Approaches towards disease resistance to filamentous pathogens

Artemis Giannakopoulou

Thesis submitted to the University of East Anglia
for the degree of Doctor of Philosophy

June 2015

© This copy of the thesis has been supplied on the condition that anyone who consults it is understood to recognise that its copyright rests with the author and that no quotation from the thesis, nor any information derived therefrom, may be published without the author's prior written consent.

ABSTRACT

In the co-evolutionary arms race between plants and pathogens, plants have developed a multifaceted armory consisting of diverse defence responses, such as the production of antimicrobial compounds and the activation of immunity via specific receptors. This work examines the use of the phytoalexin capsidiol and synthetic NLR immune receptors as disease resistance approaches against oomycete and fungal plant pathogens. The production of phytoalexins constitutes an important aspect of plant defence. Capsidiol, a pepper phytoalexin, differentially inhibits the growth of two *Phytophthora* species, the late-blight pathogen *P. infestans* and the vegetable pathogen *P. capsici*. The differential effect of capsidiol towards these two oomycetes was determined and quantified. I also monitored intraspecific variation among various *P. infestans* isolates in their sensitivity towards capsidiol. Plant defence machinery also involves intracellular immune receptors of the Nucleotide-binding Leucine-rich Repeat-containing protein family (NLRs). NLRs typically recognize pathogen effector proteins with avirulence activities, leading to a response known as effector-triggered immunity (ETI). R3a and I2 are orthologous NLRs from potato and tomato responding to effectors of *P. infestans* and the wilt fungus *Fusarium oxysporum f. sp. lycopersici*, respectively. Yet, particular races of these pathogens have evolved stealthy effectors that evade recognition by R3a and I2. I assessed whether previously identified mutations in R3a, with expanded response specificities to *Phytophthora spp*. effectors, can be transferred to I2 with similar beneficial effects. I recovered I2 mutants with expanded response spectrum to effectors from both *P. infestans* and *F. oxysporum f. sp. lycopersici*. Infection assays in both transient and stable transgenic systems suggested this expanded response correlates with resistance. I finally investigated whether the *I2* locus is a determinant of tomato resistance against *P. infestans*. Overall, these findings generate new insights into the molecular interactions underlying plants response to pathogens, and open up applied perspectives for sustainable crop disease resistance.

Table of Contents

ACKNOWLEDGEMENTS

I would first like to thank Ballet, through which I learnt the virtues of discipline and professionalism that have helped me enormously while pursuing my PhD.

Next, I would like to express my sincere gratitude to my supervisor Sophien Kamoun for being an excellent example of a Leader and for pushing me to my limits to reach my full potential. Many thanks as well for giving me the opportunity to join your research group, for trusting me, for your endless support and for teaching me how to focus on the benefits of every situation. I also want to thank my mentors; Sebastian Schornack for helping me in my first steps during my PhD and Marina Pais for her critical suggestions, endless help and the hours she spent correcting every piece of my writing throughout my PhD.

Needless to say how lucky I feel to have been a member of the Kamoun group, I am thankful to all the members, past and present, and each of them individually for their support and help during the good and bad days of driving this research. Special thanks to both Angela Chaparro-Garcia and Tolga Bozkurt, for bearing my questions with patience and for insightful discussions.

I owe a big thank you to all the researchers that make The Sainsbury Laboratory one of the best places to learn and do science. I will always admire their passion for science and their willingness to offer valuable help! Also I want to thank all the TSL/JIC students for going together through this unique experience, for all the exciting and all the crazy moments as well!

I would also like to express my sincere gratitude to Onassis Foundation for supporting my studies. I am very honored to have been selected for this award.

None of this would have been possible without the guidance of my very first supervisor Dr. Dimitrios Tsitsigiannis. His motivation and passion inspired me to follow science. I also want to thank Sofia Kountouri who taught me pipetting and helped with my first PCR reaction.

I finally want to thank my mom without whom I would have not been who I am, or have accomplished what I have. I want to thank SA for believing in me and for providing me with an excuse to travel often. I feel the luckiest person in the universe to have Sofia as my best friend. Sofia, thank you for being who you are. Thank you for standing by my side, for inspiring me, for being the definition of true friend and for constantly reminding me that anything is possible!

One last thank you to all those who wished me Good morning with a smile on their face on a daily basis these past four years. Thank you for contributing on a beautiful beginning of each day.

To Sofia and ~~AA~~ for being an endless inspiration

ABBREVIATIONS

CC	**Coiled-Coil domain**
CNL	**Coiled-coil Nucleotide-binding Leucine-Rich-Repeat protein**
Dpi	**Days post inoculation**
ETI	**Effector triggered immunity**
Fol	***Fusarium oxysporum f. sp. lycopersici***
h	**Hours**
HR	**Hypersensitive response**
kDa	**KiloDaltons**
L	**Liter**
LC/MS	**Liquid Chromatography / Mass spectrometry**
LRR	**Leucine-Rich-Repeat domain**
LSD	**Least Significant Difference**
M	**Molar**
mg	**Miligram**
ml	**Millilitre**
mm	**Milimeters**
NB-ARC	**Nucleotide Binding domain**
ng	**Nanogram**
NLR	**Nucleotide-binding Leucine-Rich-Repeat protein**
nM	**Nanomolar**
nm	**Nanometers**
NMR	**Nuclear Magnetic Resonance spectroscopy**
OD600	**Optical Density at 600 nanometers**

ppm	**Parts per million**
PTI	**PAMP-triggered immunity**
R	**Resistance**
R_f	**Retardation factor**
RFU	**Red Fluorescent Units**
RLK	**Receptor-like kinase**
RLP	**Receptor-like protein**
rpm	**Rounds per minute**
SIM	**Selected Ion Monitoring**
TIM	**Total Ion Chromatogram**
TIR	**Toll/interleukin-1**
TLC	**Thin Layer Chromatography**
TNL	**Toll/interleukin-1 NLR protein**
ug	**Microgram**
ul	**Microliter**
um	**Micrometer**
uM	**Micromolar**
WB	**Western blot**

CHAPTER 1: General introduction

Plants are continuously exposed to a wide range of disease-causing entities, such as viruses, bacteria, fungi, oomycetes, nematodes, insects and other parasitic plants (Agrios 2005, Westwood, Yoder et al. 2010). Yet, one general concept in plant pathology is that disease is the exception and resistance is the rule, as most plants are resistant to most pathogens. In order for plants to defend themselves against the rapidly evolving pathogenic organisms, they have evolved a sophisticated multi-layered arsenal defence mechanisms. This arsenal responds to external stimuli and includes both constitutive and inducible components as diverse as antimicrobial secondary metabolites and specialized intracellular immune receptors. Cell walls, and waxy epidermal cuticles are examples of constitutive defense components, which act as a first layer of defence against invading pathogens. In addition to these barriers, plant invasion triggers inducible defenses such as the production of chemical compounds (antimicrobial secondary metabolites), the activation of immune receptors (recognizing specific pathogen-derived molecules) and even cell death (Agrios 2005, Beattie 2008).

The process of fast adaptation of pathogens to resistant plants, and the counter evolution of plants to develop new resistance traits has led to a never ending so-called “arms race” between plants and pathogens (Favaron, Lucchetta et al. 2009). Plant diseases constitute one of the main threats in modern human life, and the need for sustainable crop resistance is becoming evident (Fisher, Henk et al. 2012). Conventional breeding and the use of pesticides are no longer sufficient practices to sustain food production in pace with the escalating demand posed by an ever-growing human population. Unraveling the mechanisms underpinning plant-microbe interactions could provide a better insight on how to succeed in developing targeted strategies for broad-spectrum disease resistance.

1.1. Secondary metabolites as part of the plant defence arsenal

Plants synthesize a range of metabolites, which can be divided into two classes of compounds: primary and secondary metabolites. Primary metabolites include hormones (gibberellins and brassinosteroids), photosynthetic pigments (carotenoids), membrane components (sterols) and electron carriers (chlorophylls), and are vital for the functioning of essential plant systems (Liu, Wang et al. 2005). Secondary metabolites, although not vital for plant survival, have diverse functions

such as insect attractants (essential oils and flower colours), antimicrobial compounds (phytoanticipins and phytoalexins) and defences against herbivores (antifeedants) (Dixon 2001). In short, secondary metabolites are essential for ecological viability as they mediate important interactions between plants and other organisms.

An important aspect of the plant innate immunity is the inducible production of secondary metabolites resulting from pathogenic invasion (Kuc 1995, Mithoefer and Boland 2012). Initial plant responses after pathogen attack involve cytoskeletal rearrangements, callose, extensin and lignin deposition, production of enzymes such as chitinases and glucanases and the hypersensitive response (HR). The HR restricts the pathogen from further spread to adjacent tissues where the cells surrounding the site of infection undergo apoptosis, a form of cell death (Kuc 1995). A long-term lasting response, known as systemic acquired resistance (SAR) (Vlot, Dempsey et al. 2009) will follow, involving plant hormones such as jasmonic acid, ethylene, absicic acid, salicylic acid, gibberellins and cytokinins which will act as hormonal signal transporters to the rest of the plant (Dempsey and Klessig 2012, Pieterse, Van der Does et al. 2012, Thaler, Humphrey et al. 2012, Gimenez-Ibanez and Solano 2013). Perception of the signal results in diverse changes, including the induction of genes involved in the production of diverse secondary metabolite compounds.

Several studies provide evidence that some of these secondary metabolites have antimicrobial properties and represent a great source of candidates in view of the generation of new antimicrobial agents (Stoessl, Unwin et al. 1973, Jones, Unwin et al. 1975, Ward 1976, Hargreaves, Mansfield et al. 1977, Kurosaki and Nishi 1983, Hoffman and Heale 1987, Milat, Ducruet et al. 1991, Milat, Ricci et al. 1991, Delserone, Matthews et al. 1992, Mercier, Arul et al. 1993, Echeverri, Torres et al. 1997, Keller, Czernic et al. 1998, Ma 2008, Favaron, Lucchetta et al. 2009, Grosskinsky, Naseem et al. 2011, Timperio, D'Alessandro et al. 2012, Lachhab, Sanzani et al. 2014). These compounds include alkaloids, flavonoids, lignins, phenolic compounds and terpenoids. The family of terpenoids (or isoprenoids) in plants is one of the largest, consisting of over 30,000 members, many of which have been characterized and are known to impair pathogenicity of diverse microorganisms (Harborne 1999, Gershenzon and Dudareva 2007).

1.1.1. Phytoalexins

Phytoalexins are plant antimicrobial secondary metabolites that rapidly accumulate at pathogen infection sites (Hammerschmidt 1999). Müller and Börger back in 1940 were the first to propose the concept of phytoalexins as low molecular weight antimicrobial compounds that accumulate in plants after infection or stress (Müller 1940). They found that tissue of potato tubers, previously infected with an incompatible race of the oomycete pathogen *Phytophthora infestans* induced resistance to a compatible race of the pathogen. The hypothesis proposed was that the tuber tissue had produced compounds (phytoalexins) that stopped the pathogen during the incompatible interaction and further protected from infection of compatible races of the pathogen (Müller 1940). The concept of phytoalexins which as a term means "to ward-off, protect" in Greek, was established in line with two important phenomena; first, that a plant cell could actively respond to an assayed infection and second that plants were resistant after they had been exposed to microorganisms (Deverall 1982). These compounds are extremely diverse chemically but can be categorized in three major classes: terpenoids, alkaloids and glycosteroids. Phytoalexins are part of the plant's defence arsenal against phytopathogenic microorganisms. They are broad-spectrum pathogen inhibitors including fungi, oomycetes, bacteria and viruses while they also exert phytotoxic activities (Smith 1982, Kuc 1995, Jeandet, Clement et al. 2013). Garlic allixin was the first phytoalexin to be isolated from plants, obtained from plants that were grown under continuous stress (Kodera, Matsuura et al. 1989). This phytoalexin has been shown to have diverse and yet unique biological properties, including numerous anti-oxidative and anti-microbial properties, anti-tumor promoting effects, inhibition of aflatoxin B2 DNA binding, neurotrophic effects, anti-*Helicobacter pylori* induced gastric inflammatory effects (Nishino 1990, Yamasaki, Teel et al. 1991, Dorant, Vandenbrandt et al. 1993, Agarwal 1996, Moriguchi, Matsuura et al. 1997, Mahady, Matsuura et al. 2001).

Phytoalexin members that received great attention until the 1980s were been mostly from plants in the families of Leguminosae or Fabaceae and Solanaceae (Ingham 1982, Kuc 1982, Jeandet, Clement et al. 2013). In Solanaceae, there are currently four classes that phytoalexins can be grouped into: the class of phenylpropanoid-related phytoalexins with caffeic acid and chlorogenic acid (Kuc 1957) the class of steroids glycoalkaloids with a-solanine and a-chaconine (Locci 1967, Jeandet, Clement et al. 2013), the sesquiterpenoids class whose members are rishitin,

lubimin, capsidiol (Katsui 1968, Tomiyama, Sakuma et al. 1968, Birnbaum 1974, Katsui 1974, Jeandet, Clement et al. 2013) and the class of coumarin, scopoletin (Reuveni and Cohen 1978, Jeandet, Clement et al. 2013).

1.1.1.1. Phytoalexins can contribute to pathogen resistance

Several studies have highlighted the important role of various phytoalexins as antimicrobial compounds. Two of the most well studied phytoalexins in grape (*Vitis vinifera*), the stilbenes *trans*-resveratrol and delta-viniferin, are produced after infection of the fungal pathogen *Botrytis cinerea* and the oomycete *Plasmopara viticola* respectively and are implied to contribute to the resistance of *Vitis spp.* towards those pathogens (Schnee, Viret et al. 2008, Favaron, Lucchetta et al. 2009, Alonso-Villaverde, Voinesco et al. 2011, Ahuja, Kissen et al. 2012, Timperio, D'Alessandro et al. 2012). Glyceollin and coumestrol isoflavonoids from *Glycine max* rapidly accumulate after infection of the fungus *Fusarium solani* and are thought to be implicated to the partial resistance towards that pathogen (Lozovaya, Lygin et al. 2004). Camalexin, the major phytoalexin from *Arabidopsis thaliana* is known to be involved to the resistance to many pathogens; the necrotrophic fungi *Alternaria brassicicola*, *Botrytis cinerea* and *Plectosphaerella cucumerina* (Kliebenstein, Rowe et al. 2005, Nafisi, Goregaoker et al. 2007, van Baarlen, Woltering et al. 2007, Sanchez-Vallet, Ramos et al. 2010, Ahuja, Kissen et al. 2012) the hemibiotrophic oomycete and fungus, *Phytophthora brassicae* and *Leptosphaeria maculans* respectively (Rogers, Glazebrook et al. 1996, Bohman, Staal et al. 2004, Staal, Kaliff et al. 2006, Ahuja, Kissen et al. 2012) and the biotrophic fungi *Golovinomyces orontii*, *Blumeria graminis* and *Erisiphe pisi* (Consonni, Bednarek et al. 2010, Pandey, Roccaro et al. 2010, Bednarek, Pislewska-Bednarek et al. 2011, Ahuja, Kissen et al. 2012). The major phytoalexins from *Vicia faba*, including isoflavonoid medicarpin and wyerone acid, are also known to impact the germ tubes of several species of the necrotrophic fungus genus *Botrytis* (Hargreaves, Mansfield et al. 1977). Another example is the case of two phytoalexins; pisatin and maackiain, from garden pea and red clover respectively, that can inhibit growth of 19 fungal species (Delserone, Matthews et al. 1992).

Finally, one well studied phytoalexin, capsidiol, is produced in pepper or tobacco after infection by pathogens such as the oomycete *Phytophthora capsici,* and affects a wide range of pathogens (Stoessl, Unwin et al. 1973, Jones, Unwin et al. 1975, Ward 1976, Milat, Ducruet et al. 1991, Milat, Ricci et al. 1991, Keller, Czernic et al.

1998, Ma 2008, Grosskinsky, Naseem et al. 2011).

1.1.2. Capsidiol and its antimicrobial properties

Capsidiol is a bicyclic sesquiterpenoid compound and a member of the isoprenoid class of phytoalexins and is the main phytoalexin produced in pepper and tobacco after infection of several pathogens (Zhang, Foerster et al. 2005, Literakova, Lochman et al. 2010). Similar to all sesquiterpenes, capsidiol derives from a common substrate: farnesyl diphosphate (FPP) (Cane 1990). There are two key enzymes responsible for the biosynthesis of capsidiol. The first step in the biosynthetic pathway is the cyclization of FPP by the 5-*epi*-aristolochene synthase (EAS) to produce the intermediate 5-*epi*-aristolochene. Then the 5-*epi*-aristolochene dihydroxylase (EAH) mediates the two hydroxylation steps at positions C-1 and C-3 of 5-*epi*-aristolochene to yield capsidiol (Ralston, Kwon et al. 2001). The dihydroxylase works in parallel with a cytochrome P450 reductase (CPR; NADPH-ferrihemoprotein reductase), which transfers electron equivalents for EAH reactions (Fig. 1.1). General elicitors of capsidiol in pepper include hydrogen peroxide, methyl jasmonate and cellulase (Padmanabhan, Gorepoker et al. 2005, Padmanabhan, Shiferaw et al. 2006) while infection by the necrotroph *Botrytis cinerea*, or the oomycetes *Phytophthora nicotianae* and *Phytopathora palmivora* trigger capsidiol accumulation in *Nicotiana tabacum* (Domingo, Andres et al. 2009, Erb, Meldau et al. 2012). A number of studies dating back to the 1970s described the ability of capsidiol to differentially affect growth of two notorious oomycetes, *Phytophthora infestans* and *Phytophthora capsici* (Jones, Unwin et al. 1975, Ward 1976, Egea, Alcazar et al. 1996). Jones *et al.* showed that *P. infestans* is more sensitive (~10 fold) to capsidiol than *P. capsici*, both in spore germination and growth assays, and further showed that the effect is reversible below a certain threshold (Jones, Unwin et al. 1975). Several studies have used capsidiol as a defence marker (Milat, Ducruet et al. 1991, Keller, Czernic et al. 1998, Ahmed Sid, Perez Sanchez et al. 2000, Maldonado-Bonilla, Betancourt-Jimenez et al. 2008), however there have not been many studies focusing on the capsidiol-*Phytophthora* pathosystem. In a later study, Shibata *et al*. proposed a positive role for capsidiol in the resistance of *Nicotiana benthamiana* against *P. infestans* (Shibata, Kawakita et al. 2010). They showed that silencing of two ethylene-regulated genes for capsidiol biosynthesis, *NbEAS* and *NbEAH*, negatively impacted resistance (Shibata, Kawakita et al. 2010).

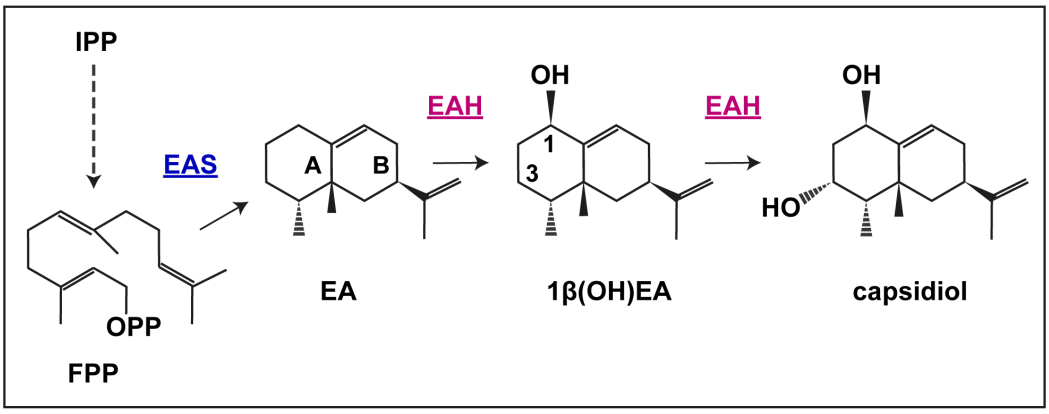

Figure 1.1: Schematic illustration of capsidiol biosynthetic pathway in plants. Farnesyl diphosphate (FPP) constitutes the substrate for the capsidiol biosynthesis. The first step involves cyclization of FPP by the action of 5-*epi*-aristolochene synthase (EAS) to generate the intermediate 5-*epi*-aristolochene (EA). Successive hydroxylations of EA at C-1 and C-3 positions by the 5-*epi*-aristolochene dihydroxylase (EAH) enzyme lead to capsidiol. Isopentenyl diphosphate (IPP) is the central intermediate in the biosynthesis of isoprenoids in all organisms; dotted line represents multiple steps.

1.2. Plants have immune receptors that recognise pathogen molecules

In addition to the secondary antimicrobial compounds, plants have also evolved specialized immune receptors. During pathogen attack, conserved microbial molecules known as pathogen- or microbe-associated molecular patterns (PAMPs/MAMPs) are recognised by the host. This occurs at the cell periphery and is mediated by cell surface pattern recognition receptors (PRRs) (Monaghan and Zipfel 2012). As a result, PAMP-triggered immunity (PTI) is launched and this process usually leads to broad-spectrum but typically incomplete resistance (Monaghan and Zipfel 2012). Pathogens however, have evolved mechanisms to overcome PTI, by secreting effector molecules to the host interface or inside host cells that suppress PTI and modulate host cell processes to their benefit (Bonardi and Dangl 2012, Win, Chaparro-Garcia et al. 2012). On the other side, plants have evolved intracellular immune receptors known as resistance (R) proteins that specifically recognise pathogen effectors triggering further immune responses which lead to resistance (Jones and Dangl 2006, Ooijen, Burg et al. 2007, Dodds and Rathjen 2010, Win, Chaparro-Garcia et al. 2012).

1.2.1. Pathogen effectors

Plant pathogenic organisms such as fungi, oomycetes, bacteria, nematodes and insects although biologically diverse, have evolved similar ways to facilitate their colonization and manipulate the host immune responses. One common tactic of plant pathogens is the secretion of effector molecules to the apoplastic space or to different compartments of the plant cell cytoplasm (Hogenhout, Van der Hoorn et al. 2009, Dodds and Rathjen 2010, Bozkurt, Schornack et al. 2012, Win, Chaparro-Garcia et al. 2012).

Win *et al*. (2012) defined effectors as "microbial secreted molecules that influence host cell processes or structure to promote the microbe's lifestyle" (Win, Chaparro-Garcia et al. 2012). Effector functions can be very diverse, ranging from enhancing access to the host nutrients to suppressing immune responses. Effectors can also be used as molecular probes in order to unravel novel components of the plant immune system and to even reprogram cellular processes (Bozkurt, Schornack et al. 2012, Win, Chaparro-Garcia et al. 2012).

Unlike plant resistance proteins, effector proteins do not appear to be generally conserved between species, and can even be diverse in amino acid sequence between different isolates of a given pathogen (Ooijen, Burg et al. 2007). As mentioned previously, effectors are secreted by the pathogen either to the host cell apoplast or to the cell interior. Pathogens have evolved various mechanisms to translocate their effectors inside the host cell (Hogenhout, Van der Hoorn et al. 2009). For example, Gram-negative bacteria utilize the Type III Secretion System as a machinery to effectively deliver effectors into the plant cell (Alfano and Collmer 2004). Our knowledge on how fungal and oomycete pathogens deliver their effectors is very poor. However, recent studies have shown that some effectors accumulate at specialized pathogenic structures of fungi and oomycetes, called haustoria (Rafiqi, Gan et al. 2010, Bozkurt, Schornack et al. 2012, Saunders, Breen et al. 2012) suggesting that haustorium-forming organisms could use these structures to successfully deliver their effectors besides the uptake of nutrients (Mendgen, Struck et al. 2000, Szabo and Bushnell 2001, Voegele, Struck et al. 2001, Voegele and Mendgen 2003, Catanzariti, Dodds et al. 2006, Whisson, Boevink et al. 2007, Rafiqi, Gan et al. 2010, Garnica, Nemri et al. 2014).

1.2.2. NLRs are the largest class of R proteins

The largest family of intracellular immune receptors is the nucleotide binding-leucine-rich repeat (NB-LRR or NLR) protein family, and is an important element of defence in both plants and animals (Maekawa, Kufer et al. 2011, Jacob, Vernaldi et al. 2013). NLRs can be clustered in two major classes depending on their N-terminal part: those carrying a domain with a predicted coiled-coil (CC) structure, called CC-NB-LRR or CNL proteins, and those carrying a Toll/interleukin-1 receptor (TIR) domain, called TIR-NB-LRR or TNL proteins (Pan, Wendel et al. 2000, Andolfo, Jupe et al. 2014). The central nucleotide-binding domain (NB), also known as NB-ARC, is shared by the mammalian protein Apaf-1, plant resistance proteins, and the nematode *Caenorhabditis elegans* Ced-4 protein. Together, these proteins represent a clade of the signal-transduction ATPases with numerous domains (STAND) (Leipe, Koonin et al. 2004, Takken and Tameling 2009). This central domain has been suggested to act as a switch between the resting state of the protein (ADP-bound) and the activated (ATP-bound) state (Takken, Albrecht et al. 2006, Tameling, Vossen et al. 2006, Maekawa, Kufer et al. 2011, Takken and Goverse 2012). The C-terminal LRR domain tends to be more polymorphic with the number and length of the LRR repeats highly variable between different NLR proteins (Takken and Goverse 2012).

Recent reports of crystal structures of individual NLR-protein domains have provided a better insight into how these proteins function (Bernoux, Ve et al. 2011, Maekawa, Cheng et al. 2011, Hao, Collier et al. 2013) but structural data of full-length plant NLR receptors are still lacking.

1.2.3. NLR activation

In the absence of the pathogen, NLR proteins are retained in an inactive conformation, to avoid unnecessary triggering of immune responses that could have detrimental effects on the plant's lifestyle (Takken, Albrecht et al. 2006, Marquenet and Richet 2007). There are three distinct steps that mediate NLR activation according to the current model (Bonardi and Dangl 2012) (Fig 1.2); (1) The presence of a microbial molecule or an effector, or the outcome of their action inside the host cell, is perceived by the NLR protein, which releases the LRR domain from the NB domain. (2) This conformational change of the receptor allows the NB domain to become an accessible platform for nucleotide exchange (ADP➔ATP) and the NLR

protein is activated. (3) Repetitive cycles of nucleotide exchange lead to a second conformational change, which further releases the N-terminal part of the protein from the NB domain. This last rearrangement is hypothesized to increase the interaction surface of the N-terminal part of the protein with downstream signaling components (Bonardi and Dangl 2012).

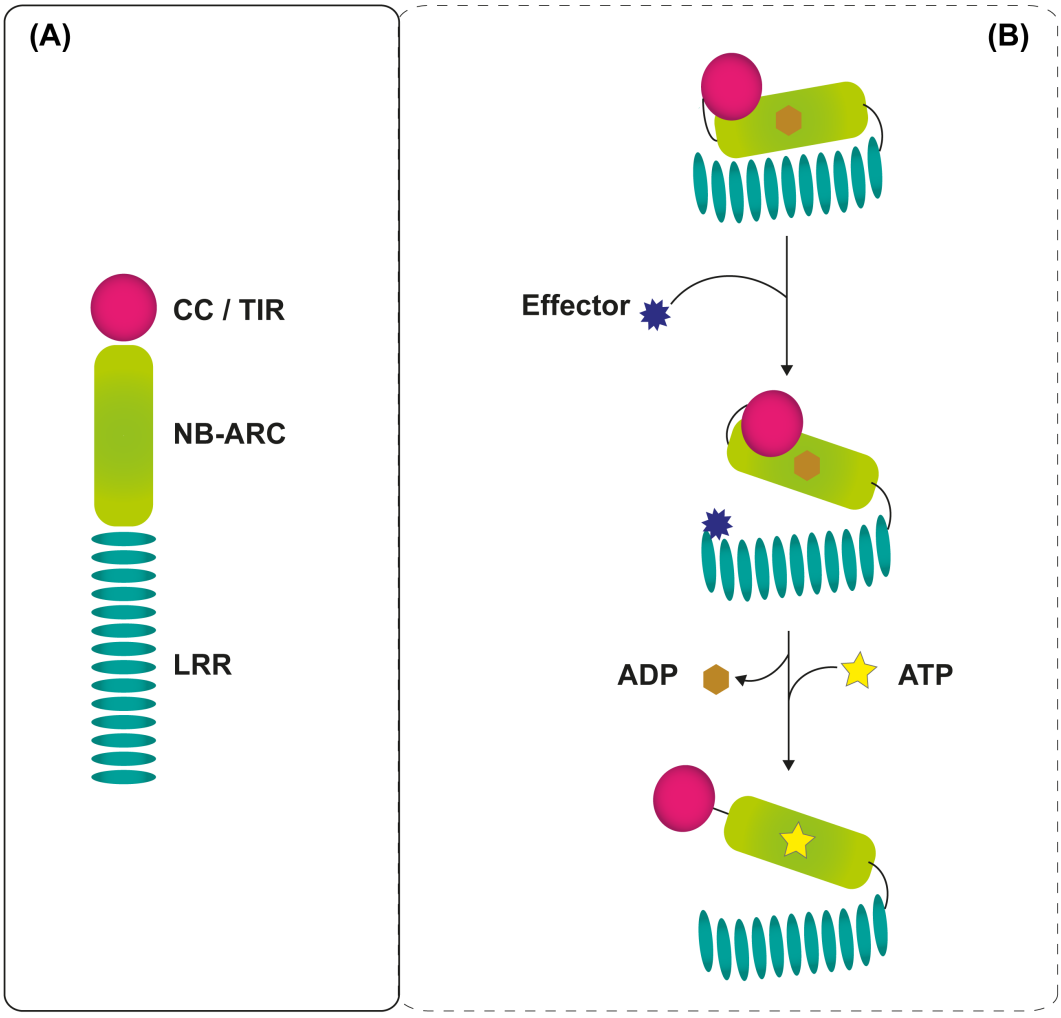

Figure 1.2: Representation of the intramolecular interactions during NLR activation in plants.
A, Domains of an NLR protein in plants. B, The LRR domain maintains NLRs an "off" state in the absence of a pathogen (top). Recognition of a pathogen effector triggers a first conformational change, nucleotide exchange ensues and the NLR protein gets activated (middle). A second conformational change is driven by the NB-ARC domain catalytic activity which results to further exposes of the N-terminal domain of the protein (bottom). Adapted by Bonardi *et al.* (Bonardi and Dangl 2012).

1.2.4. Effector triggered immunity (ETI)

As mentioned previously, during parasitic invasion, pathogens secrete effector proteins. Host-specific NLR proteins, encoded by *R* loci, will then perceive the cognate effectors from a pathogen directly (Dodds and Rathjen 2010) or indirectly (Dangl and Jones 2001, van der Hoorn and Kamoun 2008) and initiate further immune responses, which result in disease resistance. This process is known as effector-triggered immunity (ETI) (Jones and Dangl 2006, Ooijen, Burg et al. 2007, Dodds and Rathjen 2010, Win, Chaparro-Garcia et al. 2012) and it was first described by Flor (1955) as a "gene-for-gene" interaction (Flor 1955). The activation of NLR receptors usually results in HR, which will eventually limit pathogen growth (Kamoun, Huitema et al. 1999, Vleeshouwers, van Dooijeweert et al. 2000, Win, Chaparro-Garcia et al. 2012).

Several models describe the mechanisms underlying the recognition of effectors by NLR proteins. One of them suggests a direct interaction between the plant NLR protein and the pathogen effector, by means of physical interaction (Dangl and Jones 2001). Direct interaction between plant receptors and effectors has been described so far for some cases (Jia, McAdams et al. 2000, Deslandes, Olivier et al. 2003, Dodds, Lawrence et al. 2006, Ueda, Yamaguchi et al. 2006, Narusaka, Shirasu et al. 2009, Catanzariti, Dodds et al. 2010, Kanzaki, Yoshida et al. 2012, Cesari, Thilliez et al. 2013, Williams, Sohn et al. 2014, Zhai, Zhang et al. 2014). The rice CNL protein Pi-ta was the first one shown to directly bind to the *Magnaporthe oryzae* effector protein AVRPita (Jia, McAdams et al. 2000). Physical interaction was also shown between RRS1-R, an *Arabidopsis thaliana* TNL protein, PopP2, a *Ralstonia solanacearum* type III effector and AVRRPS4, a *Pseudomonas syringae* effector (Deslandes, Olivier et al. 2003, Narusaka, Shirasu et al. 2009, Williams, Sohn et al. 2014). Flax NLR proteins L5, L6, L7 and M were also shown to directly interact with different variants of the effectors AVRL567 and AVRM respectively, which are expressed during infection by the rust fungal pathogen *Melampsora lini* (Dodds, Lawrence et al. 2006, Catanzariti, Dodds et al. 2010). Another example is the case of the tobacco resistance protein N, where the ATP-bound form of the protein was found to bind the Tobacco mosaic virus helicase domain p50 (Ueda, Yamaguchi et al. 2006). Recent studies showed that AVR1-CO39 and AVR-Pia effectors from *Magnaporthe oryzae* bind to the rice CNL protein RGA5, and also AVR-Pik from the same pathogen binds to the rice CNL protein Pik-1 (Kanzaki, Yoshida et al. 2012, Cesari, Thilliez et al. 2013, Zhai, Zhang et al. 2014).

An alternative model for effector recognition by NLR proteins is the so-called “guard hypothesis”. In this model, the NLR protein in the host monitors effector-triggered modifications of other host proteins (known as guardees), which are the targets of the pathogen effectors (Mackey, Holt et al. 2002, Axtell and Staskawicz 2003, Rooney, van 't Klooster et al. 2005). Examples of NLR protein/effector pairs that are consistent with that model are the *A. thaliana* CNL protein RPM1 with *P. syringae* AVRB effector, RPM1 with *P. syringae* AVRRpm1 effector and the *A. thaliana* CNL RPS2 with the *P. syringae* effector AVRRpt2; all of these effectors interact with another *A. thaliana* protein, RIN4 and perturbations of RIN4 are then detected by the cognate NLR proteins (Mackey, Holt et al. 2002, Martin, Bogdanove et al. 2003, Dodds and Rathjen 2010).

Finally, another model that describes an indirect interaction between R proteins and effectors was proposed a few years ago (van der Hoorn and Kamoun 2008). The key players implicated in this model are: (1) the effector, (2) the decoy (effector target required for the function of the NLR protein but without any function in defence in its absence, and/or with no effect on the pathogen’s fitness), (3) the operative target (a host target, whose manipulation by the effector results in enhanced fitness for the pathogen), and (4) the NLR protein. According to the decoy model, the host NLR protein monitors alterations of the decoy, which mimics the operative effector target only in terms of perception of pathogen effectors, without contributing to the pathogen’s fitness in the absence of the cognate NLR protein. In that sense, decoys will compete with operative targets for binding to the effector. A representative example of the decoy model is the interaction between the *P. syringae* kinase inhibitor AVRPto and the tomato CNL protein Prf. During *P. syringae pv. tomato* JL1065 infection, AVRPto is translocated into the host cell, where it localizes to the plasma membrane (Shan, Thara et al. 2000). There, it physically interacts with the tomato kinase protein Pto (the decoy) (Xiao, He et al. 2007) and this interaction is then perceived by Prf (NLR protein) leading to ETI (Block, Li et al. 2008). It has been also suggested that the receptor-like kinase FLS2 is the operative target in this system (van der Hoorn and Kamoun 2008), since AVRPto inhibits the kinase activity of FLS2 and when FLS2 is absent, AVRPto contributes to virulence of *P. syringae* (Xiang, Zong et al. 2008).

In a more recent study, an “integrated decoy model” was suggested to explain effector recognition in some cases of paired NLR proteins, such as the rice NLR protein pair RGA4/RGA5 and the *A. thaliana* resistance protein pair RPS4/RRS1

(Cesari, Bernoux et al. 2014). This model is proposed as an extension of the decoy model described above (van der Hoorn and Kamoun 2008) and in this case, the decoy is integrated in the structure of the NLR protein as an extra domain allowing recognition of the effectors (Cesari, Bernoux et al. 2014). However, Wu *et al*. commenting on this latest study proposed instead the term integrated "sensor domains" (SD) (Wu, Krasileva et al. 2015). As highlighted in the commentary, the possibility that these NLR-integrated domains are not decoys (as in defective mimics) but still retain the biochemical activity of their ancestral effector target (ET) cannot be excluded (Wu, Krasileva et al. 2015). Therefore, further genetic and biochemical experiments are required to draw any final conclusions on the nature of these domains (Wu, Krasileva et al. 2015).

1.3. *Fusarium oxysporum f. sp. lycopersici*

1.3.1. Classification and life style

The name of the genus *Fusarium* has its origin in the Latin word fusus, which means a spindle, reminiscent of the shape of the pathogen's spores. Most of the genus species are soil inhabitants and are saprobes that are not known to cause plant diseases. A few known species produce mycotoxins (mostly fumonisins and trichothecenes) in cereal crops, and incorporation of these in the food chain can affect human health (W. F. O. Marasas 1987). The species *Fusarium oxysporum* first described by Snyder and Hansen (Snyder 1940) infects numerous agricultural and floricultural crops and is the causal agent of *Fusarium* wilt disease (Armstrong 1981, Agrios 2005, Divon and Fluhr 2007). *F. oxysporum* includes more than 120 forma speciales according to the host specialization of each member with *F. oxysporum f. sp. lycopersici* being a notorious and exclusive pathogen of tomato (Armstrong 1981).

1.3.1.1. Biology of the pathogen

F. oxysporum f. sp. lycopersici is a very important pathogen of tomato, causing significant losses in the worldwide tomato production. The pathogen infects tomato by direct penetration through the roots. Then, the pathogen will reach the xylem vessels, extensive colonization of which results in the characteristic wilting symptom "brown discoloration". Soon the wilting symptoms appear at the outside of the plant and the plant will eventually die (Agrios, Webster). There are three kinds of asexual

spores, microconidia, macroconidia and chlamydospores. Chlamydospores are known to survive for many years in the soil, whereas microconidia are the most abundant as they are produced under all conditions. Macroconidia are the typical spores of *Fusarium* and are found on the surface of plants killed by the pathogen (Agrios 2005, Webster J 2007).

1.3.1.2. Development of the disease

F. oxysporum f. sp. lycopersici is a soil-borne pathogen that can survive in infected plant debris in the soil as mycelium or any spore form. However, as mentioned above, chlamydospores are the type of spores that survive longer, especially in regions with cool temperatures. Dispersion of the pathogen over short distances is caused by water and contaminated farm equipment while infected transplants are the most common cause over longer distances. Unfortunately, “regions that become infested with *Fusarium*, remain so indefinitely” (Agrios 2005). The disease initiates when healthy plants grow in contaminated soils. As mentioned above, the spores will directly penetrate either through the root tips or through the positions that the lateral roots are formed. The mycelium follows the root cortex intercellularly, and later enters the xylem vessels. The mycelium will branch and produce microconidia, which will travel through the sap stream, germinate and colonize new vessels.

The accumulation of mycelium, spores, polysaccharides, gels and gums in the vessels will result in the so-called clogging of the vessels. This process will affect and break down the water economy of the plant; leaves will start wilting and die, subsequently affecting the rest of the plant. The brown discoloration of the vessels is thought to be caused by the oxidation and translocation of some breakdown products. After the plant has died, extensive colonization of the remaining tissues occurs and the pathogen reaches the surface where it starts to sporulate. Dispersion of the spores to adjacent plants will initiate a new disease cycle (Agrios 2005, Webster J 2007).

It is possible that the pathogen penetrates the fruit and contaminates the seeds, however in such cases, the light weight of the seeds will exclude their use and prevent further spread of the pathogen (Agrios 2005).

1.3.1.3. Control of the disease

The only effective measure in the fields is the use of resistant tomato varieties. The use of fungicides, even though recommended requires extra care as there is the danger of toxicity in fruits (Amini and Sidovich 2010).

Few studies have looked into the processes mediating *Fusarium*-tomato interaction in order to identify ways to control the disease. Analysis of the plant transcriptome during a tomato-*F. oxysporum f. sp. lycopersici* incompatible interaction, revealed a number of overexpressed genes related to maintenance of cellular structure and homeostasis (Andolfo, Ferriello et al. 2014). *F. oxysporum f. sp. lycopersici* follows a necrotrophic lifestyle and kills the host cells prior to infection which eventually induces cell death. Therefore expression of anti-apoptosis genes could provide resistance against the pathogen (Paul, Becker et al. 2011). Indeed, Andolfo *et al*., studying an incompatible tomato-*F. oxysporum f. sp. lycopersici* interaction found up-regulation of a homolog of *NF-kB*, a master gene of inflammation known to inhibit apoptosis by preventing the Mitogen Activated Protein Kinase (MAPK) cascade activation (Andolfo, Ferriello et al. 2014). MAPKs were found down-regulated in this system confirming the hypothesis. Auxin genes were also found to be up-regulated in this interaction, which was not surprising as auxin is known to regulate resistance to necrotrophic fungi (Llorente, Muskett et al. 2008). Jasmonate regulators and abscisic acid receptors were also up-regulated, confirming that these hormones mediate resistance in necrotrophic interactions (Anderson, Badruzsaufari et al. 2004, Koornneef, Verhage et al. 2008). Finally, as expected, the salicylic acid (SA) pathway was down-regulated (Andolfo, Ferriello et al. 2014), and silencing of a tomato gene encoding a SA methyltransferase resulted in increased resistance towards *F. oxysporum f. sp. lycopersici* (Ament, Krasikov et al. 2010).

According to a recent study, priming of tomato seeds with methyl jasmonate induces the resistance of the plants to *F. oxysporum f. sp. lycopersici* through the accumulation of a jasmonic acid precursor (12-oxo-phytodienoic acid, OPDA), salicylic acid and flavonol (P. Król 2015).

1.3.2. *Fusarium oxysporum f. sp. lycopersici* emergence of races

As mentioned previously, most *F. oxysporum* strains are host specific and strains infecting the same host belong to the same group or form, else known as *forma*

specialis (*f. sp.*) (Armstrong 1981, Katan 1999, Katan and Di Primo 1999). Effectors in *F. oxysporum f. sp. lycopersici* are usually small, cysteine-rich "secreted-in-xylem" (SIX) proteins, without sequence homology to any other known proteins (Rep 2005, Houterman, Speijer et al. 2007, Lievens, Houterman et al. 2009, Blum, Waldner et al. 2010, Schmidt, Houterman et al. 2013). The first effector genes to be identified in *F. oxysporum f. sp. lycopersici*-infected tomato plants were *Avr1* (*Six 4*), *Avr2* (*Six 3*) and *Avr3* (*Six 1*), different combinations of which are found in the three *F. oxysporum f. sp. lycopersici* races known thus far (Rep, van der Does et al. 2004, Houterman, Cornelissen et al. 2008, Houterman, Ma et al. 2009). *Avr1* is found only in race 1, *Avr2* is present in both races 1 and 2 and finally *Avr3* is present in all three races (Rep, van der Does et al. 2004, Houterman, Ma et al. 2009). The cognate resistance genes in tomato are termed *I* and *I1*, *I2* and *I3*, with *I2* and *I3* being the only ones currently cloned (Ori, Eshed et al. 1997, Simons, Groenendijk et al. 1998, Takken and Rep 2010, Catanzariti, Lim et al. 2015) (Fig. 1.3).

(A)

***F. oxysporum f. sp. lycopersici* races effectors**

1	*Avr1 Avr2 Avr3*
2	- *Avr2 Avr3*
3	- *avr2 Avr3*

(B)

Resistance *(R)* genes in tomato and corresponding effectors in *F. oxysporum f. sp. lycopersici*

R gene	Introgressed from:	Cognate Effector genes
I	*Solanum pimpinellifolium*	*Avr1*
I1	*Solanum pennellii*	*Avr1*
I2	*Solanum pimpinellifolium*	*Avr2*
I3	*Solanum pennellii*	*Avr3*

Figure 1.3: Relationship between races of *F. oxysporum f. sp. lycopersici* and tomato.

A, Effector combination in each of the three known races of *F. oxysporum f. sp. lycopersici. Avr3* is present in all three races. *Avr2* is present in races 1 and 2 while *Avr1* is only present in race 1. B, Tomato *R* genes and their effector recognition spectrum. Effector gene *Avr1* is recognised by the non-allelic genes *I* and *I1*. *Avr2* is recognised by *I2* and *Avr3* by *I3*.

There are two current models that describe the emergence of races in *F. oxysporum f. sp. lycopersici.* The first one suggests the following evolutionary path: a non-pathogenic strain of *F. oxysporum f. sp. lycopersici* acquired a small chromosome carrying all three *Avr1*, *Avr2* and *Avr3* effector genes and became race 1. Deletion of *Avr1* locus in race 1 had as consequence the emergence of race 2 (−, *Avr2, Avr3*), and point mutations in *Avr2* resulted in race 3 appearance (−, *avr2*, *Avr3*) (Houterman, Ma et al. 2009). The second supports the idea that *Avr1* lost its function due to transposon insertion resulting in race 2 (*avr1, Avr2, Avr3*), and then point mutations in *Avr2* led to race 3 (*avr1, avr2, Avr3*) (Inami, Yoshioka-Akiyama et al. 2012). The second scenario is supported by the discovery of a Japanese race 3 *F. oxysporum f. sp. lycopersici* isolate, KoChi-1, where *Avr1* was truncated by a class II DNA transposon of the *hAT* family (*Hormin*) (Inami, Yoshioka-Akiyama et al. 2012). So far, the evidence points to a scenario in which the appearance of races was driven by the varieties deployed in the field.

Race 1 *F. oxysporum f. sp. lycopersici* was first described in England back in 1886 (Booth 1971). The first gene to be introduced for race 1 resistance was *I* from *S. pimpinellifolium* in the 1940s (Bohn and Tucker 1939). We now know that the strains that were retrieved back then from infected tomato plants did not have *Avr1* (Alexander 1945, Takken and Rep 2010). Race 2 strains lacking *Avr1* quickly emerged after that, with the first report in 1945 in Ohio (Alexander 1945). This could be a result of their pre-existence in areas in which tomatoes were cultivated, or a very strong selection with concomitant high frequency of *Avr1* loss (Takken and Rep 2010). Introduction of the *I2* gene, also from *S. pimpinelifollium*, in the 1960s to control race 2 lasted for about 20 years when race 3 emerged in the early 1980s (Volin and Jones 1982). Race 3 was first reported in Australia (Grattidge and Obrien 1982), soon after in Florida (Volin and Jones 1982) and later on in California (Davis, Kimble et al. 1988). The three AVR2 variants in race 3 emerged as a result of the I2 deployment in the field, as pre-existence of these mutations in race 1 was never reported (Houterman, Ma et al. 2009). A single dominant gene, *I3*, identified in *S. penellii* accessions PI414773 (McGrath, Gillespie et al. 1987) and LA716 (Scott and Jones 1989) was then introduced in cultivated tomato to resist race 3 of the pathogen (McGrath and Maltby 1989). Tomato varieties exclusively carrying it are not expected to be effective, due to the presence of the *Avr1* suppressor in race 1 (Houterman, Cornelissen et al. 2008). *I1* and *I3* should provide durable resistance against *F. oxysporum f. sp. lycopersici.* Such an assumption however endeavors the danger that single point mutations in *Avr3* in a race 3 background could lead to the

emergence of a new race (race 4) (Takken and Rep 2010).

1.3.3. *Fusarium oxysporum f. sp. lycopersici* effectors and pathogenicity

AVR2 and AVR3 are genuine effectors as they are required for full pathogenicity of *F. oxysporum f. sp. lycopersici* but they also trigger resistance in tomato plants carrying the cognate *I2* and *I3 R* genes respectively (Rep, van der Does et al. 2004, Rep 2005, Houterman, Ma et al. 2009). The *Avr1* effector gene, although recognised by *I-* and *I1*-carrying tomato plants, does not contribute directly to the virulence of the pathogen. However, it specifically suppresses the ability of *I2* and *I3* to confer resistance against *F. oxysporum f. sp. lycopersici* races that secrete AVR2 and AVR3 (Houterman, Cornelissen et al. 2008). This makes *Avr1* the first cloned fungal-effector gene to supress *R* gene-mediated disease resistance in plants (Jones 1988). The only known sequence polymorphisms in *F. oxysporum f. sp. lycopersici* are found in *Avr3* and *Avr2* effector genes. The first is a DNA polymorphism in *Avr3* (G490A), which leads to an amino acid change (E164K). This confers a higher virulence to *F. oxysporum f. sp. lycopersici* than the E164 variant (Rep 2005). *Avr2* is also polymorphic with three polymorphisms in close proximity (G121A, G134A, G137C), all leading to an amino acid change that prevents recognition by I2 (Takken and Rep 2010).

Eleven other SIX proteins have been also identified in *F. oxysporum f. sp. lycopersici*. Chromosome 14 appears to be a hot spot of *Six* genes in this pathogen, as revealed by genome analysis (Blum, Waldner et al. 2010, Schmidt, Houterman et al. 2013). Horizontal transfer of this specific chromosome to a non-pathogenic strain of *F. oxysporum f. sp. lycopersici,* renders it pathogenic, highlighting the importance of this chromosome for the virulence of the fungus (Blum, Waldner et al. 2010). AVR2 and SIX5 are the only two effectors thus far exclusively present in *F. oxysporum f. sp. lycopersici*, whereas for other SIX proteins (AVR1, SIX6, SIX7, SIX8, SIX9) homologs are found in other *formae speciales* (Lievens, Houterman et al. 2009, Chakrabarti, Rep et al. 2011, Thatcher, Gardiner et al. 2012). Surprisingly, SIX6 is the only *F. oxysporum f. sp. lycopersici* effector found thus far as having homologs in two other fungal pathogens; *Colletotrichum orbiculare* and *C. higginsianum* (Kleemann, Rincon-Rivera et al. 2012, Gan, Ikeda et al. 2013). This effector is also required for full pathogenicity of *F. oxysporum f. sp. lycopersici* and recently has been proven to suppress the I2-mediated cell death (Gawehns, Houterman et al. 2014).

1.3.4. *Fusarium oxysporum f. sp. lycopersici* effector AVR2

AVR2 or SIX3 as it is alternatively called, is one of the several small proteins that have been identified to be secreted by *F. oxysporum f. sp. lycopersici* during colonization of tomato plants (Houterman, Speijer et al. 2007). The *Avr2* gene is intronless and after cleavage of the predicted N-terminal signal peptide, it is predicted to encode a 15.7-kDa mature protein (Houterman, Ma et al. 2009). Like all SIX proteins, it bears no homology to any known protein. As stated previously, AVR2 is a genuine effector of *F. oxysporum f. sp. lycopersici*, since deletion mutants cannot develop full symptoms of the disease (Houterman, Ma et al. 2009). Overexpression of the full length or truncated versions of AVR2 with I2 in *N. benthamiana* leaves triggers hypersensitive response, suggesting that they form a gene-for-gene pair (Houterman, Ma et al. 2009, Ma, Cornelissen et al. 2013). A truncated form of AVR2 lacking the first predicted random coil downstream of the signal peptide, showed the fastest HR (20-24 hours) after co-expression with I2, whereas cell death induced when full length AVR2 was used, appeared 10-14 hours later (Ma, Cornelissen et al. 2013). These observations led Ma *et al*. to suggest that AVR2 can be functionally divided in two parts; a small N-terminal part that is not required for the I2-dependent cell death and the C-terminal large region that includes two cysteines and is required for this action.

Avr2 is highly expressed in roots and xylem colonizing hyphae after 3 days of inoculating tomato roots. Full-length AVR2 localizes mainly in the apoplastic space while a version lacking the signal peptide was localized in the cytosol and nucleus of plant cells (Ma, Cornelissen et al. 2013). This nuclear localization has been found indispensable to trigger the I2-dependent cell death in *N. benthamiana*, suggesting that AVR2 is perceived by I2 in the nucleus (Ma, Cornelissen et al. 2013). Point mutations in *Avr2* (G121A, G134A and G137C, corresponding to amino acid changes V41M, R45H, and R45P respectively), abolish the ability of I2 to recognise the AVR2 effector variants, without altering the virulence of the fungus (Houterman, Ma et al. 2009). It has also been shown that AVR2 forms dimers in plants and in yeast; however, this dimerization alone is not sufficient to induce the I2-mediated cell death (Ma, Cornelissen et al. 2013). Interestingly, the region of the effector that is required for homodimerization contains the “RIYER” motif, which has been proposed to be an “RXLR-like” motif (conserved motif in many pathogen effectors, thought to be crucial for translocation of the effector into the cytoplasm of the host cell (Kamoun 2006)), potentially involved in the entry of the effector inside the host cells (Kale, Gu

et al. 2010). Expression of *Avr2* and some other *Six* genes including *Avr3*, *Six2* and *Six5* is regulated by the transcription factor Sge1. The knock-out of the *Sge1* gene abolishes the expression of *Six* genes and also affects pathogenicity of the fungus (Michielse, van Wijk et al. 2009).

1.4. *Phytophthora infestans*

1.4.1. Classification and life style

Phytophthora is a genus of plant-pathogenic oomycetes ('water molds'). The name of this genus originates from the Greek language. It combines two words: φυτόν (phytón), which means "plant" and φθορά (phthorá) which means "destruction", to describe these pathogens as "plant-destroyers". The specific epithet, "*infestans*", originates form the latin verb "*infestare*" meaning to attack or to destroy. *Phytophthora* belongs to the phylum of Stramenopiles (or Heterokonta), that causes significant damage in natural ecosystems and considerable economic losses for global agriculture (Kamoun and Goodwin 2007). In year 1875 Heinrich Anton de Bary first described the pathogen and so far 100 *Phytophthora* species have been characterized. However, a common belief is that an additional 100 to 500 *Phytophthora* new species exist (Brasier 2009). *Phytophthora spp.* are mostly pathogens of dicotyledons, and are relatively host-specific. A historically notable member that has been troubling human kind for many years, *Phytophthora infestans*, is the notorious oomycete that triggered the Irish potato famine in 1845 and still remains a recurrent threat for potatoes and tomatoes worldwide. As Berg placed it back in 1926, "*Phytophthora*…has been the subject of so many investigation and controversies that it fills one of the most romantic chapters in the history of biological research" (Berg 1926).

P. infestans was originally considered to be a fungus due to its filamentous characteristics. However, Kamoun and Smart established that it is closer to brown algae than to true fungi (Kamoun and Smart 2005).

1.4.1.1. Biology of the pathogen

P. infestans is a heterothallic hemibiotrophic oomycete pathogen. Its mycelium consists of branched sporangiophores, which form lemon-shaped sporangia at their tips. Whether sporangia will germinate by releasing zoospores (asexual spores) or

directly by forming a germ tube is dependent on the temperature conditions. At low temperatures up to 15°C sporangia usually form zoospores whereas above 15°C sporangia are more likely to form a germ tube (Melhus 1915). Zoospores are equipped with two flagella that they use to swim towards a host plant. As stated previously, *P. infestans* is a heterothallic pathogen, and for its sexual reproduction it needs two mating types (A1 and A2) (Gallegly and Galindo 1958, Smoot, Gough et al. 1958, Galindo and Gallegly 1960). The female hypha will either grow through the male reproductive cell, (antheridium) forming an oogonium (amphiginy) or the antheridium attaches to the oogonium (paragyny). The outcome of the fertilization is the production of an oospore which is a critical survival structure of the pathogen especially in low temperatures (Fay and Fry 1997, Fry 2008).

1.4.1.2. Development of the disease

A very important factor for the development of late blight and initial infection is the temperature, as the pathogen cannot cope with high temperatures (Jones 1912). However different *P. infestans* clonal lineages have different temperature responses (Mizubuti and Fry 1998, Fry 2008) making the identification of a catholic optimal temperature impossible. The ability of sporangia to germinate is also intrinsically dependent on the presence of free moisture on the host surface. Sporangia can disperse through the air, which constitutes an important step in the dispersal of the pathogen, but cannot survive for long periods of time (Fry 2008). Oospores can survive however in the soil for long (3-4 years) and they constitute a great source of recombination for the emergence of new strains (Shattock 1986, Judelson 1997, Judelson 1997, Agrios 2005).

In the first stage of infection, *P. infestans* requires living host cells. Spreading necrosis of the host tissue will follow indicating complete colonization and sporulation ensues. The zoospores will swim on the leaf surface, encyst and then germinate flagging the beginning of infection (Kamoun and Smart 2005). Production of a germ tube and an appresorium at the penetration site are the next steps for the establishment of the infection. Mycelia are then grown between the host cells and colonization continues by directing long curled haustoria structures inside the host cells (Agrios 2005). After a few days of extensive colonization, new sporangiophores will appear in the surface of leaves, producing sporangia, aerial dispersion of which can lead to a new infection (Agrios 2005).

1.4.1.3. Control of the disease

One of the very early efforts to foresee late blight outbursts was the use of forecasts, mostly based on the prognosis of temperature and humidity conditions that would potentially favor the pathogen (Fry 2009). However, this measure quickly proved to be problematic as the variation of the different *P. infestans* populations for environmental conditions was a major issue (Fry 2009). To date, a combination of sanitary measures, resistant varieties and well-timed chemical sprays is the only promising practice for a successful control of the disease. General practices include use of healthy collection of seed tubers, burning of plant debris before panting in Spring and use of strong herbicides to kill all sprouts or green growth (Agrios 2005).

The use of resistant varieties, although necessary, is not always easy or highly effective. One challenge is that usually the commercial potato varieties (the ones that are desirable by the consumers because of specific traits) are not highly resistant (Fry 2008). Breeders have to face an extra issue with potatoes being tetraploids and highly heterozygous, making it difficult to get the desirable phenotype (Fry 2008). Even so, the outcome of such a breeding project could be rejected by the consumers.

Several broad-spectrum and systemic fungicides are used for late blight control, however the amounts that are required are massive and also extremely costly. The use of metalaxyl/menefoxam was very effective for a while however new resistant strains emerged rendering the product ineffective (Fry 2008). An optimistic project would be the production of a *P. infestans* specific fungicide, however history proves that the adaptability of pathogens would quickly overcome that. Identification of new powerful *R* genes targeting crucial *P. infestans* effectors is still an open challenge.

1.4.2. *Phytophthora infestans* secreted effectors

Effectors secreted by the late-blight oomycete *P. infestans* can be divided into two classes, apoplastic or cytoplasmic, depending on their host cellular target. Apoplastic effectors are secreted in the plant extracellular space where they interact with and inhibit pathogenesis-related (PR) proteins, such as proteases, hydrolytic enzymes or glucanases. On the contrary, cytoplasmic effectors are translocated inside the host cell, through yet an unknown mechanism (most likely via the haustoria) (Kamoun 2007). Examples of apoplastic effectors in *P. infestans* are EPI1 and EPI10, two

serine proteases of the Kazal family that are known to interact with and inhibit the tomato pathogenesis-related protein P69B (Tian, Huitema et al. 2004). The presence of the following conserved motifs: RXLR or LFLAK at their N-terminal part can further classify cytoplasmic effectors in two groups. It has been suggested that the N-terminal RXLR motif could have a role in the translocation of the effector into the host cells, due to its similarity to a target signal from the malaria-causing protozoan *Plasmodium falciparum* (Kamoun 2006).

The LFLAK motif, also located N-terminally, is characteristic of the Crinkler (CRN) effector family and is also required for host translocation (Schornack, van Damme et al. 2010). An example of a CRN effector is CRN8, a *P. infestans* secreted kinase that undergoes auto-phosphorylation inside the host cell. The induction of CRN8 cell death does not depend directly on its kinase activity, but it is supposed to be a result of its phosphorylated state (van Damme, Bozkurt et al. 2012).

1.4.3. *Phytophthora infestans* effector AVR3a

One of the best-studied effectors of *P. infestans* is AVR3a, also known as Pex147 (*Phytophthora* extracellular protein 147). AVR3a is an RXLR cytoplasmic effector that was originally identified by searching expressed sequence tags (ESTs) for genes encoding secreted proteins, such as Pex147 and using association genetics (Armstrong, Whisson et al. 2005). AVR3a is polymorphic in *P. infestans* populations, with isolates carrying the AVR3a^{KI} variant ($K_{80}I_{103}$), AVR3a^{EM} ($E_{80}M_{103}$) or both. The two isoforms show perfect correlation with the recognition by the potato CNL protein, R3a; the AVR3a^{KI} variant associates with avirulence while the AVR3a^{EM} associates with virulence (Armstrong, Whisson et al. 2005). The *Avr3a* gene is expressed in sporangia, zoospores and germinating cysts, but it reaches its highest expression 48 hours after infection. *Avr3a* is flanked by two paralogs, *Pex147-2* and *Pex147-3*, but neither of them are recognised by R3a and their products are not expressed (Bos 2007). As previously mentioned, the RXLR motif bears similarity to a sequence [containing a host-targeting (HT) motif] in *P. falciparum* that is required for the export of parasite proteins to the erythrocyte (Bhattacharjee, Hiller et al. 2006). Interestingly, it has been demonstrated that the first 50 amino acids of AVR3a when fused to an ER-type signal sequence (pathogen proteins containing this signal are recruited to the parasite secretory pathway), are in fact exported to the host erythrocyte. This observation demonstrated that RXLR is able to function as a translocating signal and that this function is conserved across species

(Bhattacharjee, Hiller et al. 2006).

AVR3a has two isoforms as previously mentioned; AVR3a^{KI} and AVR3a^{EM}, which differ in only two amino acids in the mature protein (Armstrong, Whisson et al. 2005, Bos, Kanneganti et al. 2006). R3a triggers cell death in *N. benthamiana* only when co-expressed with the AVR3a^{KI} isoform but not with the AVR3a^{EM} (Armstrong, Whisson et al. 2005). As a consequence, R3a confers resistance only to *P. infestans* strains that carry *Avr3a^{KI}*. Little is known about the events occurring downstream the recognition of AVR3a by R3a. However, it has been shown that the recognition depends on SGT1, an ubiquitin ligase-associated protein and HSP90, a molecular chaperone involved in protein folding, stress responses, signal transduction and transcriptional regulation (Liu, Burch-Smith et al. 2004).

Distinct amino acids of AVR3a are known to define its virulence and avirulence activities and structural data revealed these activities are uncoupled (Bos, Kanneganti et al. 2006, Bos, Chaparro-Garcia et al. 2009). In plants lacking R3a, AVR3a^{KI} suppresses the cell death induced by the *Phytophthora* elicitin INF1 (Bos, Kanneganti et al. 2006). INF1 is a small, cysteine-rich protein (Kamoun 2006) secreted by *P. infestans* during infection. It induces cell death and systemic acquired resistance in *N. benthamiana* and is ubiquitous in all *Phytophthora* species. This elicitin is highly expressed during the necrotrophic stage of *P. infestans* infection (Kamoun, vanWest et al. 1997) and its silencing results in enhanced virulence towards *N. benthamiana* (Kamoun, van der Lee et al. 1998).

Bos *et al*. in another study showed that AVR3a mutants with loss-of-induction of R3a cell death were affected in protein stability, resulting in an inactive phenotype (Bos, Chaparro-Garcia et al. 2009). Mutations at the polymorphic position 80 in the AVR3a^{EM} background (AVR3a$^{X80/M103}$) had in most cases a gain-of-function phenotype, highlighting the importance of that residue in R3a-mediated recognition. Fifteen other mutations widespread along the protein also resulted in gain-of-function phenotypes, most of which were affected in exposed and charged residues. These results propose that protein-protein interactions are mediating the recognition by R3a, rather than AVR3a enzymatic actions (Bos, Chaparro-Garcia et al. 2009). Interestingly, out of the gain-of-function mutants screened, only one could suppress INF1 cell death like in the case of the wild type AVR3a^{KI} (Bos, Chaparro-Garcia et al. 2009). AVR3a residue 147 was shown to be indispensable for the INF1 cell death

suppression but not for the R3a-mediated cell death, suggesting that these two activities are disconnected (Bos, Chaparro-Garcia et al. 2009).

1.5. *Solanum pimpinellifolium* NLR protein I2

1.5.1. I2 is a member of the I2C tomato super cluster

I2 is a tomato immune receptor that belongs to the CNL class of NLR proteins. "I" as previously mentioned stands for immunity. This nomenclature was introduced by Bohn and Tucker for the first gene found in *S. pimpinellifolium* conferring resistance to *F. oxysporum f. sp. lycopersici*, which was therefore called '*I'* (Bohn and Tucker 1939). Ori et al, revealed that two members of a multigene family, designated *I2C* complex were at the same tomato locus, *SL8D*, as the *I2* gene and bear similarities to cytoplasmic NLR proteins (Ori, Eshed et al. 1997). The *I2* dominant gene is located in the long arm of chromosome 11 (Laterrot 1976) and was cloned using a selective restriction fragment amplification (AFLP) technique (Simons, Groenendijk et al. 1998). *I2* is a member of a tomato super cluster with six additional members, termed *I2C* genes (Simons, Groenendijk et al. 1998, Andolfo, Sanseverino et al. 2013). The super cluster can be further divided in two subclusters; the first one consisting of *I2C6, I2C5*, *I2C4* and a receptor like kinase (RLK-1), and the second including *I2*, *I2C2* (encoding the only other CNL protein in the cluster), *I2C3* and *I2C7* (Andolfo, Sanseverino et al. 2013). Ontology analysis revealed that *I2C5* was the ancestral gene in the I2C cluster (Andolfo, Sanseverino et al. 2013). Andolfo et al., hypothesized that *I2* must have originated from *I2C5*, after a reverse duplication, since these two genes share the highest pairwise identity in the cluster. Accordingly, *I2C2* originated by gene duplication of the functional *I2* gene while a reverse duplication of an *I2* and *I2C2* fragment resulted in *I2C7* and *I2C4* respectively (Andolfo, Sanseverino et al. 2013). The *I2* locus has been mapped close to *Ty-2* a resistance gene against tomato yellow leaf curl virus (TYLCY) (Ji, Scott et al. 2009).

The coding sequence of *I2* is intronless with an open reading frame (ORF) of 3801 base pairs (bp), encoding a polypeptide of 1266 amino acid residues with a relative molecular mass of 144.826 kD (Simons, Groenendijk et al. 1998). An intron of 86 bp is found just upstream the initiation codon of *I2* and two more of 399 bp and 82 bp respectively, after the stop codon (Simons, Groenendijk et al. 1998). *I2* differs from the other members of the *I2C* complex mainly due to deletions and insertions that are found in the *I2C* members. An interesting hypothesis is that ability of I2 to confer

resistance against race 2 of the wilt causing *F. oxysporum f. sp. lycopersici*, is due to three tandem copies of a 23-amino acid sequence found at the C-terminal end of its LRR domain, while different copy numbers are found in the other members of the I2C complex (Simons, Groenendijk et al. 1998).

1.5.2. I2 is a functional ATPase

Tameling *et al*., discovered that I2, like other NLR proteins, is a functional ATPase and requires a functional P-loop to exert this activity (Tameling, Elzinga et al. 2002). The presence of a divalent cation was also found to be indispensable for the ability of I2 to bind a nucleotide as it has been shown for other NLR proteins (Tameling, Elzinga et al. 2002). Mutations in conserved motifs of the I2 NB-ARC domain which affect ATP hydrolysis, resulted in an autoactive phenotype, showing cell death after transient expression in *N. benthamiana* and were also dependent on a functional P-loop (Tameling, Vossen et al. 2006). For example, point mutations in the highly conserved MHD motif in I2 resulted in either autoactive or loss-of-function phenotypes. This was also the case for other NLR proteins, indicating the importance of the MHD motif for R protein function (Takken, Albrecht et al. 2006, van Ooijen, Mayr et al. 2008). When those autoactivation-causing mutations were combined, the cell death produced was never as strong as the one caused by single mutations in the MHD motif (Van Ooijen, Mayr et al. 2008). This observation led to the assumption that an MHD mutant reaches the maximum activation potential, highlighting the importance of this motif as a negative regulator of NLR protein activity (Van Ooijen, Mayr et al. 2008).

1.5.3. I2 interacting proteins

The C-terminal LRR domain of NLR proteins is known to mediate both intra- and intermolecular interactions (Lukasik and Takken 2009). Common examples of intermolecular interactions are those with chaperones; the heat shock protein 90 (HSP90) is one of the best studied chaperones that interacts with the LRR domain of many NLR proteins, including I2, RPM1, N and Rx (Hubert, Tornero et al. 2003, Lu, Malcuit et al. 2003, Liu, Burch-Smith et al. 2004, van Bentem, Vossen et al. 2005). Proteins that depend on HSP90 for their stability and function are generally referred to as client proteins (Pearl and Prodromou 2006). Co-chaperones regulate the activity of HSP90 and in some cases these co-chaperones directly interact with the HSP90 client proteins as well. I2 is a client protein of HSP90 and the N-terminal part

of the I2 LRR region (LRRs 1-11) is the one required for the interaction (van Bentem, Vossen et al. 2005). A HSP90 co-chaperone, protein phosphatase 5 (PP5), was also found to interact with a region comprising the LRRs 12-22 of I2 (van Bentem, Vossen et al. 2005). Silencing of HSP90 abolishes the cell death mediated by an autoactive form of I2, while silencing of PP5 results in a less strong HR (van Bentem, Vossen et al. 2005, van Ooijen, Lukasik et al. 2010). Co-chaperones RAR1 and SGT1 also interact with HSP90 in plants (Hubert, Tornero et al. 2003, Takahashi, Casais et al. 2003, Liu, Burch-Smith et al. 2004). SGT1 silencing was shown to reduce the HR mediated by an autoactive version of I2, similarly to the HSP90 silencing (van Bentem, Vossen et al. 2005), however RAR1 silencing only weakly affected the cell death produced (van Bentem, Vossen et al. 2005, van Ooijen, Lukasik et al. 2010). Overall, the combined activities of the three HSP90 co-chaperones affect stability and accumulation and thus NLR protein-mediated signaling responses (Zhang, Dorey et al. 2004, Azevedo, Betsuyaku et al. 2006, Boter, Amigues et al. 2007).

Van Ooijen *et al*., also showed that I2 is a client protein of a heat shock protein 20 (HSP20) chaperone, RSI2, and further identified that this interaction required the LRRs 15-19 of I2 (van Ooijen, Lukasik et al. 2010). HSP20 chaperones are known to help in preventing degradation of unfolded proteins (Lee, Roseman et al. 1997, Lee and Vierling 2000). Interestingly, RSI2 silencing in *N. benthamiana* plants abolished the autoactive I2-mediated HR and also the accumulation of full length I2, while SGT1 or HSP90 silencing led to the accumulation of I2 breakdown products (van Ooijen, Lukasik et al. 2010). These results suggest that RSI2 is not only involved in the stabilization of I2 but is also required for its function (van Ooijen, Lukasik et al. 2010).

Two more proteins have been found to specifically interact with the N-terminal part of I2; *Sl*Formin, a member of the Formin gene family [actin-regulating proteins that accelerate actin polymerization (Faix and Grosse 2006)] and *Sl*Trax, a protein bearing homology to the human translin associated factor X [proteins involved in microtubule-depended mRNA trafficking and translational repression (Aoki, Ishida et al. 1997, Cho, Chennathukuzhi et al. 2004)] (Lukasik-Shreepaathy, Vossen et al. 2012). Different domains of I2 were shown to be required for the two interactors, with the CC domain to be sufficient for the *Sl*Formin interaction while both CC and NB domain were required for the interaction with *Sl*Trax (Lukasik-Shreepaathy, Vossen et al. 2012). Interestingly, the ability of I2 to interact with one or the other correlated

with the two conformations that I2 can have *in vivo* (Lukasik-Shreepaathy, Vossen et al. 2012): active and resting (Tameling, Vossen et al. 2006). Binding to the *Sl*Formin correlated with the active I2 state, while *Sl*Trax-binding was associated to the resting inactive state (Lukasik-Shreepaathy, Vossen et al. 2012). Silencing of both interactors did not affect however neither the I2-mediated disease resistance nor the *F. oxysporum f. sp. lycopersici* race 3 susceptibility in the bioassays performed. This is so far the first report where the ability of an NLR protein to interact with specific proteins is correlated with the proposed nucleotide-depended conformations (Lukasik-Shreepaathy, Vossen et al. 2012).

1.5.4. I2 spatial and subcellular localization

Macroscopical and histochemical analyses on tomato plants revealed that *I2* is expressed in cells surrounding xylem vessels, suggesting a co-localization with the site of fungal infection in resistant plants (Mes, van Doorn et al. 2000). The subcellular localization of I2 is currently unknown and its determination is hampered by the loss-of-function of I2 tagged versions and the lack of sensitive enough antibodies (Tameling, Elzinga et al. 2002, Takken and Rep 2010). Like most NLR proteins, I2 is predicted to be localized in the cytosol (Simons, Groenendijk et al. 1998). A truncated version of the I2 protein lacking the LRR domain localizes both in the nucleus and cytosol when transiently expressed in *N. benthamiana* (F. Takken unpublished data). As mentioned previously, nuclear localization of its cognate effector, AVR2, is required to activate I2, suggesting that AVR2 is recognised by I2 in the nucleus (Ma, Cornelissen et al. 2013). Simons *et al*. predicted a potential Nuclear Localization Signal motif (NLS) in the CC domain of I2 (Simons, Groenendijk et al. 1998). Taken together these observations suggest that I2 could be localized also in the nucleus (Ma, Cornelissen et al. 2013).

1.5.5. Mechanisms mediating the I2/AVR2 interaction

Our knowledge on the mechanisms underlying the I2/AVR2 interaction is yet very limited. Recognition of the xylem-colonizing fungus *F. oxysporum f. sp. lycopersici* by I2 does not typically involve the induction of HR. Instead, this defence response, which happens in the parenchyma cells adjacent to vessel elements, involves mainly callose deposition, the accumulation of phenolic compounds, and the formation of tyloses and gels produced in the infected cells (Beckman 2000, Takken and Rep 2010). Transient co-expression of I2 and AVR2 in *N. benthamiana* results in HR

(Houterman, Ma et al. 2009). Takken and Rep in a recent study showed that AVR2 is perceived inside the host cell by I2. This suggests that I2 is not likely to be guarding an extracellular target (Takken and Rep 2010). In race 3 of *F. oxysporum f. sp. lycopersici*, three AVR2 variants can be found, each possessing a single amino acid change (V41M, R45H, and R45P). These AVR2 variants are not recognised by I2, and do not alter the virulence function of the fungus (Houterman, Ma et al. 2009). These observations led Houterman *et al.* to conclude that I2 cannot just be detecting changes in a virulence target, because the interaction with the virulence target is unaffected by these mutations (Houterman, Ma et al. 2009). Consequently, there are the following possibilities: a direct interaction or the recognition of an AVR2-decoy or AVR2-target complex. So far, yeast two-hybrid and pull-down experiments have been unsuccessful in revealing a direct interaction between I2 and AVR2 (F. Takken and M. Rep, unpublished results). Future experiments to identify AVR2-interacting proteins could provide more insights into the mechanisms mediating this interaction.

1.5.6. I2 is targeted by miRNAs

Ectopic activation of immune responses, and particularly of *R* genes, could pose threats to plant fitness and survival (Tian, Traw et al. 2003). It was shown that *R*-gene expression is down-regulated by microRNAs (miRNAs), which cleave the *R*-gene mRNAs and generate trans-acting small interfering RNA (tasiRNAs). The tasiRNAs repress gene expression in plants through post-transcriptional gene silencing (Li, Pignatta et al. 2012). *I2* homologs in potato were found to be targeted by *miR482* (Li, Pignatta et al. 2012), while *miR6024* was the one targeting the *I2* family in tomato (Wei, Kuang et al. 2014). *miR6024* was also found in distant related genus (*Nicotiana* and *Solanum*) suggesting that it originated in the common ancestor of Solanaceae (Wei, Kuang et al. 2014). In the presence of pathogens however, *R* genes are free to function, due to the suppression of the silencing machinery of the host plants by pathogens (Li and Ding 2006, Weiberg, Wang et al. 2013).

1.6. *Solanum demissum* NLR protein R3a

Taking advantage of the high colinearity among the Solananaceae genomes, comparative genomics led to the identification of *R3a*, a gene analogue of *I2* (Huang, van der Vossen et al. 2005). *R3a* is a member of the *R3* locus on chromosome 11 in potato and has been shown to be constitutively expressed (Huang, van der Vossen et al. 2005). It is one of the very first late blight *R* genes to be used in potato

breeding, encoding an immune receptor responding to the AVR3a^{KI} variant and very weakly to AVR3a^{EM} from *P. infestans* (Armstrong, Whisson et al. 2005, Bos, Kanneganti et al. 2006, Morgan and Kamoun 2007, Birch, Boevink et al. 2008). *R3a* plants are susceptible to *P. infestans* strains homozygous for the *Avr3a^{EM}* allele (Armstrong, Whisson et al. 2005, Bos, Kanneganti et al. 2006, Bos, Chaparro-Garcia et al. 2009, Segretin, Pais et al. 2014).

A few recent studies have generated R3a mutants with expanded response specificities to the stealthy AVR3a^{EM} variant of *P. infestans* (Chapman, Stevens et al. 2014, Segretin, Pais et al. 2014). Segretin *et al.*, performed a random mutagenesis upon the full-length *R3a* coding sequence and identified eight single-site R3a+ mutant clones with expanded response specifies to the AVR3a^{EM} isoform (Segretin, Pais et al. 2014). In total, eight single-amino acid mutants were generated across the R3a protein, with six of them clustered in the LRR domain, one on the NB-ARC and one in the CC domain. All these mutants showed expanded response to the AVR3a^{EM} isoform while retaining the response to AVR3a^{KI}. Further, the mutants in the CC and NB-ARC domains showed gain of response to PcAVR3a4, an AVR3a homolog from *Phytophthora capsici* (Segretin, Pais et al. 2014). However, infection assays both in transient and with stable transgenic plants failed to show resistance to *P. infestans,* suggesting that HR and resistance may be uncoupled (Segretin, Pais et al. 2014). Using a similar approach, Chapman *et al.*, performed random mutagenesis, DNA shuffling and targeted mutagenesis upon *R3a*, to produce R3a* variants with a gain of recognition towards AVR3a^{EM} (Chapman, Stevens et al. 2014). Transient expression of the R3a* variants with AVR3a^{EM} yielded HR. R3a-triggered cell death has been previously suggested to be dependent on SGT1 and HSP90 (Bos, Kanneganti et al. 2006). Silencing of SGT1 and to a lesser extend HSP90, was shown to impair the cell death caused after co-expression of the R3a* mutants and AVR3a^{EM} (Chapman, Stevens et al. 2014). As was the case in the work by Segretin *et al*., stably transformed potato lines expressing those variants also failed to provide resistance to AVR3a^{EM}-carrying *P. infestans* strains (Chapman, Stevens et al. 2014). It is still possible that HR and resistance are two independent phenomena in this system, however it has also been suggested that the strength of the HR correlates with resistance levels to *P. infestans* (Vleeshouwers, van Dooijeweert et al. 2000).

There is no current evidence of a direct interaction between R3a and AVR3a^{KI}. However, Engelhardt *et al*., showed that AVR3a^{KI} relocalizes from the cytoplasm to

the late endosomes when co-expressed with R3a and that both proteins are in close proximity, while AVR3a^{EM} remains in the cytoplasm (Engelhardt, Boevink et al. 2012). The recent study by Chapman *et al*., further confirmed that both AVR3a variants travel from the cytoplasm to the late endosomes when co-expressed with the R3a* mutant clones (Chapman, Stevens et al. 2014). Taking into account that this relocalization of both R3a and AVR3a^{KI} has been shown to be a prerequisite for the development of cell death (Engelhardt, Boevink et al. 2012), it is suggested that the expanded recognition of AVR3a^{EM} by R3a* mutants resembles the mechanism underlying R3a response to AVR3a^{KI} (Chapman, Stevens et al. 2014).

1.7. Aims of the thesis

Plants are exposed to a diverse range of pathogenic organisms such as viruses, bacteria, fungi, oomycetes, nematodes, insects and other parasitic plants (Agrios 2005, Westwood, Yoder et al. 2010). Therefore, they have evolved a sophisticated multi-layered immune system, as diverse as secondary metabolites and intracellular immune receptors, in order to protect themselves from pathogenic attacks.

As previously described, the interaction between plants and pathogens only rarely results in the development of disease symptoms, as most plants are resistant to most pathogens, also known as non-hosts of the pathogen (Jones and Dangl 2006). Some pathogens have a broad range of hosts, while others can infect only a limited number of plants and many times the success of the infection relies on the certain types of tissues, organs and/or age of the plant under attack (Agrios 2005). The ability of a certain pathogen to cause disease on different plant species depends on the different repertoire of resistance genes and molecular mechanisms mediating each host-pathogen interaction (Beattie 2008).

In this study, I focused on two important mechanisms in the plant defence system (Fig. 1.4); the use of phytoalexins, and the deployment of intracellular immune receptors with expanded response specificities as two approaches to engineer disease resistance to filamentous pathogens. The main objectives of this thesis were 1) to examine whether plant-derived antimicrobial compounds can determine host specificity in plant-microbe interactions and 2) to provide insights on how synthetically engineered immune receptors could open up new possibilities for breeding crop plants with a broad spectrum of disease resistance.

In chapter 3, my objective was to examine whether the differential effect of the pepper phytoalexin capsidiol towards two *Phytophthora* species (*P. infestans* and *P. capsici*) is consistent with their host range. Previous studies back in the 1970s had monitored the ability of capsidiol to differentially affect growth of these two *Phytophthora* species (Jones, Unwin et al. 1975, Ward 1976, Egea, Alcazar et al. 1996). Using highly pure capsidiol preparations obtained from an engineered yeast system and taking advantage of transgenic *Phytophthora* strains expressing fluorescent markers, the differential effect to *P. infestans* and *P. capsici* was addressed.

In chapters 4 and 5, my objective was to investigate whether gain-of-response mutations are transferable between orthologous *R* genes. *R3a* is a potato *R* gene conferring resistance against *P. infestans* strains that carry *Avr3a*^{KI} but cannot defeat *P. infestans* homozygous for *Avr3a*^{EM} (Armstrong, Whisson et al. 2005, Bos, Kanneganti et al. 2006, Bos, Chaparro-Garcia et al. 2009, Segretin, Pais et al. 2014). The R3a immune receptor responds strongly to the *P. infestans* RXLR-type host-translocated AVR3a^{KI} but weakly to AVR3a^{EM} (Armstrong, Whisson et al. 2005, Bos, Kanneganti et al. 2006). In a previous study, Segretin *et al*., discovered eight R3a+ mutant clones, with single-amino acid substitutions widespread in the R3a protein, with expanded response specificities to the AVR3a^{EM} variant from *P. infestans* and to another AVR3a homolog from *P. capsici* (Segretin, Pais et al. 2014). To determine the extent to which these mutations could also extend the response spectrum of I2, an R3a homolog in tomato, I2 mutants carrying the equivalent R3a+ mutations were generated. I2 is known to respond to the *F. oxysporum f. sp. lycopersici* effector AVR2 found in race 2 of the pathogen (Simons, Groenendijk et al. 1998, Houterman, Ma et al. 2009). Single-amino acid substitutions in AVR2 present in race 3 abolish the recognition by I2 (Houterman, Ma et al. 2009). I evaluated the response of the I2 wild-type and I2 mutant proteins generated against both AVR3a and AVR2 effectors from *P. infestans* and *F. oxysporum f. sp. lycopersici* respectively. I also examined the degree to which tomato lines carrying *I2* gain-of-response mutants can provide resistance against *P. infestans* and *F. oxysporum f. sp. lycopersici*.

In chapter 6, I examined the possibility of the *I2 locus* being a contributing factor to the resistance of tomato cultivar PVO 43143 against *P. infestans* NL00228 strain carrying *Avr3a*^{KI}.

As previously discussed, plant diseases constitute a never-ending threat for modern human life making the need for sustainable crop disease resistance increasingly urgent (Pennisi 2010, Fisher, Henk et al. 2012). So far, sustainable crop improvement approaches based on the use of single or combinations of NLR receptors are easily overcome by the rapidly evolving plant pathogens (Cook 2000, Michelmore, Christopoulou et al. 2013, Jones, Witek et al. 2014). Overall, this study addressed how basic research on two of the various mechanisms mediating plant-microbe interactions can be translated to targeted disease control strategies in the field. The role of phytoalexins as potential determinants of host specificity and the use of synthetic intracellular immune receptors with expanded response specificities

against divergent pathogens were assayed. The knowledge generated created novel opportunities for engineering disease resistance in agriculture.

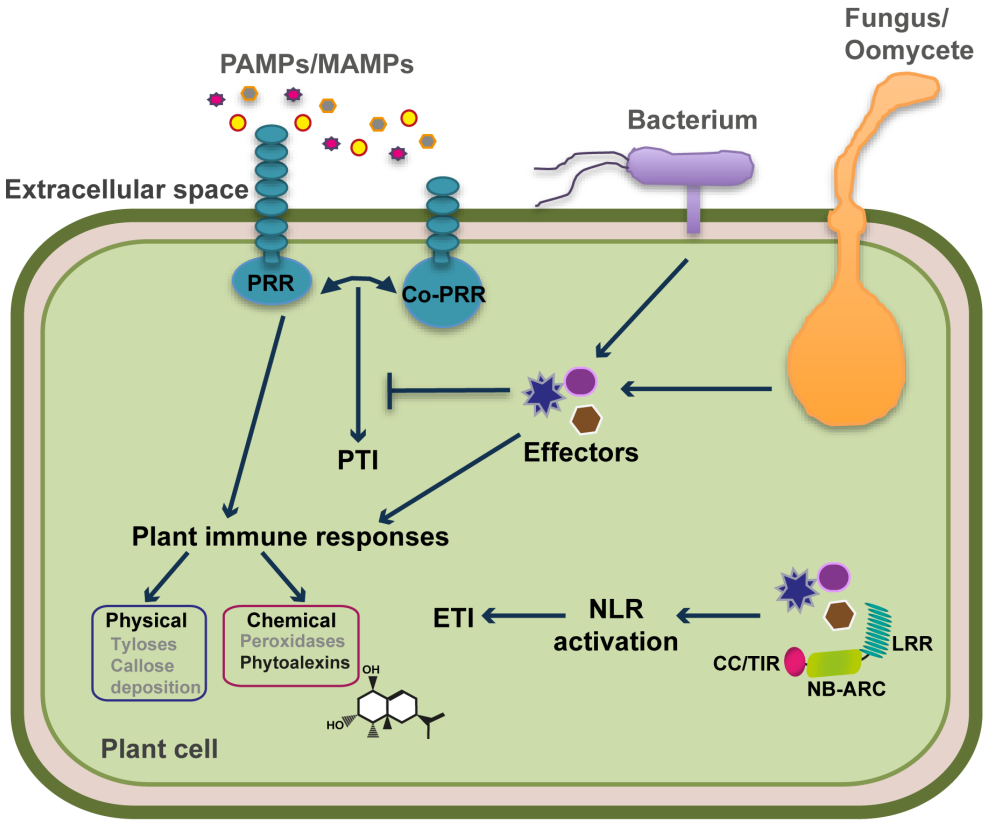

Figure 1.4: Schematic representation of the plant immune system
Plants perceive PAMPs/MAMPs secreted by pathogens of all lifestyles, using extracellular (PRRs) receptors and initiate the PRR-mediated immunity (PTI). Effectors are secreted by the pathogen both to the cell apoplast to block PTI and to the cell interior. Intracellular NB-ARC-LRR (NLR) receptors sense the effectors leading to effector-triggered immunity (ETI). All these processes activate immune responses, which arrest pathogen growth and lead to disease resistance. Adapted by Jeffery L. Dangl, Diana Horvath *et al.*, 2013; Yadeta and Thomma, 2013 (Dangl, Horvath et al. 2013, Yadeta and Thomma 2013).

CHAPTER 2: Materials and Methods

2.1. Yeast growth (by Dr. Dave Haart)

The yeast strain EPY300 was engineered to express the capsidiol biosynthetic pathway (Trinh-Don, MacNevin et al. 2012) and was used to produce capsidiol by fermentation. In brief a starter culture (around 20 ml) was prepared and inoculated into a 5 L-bioreactor containing rich media to full capacity. The media consisted in 1% Bacto yeast extract, 2% Bacto peptone (BD Biosciences, Oxford, UK), 1.8% galactose, 0.2% glucose, 150 mg/L methionine and 80 mg/L adenine hemisulphate (Sigma Aldrich Co Lt, Dorset, UK). The bioreactor was set to 30°C, with constant stirring [180 rounds per minute (rpm)] and aeration at 4 L/minute. After 96 hours (h) both stirring and aeration were stopped, and the temperature was reduced to 5°C. Once yeast cells had settled (24-48 h), the media containing the yeast-produced capsidiol was decanted for extraction.

2.2. Capsidiol extraction and purification (by Dr. Dave Haart)

Capsidiol was isolated by dichloromethane extractions of the media. The combined extracts (eg 5 L total volume) were dried, filtered and evaporated to dryness using a rotary evaporator. The crude extract (around 1,500 mg) was re-dissolved in a minimum volume of 1:1 hexane/ethyl acetate (EA) and applied to a glass sinter funnel 40×40 mm containing silica gel (previously equilibrated with hexane), and connected to an on-house pump. Purification of capsidiol was accomplished by vacuum filtration using a gradient (0–66%) of ethyl acetate/hexane. Each fraction (25 ml) was assessed for capsidiol (Retardation factor, R_f = 0. 363) content by analytical Thin Layer Chromatography (TLC) (Merck silica gel 60 (F_{254}) 7×7 cm aluminium-coated plates), using 66% ethyl acetate/hexane as the developing solvent and visualization with solution cerium ammonium molybdate solution. Fractions judged to contain exclusively capsidiol were combined together and evaporated under reduced pressure. Further (and final) purification of this material was effected by preparative TLC (Merck silica gel 60 (F_{254}) 20×20 cm glass-coated plates) previously sprayed with a 0.5% berberine chloride ethanolic solution (non-destructive visualization of capsidiol by UV at 365 nm). Briefly, the silica gel TLC plates were divided horizontally in two halves by removing a thing line of silica coating, and the sample (containing around 25 mg of product) was placed in a continuous line 1 cm above the bottom of the plate. After loading, the band was ‘focused/concentrated’ twice by

standing the plate in a tank containing pure EA until the solvent front reached 2 cm. After air-drying, the plate was finally developed using 66% ethyl acetate/hexane. The band corresponding to capsidiol (R_f = 0.363) after visualization by UV light (365 nm) was marked and scraped off avoiding the very bottom of the band, which was shown to contain an as yet unidentified more polar terpene compound. The silica gel scrapings were loaded into a pipette-column and washed using ethyl acetate.

Typically we found that 5 L fermentation yielded around 1,500 mg of crude extract, which is reduced to about 700 mg after silica column, to produce 300–400 mg of essentially pure capsidiol (>97% by 1H-NMR) after preparative TLC.

2.3. Identification of capsidiol (by Dr. Dave Haart)

Identification and purity estimation of the yeast-produced capsidiol was carried out by Nuclear magnetic resonance spectroscopy (NMR) and combined liquid chromatography-mass spectrometry (LC/MS) following the method of Literakova *et al*. (Literakova, Lochman et al. 2010) with slight modifications. In brief, we used an isocratic 75% methanol: water solvent mixture, in a C8 reverse column (Agilent 1100 MSD) with negative mode TIC (Total Ion Chromatogram) and SIM (Selected Ion Monitoring) at m/z 201, 219, 259.
In figure 3.1 (chapter 3) all the peaks carry information about each hyrdrogen atom in the molecule and each part of the spectra informs you about the unique environment of that proton. Since neighbouring protons ‘communicate’ with each other, they will split the spectrum into many peaks. The splitting effect and the position along the spectrum (ppm) are used to decode the identity of the compound. In this case, the observed splitting pattern confirms the structure of capsidiol. The inset shows a small yet quantifiable amount of contaminant.

2.4. Bacterial strains

Agrobacterium tumefaciens strain GV3101 (Hellens, Mullineaux et al. 2000), *Escherichia coli* TOP10 (Invitrogen) and DH5α (Life Technologies) were used in molecular cloning experiments and library construction. These strains were cultured as previously described (Sambrook and Russell 2001), at 28°C (for GV3101) or 37°C (for TOP10) in Luria-Bertani (LB) media supplemented with the appropriate antibiotics.

A. tumefaciens strain GV3101 was used for transient transformation of *Nicotiana benthamiana*. *A. tumefaciens* AGL1 (Lazo, Stein et al. 1991) was used for transient transformation of *Solanum lycopersicum* accession OH7814-SGN758 (David Francis, United States, Ohio state, Humid).

2.5. *Phytophthora* strains

In **Chapter 3** the following Phytophthora isolates were used:
P. infestans isolates: 88069 (van West, de Jong et al. 1998), 88069td (Whisson, Boevink et al. 2007, Bozkurt, Schornack et al. 2011), T30-4 (Haas, Kamoun et al. 2009), 06_3928A (Cooke, Cano et al. 2012), VK98014 (Li, van der Lee et al. 2012), EC1-3527, EC1-3626, 2004_7804B (Cooke, Cano et al. 2012), 2011_8410B (Cooke, Cano et al. 2012) and NL08645 (Haas, Kamoun et al. 2009) (Table 2.5.1)
P. capsici isolates: *P. capsici* LT1534 and *P. capsici* LT1534 tdtom (Jupe, Stam et al. 2013) strains.

Td and tdtom strains are transgenic strains expressing the red fluorescent marker tandem dimer RFP, known as tdTomato.

Table 2.5.1: Provenance of *Phytophthora infestans* samples

Isolate ID	Country of origin	Collection year	Host species	Reference
88069	The Netherlands	1988	*Solanum lycopersicum*	(van West, de Jong et al. 1998)
88069td				(Whisson, Boevink et al. 2007)
T30-4				(Haas, Kamoun et al. 2009)
06_3928A	United Kingdom	2006	*Solanum tuberosum*	(Cooke, Cano et al. 2012)
VK98014	The Netherlands	1998	*Solanum tuberosum*	(Li, van der Lee et al. 2012)
EC13527	Ecuador	2002	*Solanum andreanum*	World Oomycete Genetic Resource Collection at UC Riverside, CA
EC13626	Ecuador	2003	*Solanum tuberosum*	World Oomycete Genetic Resource Collection at UC Riverside, CA
2004_7804B	Scotland	2004	*Solanum tuberosum*	(Cooke, Cano et al. 2012)

2011_8410B	United Kingdom	2011	*Solanum tuberosum*	(Cooke, Cano et al. 2012)
NL08645	The Netherlands	2008	*Solanum venturii*	(Li, van der Lee et al. 2012)

In **Chapter 4** the following isolates were used in the *P. infestans* infection assays: NL00228 (Zhu, Li et al. 2012), 88069 (van West, de Jong et al. 1998) and 88069td (Whisson, Boevink et al. 2007). *P. infestans* strains were grown on rye sucrose agar as previously described at 18°C in the dark.

2.5.1. *Phytophthora* infection assays

Nicotiana benthamiana plants (four- to five-week-old) were transiently transformed with *A. tumefaciens* expressing the construct of interest and one day post-infiltration leaves were detached and placed on a clear tray under high humidity conditions. *P. infestans* strains were grown on rye sucrose agar (RSA) at 18°C in the dark and zoospores suspensions were collected by 7 to 17-day-old plates by flooding the agar plates with chilled water and incubated for 3 hours at 4°C. Zoospores concentration was measured with a hemacytometer and adjusted to 100 zoospores/ul. Leaves were droplet (10 ul, 4 spots per leave) inoculated with the zoospore suspension on the abaxial side and incubated at 16-18°C. Disease lesions were measured (in mm) starting at 2 days post inoculation (dpi) until 6 or 7 dpi. Quantification of the total area of infection was carried out using the Image J software (Schneider, Rasband et al. 2012) described below. Disease scoring data was subjected to statistical analysis using one-way analysis of variance (ANOVA) which was followed by Fisher's Least Significant Difference (LSD) procedure as a Multiple Range test with a 95% confidence interval. The analysis was performed with Statgraphics software package.

2.5.2. Plug and zoospore inhibition assays

Phytophthora strains were grown on rye sucrose agar as previously described at 20°C in the dark (*P. infestans*) or on V8 vegetable juice agar plates (*P. capsici*) at 25°C and illumination. For the plug inhibition assays, 5 mm diameter plugs were taken from two- to three-week-old *Phytophthora* plates and placed in the wells of a 24-well plate, previously filled with 1 ml of Plich medium. Washes were applied to the plates containing the *Phytophthora* plugs by carefully removing the Plich media from the wells, adding distilled water, expose for 1 to 2 minutes and remove. This step

was repeated at least 2 times. Finally 1 ml of fresh Plich media was added and plates were kept at 20°C in the dark (*P. infestans*) and 25°C and illumination for *P. capsici*.

For the zoospores inhibition assays, spores were harvested as previously described for *P. infestans.* For *P. capsici* zoospore suspensions were collected by 7 to 17-day-old plates by flooding the agar plates with chilled water and incubated for 1 hour at room temperature and illumination. Zoospore suspension of both Phytophthora species were diluted to 50,000 spores/ml. Droplets of 10 µl were added to each well of a 96-well plate, previously filled with 250 µl of Plich medium, covered with a plastic lid and sealed with Parafilm. Plates were kept at 20°C in the dark and 25°C and illumination for *P. infestans* and *P. capsici* respectively over 10 days. At regular intervals, mycelial growth was monitored using a Varioscan Flash Multimode Reader (Thermo Scientific) by measuring light absorption at OD600 as well as emission of red fluorescence (excitation at 360 nm, emission at 465 nm).

2.6. Light microscopy

Mycelia grown in 96-well microtitre plates (of the zoospore inhibition assays-chapter 3) were imaged using a Zeiss Axiovert 25 microscope in transmission light mode with 10x magnification. Pictures were taken using a Cannon E0S-D30 camera.

Mycelial growth of *P. infestans* 88069td strain in *N. benthamiana* leaves (Appendix 2) was visualized using a Leica Stereomicroscope (Leica Microsystems CMS GmbH) mounted with a CCD (Charged Coupled Device) camera under UV (Ultra Violet) LED (Light Emitting Diode) illumination and filter settings for DsRed. In this case images were processed as described below (In collaboration with Dr. Ji Zhou, at The Sainsbury Laboratory, TSL).

2.7. Infect measure analysis

2.7.1. Image J analysis

The Image J analysis software was used to quantify *P. infestans* infection assays carried upon *N. benthamiana* and *S. lycopersicum* leaves. Briefly, the following analysis was carried out. Raw data pictures were imported to Image J and adjusted for brightness and/or contrast. Measurement scale was set using a defined distance

inside the raw data figure (ruler usually included in every raw data figure). Using the free area or the circle selection tool from the toolbox, every infection spot was circulated. Following the “analysis” and “measure” selection, a spreadsheet was created with data points correlating to the infected area (in mm^2) of each individual infection spot selected.

2.7.2. Measure analysis (by Dr. Ji Zhou)

Mycelial growth of *P. infestans* 88069td strain was visualized using a Leica Stereomicroscope (Leica Microsystems CMS GmbH) mounted with a CCD camera under UV LED illumination and filter settings for DsRed. In this case, the lesion area was monitored using bioimage analysis software. The software plugin was designed so that it could batch process a series of TIFF microscope images based on a number of core ImageJ/FIJI libraries. The algorithm extracted the intensity plane from the TIFF images, based on which masking methods were applied to identify regions with high intensity and contrast values. Tailored feature selection functions were implemented to detect objects such as the scale (pixel to μm) and infection areas on every image. Finally, a 2D convex hull method was applied to measure recognised infection areas and score the size/perimeter of the infection (in both pixel and μm).

The algorithm reads a series of TIFF files into the AcapellaTM image analysis platform. TIFF images are split into three planes – hue, saturation, and intensity value. Only intensity plane is used in the image analysis. Whilst splitting the image, a convolution method is used to harmonize intensity values. Image masks are applied to identify regions with high intensity/contrast values – generated masks are randomly coloured and treated as a set of image objects. A filtering system is used to detect the scale (pixel to um) according to its unique intensity, contrast, and width/length ratio. Another filtering system is used to filter out objects such as letters and experiment errors (inappropriate intensity, size, contrast, and location (attached to the image border). After screening, only genuine infected areas are retained.

Since the aim was to measure the area and the perimeter of the infected area, which contains many dark regions, we could not rely on measurement based on bright pixels. Hence, to perform the calculation, the algorithm firstly splits the detected infected areas into many smaller objects. Based on the split objects, the algorithm detects the center as well as finds the most left/top/bottom/right pixels of the

infection areas. Based on coordinates of those most left/top/bottom/right pixels, minor radius and major radius of the infection areas are calculated and refined. To calculate the area and the perimeter of the infected regions a calculation is based on the calculated minor radius and major radius. For example, the formula used for computing area is:

Area=παb (*α*, major radius; b, minor radius)

The formula used for computing perimeter is:

$$C \approx \pi \left[3(a+b) - \sqrt{(3a+b)(a+3b)}\right] = \pi \left[3(a+b) - \sqrt{10ab + 3(a^2+b^2)}\right]$$

(*α*, major radius; b, minor radius)

2.8. *Fusarium oxysporum f. sp. lycopersici* strains and growth conditions

In **Chapter 5**, the following *F. oxysporum f. sp. lycopersici* isolates were used: Fol007, Fol029, Fol035 and Fol067 (Table 2.8.1).
All *F. oxysporum f. sp. lycopersici* isolates were grown on potato dextrose agar plates in the dark at 22°C.

Table 2.8.1: Provenance of *Fusarium oxysporum f. sp. lycopersici* strains

Strain number	Origin	Race	AVR2 mutation	Reference
Fol007	France	2		(Houterman, Ma et al. 2009)
Fol029	USA (Florida)	3	R45H	(Houterman, Ma et al. 2009)
Fol035		3	R46P	(Houterman, Ma et al. 2009)
Fol067	USA (Arkansas)	3	V41M	(Houterman, Ma et al. 2009)

2.8.1. *Fusarium oxysporum f. sp. lycopersici* infection assays

To test virulence of *F. oxysporum f. sp. lycopersici* isolates on tomato lines the root dip inoculation method was used (F.L. 1939). Briefly, spores were collected from 5-

day-old cultures in potato dextrose broth, filtered using autoclaved muslin (E. Russum & Sons LTD) and used for root inoculation of 10 to 12-day old tomato plants at a spore density of 10^7 ml^{-1}. The seedlings were then potted individually. Three weeks after inoculation disease index was scored based on the plant weight above cotyledons. Disease scoring data was subjected to statistical analysis using one-way ANOVA and Fisher's LSD test with a 95% confidence interval.

2.9. Plant material

2.9.1. *Nicotiana benthamiana*

N. benthamiana plants were grown under controlled environmental conditions at an average temperature of 23°C, with 45-65% humidity in long day conditions (16 hours of light).

2.9.2. *Solanum lycopersicum*

The following *S. lycopersicum* cultivars were used (Table 2.10.1). Tomato plants were grown at an average temperature of 23°C in long day conditions (16 hours of light).

Table 2.9.1: Provenance of the tomato varieties used in this study

Tomato variety	Alternative name	Sol genomics ID	Genotype
MoneyMaker	-	SGN950	*i2i2*
HEINZ H1706	LA4345	SGN676	*i2i2*
MoneyMaker CF0 *	-	-	*i2i2*
PVO 43143	Motelle (LA2823)	SGN3796	*I2I2*
OH7816	Ohio 7816	SGN758	*i2i2*

(*): This MoneyMaker line carrying no detectable resistance genes for *Cladosporium fulvum* (Cf0) was obtained from R. Oliver (University of East Anglia, Norwich, UK)

2.9.2.1. *Solanum lycopersicum* transgenic plants

S. lycopersicum wild type plants were transformed with *A. tumefaciens* AGL1 carrying the gene of interest (Table 2.10.2) and transgenic plants were regenerated

according to the method of Fillatti, Kiser *et al*. 1987 for tomato (Fillatti, Kiser et al. 1987) by Mr. Matthew Smoker. Primary transformants (T0) were selected in Murashige-Skoog salts (MS) media containing the appropriate antibiotic for selection (kanamycin). The tomato plants were grown in Levington's M3 compost (Levington Horticulture Ltd., Fisons, Ipswich, UK) in a greenhouse with an average temperature between 22°C and 27°C in the light and 12°C to 16°C in the dark. Sixteen hours of light were supplied at a photon flux density of 300 to 650 uE m^{-2} sec^{-1} at the plant surface, and the relative humidity was between 70 and 80%.

Table 2.9.2: *Solanum lycopersicum* transgenic tomato lines used in this study

Line ID	Construct	Transformation ID	Chapter
B8	35S::I2	SLSK139	Ch. 4, 5
B14	35S::I2	SLSK139	Ch. 4, 5
A36	35S::*I2*^{I141L}	SLSK143	Ch. 4, 5
B2	35S::*I2*^{I141L}	SLSK143	Ch. 4, 5
A16	35S::*I2*^{I141V}	SLSK144	Ch. 4, 5
A49	35S::*I2*^{I141V}	SLSK144	Ch. 4, 5
B15	35S::*I2*^{N330K}	SLSK141	Ch. 4, 5
B16	35S::*I2*^{N330K}	SLSK141	Ch. 4, 5
B25	35S::*I2*^{C967R}	SLSK140	Ch. 4,5
B26	35S::*I2*^{C967R}	SLSK140	Ch. 4,5
EV1	pk7WG2	SLSK145	Ch. 4,5
EV2	pk7WG2	SLSK145	Ch. 4,5

2.10. *Agrobacterium*-mediated transient expression

Agrobacterium cells carrying the desired insert were grown over night at 28°C in Luria - Bertani (LB) medium with the appropriate antibiotics. Cells were harvested by centrifugation at 4500 rpm and resuspended in MES + $MgCl_2$ medium to a final OD600mm of 0.3 or 0.6 (depending on the experiment). Acetosyringone was added to the resuspended cultures at a final concentration of 150 uM and left at room temperature for 2 hours before infiltration. Infiltrations on *N. benthamiana* were

mostly carried out using four- to five-week old plants on the abaxial side of the plant using a 1 ml syringe without needle.

2.11. Hypersensitive response assays

Wild-type and mutant I2 and R3a clones were co-agroinfiltrated in *N. benthamiana* leaves to compare their relative response to different effector proteins. Each combination of wild-type or mutant R protein and effector protein (or negative control) was infiltrated as 16 to 20 replicates per experiment and every experiment was repeated at least 3 times. Briefly, 10 ml-LB media cultures with antibiotics [rifampicin at 50 mg/liter, gentamicin at 20 mg/liter, and spectinomycin at 50 mg/liter (I2 and AVR2 constructs) or ampicillin at 100 mg/ liter (R3a and AVR3a constructs)] were inoculated with the library clones and grown at 28°C for 48 hours (to reach an optical density at 600 nm [OD600] of 1 to 1.2). Cultures were pelleted by centrifugation (5 minutes at 3,500 rpm and 15°C) and resuspended with infiltration buffer to a final OD600 of 0.1. In all the agroinfiltration experiments pGR106-FLAG-AVR3a^{KI}, pGR106-FLAG-AVR3a^{EM} (amino acids 23 to 147) constructs were used to express AVR3a mature proteins (without signal peptide) (Armstrong, Whisson et al. 2005, Bos, Kanneganti et al. 2006, Bos 2007, Bos, Chaparro-Garcia et al. 2009). *A. tumefaciens* GV3101 transformed with pGR106-ΔGFP [containing a truncated version of GFP as described by Bos and colleagues (Bos, Kanneganti et al. 2006)] was grown as the AVR3a clones. In addition, CTAPi-AVR2, CTAPi-AVR2$^{V>M}$, CTAPi-AVR2$^{R>P}$, CTAPi-AVR2$^{R>H}$ (Houterman, Ma et al. 2009) were used to express AVR2 mature proteins (without signal peptide). *A. tumefaciens* GV3101 transformed with CTAPi (Rohila, Chen et al. 2004) was grown as the AVR2 clones. For transient co-expression of *R* gene clones and effector clones, the cells resuspended in infiltration buffer were mixed to have a final OD600 of 0.1 (R clones) and 0.5 (effector clones). Agroinfiltration experiments were performed on four-week-old *N. benthamiana* plants. Plants were grown and maintained throughout the experiments in a controlled environment room with a temperature of 22 to 25°C and high light intensity. HR phenotype development was monitored from 3 to 7 dpi according to an arbitrary scale from 0 (no HR phenotype observed) to 3 (confluent necrosis on the infiltrated area) (Appendix 2, Fig. A2.1). The arbitrary scale was based on a previously established HR scale (Segretin, Pais et al. 2014), to measure induction of HR (Bos, Kanneganti et al. 2006).

The HR-associated autofluorescence in agroinfiltrated *N. benthamiana* leaves was monitored as follows: A Nikon D4 with a 60 mm macro lens (International Organization of Standardization-ISO set to 1250 or 1600) equipped with a yellow filter (Kodak Wratten No. 8). UV (Ultra Violet) Blak-Ray® longwave (365 nm) lamps B-100AP were spotlights and were moved around the subject during the exposure to give a more even illumination. The autofluorescence under exposure to UV light is associated with accumulation of phenolic compounds (Klement, Rudolph et al. 1990).

Statistical analysis for all the HR experiments was carried out by calculating the standard deviation of the values obtained, to reveal how variable the HR response is in this system, as has previously been shown in the literature (Bos, Kanneganti et al. 2006, Segretin, Pais et al. 2014).

2.12. DNA and cloning methods

2.12.1. DNA methods

2.12.1.1. Colony PCR

A PCR mix contained 1X buffer (Thermo Scientific), DNA template, 0.5 uM primers, 0.2 mM dNTPs, 1 unit Dream Taq polymerase (Thermo Scientific), in a total reaction volume of 12 ul. Picked colonies with a 10 ul sterile tip (DNA template). PCR cycling conditions were as follows: Initial heating at 95°C for 2 minutes, then the initial denaturation, at 95°C for 2 minutes (cycle 1x), denaturation at 95°C for 30 seconds, annealing at 55°C for 30 seconds (25-30X cycles), extension at 72°C for 1 minute per kb, and a final extension at 72°C for 10 minutes (1x cycle).

2.12.1.2. Proofreading PCR reaction (for cloning)

When high fidelity was required the reaction conditions were as follows; PCR mix contained 1X Phusion buffer (New England Biolabs), cDNA template (5 ul), 3% DMSO, 0.2 mM dNTPs mix, 0.5 uM primers, 1 unit Phusion polymerase (New England Biolabs) in a total reaction volume of 50 ul.

PCR cycling conditions were as follows: Initial denaturation, at 98°C for 3 minutes (cycle 1x), denaturation at 98°C for 15 seconds, annealing at 57-70°C for 15

seconds (30-34X cycles), extension at 72°C for 1 minute per kb, and a final extension at 72°C for 10 minutes (1x cycle).

For targeted mutagenesis the previous reaction conditions were used except that 1 ul of plasmid was used as a template. The PCR product was digested with 2 units of DpnI (New England Biolabs) in 1X buffer. Reactions were incubated at 37°C overnight and 5 ul were transformed into E. coli chemical competent cells TOP10 (Invitrogen).

2.12.1.3. Sequence analysis

Plasmid DNA was isolated sequenced by GATC Sequencing Service (Constance, Germany) using several primers to allow full coverage. Base-calling and quality values were obtained using the Phred algorithm (Ewing, Hillier et al. 1998). Sequences were analyzed with MacVector 12.6 (Olson 1994).

2.12.1.4. Gel electrophoresis

Electrophoresis in a horizontal agarose gel was used to analyze PCR products. Gels contained 1X TAE (40 mM Tris, 20 mM NaAc, 1 mM EDTA, pH 7.9) plus 1 ug/ml ethidium bromide (SIGMA) for visualization purposes. Concentration of agarose was 1-1.5% (w/v). DNA samples had 0.1 volume of 6x loading buffer (Fermentas). Gels were run in 1X TAE at 100 V for 20 to 40 minutes and visualized on a short wavelength UV transilluminator (BioRad).

2.12.1.5. DNA Gel purification

DNA was visualized on a long wavelength UV transilluminator and the DNA fragment was excised using a razor blade and purified using the QIAquick spin columns.

2.12.1.6. Miniprep preparation

Liquid cultures of positive individual colonies (identified by PCR) were started and incubated over night in 10 ml of LB plus the appropriate selective antibiotics. The overnight cultures were spun down at 4500 rpm for 10 minutes and the plasmid was extracted from the bacterial pellet using QIAgen spin miniprep kit (Qiagen).

2.12.1.7. Generation of the pENTR clone for Gateway cloning

The DNA fragment was amplified using primers containing CACC and ligated pENTR - TOPO vector (Invitrogen). Reaction proceeded for 30 minutes at room temperature. The reaction was transformed into Escherichia coli chemical competent cells TOP10 (Invitrogen).

2.12.1.8. Cloning using Gateway LR reaction

The LR reaction was set up using the destination vectors series of Gateway (Karimi, Inze et al. 2002). The reaction mix had 100 ng of the pENTR vector and 300 ng of the destination vector, $T_{10}E_1$ buffer pH 8.0 to a final volume of 4 ul, 2 ul LR Clonase II mix (Invitrogen) and incubated at 25°C for 2 hours. The reaction was stopped by adding 1 ul of proteinase K (Invitrogen) and incubated for 10 minutes at 37°C. The reaction was transformed into *E. coli* chemical competent cells TOP10 (Invitrogen).

2.12.1.9. Digestion reaction

Clean PCR product (35 ul) was mixed with 2 units of enzyme, 8 ul MilliQ water and 1X of the appropriate buffer followed by incubation at 37°C for 2-3 hours. Digestion product was cleaned using the QIAgen columns and eluted in 30 ul MilliQ water.

2.12.1.10. Ligation reaction

Digested PCR product was mixed with digested destination vector as follows. 1 ul vector, 7 ul insert, 1X ligase buffer and 1 unit ligase (T4) (Promega). The reaction was left overnight at room temperature. The following day ligation product was transformed into DH5α and GV3101 competent cells for sequencing.

2.12.1.11. Chemically competent cells transformation

Ligation product (6 ul) was transferred into 50 ul TOP 10 (Invitrogen) E. coli cells (thaw on ice) and left 15 minutes on ice. Cells were subjected to a heat shock cells for 45 seconds at 42°C (water bath or dry block) and left 5 more minutes on ice. 250 ul of SOC medium were added and transformed cell were incubated for 1 hour at 37°C. Transformed cells were then plated on LB plates containing the appropriate antibiotic for selection. The following day, recombinants were analyzed by colony

PCR, using M13F primer (Life Technologies) and a reverse primer specific to the cloned fragment.

2.12.1.12. Electro-competent cells transformation

The desired plasmid was added to thaw GV3101 cells (50 ul) and the cells were transferred to an electroporation cuvette having 1 mm width and used an electroporator (Biorad) with the following settings: 1800 V with a capacity of 25 uF over 200 Ω resistance. Immediately 400 ul of SOC medium were added to the electroporated cells and incubated for 1hour at 28°C shaking at 300 rpm. Transformed cells were plated on LB plates containing the appropriate antibiotics for selection.

2.12.1.13. Primers used in this study

All primers that were used in this study (Table 2.12.1) were designed using Primer-BLAST (http://www.ncbi.nlm.nih.gov/tools/primer-blast/).

Table 2.12.1: Plasmids used in this study

Primer ID	Sequence (5'-3)	Chapter
I2G_F	CACCATGGAGATTGGCTTAGCAGTT	Ch. 4, 5
I2G_R	TTAAATATATTTCCAATCGATATTTATGATG	Ch. 4, 5
I141F_F	GGATTTGCAAGAGCAATTTGGTCTCCTTGGCTT	Ch. 4, 5
I141F_R	TTTAATGTTTCAATAGTGTCTTCCAGCTTG	Ch. 4, 5
I141X_F	GGATTTGCAAGAGCAANNNGGTCTCCTTGGCTTA	Ch. 4, 5
N330Y_F	CAAATTCGCATGGGCTTCTTGTCTACCGAAGCC	Ch. 4, 5
N330Y_R	CTCATTTCCCATCATCAAGGCAACACTGTC	Ch. 4, 5
N330X_F	CAAATTCGCATGGGCNNNTTGTCTACCGAAGCC	Ch. 4, 5
I2_GS4_F	TAAGCAACACTCGGCCCTTGAAGATGCCA	Ch. 5
I2_GS4_R	CGTCAAGATGACGCAAGTTAATCAACTTC	Ch. 5
I2_6CC10_F	ACCTTGAAGAGAATAGAGATATCTCGTTGCC	Ch. 5
I2_6CC10_R	AGTTGGCAGTATGCTAAAAGGAAAGGAG	Ch. 5
I2_Chi7_F	GGTGAGATGTTTGTGAAGTATTTGAGAGTGA	Ch. 5
I2_Chi7_R	AACTGGCGCCTCCAATTTCAATTTTGG	Ch. 5
I2_GS8_ F	GTGAATGATTGTGGTCGTGTAGATGATATAT	Ch. 5
I2_GS8_ R	TCTCAAATACTCCACAAACATCTCACCA	Ch. 5
I2_GS12_F	ATTCCTACTGCCACTAAAACTCTCCGTATTT	Ch. 5

I2_GS12_R	CAAAAACCTAGTAACGTTCTGGCAATTT	Ch. 5
I2_GS15_F	AAACTATCTATTTTCCGTTGCCCATTGCTCAC	Ch. 5
I2_GS15_R	AGAGAGGGAAGAGGGCATCCCTTTAAAT	Ch. 5
I2_CC_R	AGGTCTTCTAGTTTCTAGTTTCG	Ch. 4, 5,
I2_NBS_F	TCAACTTCTGTGGATGATGAAT	Ch. 4, 5
I2_NBS_R	CTGCTCCAATTTGTAGAGGG	Ch. 4, 5
I2_LRR1_F	TTGAGGACATTGCTTCCGATA	Ch. 4, 5
I2_LRR1_R	TTCTCTTCAAGGTAGTTGGCAG	Ch. 4, 5
I2_LRR2_F	TACAGATATCTCGTTGCCCAAAA	Ch. 4, 5
I2_NBLR_F	AGTGAAAGATGAAATAAATCAAG	Ch. 4, 5
I2_NBLR_F	CTCCACTCCAATGATAATTGC	Ch. 4, 5
I2_LRRsp_F	ATATGACGGAGTGGAAGCAATGG	Ch. 4, 5
I2_LRRsp_R	TCTGGACAATCAGACAGACGCAGT	Ch. 4, 5
35S_F	AAGACCCTTCCTCTATATAAGG	Ch. 4, 5
PK7_term_R	GATTTGTAGAGAGAGACTGGTGATTTTTGCGGACTC	Ch. 4, 5
I2hh_F*	CAAGGAACTGCGTCTGTCTGATT	Ch. 4, 5, 6
I2hh_R*	ATGAGCAATTTGTGGCCAGTATT	Ch. 4, 5, 6
Actin-F[1]	AGGCACACAGGTGTTATGGT	Ch. 4, 5, 6
Actin-R[1]	AGCAACTCGAAGCTCATTGT	Ch. 4, 5, 6
AVR2wt_F	ATGCGTTTCCTTCTGCT	Ch. 5
AVR2V>M_F	GGGTAACCCATATTGCA	Ch. 5
AVR2R>H_F	TGCGTGTTTCCCGGCCA	Ch. 5
AVR2R>P_F	GTTTCCCGGCCGCCC	Ch. 5
SIX3-F1[2]	CCAGCCAGAAGGCCAGTTT	Ch. 5
SIX3-R2[2]	GGCAATTAACCACTCTGCC	Ch. 5
FP157_F[3]	ATGAAGTACACTCTCGCTACC	Ch. 5
FP158_R[3]	GGTGAAAGTGAAAGAGTCACC	Ch. 5

(*): These primers were designed according to the results of Yu SC *et al.*, (Yu and Zou 2008)
1: These primers have been previously described by Aime *et al.*, (Aime, Cordier et al. 2008)
2: These primers have been previously described by Van der Does *et al.*, (van der Does, Lievens et al. 2008)
3: These primers have been previously described by Michielse *et al.*, (Michielse, van Wijk et al. 2009)

2.13. Protein methods

2.13.1. SDS-polyacrylamide gel electrophoresis

Gels were run in Tris-glycine buffer (25 mM Tris, 250 mM glycine pH 8.3, 0.1% (w/v) SDS) for approximately 1.5 hours at 60 to 150 V. All gels were run with a protein size marker 10-250 kDa (PageRuler Plus, Fermentas).

2.13.2. Western blotting

Two Trans-Blot® Turbo™ Transfer System sponges were equilibrated for 10 minutes in cold (4°C) transfer buffer (25 mM Tris, 192 mM glycin, 20% (v/v ethanol , pH 8.3). The polyvinylidene difluoride (PVDF) membrane membrane (BioRad) was activated for several minutes in 100% methanol. The device was assembled following the manufacturer's instructions (BioRad). The membrane was facing the anode and the gel the cathode. Transfer was carried out at room temperature with the Trans-Blot® Turbo™ Transfer System following the manufacturer's instructions (BioRad).

2.13.3. Immunoblotting

PVDF membrane containing the immobilized, denatured proteins were blocked for 1 hour in 0.1% TBS-T buffer (0.5 M NaCl, 200 mM Tris-HCl, 0.05% (v/v) Tween-20, 0.2% (v/v) Triton X-100, pH 7.5) plus 3% (w/v) BSA with gentle agitation on a platform shaker. The membrane was washed for 5 minutes in TBS-T buffer. The membrane was incubated with the primary antibody directed to the target protein in TBS-T + 3% BSA for 1 hour at room temperature. Then the membrane was washed for 40 minutes in TBS-T buffer changing the buffer every 10 minutes. Secondary antibodies covalently coupled to horseradish peroxidase (HRP) were then added. Finally the membrane was washed for 50 minutes in TBS-T buffer changing the buffer every 10 minutes. Detection of the peroxidase signal of the secondary antibody-HRP conjugate was performed with ECL (Amersham Biosciences) or SuperSignal West Femto (Pierce). Film exposure ranged from 30 seconds to 30 minutes. The film was aligned to the membrane and the protein marker was marked on the film.

Immunoblotting was performed with a polyclonal antibody raised against the CC domain of R3a (a-R3a), kindly provided by Dr. Mark J. Banfield. The primary antibody was diluted in TBS-T + 3% BSA to the following concentration: anti-R3a (1:3000). The secondary antibody was again diluted TBS-T + 3% BSA to the following concentration: anti-rabbit-HRP (1:5000, Sigma).

2.13.4. Structure predictions

Homology models of the individual CC, NB-ARC and LRR regions of I2 in chapters 4 and 5 were generated using protein fold recognition algorithms, as implemented by Intfold (Roche, Buenavista et al. 2011), and sequences covering the individual domains.

For the CC domain of I2, Intfold identified the CC domain of potato NLR protein Rx (PDB code 4m70) (Hao, Collier et al. 2013) as the top-scoring template and as there are no experimental data to guide our selection, an unbiased approach was used. Additional servers (iTASSER, Phyre2 and SWISS-MODEL) identified the CC domain of the barley NLR-protein MLA10 as the top-scoring template for modelling of the I2 CC-domain. In all these models (either of which could be valid), in each of the structures the I2 I141 position is consistently positioned to the C-terminus of the defined coiled-coil units and is therefore predicted to be located at an inter-domain region between the CC and NB-ARC domains. The NB-ARC domain was modeled using Apaf-1 (PDB code 1Z6T chain B) (Riedl, Li et al. 2005) as template, which was the top score of IntFold. That template is in agreement with previously published experimental evidence showing that I2 has ATPase activity (Tameling, Elzinga et al. 2002), as determined by positioning of the key motifs known to be required for ATPases. The LRR domain was modelled using 2 templates; Toll-like receptor 3 (PDB code 2a0z) (Bell, Botos et al. 2005) and Toll-like receptor 8 (PDB code 3w3g) (Tanji, Ohto et al. 2013) which were the top-scoring template in IntFold.

2.14. Media and buffer recipes

2.14.1. Protein extraction buffer

GTEN (10% glycerol, 25 mM Tris (pH 7.5), 1 mM EDTA, 150 mM NaCl) + 10 mM DTT + 2% (w/v) PVPP (polyvinylpolypyrolidone; not to be subsitituted with PVP (polyvinylpyrolidone) + 1% (v/v) protease inhibitor cocktail (Sigma) + 0.1% (v/v) Tween 20 or 0.15% (v/v) NP-40.

2.14.2. Dye (for DNA loading of gels)

For the loading of DNA gels two dye were used; the orange dye 6x (Thermo Scientific) and the 6x DNA blue loading dye (Thermo Scientific). The 6x orange dye

contained 10 mM Tris-HCl (pH 7.6), 0.15% orange G, 0.03% xylene cyanol FF, 60% glycerol, and 60 mM EDTA. The 6x DNA blue loading dye (Thermo Scientific) containing 10 mM Tris-HCl (pH 7.6), 0.03% bromophenol blue, 0.03% xylene cyanol FF, 60% glycerol, and 60 mM EDTA.

2.14.3. SDS-PAGE buffer (for protein loading)

For a 5X final concentration the following were added: bromophenol blue 0.2% (w/v), Tris-HCl (pH 6.8) 200 mM, Glycerol 2.5% (v/v), and SDS 4% (w/v).

2.14.4. Agroinfiltration buffer

The agroinfiltration buffer was prepared by adding 10 mM of $MgCl_2$, 10 mM of MES, and 150 uM acetosyringone in 1 L of MilliQ water. The pH was then adjusted to 5.6. Acetosyringone was added to the buffer prior use.
Acetosyringone powder was dissolved in either DMSO or ethanol for a stock solution of 100 mM and stored at -20°C.

2.14.5. Plich medium

The following were dissolved in 1 L of deionized water: 2.4 gr sucrose, 0.27 gr asparagine, 0.15 g KH_2P0_4, 0.10 gr $MgS0_4$ $7H_2O$, 10 mg cholesterol, 10 mg ascorbic acid, 2 mg thiamine HCl, 4.4 mg $ZnSO_4$ $7H_2O$, 1 mg $FeSO_4$ $7H_2O$, 0.07 mg, and $MnCl_2$ $4H_2O$. For solid media 20 g agar (Difco) were also added.

2.14.6. LB medium

The following were dissolved in 1 L of MilliQ water: 10 g of tryptone, 5 g of yeast extract, and 10 g of NaCl. Following the pH was adjusted to 7.0. For solid media 10 g of agar (Difco) were also added.

2.14.7. SOC medium

The following were dissolved in 97 ml of MilliQ water: 2 g of tryptone, 0.5 g of yeast extract, 1 ml of a solution of NaCl (1 M), 1 ml of a MgSO4 solution (1 M) and 1 ml of a $MgCl_2$ solution (1 M).

2.14.8. Murashige-Skoog salts MS medium

The following were dissolved in 1 L of MilliQ water: 4.3 g of MS salts, 0.59 g of MES, 0.1 g of myo-inositol, 1 ml of 100X MS vitamin stock, and 10 g of sucrose. Following the pH was adjusted 5.7 with KOH. For solid media 8 g of agar (Difco) were also added.

2.14.9. Potato Dextrose browth medium

The following were dissolved in 1 L of MilliQ water: 4.0 g of potato extract and 20 g dextrose. Following the pH was adjusted 5.6. For solid media 15 g of agar (Difco) were also added.

2.14.10. Antibiotics

For bacterial cultures kanamycin was used at a final concentration of 50 ug/ml, gentamycin at 25 ug/ml, carbenicillin at 100 ug/ml, rifampicin at 100 ug/ml, and Spectinomycin at 50 ug/ml. For the selection of transgenic plants, kanamycin was used at a final concentration of 50 ug/ml. All antibiotic solutions were sterilized with a 22 um filter.

CHAPTER 3: The pepper phytoalexin capsidiol affects differentially the oomycete plant pathogens *Phytophthora infestans* and *Phytophthora capsici*

3.1. Introduction

One of the many ways plants have evolved to defend themselves is the production of compounds that affect microbes in various ways. Some of these compounds are broad-spectrum, whereas others are not. Specific antimicrobial specialized metabolites termed phytoalexins, are among such defence compounds which are induced under stress conditions or upon infection by a pathogen (Stoessl, Unwin et al. 1973, Jones, Unwin et al. 1975, Ward 1976). Our knowledge on the spectrum of action of phytoalexins remains limited and, surprisingly, their contribution to species-level (also known as nonhost) resistance is not always fully appreciated.

One phytoalexin that has been well studied, capsidiol, is produced by the solanaceous plants *Capsicum annuum* (pepper) or *Nicotiana tabacum* (tobacco) after infection by pathogens such as the oomycete *Phytophthora capsici* (Stoessl, Unwin et al. 1972, Maldonado-Bonilla, Betancourt-Jimenez et al. 2008). Capsidiol has been shown to affect diverse pathogens such as fungi, oomycetes and bacteria (Stoessl, Unwin et al. 1973, Jones, Unwin et al. 1975, Ward 1976, Milat, Ducruet et al. 1991, Keller, Czernic et al. 1998, Ma 2008, Maldonado-Bonilla, Betancourt-Jimenez et al. 2008, Grosskinsky, Naseem et al. 2011). In a recent study, capsidiol was shown to be in the defence of the model plant *Nicotiana benthamiana* against *Potato virus X* (Li, Tee et al. 2015). As previously described, capsidiol is a bicyclic sesquiterpenoid and member of the isoprenoid class of phytoalexins.

Some of the most destructive plant pathogens are included in the *Phytophthora* genus, a member of the oomycete class (Kamoun 2009). *P. infestans* and *P. capsici* are two of the most notorious species, causal agents of the potato and tomato late blight and the vegetable blight and fruit rot respectively. Both species have been extensively studied at the genomic level and constitute model systems to study oomycete pathogens (Haas, Kamoun et al. 2009, Chaparro-Garcia, Wilkinson et al. 2011, Cooke, Cano et al. 2012, Jupe, Stam et al. 2013). *P. capsici* like *P. infestans* adopts two separate phases during infection; an early biotrophic one and a later one which involves extensive necrosis of host tissue (necrotrophic phase) (Kamoun and

Smart 2005). Although *P. infestans* host range is limited to solanaceous plants, particularly potato and tomato, *P. capsici* has a broader range of hosts including members from the Cucurbitaceae, Fabaceae, and Solanaceae families (Kamoun 2009). Tomato is a common host of these two *Phytophthora* species however *P. infestans* cannot infect several host plants of *P. capsici*, notably pepper.

There has not been much research on the molecular basis of host-specificity of *Phytophthora* species, such as *P. infestans* and *P. capsici*. A few studies have suggested that disease resistance genes that operate at the nonhost level are likely to be implicated (Ishizaka, Tomiyama et al. 1969), however there is evidence that phytoalexins might also be involved. Back in the 1970s, several studies had shown that capsidiol has differential activity against *P. infestans* and *P. capsici* (Jones, Unwin et al. 1975, Ward 1976). More specifically, Jones *et al*., using spore germination and growth assays revealed that *P. infestans* is more sensitive (~10 fold) to capsidiol than *P. capsici* (Jones, Unwin et al. 1975). In the same study, it was also shown that the effect of capsidiol below a certain threshold is reversible on both *Phytophthora* species (Jones, Unwin et al. 1975). Equivalent capsidiol levels are only reached *in vivo* in resistant varieties of pepper, which suggests that sensitivity to capsidiol and differential accumulation of this phytoalexin might play a role in host specificity (Egea, Alcazar et al. 1996). A few recent studies have used the role of capsidiol in *Phytophthora* pathosystems as a marker for defence (Milat, Ducruet et al. 1991, Keller, Czernic et al. 1998, Ahmed Sid, Perez Sanchez et al. 2000, Maldonado-Bonilla, Betancourt-Jimenez et al. 2008). However, Shibata *et al*. showed that silencing of two ethylene-regulated genes for capsidiol biosynthesis, *NbEAS* and *NbEAH*, negatively impacted the resistance of *Nicotiana benthamiana* against *P. infestans* proposing a positive role of capsidiol in this interaction (Shibata, Kawakita et al. 2010, Matsukawa, Shibata et al. 2013).

In this study, I revisited the effect of capsidiol on *P. infestans* and *P. capsici*, and the variation in sensitivity to this phytoalexin. The specific objectives of this study were 1) to confirm and more accurately characterize the differential sensitivity of *P. infestans* and *P. capsici* and 2) to investigate whether different *P. infestans* isolates have different levels of resistance to capsidiol. Compared to the earlier studies (Jones, Unwin et al. 1975, Egea, Alcazar et al. 1996, Ma 2008, Literakova, Lochman et al. 2010) I used highly pure preparations of capsidiol obtained in yeast engineered to express the capsidiol biosynthetic pathway (Trinh-Don, MacNevin et al. 2012). Taking advantage of transgenic *Phytophthora* strains expressing fluorescent

markers for biomass quantification and a novel fluorescence-based assay, I was able to monitor and further quantify the differential sensitivity of *P. infestans* and *P. capsici* to capsidiol. These assays showed that capsidiol alters the growth behaviour of both *Phytophthora* species. Finally, I monitored the intraspecific variation within *P. infestans* isolates to capsidiol. Most of the results presented in this chapter have been published[1].

3.2. Results

3.2.1. *P. infestans* is more sensitive to capsidiol than *P. capsici*

To examine the effect of capsidiol on *Phytophthora spp.,* I conducted inhibition assays using mycelial plugs of two to three week-old plates of *P. infestans* and *P. capsici,* which were placed in sterilized 26-well plates (Greiner Bio-one) in Plich medium, supplemented with varying concentrations of capsidiol or DMSO (control) reaching maximum concentration of 300 uM for *P. infestans* and 2 mM for *P. capsici*. To verify that the effect I was monitoring was caused by only one compound, capsidiol, a metabolically engineered yeast system (Trinh-Don, MacNevin et al. 2012) was used (by Dr. Dave Haart) to produce high purity capsidiol, as demonstrated by Nuclear Magnetic Resonance (NMR) Spectroscopy (Fig. 3.1A). Visual inspection of mycelial growth followed 10 days after original incubation of agar-grown mycelial plugs in capsidiol- or control-containing liquid medium at 20 °C in the dark for *P. infestans* and 25 °C and illumination for *P. capsici*. Reduced *P. infestans* growth was observed at capsidiol concentrations of 50 uM or above and growth was completely blocked at concentrations of 120 uM and higher. Capsidiol affected *P. capsici* growth at concentrations of 1.5 mM or higher, but did not fully inhibit growth in any of the tested capsidiol concentrations (Fig. 3.1B). To determine whether the control solution, DMSO, affects *Phytophthora* mycelial growth, 2.36% (v/v) of DMSO (representing the highest relative DMSO concentration that was used during the experiment) was added to the incubating mycelial plugs. No growth arrest was monitored in the DMSO containing cells, suggesting that DMSO has no affect in *Phytophthora* growth in the concentration used (Fig. 3.1B).

[1] **Artemis Giannakopoulou, Sebastian Schornack, Tolga O. Bozkurt, Dave Haart, Dae-Kyun Ro, Juan A. Faraldos, Sophien Kamoun, Paul E. O'Maille.** (2014). Variation in Capsidiol Sensitivity between *Phytophthora infestans* and *Phytophthora capsici* Is Consistent with Their Host Range. PLOS One **9.**

Overall, my results confirm earlier indications that *P. capsici* displays a higher degree of resistance to capsidiol than *P. infestans*. However, in my hands complete growth inhibition of *P. infestans* was achieved with 120 uM capsidiol, a value 2 times less than previously reported (Jones, Unwin et al. 1975).

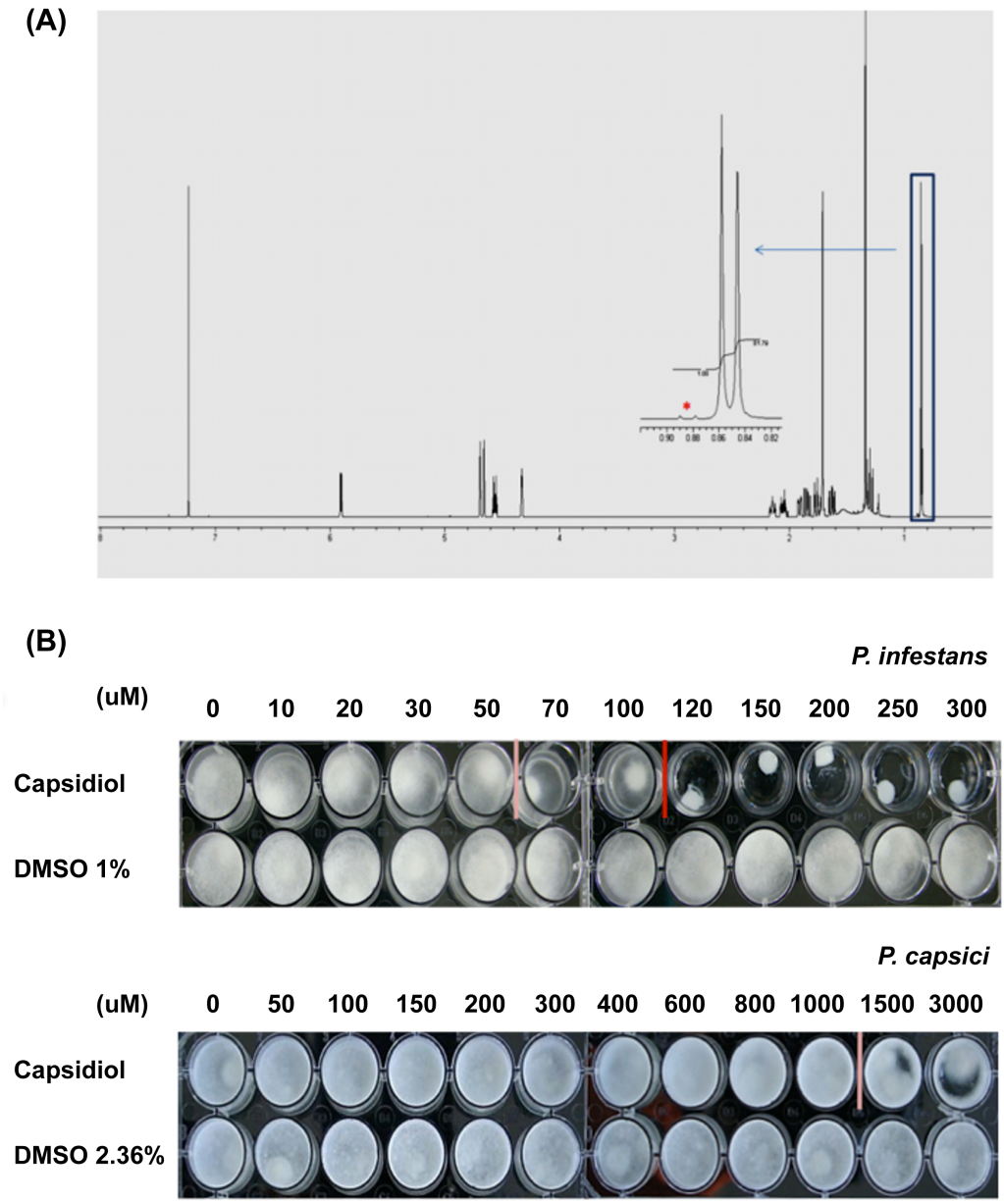

Figure 3.1: *P. infestans* is more sensitive to capsidiol than *P. capsici*.
A, Verification of capsidiol purity as tested by NMR spectroscopy (Nuclear Magnetic Resonance Spectroscopy). ^{1}H NMR ($CDCl_3$, 600 MHz) spectrum of capsidiol, by Dr. Dave Haart. NMR integrations of the diagnostic methyl doublet at δ_H 0.88 ppm (expansion) reveal a purity of greater than 98.8%. (*) Represents the impurity. B, Plugs were taken from two- to three-week-old *Phytophthora* plates and placed in the wells of a 24-well plate, previously filled with 1 ml of Plich medium. Capsidiol was added in various concentrations diluted in DMSO. Growth inhibition assay of *P. infestans* and *P. capsici* after 10 days of exposure of mycelial plugs to capsidiol. Pink

bar delineates the lowest concentration with an inhibitory effect and the red bar the concentration after which there is no longer growth. This experiment was performed 4 times.

3.2.2. Capsidiol arrests *P. infestans* growth reversibly

Previous studies have shown that the growth-inhibiting effects of capsidiol are reversible at concentrations below 5 mM (Jones, Unwin et al. 1975, Egea, Alcazar et al. 1996), higher concentrations of which are fungitoxic (Egea, Alcazar et al. 1996). To study the reversibility of the inhibitory effect of capsidiol I used the previously established *Phytophthora* microtitre plate assay (described in paragraph 3.2.1). As a starting point for this experiment I chose 10 days after original incubation of the mycelial plugs, time at which the inhibitory effects were clear (Fig. 3.2A). The Plich medium (containing either capsidiol or DMSO) was carefully removed from the wells and the overgrown plugs were washed three times with deionized water. Following that treatment, fresh Plich medium was added again to the wells. Growth restoration was observed 24 hours after the washing treatment and 10 days later the extent of mycelial growth was similar to the control that was grown without any capsidiol (Fig. 3.2B). This result confirmed previous reports that suggested that low capsidiol concentrations reversibly inhibit *Phytophthora* growth (Jones, Unwin et al. 1975).

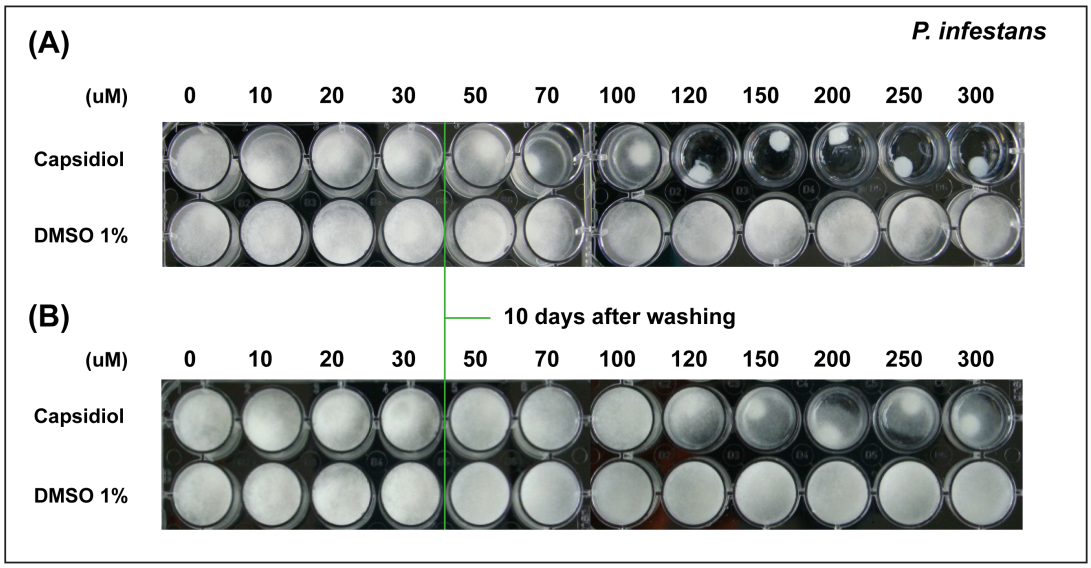

Figure 3.2: Capsidiol inhibits *P. infestans* growth reversibly.
Plugs were taken from two- to three-week-old *P. infestans* plates and placed in the wells of a 24-well plate, previously filled with 1 ml of Plich medium. Capsidiol was added in various concentrations diluted in DMSO. Washes were applied to the plates containing the *P. infestans* plugs by carefully removing the Plich media from the wells, adding distilled water, expose for 1 to 2 minutes and remove. This step was

repeated at least 2 times. Finally 1 ml of fresh Plich media was added and plates were kept at 20°C in the dark. A, Growth inhibition assay of *P. infestans* after 10 days of exposure of mycelial plugs to capsidiol. B, Restoration of growth after washing treatment. Green line indicates the point after which the washing treatment was applied. The experiment was performed 3 times with similar results. Picture was taken 10 days after the washing and 20 days after initial exposure to capsidiol.

3.2.3. Quantitative evaluation of differential growth inhibition of *P. infestans* and *P. capsici* by capsidiol

In order to quantify the effect of capsidiol on the growth of *Phytophthora* strains, I developed and applied an inhibition assay with zoospore suspension solutions and measured the amount of growing mycelia using either optical density or emitted fluorescence of transgenic *Phytophthora* strains. In this experiment the following strains were used: *P. infestans* 88069td, *P. infestans* 88069 (Chaparro-Garcia, Wilkinson et al. 2011), *P. capsici* LT1534 tdtom and *P. capsici* LT1534 (Jupe, Stam et al. 2013) strains (td and tdtom strains are transgenic strains expressing the red fluorescent marker tandem dimer RFP, known as tdTomato). The zoospores were harvested from *Phytophthora* and were subjected to incubation in Plich medium with various concentrations of capsidiol or DMSO. Scanning of the plates was performed at one to three day intervals for calculation of the Optical Density at 600 nm (OD600) and red fluorescence intensity. To directly compare the difference in sensitivity between *P. infestans* and *P. capsici*, I generated dose response curves by measuring both OD600 and fluorescence intensity at increasing concentrations (Fig. 3.3)

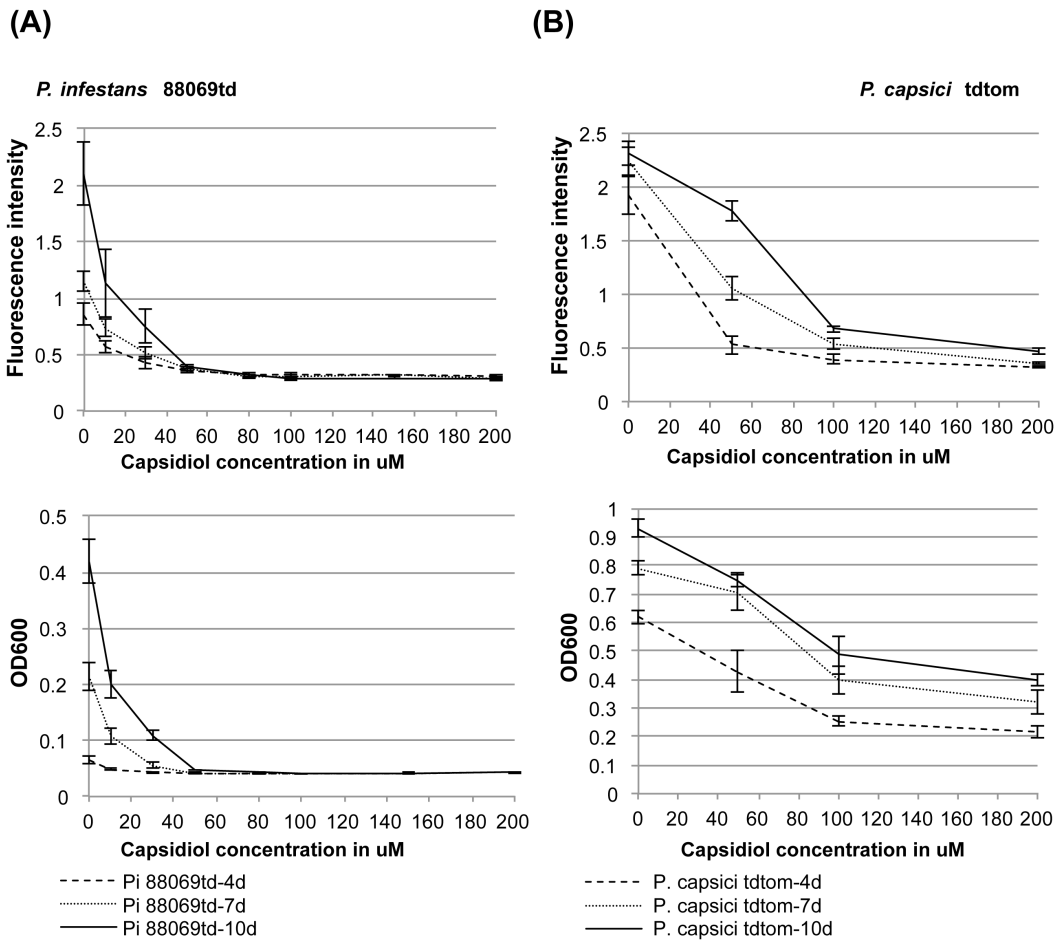

Figure 3.3: Capsidiol is not affecting *P. capsici* growth as severely as it does *P. infestans*.

Zoospores from two- to three-week-old *Phytophthora* plates were harvested and diluted to a final concentration of 50,000 spores/ml. Droplets of 10 µl were added to each well of a 96-well plate, previously filled with 250 µl of Plich medium, covered with a plastic lid and sealed with Parafilm. Plates were kept at 20°C in the dark for *P. infestans* and 25°C and illumination for *P. capsici*. At regular intervals, mycelial growth was monitored using a Varioscan Flash Multimode Reader (Thermo Scientific) by measuring light absorption at OD600 as well as emission of red fluorescence (excitation at 360 nm, emission at 465 nm). A, Dose response curves of *P. infestans* 88069td calculated at 4, 7 and 10 days for both Fluorescence intensity and OD600. B, Dose response curves of *P. capsici* tdtom calculated at 4, 7 and 10 days for both Fluorescence intensity and OD600. The experiment was performed 3 times. Error bars represent standard deviation.

3.2.3.1. Red fluorescence intensity growth curves

Notable difference between *P. infestans* and *P. capsici* was found as a result of measurements of red fluorescence emission under capsidiol treatment (Fig. 3.4). All concentrations of capsidiol above 50 uM dramatically affected the ability of *P. infestans* 88069td to emit red fluorescence. The values acquired after 10 days were at a range of 0.3 red fluorescent units (RFU), close to the value obtained with the non-fluorescent 88069 strain (Fig. 3.4A and A1.1-Appendix 1). On the contrary, *P. capsici* tdtom retained its ability to emit red fluorescence up to a concentration of 400 uM of capsidiol, after which RFU levels dropped down to the non-fluorescent *P. capsici* strain values (Fig. 3.4B and A1.1-Appendix 1).

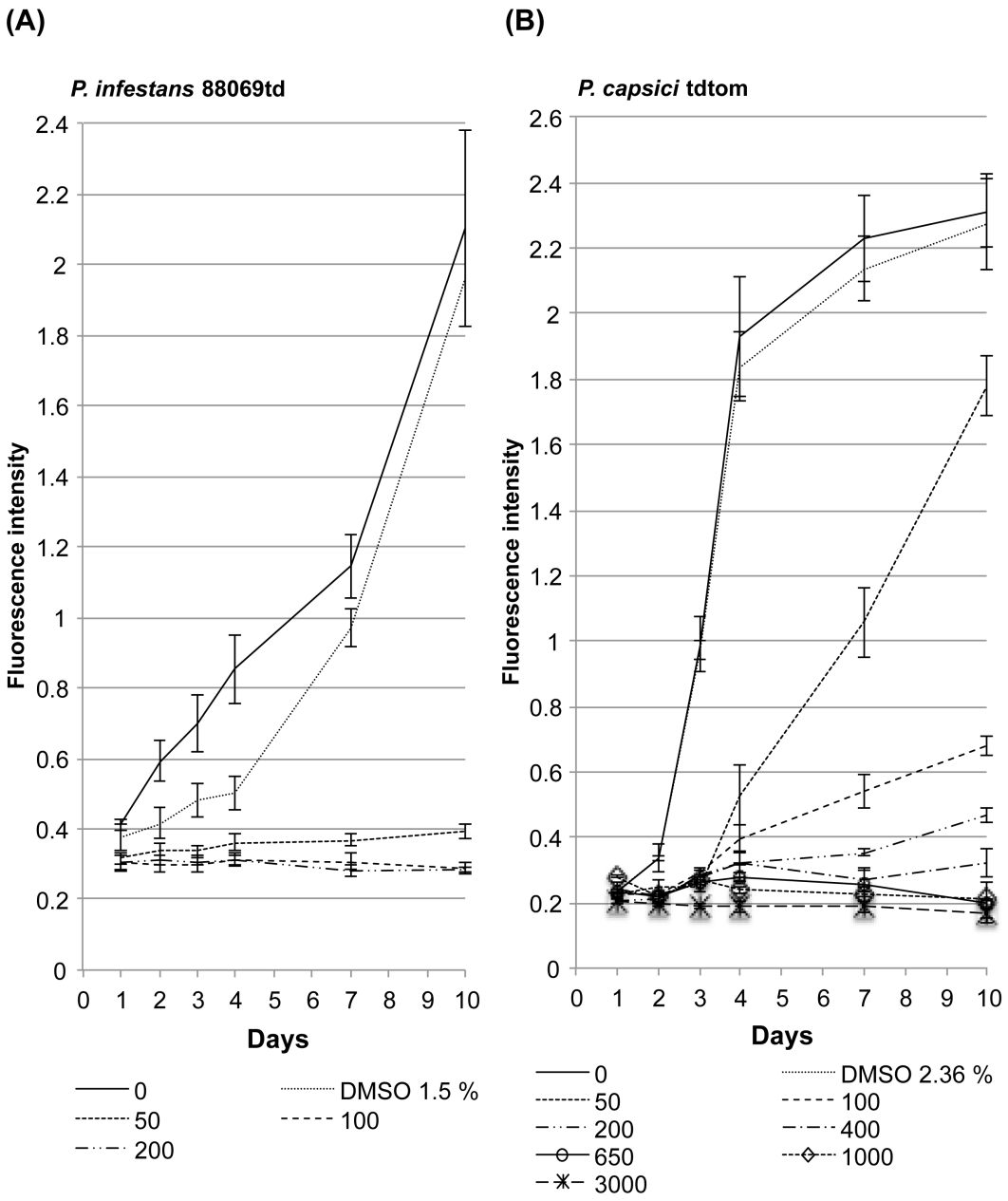

Figure 3.4: Scatter plots correlating fluorescence intensity and capsidiol concentration.

Zoospores from two- to three-week-old *Phytophthora* plates were harvested and diluted to a final concentration of 50,000 spores/ml. Droplets of 10 µl were added to each well of a 96-well plate, previously filled with 250 µl of Plich medium, covered with a plastic lid and sealed with Parafilm. Plates were kept at 20°C in the dark for *P. infestans* and 25°C and illumination for *P. capsici*. At regular intervals, mycelial growth was monitored using a Varioscan Flash Multimode Reader (Thermo Scientific) by measuring emission of red fluorescence (excitation at 360 nm, emission at 465 nm). A, Fluorescence intensity of *P. infestans* 88069td over time for a maximum of 10 days B, Fluorescence intensity of *P. capsici* tdtom over time for a maximum of 10 days. Each point in the plots represents the average value of three repeats. Error bars represent standard deviation.

3.2.3.2. Optical Density growth curves

Considerable growth differences were also confirmed by the OD600 measurements (Fig 3.5). Capsidiol concentrations of 50 uM or greater completely blocked *P. infestans* growth, as shown by the extremely low values of OD600, lower even than the control strain (Fig. 3.5A and A1.1-Appendix 1). *P. capsici* growth was severely affected at a capsidiol concentration of 650 uM and higher, as depicted by the low OD600 values that were close to the ones from the control strain (Fig. 3.5B and A1.1-Appendix 1).

The results obtained are in agreement with previous findings that *P. capsici* is more resistant to capsidiol than *P. infestans* and further reveal that the difference in sensitivity is almost 13 fold, a value not previously reported.

To determine whether DMSO had any effect on the RFU and OD600 values obtained, the same set of experiment was repeated with a concentration of 2.36% (v/v) (a value equivalent with the maximum capsidiol solution that was used during the experiment). DMSO was shown to affect neither Fluorescence intensity nor the OD600 of either *Phytophthora* species for the concentration tested (Fig. A1.1-Appendix 1).

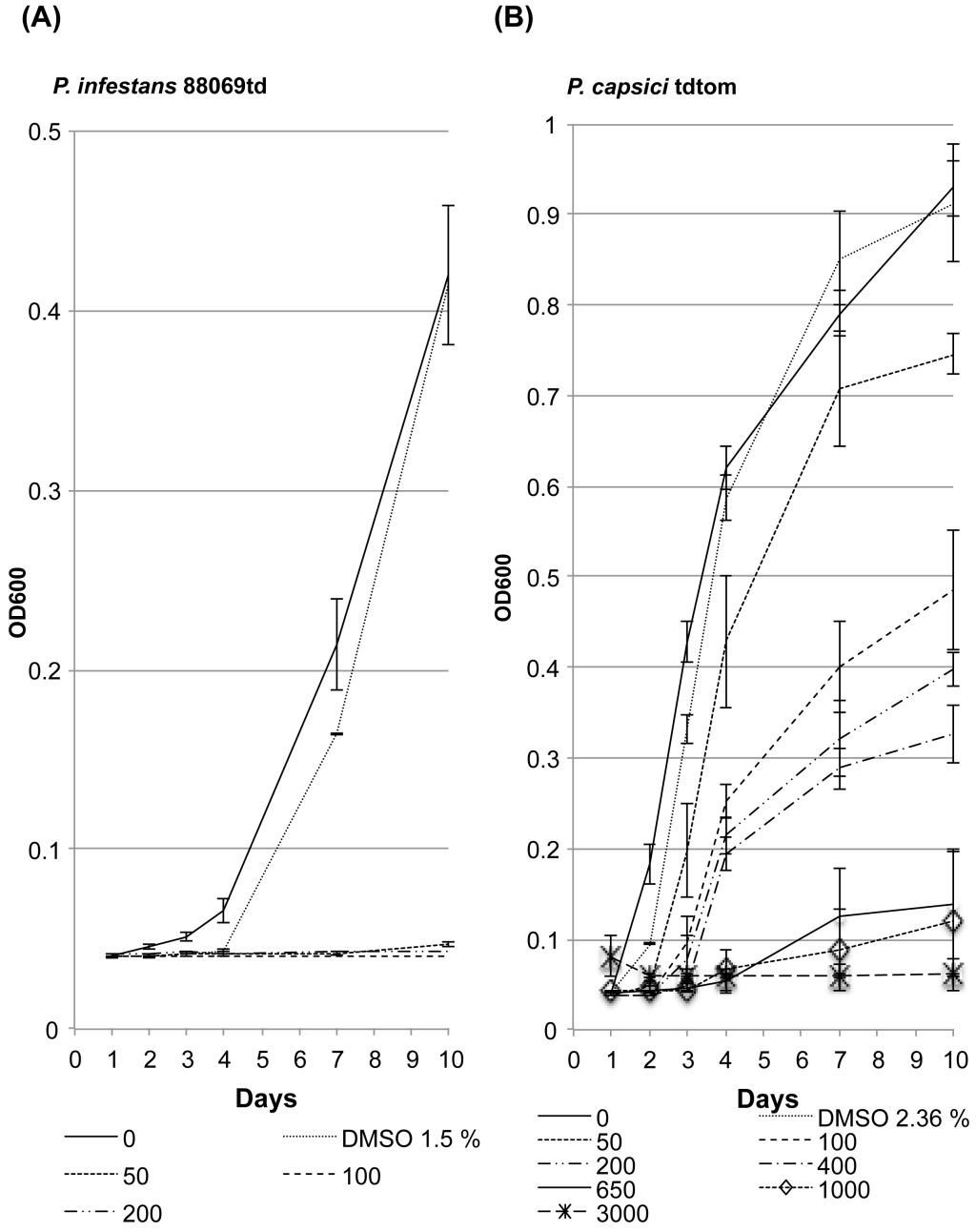

Figure 3.5: Scatter plots correlating 0D600 and capsidiol concentration.
Zoospores from two- to three-week-old *Phytophthora* plates were harvested and diluted to a final concentration of 50,000 spores/ml. Droplets of 10 µl were added to each well of a 96-well plate, previously filled with 250 µl of Plich medium, covered with a plastic lid and sealed with Parafilm. Plates were kept at 20°C in the dark for *P. infestans* and 25°C and illumination for *P. capsici*. At regular intervals, mycelial growth was monitored using a Varioscan Flash Multimode Reader (Thermo Scientific) by measuring light absorption at OD600 A, Growth of *P. infestans* 88069td over time for a maximum of 10 days B, Growth of *P. capsici* tdtom over time for a maximum of 10 days. Each point in the plots represents the average value of three repeats. Error bars represent standard deviation.

3.2.4. Capsidiol alters *P. infestans* and *P. capsici* mycelial growth

To further examine the capsidiol effects of *Phytophthora* mycelial growth, hyphal morphology was microscopically monitored during a capsidiol time course treatment at two- to four-day intervals in microtitre plates. For this experiment I used the following strains: *P. infestans* 88069td and *P. capsici* tdtom. *P. infestans* 88069td mycelial growth was severely affected by capsidiol concentrations of 10 uM, as shown by stunted branching (Fig. 3.6). A similar phenotype was observed at 400 uM of capsidiol concentration for *P. capsici* tdtom (Fig. 3.7). In more detail, *Phytophthora* showed a stunted branching in the lower capsidiol concentrations and even spore germination was affected in higher concentrations. Taking into account that the experiment was performed with zoospore suspension as the initial inoculum, it is not clear exactly by which mechanism capsidiol is affecting *Phytophthora* growth. Additional sets of experiments of Scanning Electron Microscopy (SEM) on *Phytophthora* growth after exposure to capsidiol were not successful in providing any information on the basis of this phenomenon. To confirm that the control containing medium DMSO, does not have any effect on the phenotypes observed, a similar experiment was set up using DMSO at concentrations equivalent to the maximum capsidiol that was used for each strains. No inhibitory effect was observed for any of the *Phytophthora* strains tested (Fig. A1.2-Appendix 1). These results are in agreements with the limiting capsidiol concentrations obtained in zoospore inhibition assays for both species and further suggest that capsidiol might also target developmental factors in *Phytophthora* in order to exert its role in defence.

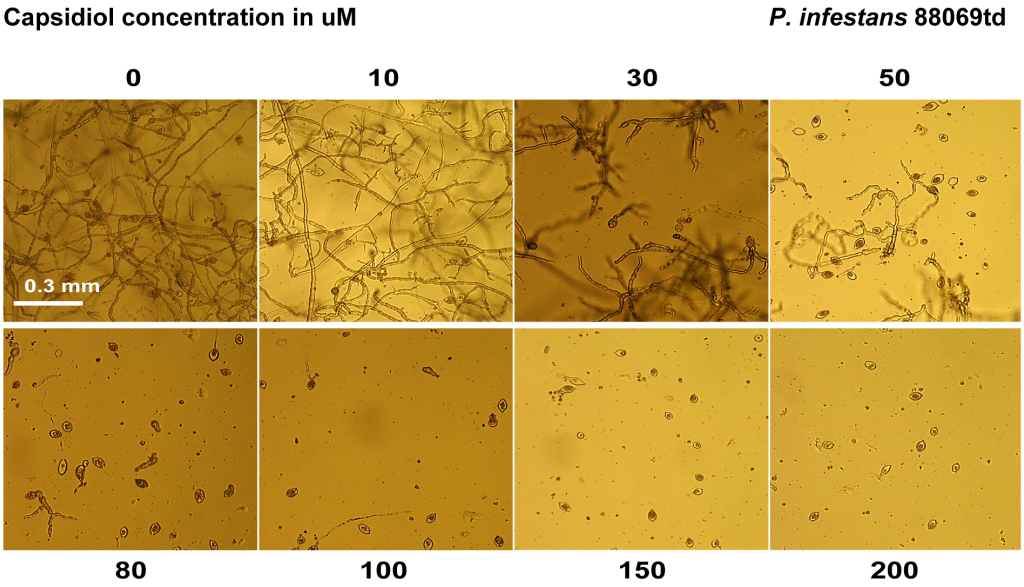

Figure 3.6: Growth behaviour of *P. infestans* 88069td, after 10 days of exposure to different capsidiol concentrations.

Zoospores from two- to three-week-old *P. infestans* plates were harvested and diluted to a final concentration of 50,000 spores/ml. Droplets of 10 µl were added to each well of a 96-well plate, previously filled with 250 µl of Plich medium, covered with a plastic lid and sealed with Parafilm. Plates were kept at 20°C in the dark. Mycelial growth was imaged using a Zeiss Axiovert 25 microscope in transmission light mode with 10x magnification at 10 days post inoculation (10 dpi). The experiment was performed 3 times with similar results.

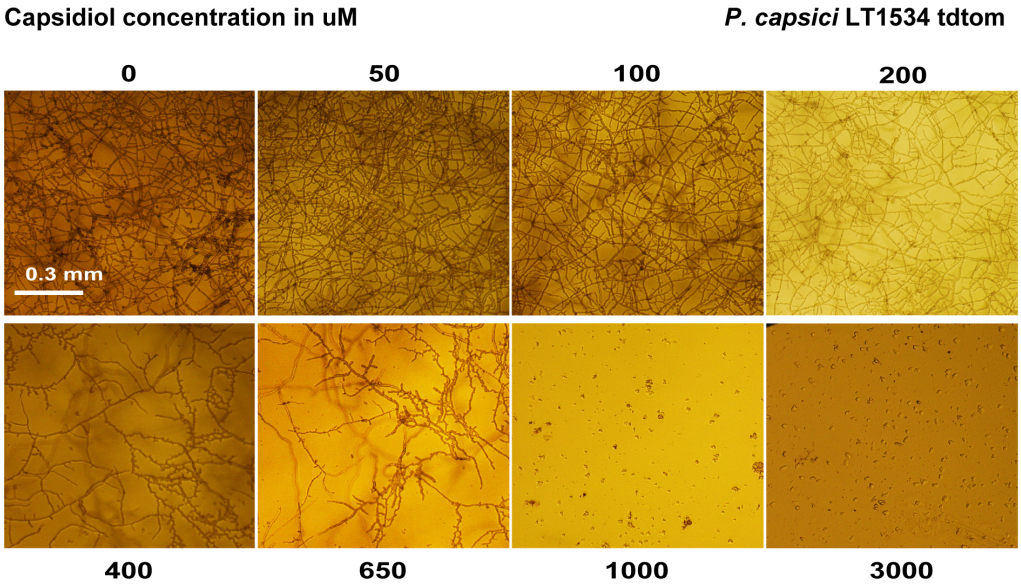

Figure 3.7: Growth behaviour of *P. capsici* tdtom, after 10 days of exposure to different capsidiol concentrations.

Zoospores from two- to three-week-old *P. capsici* plates were harvested and diluted to a final concentration of 50,000 spores/ml. Droplets of 10 µl were added to each well of a 96-well plate, previously filled with 250 µl of Plich medium, covered with a plastic lid and sealed with Parafilm. Plates were kept at 25°C and illumination.

Mycelial growth was imaged using a Zeiss Axiovert 25 microscope in transmission light mode with 10x magnification at 10 days post inoculation (10 dpi). The experiment was performed 3 times with similar results.

3.2.5. Variation in sensitivity to capsidiol among *P. infestans* isolates

To determine whether different *P. infestans* isolates exert different sensitivity towards capsidiol I conducted an experiment exposing mycelial plugs to various concentrations of capsidiol, as described previously. In this experiment the following *P. infestans* isolates were used: 88069 (van West, de Jong et al. 1998), 88069td (Whisson, Boevink et al. 2007, Bozkurt, Schornack et al. 2011), T30-4 (Haas, Kamoun et al. 2009), 06_3928A (Cooke, Cano et al. 2012), VK98014 (Li, van der Lee et al. 2012), EC1-3527, EC1-3626, 2004_7804B (Cooke, Cano et al. 2012), 2011_8410B (Cooke, Cano et al. 2012) and NL08645 (Haas, Kamoun et al. 2009) (Table 2.5.1, chapter 2). My analysis showed that only one isolate, 06_3928A, displayed a similar level of resistance to capsidiol at our reference isolate, 88069, whereas the other isolates were more sensitive with isolate NL08645 being the most sensitive to capsidiol (Fig. 3.8). Once more, DMSO was tested and did not have any effect on *Phytophthora* growth in the concentrations used. My results support that there is strain-specific variation of *P. infestans* isolates to capsidiol growth inhibition, the genetic basis of which remains to be studied.

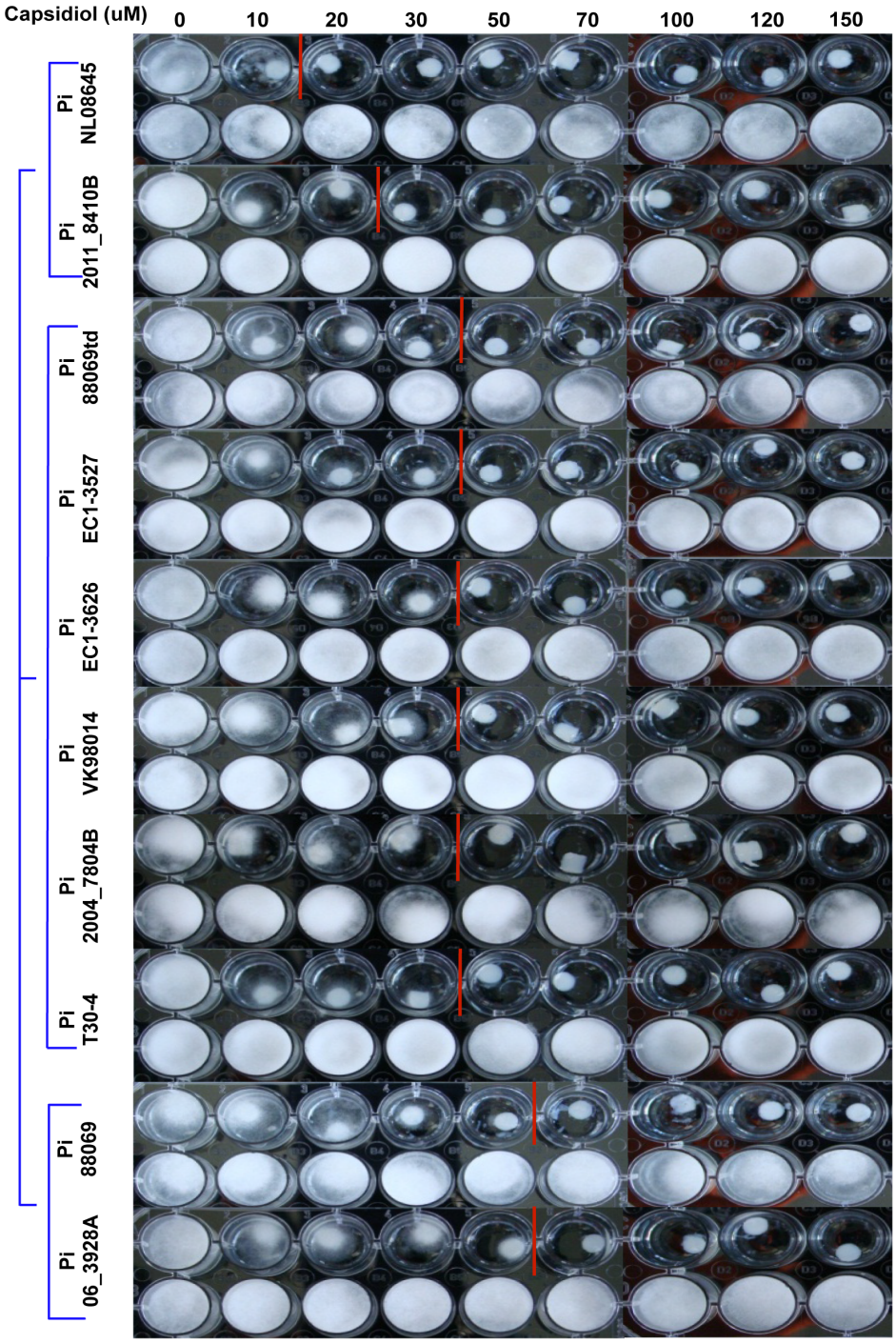

Figure 3.8: Different *P. infestans* isolates have different sensitivity to capsidiol. Isolates are clustered according to their sensitivity, starting from the most sensitive to the least. Top row of wells of each isolate represents capsidiol treatment (capsidiol was dissolved in DMSO/Plich media) in µM and the lower row represents treatment with 1% (v/v) DMSO/Plich (negative control). The experiment was performed 3 times.

3.3. Discussion

In this study, I developed new assays to examine the effect of the phytoalexin capsidiol on two *Phytophthora* species that differ in their host range. The results presented are overall consistent with a 1975 report that *P. infestans* is more sensitive to capsidiol than *P. capsici* (Jones, Unwin et al. 1975). Using highly pure preparations of capsidiol, I monitored a major (>10-fold) differential effect of capsidiol between species in both mycelial and zoospore inhibition assays. Taking into account that this phytoalexin is produced by pepper but not potato, it remains to be determined whether capsidiol contributes to nonhost resistance of pepper to *P. infestans*.

All the previous studies on capsidiol have been using pepper fruits or tobacco cell cultures to produce capsidiol (Jones, Unwin et al. 1975, Egea, Alcazar et al. 1996, Ma 2008, Literakova, Lochman et al. 2010). Using a recently developed method in yeast (Trinh-Don, MacNevin et al. 2012), highly pure capsidiol was produced. This gave me the confidence of reduced likelihood that contaminating phytochemicals may have affected the experiments. It further allowed me to directly assess the effect of capsidiol on *Phytophthora* species and helped me to more accurately estimate the inhibitory doses of capsidiol on *Phytophthora* growth. The use of fluorescently labeled *Phytophthora* strains enabled me to also calculate biomass and estimate growth in the inhibition assays. Although my findings are consistent with the earlier studies, I could more accurately estimate the difference in sensitivity. The results suggest that 120 uM of capsidiol completely inhibit *P. infestans* growth both in mycelial and zoospore assays, whereas Jones *et al*., concluded that this effect started at 200 uM of capsidiol (Jones, Unwin et al. 1975). However, I cannot rule out that these differences are probably due to the assays used. My zoospore assays were more consistent with the results of Jones *et al*., who concluded that capsidiol has a fungistatic effect at 3.75 mM and is fungitoxic at concentrations that exceed 5 mM (Jones, Unwin et al. 1975, Egea, Alcazar et al. 1996). In this study I also found that that the two *Phytophthora* species examined differ in their ability to cope with capsidiol, and this difference was calculated at a level of approximately 13-fold, which is in in agreement with earlier studies that showed *P. capsici* to be at least 10 times more resistant to capsidiol than *P. infestans* (Jones, Unwin et al. 1975). It is important to highlight here that *P. capsici* grew faster and reached a higher OD600 value in the absence of capsidiol, than *P. infestans*, indicating the higher aggressiveness of this pathogen compared to *P. infestans*. Also, the minor

inconsistencies that arose between the OD600 and fluorescence values can be explained by the limitations of the method used in the Varioscan mashing during the scanning of plates. This study also suggested that capsidiol might have a role in suppressing developmental mechanisms in *Phytophthora*, since a stunted branching or no branching at all was observed at inhibitory concentrations. Finally, I showed that the level of sensitivity between different *P. infestans* isolates varies, providing a basis for studying the underlying genetic variation.

It has been previously shown that other phytoalexins, like capsidiol, show a differential toxicity to phytopathogenic organisms. For example, it has been shown that the major phytoalexins from *Vicia faba* including isoflavoinoid medicarpin and wyerone acid have a greater impact on germ tubes produced by the necrotrophic fungus *Botrytis cinerea*, than *B. fabae* (Hargreaves, Mansfield et al. 1977). A differential toxicity in wyerone derivatives than medicarpin was also shown in that study (Hargreaves, Mansfield et al. 1977). Studying the role of the garden pea and red clover phytoalexins, pisatin and maackiain respectively against 19 fungal species, Delserone *et al*., revealed that nonhost phytoalexins have a greater effect inhibiting growth of the pathogens tested than the phytoalexins naturally occurring in the host (Delserone, Matthews et al. 1992). These studies all support the idea that that differential activity of phytoalexins is a common phenomenon and further highlight the importance of understanding how different pathogens have evolved to cope with them.

What could be the nature of the differential effect of capsidiol on the two *Phytophthora* species? A detoxification mechanism of capsidiol by *P. capsici* was never confirmed, instead it was suggested that *P. capsici* does not induce high enough levels of capsidiol during infection of its host plant pepper (Ward and Stoessl 1972, Jones, Unwin et al. 1975, Jones, Unwin et al. 1975). The process of detoxification would probably involve oxidation of capsidiol to a less fungitoxic ketone, capsenone, as has been noted in *in vitro* assays with the fungi *Botrytis cinerea* and *Fusarium spp.* and this ketone was never detected in pepper tissue infected with *P. capsici* (Ward and Stoessl 1972, Stoessl, Unwin et al. 1973). This suggests that the pathogen may evade the phytoalexin by limiting its induction (Ward and Stoessl 1972, Stoessl, Unwin et al. 1973). An alternative hypothesis is that ATP-binding cassette (ABC) transporters may be involved as an efflux pump. For the rot causing ascomycete *Nectria haematococca,* it has been shown that it overcomes the effect of the pea phytoalexin pisatin using two mechanisms (Coleman, White et al.

2011). The first mechanism involves the production of a cytochrome P450 that is responsible for the detoxification of pisatin and the second lies on the use of a specific ABC transporter, NhABC1, which enhances the tolerance of the fungus to the phytoalexin (Coleman, White et al. 2011). These results suggest that a successful pathogen has evolved multiple ways to overcome these plant antimicrobial compounds (Coleman, White et al. 2011). NhABC1 has been shown to also tolerate the potato phytoalexin rishitin and it phylogenetically resides to a clade of ABC transporters involved in virulence (Coleman, White et al. 2011).

Since there is no evidence that *P. capsici* can detoxify capsidiol, it is possible that it relies on ABC transporters to cope with capsidiol. In a more recent study, Judelson *et al*., studying the role of ABC transporters in fungicide sensitivity of *P. infestans,* failed to show correlation between up-regulation of ABC transporter genes in strains less sensitive to fungicides (Judelson and Senthil 2006). Whether inter- or intra-specific variation in expression of ABC transporter genes explains differences in capsidiol sensitivity in *Phytophthora* remains to be determined.

The difference in sensitivity to capsidiol between *P. infestans* and *P. capsici* could also be explained by a genetic difference in the target of capsidiol in these two species. Capsidiol has been shown to have a bacteriostatic effect against the human gastritis pathogen *Helicobacter pylori in vitro* although the mode of action remains unknown (De Marino, Borbone et al. 2006). Identifying the molecules that are targeted by capsidiol in *Phytophthora* would be of great interest so as to unravel the mechanisms mediating that interaction. Transcriptome dynamics in response to capsidiol would be a promising approach given that the genomes of both *P. infestans* and *P. capsici* are available (Haas, Kamoun et al. 2009, Cooke, Cano et al. 2012, Lamour, Mudge et al. 2012). From an evolutionary perspective, it would be of great interest to examine the response of *Phytophthora* to other sesquiterpenes that emerged during the functional divergence of terpene synthases in solanaceous plants (O'Maille, Malone et al. 2008).

The different levels of tolerance that were observed among the various *P. infestans* isolates tested could reflect the remarkable level of diversity noted in this highly adaptable plant pathogen species (Raffaele, Farrer et al. 2010, Cooke, Cano et al. 2012). Remarkably the variation noted is reminiscent of what has been monitored for sensitivity to fungicides in *P. infestans* and other oomycetes (Blum, Boehler et al. 2010, Blum, Waldner et al. 2010, Randall, Young et al. 2014). There are some cases

where the genetic basis of chemical sensitivity has been identified. For example, Randall *et al*., revealed that sequence polymorphisms in the large subunit of RNA polymerase I (RPA190) contributes to *P. infestans* insensitivity to the oomycete-specific control chemical Mefenoxam (Randall, Young et al. 2014). Another study also demonstrated that for the two oomycete pathogens, *Plasmopara viticola* and *P. infestans*, an amino acid change in a protein known to be involved in cellulose biosynthesis (PvCESA3 and PiCESA3 in the two pathogens respectively) confers insensitivity to Mandipropamide (Blum, Boehler et al. 2010, Blum, Waldner et al. 2010).

According to my analysis, sensitivity to capsidiol ranged ~5 fold in the *P. infestans* isolates tested. Which could be the biological significance for these differences? Even though potato does not produce capsidiol, I cannot exclude the possibility that *P. infestans* has evolved mechanisms to tolerate other terpenoids produced by potato, which might contribute to host immunity. Indeed, potato is know to accumulate rishitin, another bicyclic sesquiterpene phytoalexin that is related to capsidiol (Ishizaka, Tomiyama et al. 1969). In the future, it would be interesting to examine whether there is any correlation between aggressiveness and tolerance to capsidiol among various *P. infestans* isolates.

Overall, this study suggests that a biotechnological approach to engineer resistance to *P. infestans* could be taken. Genetic manipulation of capsidiol production in *N. benthamiana*, a *P. infestans* host plant that produces capsidiol, has already indicated that this phytoalexin contributes to disease resistance (Shibata, Kawakita et al. 2010, Matsukawa, Shibata et al. 2013). Interestingly, *P. capsici* is markedly more aggressive pathogen of *N. benthamiana* than *P. infestans* (Chaparro-Garcia, Wilkinson et al. 2011). This suggests again that *P. capsici* can tolerate the capsidiol produced by this plant. Ultimately, capsidiol biosynthetic genes could be transferred from pepper or tobacco to potato and tomato as a potential strategy for disease resistance against *P. infestans*. The first example of a nonhost phytoalexin expressed to a novel plant was the case of the grapevine resveratrol, back in 1993 (Hain, Reif et al. 1993). In that study, Hain *et al*., expressed the two sesquiterpene synthase genes (*STS*) for resveratrol biosynthesis (*Vst1* and *Vst2*) in tobacco resulting in higher disease resistance against *Botrytis cinerea* (Hain, Reif et al. 1993). Several other studies have successfully transferred *STS* genes in many plants conferring resistance to several pathogens (Hain, Reif et al. 1993, StarkLorenzen, Nelke et al. 1997, Thomzik, Stenzel et al. 1997, Leckband and Lorz

1998, Hipskind and Paiva 2000, Liang, Zheng et al. 2000, Coutos-Thevenot, Poinssot et al. 2001, Zhu, Agbayani et al. 2004, Lim, Yun et al. 2005, Serazetdinova, Oldach et al. 2005, Liu, Zhuang et al. 2011). However, there have been reports where plants transformed with *STS* genes did not result in increased resistance (Kobayashi, Ding et al. 2000, Giorcelli, Sparvoli et al. 2004, Seppanen, Syrjala et al. 2004). Therefore, whether transgenic STS potato and/or tomato plants expressing capsidiol will be able to limit *P. infestans* growth is an open question.[2]

[2] It should be noted that my involvement in this project was terminated here; therefore no further experimentation was carried out.

CHAPTER 4: I2 immune receptor mutant confers partial resistance to the Irish potato famine pathogen *Phytophthora infestans*

4.1. Introduction

Plant diseases constitute a never-ending threat for modern human life making the need for sustainable crop disease resistance increasingly urgent (Pennisi 2010, Fisher, Henk et al. 2012). Sustainable crop improvement approaches based on plant defence mechanisms, often involve *R* genes - plant loci that encode immune receptors (Cook 2000, Michelmore, Christopoulou et al. 2013, Jones, Witek et al. 2014). A very challenging project is to engineer plants with broad-spectrum disease resistance, meaning that the plants will be able to defend themselves against a wide spectrum of pathogens. Although a typical approach to achieve this goal is by pyramiding multiple immune receptors with different pathogen resistance spectra, single *R* genes that function against multiple pathogens do occur. One characteristic example is the tomato gene *Mi-1.2*, which confers resistance to pathogens from different phyla: arthropods (aphids and whiteflies) and a nematode (Nombela, Williamson et al. 2003, Atamian, Eulgem et al. 2012). Cf-2, an extracellular immune receptor in tomato again, also mediates resistance to both the fungus *Cladosporium fulvum* and the root parasitic nematode *Globodera rostochiensis* (Lozano-Torres, Wilbers et al. 2012). In Arabidopsis, a pair of two immune receptors, RPS4 and RRS1, mediates resistance to the bacteria *Pseudomonas syringae* and *Ralstonia solanacearum* but also to the fungus *Colletotrichum higginsianum* (Gassmann, Hinsch et al. 1999, Deslandes, Olivier et al. 2003, Birker, Heidrich et al. 2009, Narusaka, Shirasu et al. 2009). Pathogens however, as part of the same co-evolutionary arm race with plants, develop ways to overcome immunoreceptor-specific mediated disease resistance with the emergence of new races. The ultimate challenge for plant breeders and biotechnologists is to generate new resistance gene specificities rapidly enough to keep up with the pathogen evolution. Engineering wide-spectrum immune receptors that target more than one pathogen is one approach to rapidly deliver agronomically useful resistance genes.

Plants, in order to resist pathogenic invasion, deploy cell surface and intracellular immune receptors that recognise pathogen-secreted molecules and further activate immune responses (Dodds and Rathjen 2010, Win, Chaparro-Garcia et al. 2012). As

previously described, the nucleotide binding-leucine-rich repeat (NLR) protein family, is the largest family of intracellular immune receptors and an important element of defence against pathogens in both plants and animals (Maekawa, Kufer et al. 2011, Jacob, Vernaldi et al. 2013). NLR proteins in plants, recognise effectors, pathogen secreted molecules that normally modulate host cell processes to the benefit of the pathogen (Hogenhout, Van der Hoorn et al. 2009, Dodds and Rathjen 2010, Bozkurt, Schornack et al. 2012, Win, Chaparro-Garcia et al. 2012). Recognition of one or a limited number of effectors by NLRs results in the so-called NLR-triggered immunity or effector-triggered immunity (Jones and Dangl 2006, Ooijen, Burg et al. 2007, Dodds and Rathjen 2010, Win, Chaparro-Garcia et al. 2012). NLR proteins, as previously mentioned are grouped in two major classes depending on their N terminal domains: CC-NB-LRR or CNL proteins with a predicted coiled-coil (CC) structure and TIR-NB-LRR or TNL proteins with a Toll/interleukin-1 receptor (TIR) domain (Pan, Wendel et al. 2000, Andolfo, Jupe et al. 2014). Activation of NLR receptors usually results in a hypersensitive response, which is associated with restricting pathogen colonization of the host tissue (Spoel and Dong 2012, Win, Chaparro-Garcia et al. 2012).

In the Solanaceae (nightshade) botanical family the CNL class of NLRs has dramatically expanded (Andolfo, Jupe et al. 2014). In tomato, for example, 18 distinct clades of CNL genes are present in every chromosome, whereas only a single TNL clade occurs (Andolfo, Jupe et al. 2014). Two agronomically important genes occur in the Solanaceae CNL-8 clade. *R3a* and *I2* as discussed earlier, mediate resistance to the late blight oomycete pathogen *Phytophthora infestans* and the wilt fungus *Fusarium oxysporum f. sp. lycopersici* respectively (Ori, Eshed et al. 1997, Simons, Groenendijk et al. 1998, Armstrong, Whisson et al. 2005, Bos, Kanneganti et al. 2006, Takken and Rep 2010). *F. oxysporum f. sp. lycopersici* secretes the effector AVR2, which activates I2 immunity. As stated previously, pathogens evolve to overcome the NLR-mediated disease resistance by emerging new races. Similarly in this system, in races 3 of *F. oxysporum f. sp. lycopersici*, single point mutations of AVR2 abolish recognition by I2 and break the I2-mediated resistance (Houterman, Ma et al. 2009, Takken and Rep 2010).

S. demissum R3a is one of the first late blight *R* genes to be bred in cultivated potato (Hawkes 1990, Gebhardt and Valkonen 2001, Huang, van der Vossen et al. 2005). The R3a immune receptor as previously described in chapter 1 strongly responds to the *P. infestans* RXLR-type host-translocated effector $AVR3a^{KI}$ but weakly to

AVR3a^{EM}, which differ in only two amino acids in the mature protein (Armstrong, Whisson et al. 2005, Bos, Kanneganti et al. 2006). Strains of *P. infestans* that carry *Avr3a^{KI}*, either in a homozygous or heterozygous configuration, are avirulent on R3a potatoes (Armstrong, Whisson et al. 2005, Bos, Kanneganti et al. 2006, Bos, Chaparro-Garcia et al. 2009, Segretin, Pais et al. 2014). *P. infestans* strains homozygous for *Avr3a^{EM}* are virulent on R3a and have increased in frequency in *P. infestans* populations since the 19th century to become dominant in many potato growing regions of the world (Cooke, Cano et al. 2012, Chowdappa, Kumar et al. 2013, Li, van der Lee et al. 2013, Yoshida, Schuenemann et al. 2013, Yoshida, Burbano et al. 2014).

In a previous study, Segretin *et al.*, using random mutagenesis on the full length of *R3a*, managed to expand the response spectrum of R3a to AVR3a^{EM} variant of *P. infestans*. In that study, eight single-amino acid mutants, termed R3a+, gained response to AVR3a^{EM} while retaining the ability to respond to AVR3a^{KI} (Segretin, Pais et al. 2014). Six of these R3a+ mutations locate to the LRR domain, one in the NB-ARC and one in the CC. Interestingly, the two mutants in the CC and NB-ARC domains, R3a^{I148F} and R3a^{N336Y}, respectively, showed further gain-of-response to PcAVR3a4, an AVR3a homologue from the pepper pathogen *Phytophthora capsici*. Segretin *et al*., proposed that these mutants are sensitized, "trigger-happy" mutants, with a lower threshold for activation of the NLR receptor resulting in enhanced response to weak elicitors (Segretin, Pais et al. 2014). However, the R3a+ mutants, and similar multiple site R3a mutants described by Chapman *et al.*, (Chapman, Stevens et al. 2014) did not translate in enhanced resistance to *P. infestans* isolates homozygous for the *Avr3a^{EM}* allele, indicating that the observed gain-of-response in the cell death assay did not translate into a gain of late blight resistance.

In this study, I took advantage of the relatively high sequence similarity between *S. demissum* R3a and its tomato ortholog I2 to test the extent to which gain-of-function mutants identified in one NLR can be transferred to a homologous receptor from another plant species. The specific objectives of this chapter were 1) to investigate whether transfer of the R3a+ mutations, residing at the N-terminal part of the protein, to the equivalent positions in I2 can expand the response spectrum to the stealthy AVR3a^{EM} variant of *P. infestans*; and 2) to test if I2 mutants with expanded response spectrum specificities provide resistance towards *P. infestans* strains carrying either of the AVR3a variants. This study was based on the initial observation that two residues mutated in the R3a+ mutants, R3a^{I148F} and R3a^{N336Y}, are conserved in I2

(Huang, van der Vossen et al. 2005), and the hypothesis that these residues are hotspots for sensitized phenotypes in the R3a/I2 class of NLRs. These experiments revealed that transfer of the two R3a+ mutations to I2 resulted in a loss-of-response for $I2^{I141F}$ and autoactivity for $I2^{N330Y}$ mutants. I then reasoned that other amino acid substitutions at the same positions might yield an expanded response phenotype, and therefore generated I2 mutant proteins carrying all possible amino acids in positions 141 and 330. Remarkably, one mutant, $I2^{I141N}$, displayed expanded response to both $AVR3a^{KI}$ and $AVR3a^{EM}$, and conferred partial resistance to *P. infestans* strains carrying either of the AVR3a variants. Further assays showed that in addition $I2^{I141N}$ responded to two stealthy *F. oxysporum f. sp. lycopersici* AVR2 effector variants that evade response by the wild-type I2 receptor. Most of the results presented have been used for publication[3].

4.2. Results

4.2.1. I2 responds weakly to $AVR3a^{KI}$

Given that *I2*[4] and *R3a* are orthologous genes, I first determined whether I2 responds to the two AVR3a variants from *P. infestans*. I co-expressed I2 with each of the AVR3a isoforms using *Agrobacterium tumefaciens*-mediated transient transformation (agroinfiltration) in the model plant *Nicotiana benthamiana* and scored for hypersensitive cell death phenotypes. Statistical analysis for all the HR experiments was carried out by calculating the standard deviation of the values obtained, to reveal how variable the HR response is in this system, as has previously been shown in the literature (Bos, Kanneganti et al. 2006, Segretin, Pais et al. 2014). I found that I2 responds weakly to $AVR3a^{KI}$ (HR index typically between 0.5 and 1.2 on a scale of 0 to 3 at 6 days post-infiltration (dpi)) (Fig. 4.1 and A2.2, A2.3-Appendix 2). Occasionally, I2 showed a weak response to $AVR3a^{EM}$ (HR index less than 0.5) (Fig. 4.1). Both AVR3a variants were expressed alone in *N. benthamiana* to exclude any possibility of weak autoactivity of these constructs (Fig. A2.4-Appendix 2). No cell death reaction was seen upon transient expression of neither AVR3a variant (Fig. A2.4-Appendix 2), suggesting that the I2/AVR3a cell death is specific. These findings, together with the high amino acid sequence similarity between R3a and I2,

[3] **Artemis Giannakopoulou, John F. C. Steele, Maria-Eugenia Segretin, Tolga O. Bozkurt, Ji Zhou, Silke Robatzek, Mark J. Banfield, Marina Pais and Sophien Kamoun**. (2015) Tomato I2 immune receptor can be engineered to confer partial resistance to the oomycete *Phytophthora infestans* in addition to the fungus *Fusarium oxysporum* MPMI.

[4] In this study we used the I2 clone GenBank number KR108299-see Appendix 2 (Fig. A2.1-Appendix 2) for more details.

prompted me to test the possibility that transferring previously identified R3a+ mutations to I2 expands the response profile of this NLR receptor.

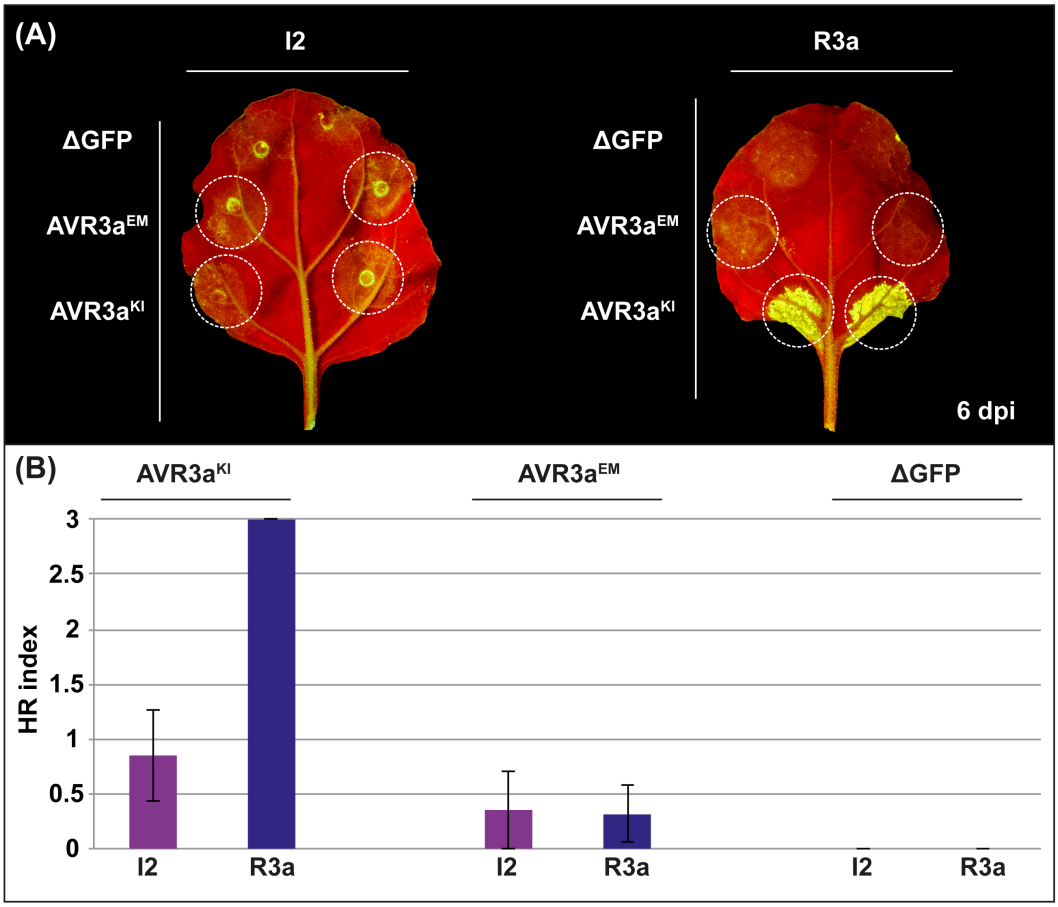

Figure 4.1: The tomato resistance protein I2 responds to AVR3a^{KI} from *Phytophthora infestans*.

A, Hypersensitive response (HR) phenotypes of wild-type I2 after co-expression with the *P. infestans* AVR3a variants in *N. benthamiana* leaves. Wild-type *I2* was under transcriptional control of the *Cauliflower mosaic virus* 35S promoter and AVR3a^{KI}, AVR3a^{EM} or a truncated version of green fluorescent protein (ΔGFP) were expressed from a *Potato Virus X* (PVX)-based vector. The picture was taken at 6 days post-infiltration (dpi). B, HR indices corresponding to the experiment described in A. Values scored at 6 dpi are plotted. Bars represent the average of 20 replicas for each combination of constructs; error bars represent standard deviation. Scoring of the HR was obtained according to an arbitrary scale (Fig. A2.2), as previously described (Bos, Kanneganti et al. 2006, Segretin, Pais et al. 2014). Circulated areas represent examples of different levels of HR.

4.2.2. Homology models of the NB-ARC domain highlight conserved R3a+ residues

R3a and I2 share a relatively high similarity (83% amino acid similarity) overall, with the NB-ARC domain displaying the highest sequence conservation (Huang, van der

Vossen et al. 2005) (Fig. 4.2A). Homology structure models of the conserved CC and NB-ARC domains were generated based on protein fold recognition algorithms implemented by IntFold (Fig. 4.2B) (Roche, Buenavista et al. 2011).

Sequence alignment of the protein domains revealed that R3a and I2 are conserved in the amino acid positions rendering the R3a+ mutations (highlighted in yellow I148, N336 and I141, N330 for R3a and I2 respectively) (Fig. 4.2A). For the CC domain the model was based on the CC domain of the potato NLR protein Rx (PDB code 4m70) (Hao, Collier et al. 2013), which appeared as the top-scoring template and since ~~as~~ there are no experimental data to guide our selection, an unbiased approach was used. Additional servers (iTASSER, Phyre2 and SWISS-MODEL) identified the CC domain of the barley NLR protein MLA10 as the top-scoring template for modelling of the I2 CC-domain. In all these models (either of which could be valid), in each of the structures the I2 I141 position is consistently positioned to the C-terminus of the defined coiled-coil units and is therefore predicted to be located at an inter-domain region between the CC and NB-ARC domains (Fig. 4.2B).

The template for the NB-ARC domain was Apaf-1 (PDB code 1Z6T chain B) (Riedl, Li et al. 2005), as the crystal structure of this template has been determined to the highest resolution and the residues forming the ATPase active site are appropriately positioned, in agreement with previously published experimental evidence showing that I2 has ATPase activity (Tameling, Elzinga et al. 2002). The I2 N330 position maps to the junction of the NB and ARC1 regions (Fig. 4.2B), near the NB binding site and adjacent regions that have been implicated in nucleotide exchange events in plant NLR proteins and associated with activity (Van Ooijen, Mayr et al. 2008).
The structural models indicate that the two R3a+ positions in the I2 CC and NB-ARC domain occur in inter-domain regions and mutations at these positions may affect the overall conformation dynamics of the protein. I therefore proceeded with the generation of I2 mutants in these positions.

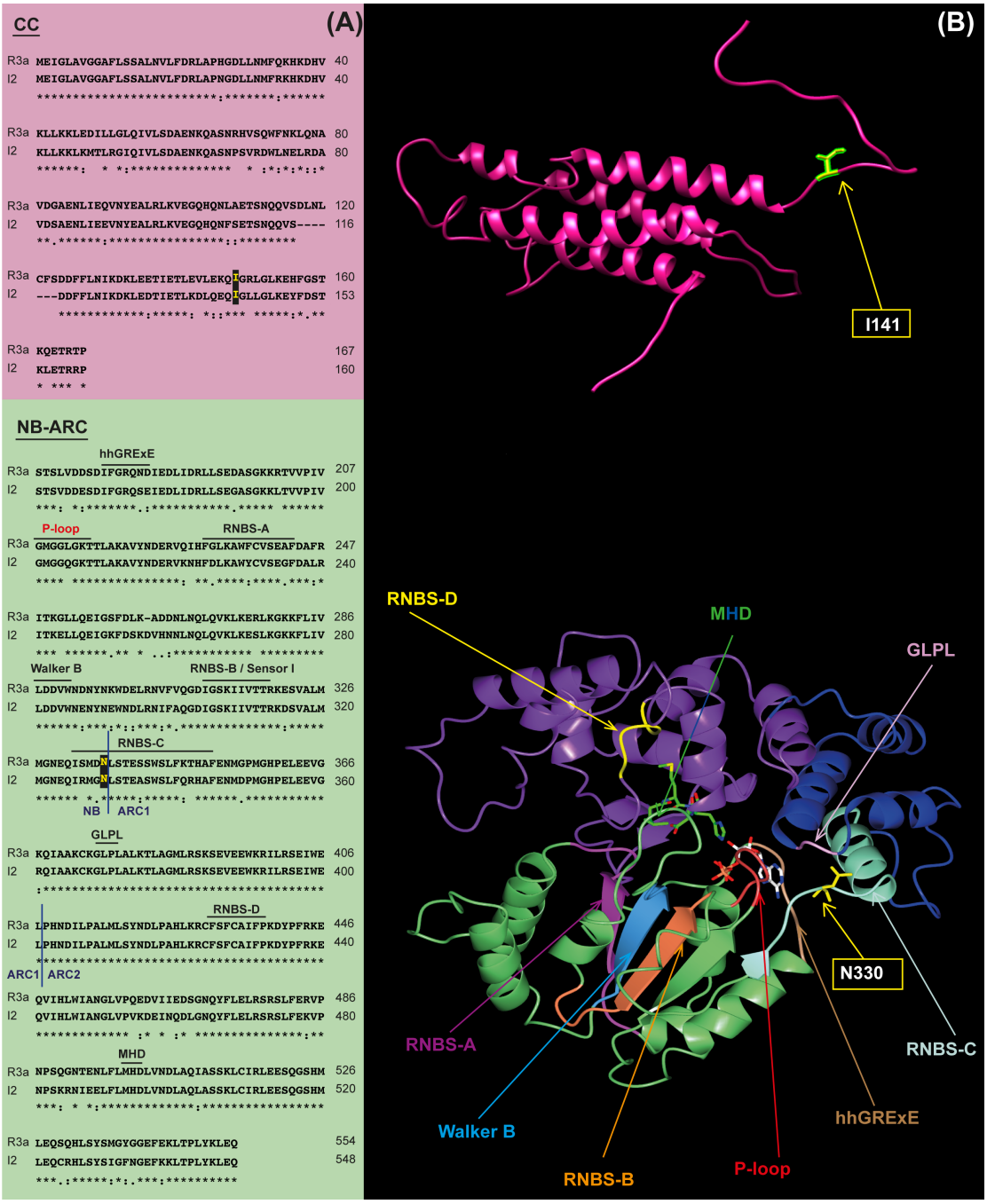

Figure 4.2: I2 and R3a are highly similar in the N-terminal region.

A, Protein sequence alignment of the CC and NB-ARC domains of I2 and R3a. The amino acid positions that were subjected to mutation are highlighted in yellow. Conserved R-protein motifs in the NB-ARC domain are overlined according to Ooijen *et al.*, (Ooijen, Burg et al. 2007). Blue lines delimit the 3 subdomains of the NB-ARC: NB, ARC1 and ARC2. B, Structural model of the CC and NB-ARC domains of I2. Models were generated by remote homology modeling using the INTFold2 server (Roche, Buenavista et al. 2011). The CC domain is shown in pink and the NB-ARC is shown in three different colours depending on the subdomain: NB (green), ARC1 (purple), ARC2 (blue). Amino acids corresponding to the single-residue I2 mutations are shown in yellow stick representation. The carbon atoms of ATP are shown in white. The locations of R-protein motifs are indicated with arrows.

4.2.3. The $I2^{I141F}$ and $I2^{N330Y}$ mutants are nonfunctional and autoactive, respectively

I generated I2 mutants carrying the equivalent to $R3a^{I148F}$ and $R3a^{N336Y}$ in the CC and NB-ARC domains. These I2 mutants, $I2^{I141F}$ and $I2^{N330Y}$, were tested with $AVR3a^{KI}$ and $AVR3a^{EM}$ using agroinfiltration in *N. benthamiana*. $I2^{I141F}$ showed a loss-of-response as it did not trigger any cell death when co-expressed with either one of the AVR3a isoforms (Fig. 4.3). $I2^{N330Y}$ showed an autoactive phenotype, as it triggered strong cell death (HR index 3) even in the absence of effector proteins (Fig. 4.3). These results indicate that the specific R3a+ amino acid substitutions do not confer the desirable expanded response phenotypes to I2, however highlight the importance of these two positions for I2 activity.

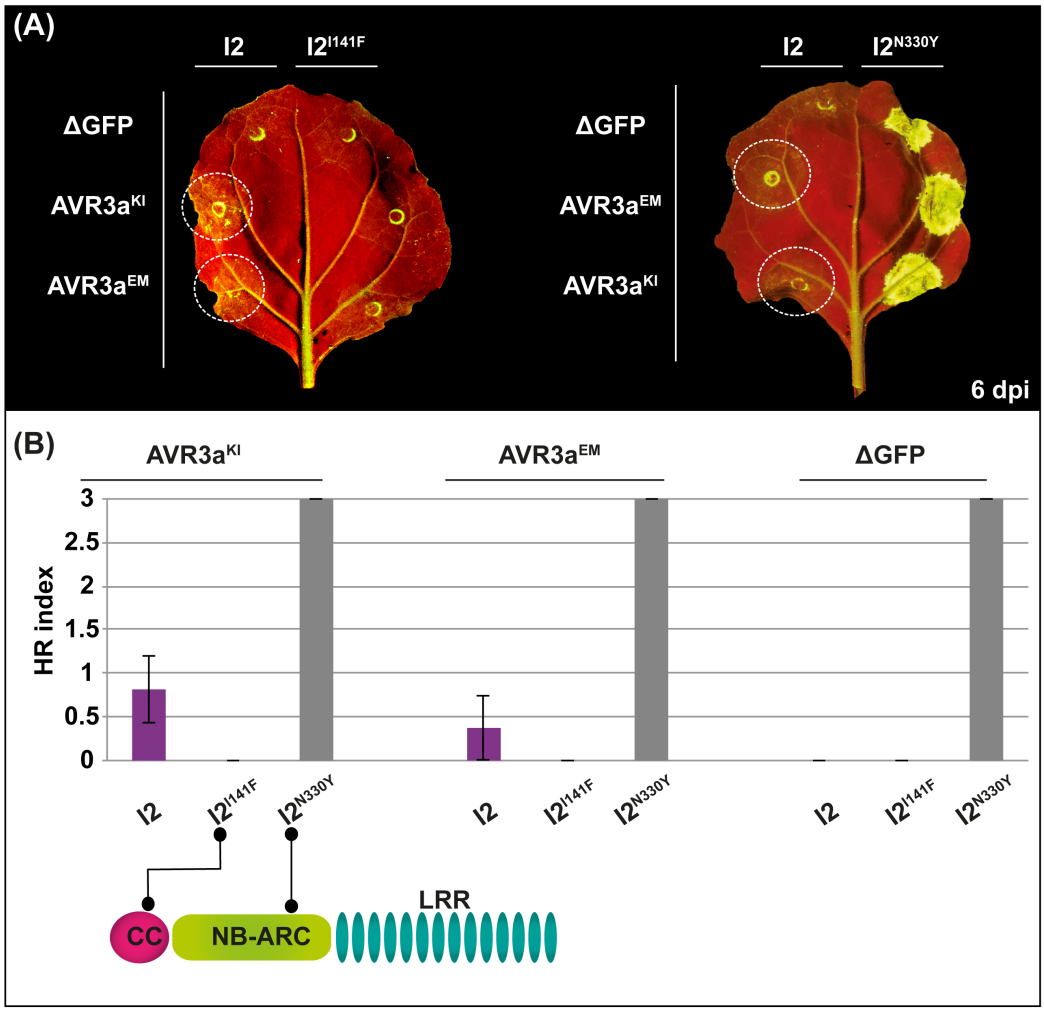

Figure 4.3: I2 mutants carrying the precise R3a+ single-amino acid mutations in the CC and NB-ARC domains show a loss-of-response and an autoactive phenotype respectively.
A, Hypersensitive response (HR) phenotypes of wild-type I2, $I2^{I141F}$ and $I2^{N330Y}$ after co-expression with the *Phytophthora infestans* AVR3a variants in *N. benthamiana*

leaves. Wild-type *I2* and *I2* mutants were under transcriptional control of the *Cauliflower mosaic virus* 35S promoter and AVR3a^{KI}, AVR3a^{EM} or a truncated version of green fluorescent protein (ΔGFP) were expressed from a *Potato Virus X* (PVX)-based vector. The pictures were taken at 6 days post-infiltration (dpi). B, HR indices corresponding to the experiment described in A. Values scored at 6 dpi are plotted. The cartoon indicates the approximate positions of the mutations. Bars represent the average of 16 replicas for each combination of constructs; error bars represent standard deviation. Scoring of the HR was obtained according to an arbitrary scale (Fig. A2.2), as previously described (Bos, Kanneganti et al. 2006, Segretin, Pais et al. 2014). Circulated areas represent examples of different levels of HR.

4.2.4. I2 mutants at positions 141 and 330

To test whether additional amino acid substitutions at I2 positions 141 and 330 yield an expanded response to AVR3a, I randomly mutagenized I2 codons 141 and 330 (Fig. 4.4A). Mutagenized *I2* molecules were then cloned in the binary vector pk7WG2 (Karimi, Inze et al. 2002) under the transcriptional control of the *Cauliflower mosaic virus* 35S promoter, and transformed into *A. tumefaciens.* Mutants representing all different amino acids were obtained only for position 330, whereas I only generated a library with 12 amino acids for position 141. The generated mutant clones were screened by co-expression with the AVR3a isoforms in *N. benthamiana*. The cell death phenotypes I acquired grouped the I2 mutant clones in four categories: strongly autoactive (HR index = 3 in the absence of effectors), loss-of-response (no HR phenotype), similar profile to wild-type I2, and gain-of-response (expanded response to AVR3a^{EM}). Substitutions of the Asn in position 330 with Cys, His, Leu, Tyr, Arg, Thr, Ser, Val, Trp, Phe, Met and Ile resulted in autoactive mutants; Glu, Pro and Asp gave a loss-of-response phenotype and Lys, Gln, and Ala had a similar response profile to the wild-type I2 (Fig. 4.4). Substitution of the Ile in position 141 with Tyr resulted in an autoactive mutant; Arg, Pro, Val, Ala, Lys, Leu, Thr and Asp showed a loss-of-response phenotype. Interestingly, I2^{I141N}, which carries a substitution of Ile to Asn in position 141, responded more strongly to AVR3a^{EM} compared to the wild-type I2 (Fig. 4.5).

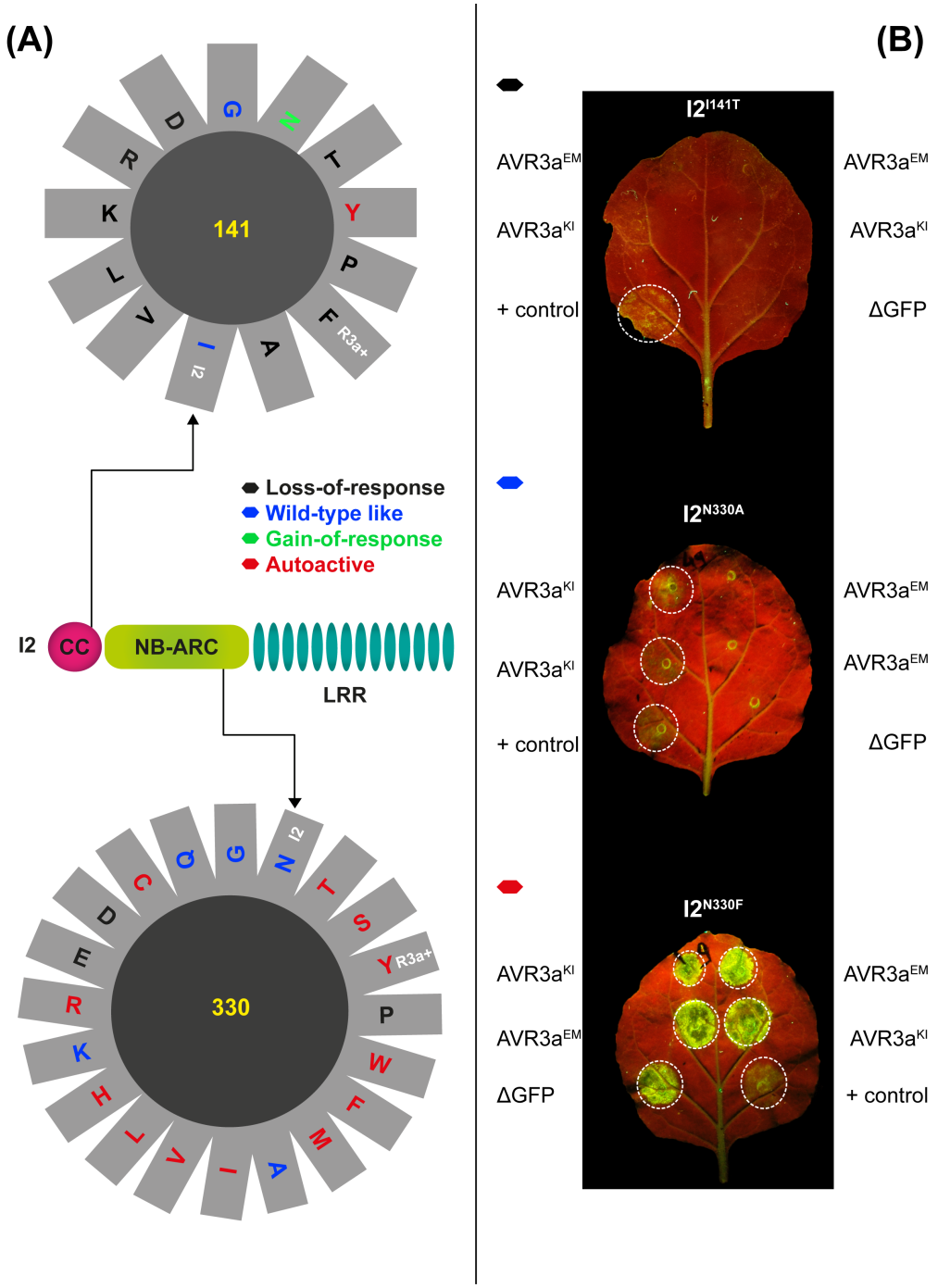

Figure 4.4: I2 mutant libraries carrying randomized amino acids at positions 141 and 330.

The full length *I2* coding sequence (3,801 bp) was used as template for a polymerase chain reaction-based mutagenesis targeted to the corresponding coding sequence positions. Amplification products were cloned in the binary vector pK7WG2 (under transcriptional control of the *Cauliflower mosaic virus* 35S promoter) and transformed into *A. tumefaciens*. The library was screened for gain-of-response phenotypes by co-agroinfiltration in *N. benthamiana* of the I2 mutant clones with *Phytophthora infestans* AVR3a^{KI} and AVR3a^{EM} expressed from a *Potato virus X* (PVX)-based vector. A, Amino acid substitutions are coloured according to the response phenotypes obtained: black (loss-of-response), blue (wild-type like), green (gain-of-response), red (autoactive). Wild-type amino acids at these positions and amino acids corresponding to the R3a+ mutants are indicated by the I2 and R3a+

labels respectively. B, Hypersensitive response (HR) phenotypes of selected I2 mutants generated in this library ($I2^{I141T}$, $I2^{N330A}$, $I2^{N330F}$) after co-expression with the *Phytophthora infestans* AVR3a variants in *N. benthamiana* leaves, representing a loss-of-response, a wild-type like and an autoactive phenotypic example respectively. Circulated areas represent examples of different levels of HR.

4.2.5. A single amino acid change expands the response of I2 to $AVR3a^{EM}$

The gain-of-response $I2^{I141N}$ identified in the screen was selected for further characterization. To determine the extent to which the single-site I141N mutation in the CC domain of I2 expands its response profile to the $AVR3a^{EM}$ variant, I co-expressed $I2^{I141N}$ with both AVR3a isoforms using *N. benthamiana* agroinfiltration. $I2^{I141N}$ responded to $AVR3a^{EM}$ (HR index between 2.5 and 3 in a scale of 0 to 3), and also exhibited a stronger response to $AVR3a^{KI}$ when compared to wild-type I2 (HR index ~2 vs 0.7 for the wild-type) (Fig. 4.5). $I2^{I141N}$ also exhibited a weak response in the absence of effector (HR index ~1), which was lower than the response to the two AVR3a variants. These results indicate that a single-amino acid change in the CC domain of I2 (I141N) is sufficient to expand the response profile of the wild type I2 receptor to $AVR3a^{EM}$ and increase its response to the $AVR3a^{KI}$ isoform.

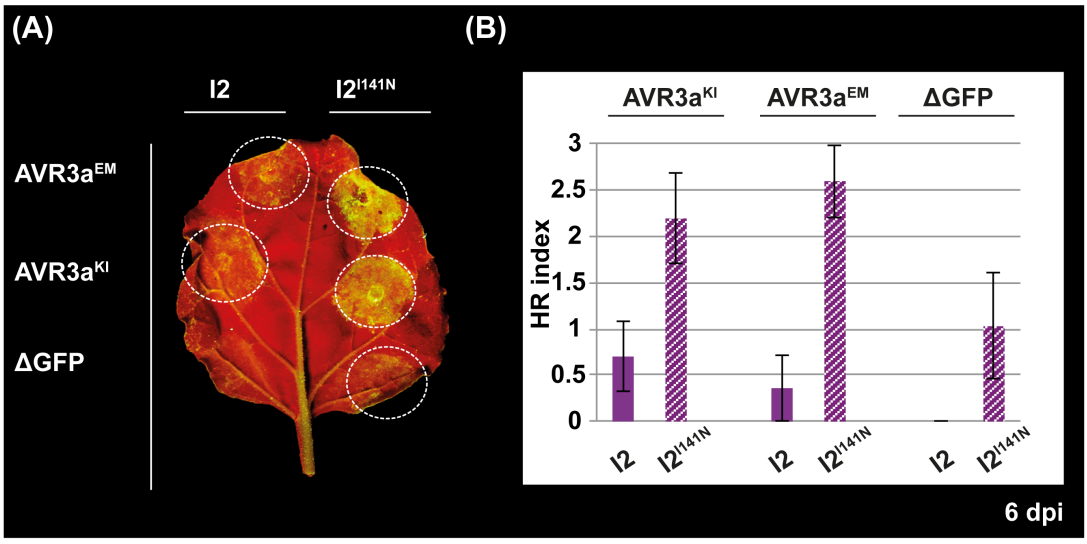

Figure 4.5: $I2^{I141N}$ responds to $AVR3a^{EM}$ while retaining the response to the $AVR3a^{KI}$ isoform.

A, Hypersensitive response (HR) phenotypes of wild-type I2 and $I2^{I141N}$ after co-expression with the *Phytophthora infestans* AVR3a variants in *N. benthamiana* leaves. The wild-type and mutant *I2* were under transcriptional control of the *Cauliflower mosaic virus* 35S promoter and $AVR3a^{KI}$, $AVR3a^{EM}$ or a truncated version of green fluorescent protein (ΔGFP) were expressed from a *Potato Virus X* (PVX)-based vector. The picture was taken at 6 days post-infiltration (dpi). B, HR indices corresponding to the experiment described in A. Values scored at 6 dpi are

plotted. Bars represent the average of 20 replicas for each combination of constructs; error bars represent standard deviation. Scoring of the HR was obtained according to an arbitrary scale (Fig. A2.2), as previously described (Bos, Kanneganti et al. 2006, Segretin, Pais et al. 2014). Circulated areas represent examples of different levels of HR.

4.2.6. I2^{I141N} protein has altered accumulation levels compared to wild-type I2 protein

The effect of the I141N mutation on the stability of the I2 protein was investigated by performing western blot assays where I used a polyclonal antibody raised against the CC domain of R3a. Samples were collected at 2, 3 and 5 dpi, as I reasoned that this range of time points would allow me to detect potential differences in the protein levels between I2 and I2^{I141N}. Interestingly, at 2 and 5 dpi, wild-type I2 yielded a more intense signal than the I2^{I141N} mutant (Fig. 4.6). As an additional control in this experiment I used the loss-of-response mutant protein I2^{I141T} which only yielded a weak signal at 5 dpi (Fig. 4.6). Additional analysis on the remaining loss-of-response mutants showed that all of them are expressed with most of them giving a weaker signal than the wild-type I2 protein (Fig. A2.5-Appendix 2).

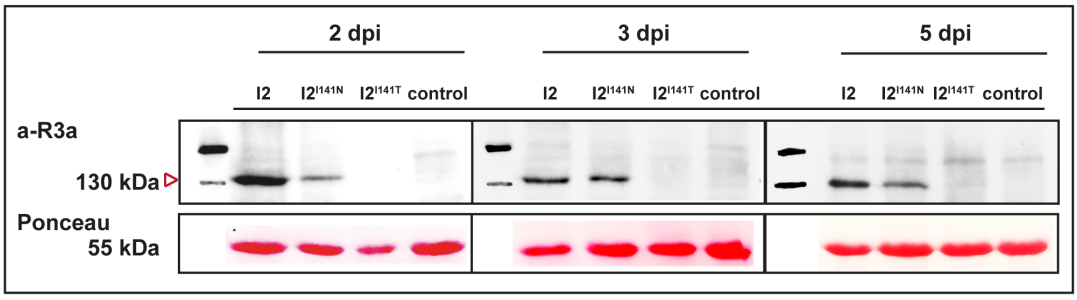

Figure 4.6: The I2^{I141N} gain-of-response mutant has altered accumulation compared to wild-type I2 *in planta*.
Nicotiana benthamiana leaves were agroinfiltrated with constructs to express wild-type and mutant I2 or a truncated version of green fluorescent protein, ΔGFP (control). Total protein extracts from leaves sampled at 2, 3 and 5 days post-infiltration (dpi) were subjected to SDS-PAGE followed by immunoblotting with a polyclonal antibody raised against the CC domain of R3a (a-R3a, upper panel). A band of approximately 145 kDa, indicated with a red arrow, corresponding to I2 was present in total extracts of the leaves infiltrated with the *I2* and *I2^{I141N}* constructs. Ponceau S staining of Rubisco (lower panel) is shown as control of the amount of protein loaded and transferred in each lane. Sizes (in kDa) are indicated on the left. I2^{I141T} is a loss-of-response I2 mutant and was included as an additional negative control in this experiment. Different boxes indicate different blots.

4.2.7. R3a^{I148N} has a response profile similar to that of wild-type R3a

To examine whether the I141N mutation in the CC domain of I2 could also alter the response profile of R3a, I introduced this mutation in R3a and generated the R3a^{I148N} mutant. R3a^{I148N} was then co-expressed with the AVR3a variants using agroinfiltration assays in *N. benthamiana* and I scored the intensity of the cell death developed. The response of R3a^{I148N} to the two AVR3a isoforms was similar to that of wild-type R3a, as a potent hypersensitive response was detected only when the protein was co-expressed with AVR3a^{KI} (HR index ~3) (Fig. A2.6-Appendix 2). As previously reported (Bos, Chaparro-Garcia et al. 2009), a weak response was sometimes observed when the wild type R3a protein was co-expressed with the AVR3a^{EM} variant, a trend that was also observed for the R3a^{I148N} mutant (HR index < 0.2, Fig. A2.6-Appendix 2). These results indicate that, even though the 141/148 amino acid position in the CC domain is important for the activities of I2 and R3a, different amino acid substitutions are necessary to expand the response spectrum of these immune receptors.

4.2.8. I2^{I141N} confers partial resistance to a *P. infestans* strain expressing *Avr3a^{EM}*

To determine the degree to which the expanded response profile of I2^{I141N} translates into a wider resistance spectrum, I performed infection assays in *N. benthamiana* leaves expressing I2 and I2^{I141N} with different strains of *P. infestans*. I2 and I2^{I141N} proteins were expressed using *A. tumefaciens*-mediated transformation in leaves of three to four-week-old *N. benthamiana* plants. Inoculation of infiltrated leaves with *P. infestans* zoospore suspensions started approximately 15 hours after agroinfiltration. I first examined the effect of the wild-type I2 protein on *P. infestans* strain NL00228 homozygous for *Avr3a^{KI}* (Zhu, Li et al. 2012), or strain 88069 homozygous for *Avr3a^{EM}* (van West, de Jong et al. 1998). I2 expression restricted infection by *P. infestans* NL00228 as illustrated by the development of smaller lesion sizes compared to those observed in leaves expressing a control construct (Fig. 4.7). In contrast, I2 did not impact infection by strain 88069 resulting in no significant differences in lesion sizes (Fig. 4.7). Remarkably, the I2^{I141N} mutant protein restricted infection by both strains of *P. infestans*. I2^{I141N} expression restricted infection of *P. infestans* NL00228 to a similar level to the wild-type I2. Strikingly, expression of this mutant restricted infection by the *Avr3a^{EM}*-expressing *P. infestans* 88069 strain, as depicted by the smaller lesion sizes developed compared to those observed in

leaves expressing a control construct (Fig. 4.7 and A2.7-Appendix 2). These findings suggest that the $I2^{I141N}$ mutant has an expanded resistance profile to *P. infestans* relative to the I2 wild-type receptor.

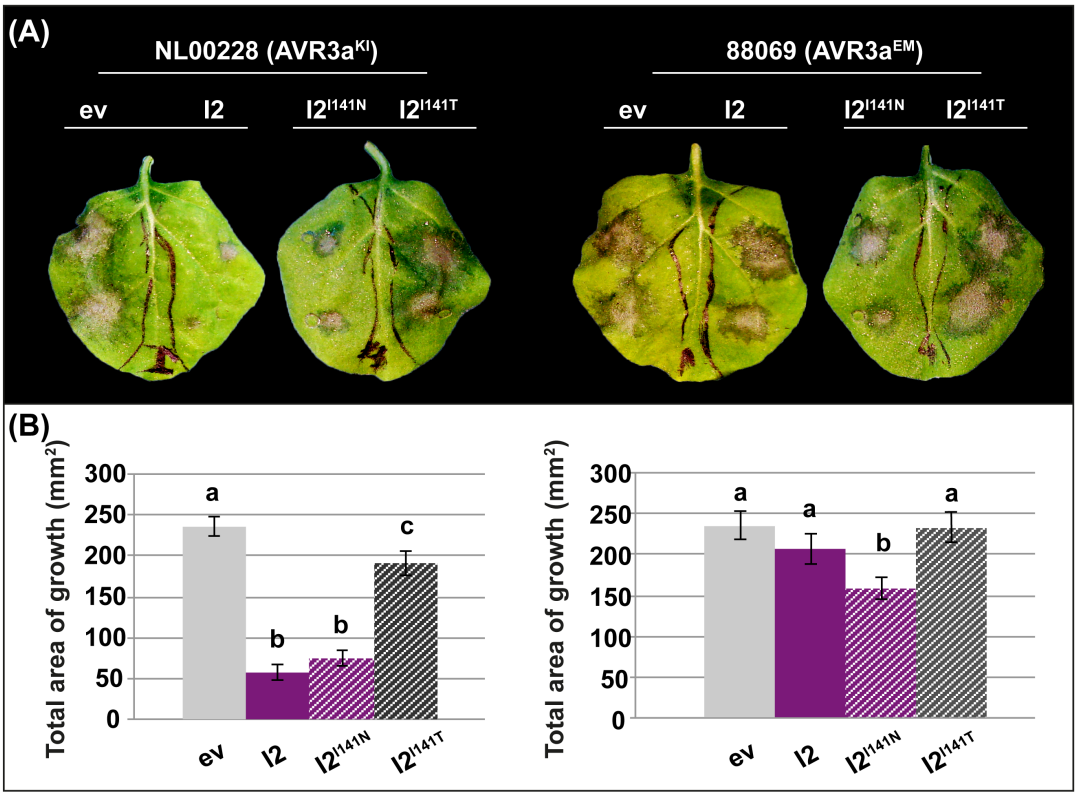

Figure 4.7: Wild-type I2 and $I2^{I141N}$ confer partial resistance to strains of *Phytophthora infestans*.

A, Wild-type I2 and I2 mutants were expressed in *N. benthamiana* leaves under transcriptional control of the *Cauliflower mosaic virus* 35S promoter. After approximately 15 hours, the infiltrated leaves were drop-inoculated with *P. infestans*-zoospore suspensions corresponding to the strains NL00228 (carrying $Avr3a^{KI}$) and 88069 (carrying $Avr3a^{EM}$). The pictures were taken at 6 days post-inoculation. B, The total area of *P. infestans* growth was determined with Image J software (Schneider, Rasband et al. 2012) (paragraph 2.7.1). Values corresponding to 6 days post-inoculation are plotted. Bars represent the average of 24 replicas for each treatment; error bars represent standard deviation. The experiment was performed 4 times and a representative repeat is shown. The Gateway binary vector pK7WG2 was included as negative control (empty vector, ev). $I2^{I141T}$ is a loss-of-response I2 mutant and was used as an additional negative control in this experiment. Significant differences between the groups are indicated by letters and were determined in an analysis of variance (ANOVA) followed by a Fisher's Least Significance Difference (LSD), with a 95% confidence interval ($p \leq 0.05$).

4.2.9. I2^{I141N} responds to *F. oxysporum f. sp. lycopersici* stealthy effectors AVR2$^{V>M}$ and AVR2$^{R>H}$

Given the expanded response phenotype of the I2^{I141N} mutant towards the AVR3a variants from *P. infestans*, I further investigated the extent to which I2^{I141N} has altered response to AVR2 effectors of *F. oxysporum f. sp. lycopersici* (Takken and Rep 2010). To achieve this, both I2 wild-type and I2^{I141N} mutant proteins were co-expressed with the AVR2 effector variants from *F. oxysporum f. sp. lycopersici* using agroinfiltration in *N. benthamiana*. Remarkably, I2^{I141N} responded to two out of the three stealthy AVR2 variants: AVR2$^{V>M}$ (HR index ~3) and AVR2$^{R>H}$ (HR index ~1.2), while it retained the capacity to respond to AVR2 from *F. oxysporum f. sp. lycopersici* race 2 (HR index ~2.5) (Fig. 4.8). These results indicate that the gain-of-response mutation identified based on one pathogen effector displays also increased response spectrum to effectors from another pathogen. The I2^{I141N} mutant of I2 has, therefore, expanded response to effectors from oomycetes and fungi, two phylogenetically unrelated plant pathogens.

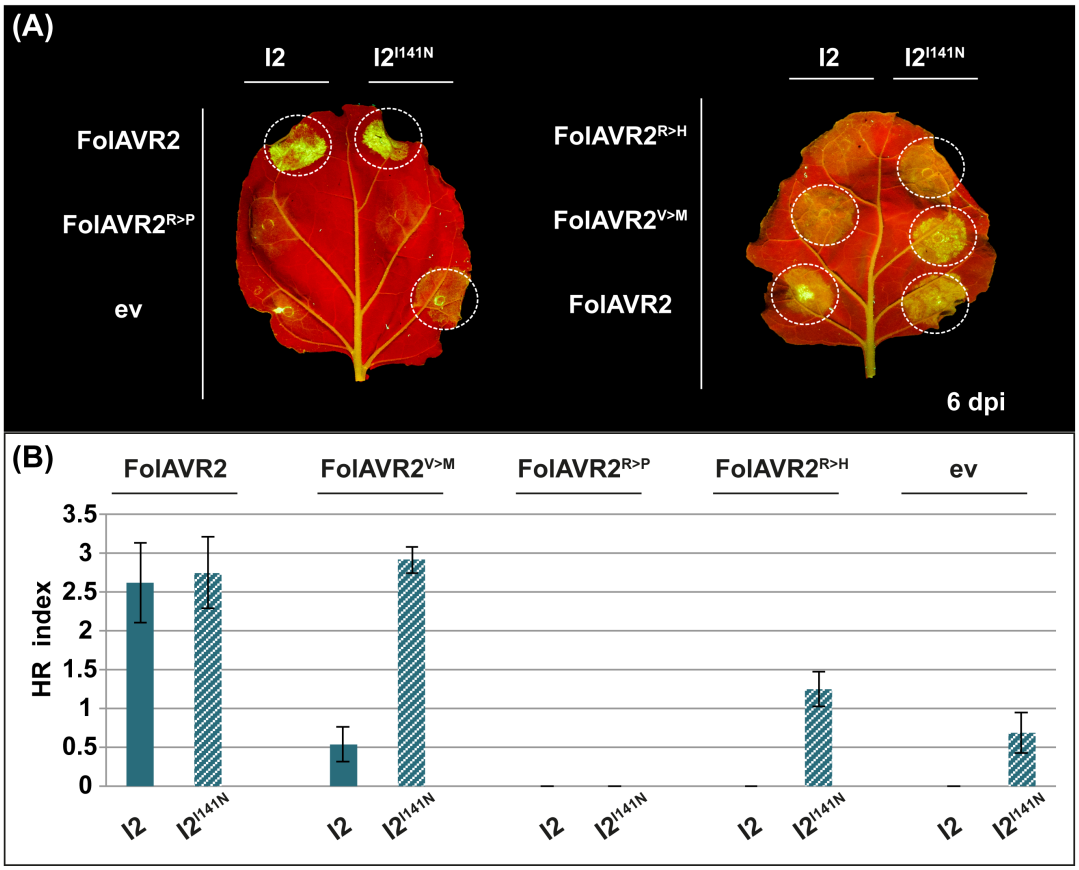

Figure 4.8: I2^{I141N} shows expanded response to *Fusarium oxysporum f. sp. lycopersici* (Fol) AVR2 variants from race 3.
A, Hypersensitive response (HR) phenotypes of wild-type I2 and I2^{I141N} after co-expression with the FolAVR2 variants from race 3 in *N. benthamiana* leaves. Wild-

type and mutant *I2* were under transcriptional control of the *Cauliflower mosaic virus* 35S promoter while FolAVR2, FolAVR2$^{V>M}$, FolAVR2$^{R>P}$ and FolAVR2$^{R>H}$ were expressed from the binary vector CTAPi. The CTAPi empty vector (ev) was included as negative control. The picture was taken at 6 days post-infiltration (dpi). B, HR indices corresponding to the experiment described in A. Values scored at 6 dpi are plotted. Bars represent the average of 18 replicas for each combination of constructs; error bars represent standard deviation. Scoring of the HR was obtained according to an arbitrary scale (Fig. A2.2), as previously described (Bos, Kanneganti et al. 2006, Segretin, Pais et al. 2014). Circulated areas represent examples of different levels of HR.

4.2.10. Preliminary results suggest that *I2^{I141N}* tomato lines are partially resistant to *P. infestans*

To investigate whether the expanded response phenotype of I2^{I141N} mutant immune receptor towards both AVR3a variants from *P. infestans*, translates to resistance, tomato plants (*S. lycopersicum* accession OH7814 - SGN758) were transformed via *A. tumefaciens* with *I2* wild-type and *I2^{I141N}*, *I2^{I141T}* mutant genes (under transcriptional control of the *Cauliflower mosaic virus* 35S promoter). Infections were performed on excised leaves upon which *P. infestans* zoospore droplets were placed. For this experiment I used primary transformant tomato lines (T0 generation) carrying *I2^{I141N}* and T2 generation plants carrying *I2* or plants that had been transformed with the empty vector pK7WG2 (EV). The reason for that selection was that the transformation process did not take place at the same time for all I2 constructs. Because the transformation using *I2^{I141T}* was not successful, as an additional control for the *I2^{I141N}* T0 lines, I included T0 lines that contained a truncated version of the *I2* gene.

All the *I2^{I141N}* tomato lines tested displayed no phenotypic abnormality suggesting that the slight autoactivity that the protein showed in the HR transient assays (Fig. 4.5 and 4.8) does not result in obvious morphological changes in the transgenic lines. In total I tested eight *I2^{I141N}* T0 plants, eight T0 plants containing a truncated version of *I2* (referred to as *I2^{X}* from now on), two *I2* T2 plants and 2 EV T2 plants. Wild-type OH7814 tomato lines were also included as additional controls in this experiment. Infection was carried out with *P. infestans* strains homozygous for either *Avr3a^{KI}* (NL00228) or for *Avr3a^{EM}* (88069). As expected, the *I2* T2 plants tested were resistant to *P. infestans* NL00228 (AVR3a^{KI}) as they developed significantly smaller lesions than the EV and wild-type OH7814 tomato lines (Fig. 4.9A and C). All the *I2^{I141N}* T0 plants tested were resistance *P. infestans* NL00228 (AVR3a^{KI}) as they

developed very small lesions, even smaller than the *I2* plants (Fig. 4.9A and C). Interestingly, one *I2*^{I141N} tomato plant, *I2*^{I141N}-5 had no apparent lesions, suggesting that this plant could not be infected. The *I2*^{X} T0 plants were depicted as susceptible as they developed lesions to a similar size to the EV and wild-type OH7814 tomato lines (Fig. 4.9A and C).

I2, EV and wild-type OH7814 tomato plants were all susceptible to *P. infestans* 88069 (AVR3a^{EM}) as they all developed similar size lesions (Fig. 4.9B and C). The *I2*^{I141N} T0 plants tested showed partial resistance to *P. infestans* 88069 (AVR3a^{EM}) as they developed smaller sizes than the *I2*, EV and wild-type OH7814 tomato lines (Fig. 4.9B and C). In more detail, *I2*^{I141N}-1, *I2*^{I141N}-3, and *I2*^{I141N}-7 T0 plants were the least infected, as revealed by the reduced lesions and subsequent statistical analysis of the infection, while *I2*^{I141N}-2, *I2*^{I141N}-4, *I2*^{I141N}-6 and *I2*^{I141N}-8 were infected to a greater extend, but still significantly lower that the control plants (Fig. 4.9B and C). Again, *I2*^{I141N}-5, was the only T0 plant that showed no lesion development (Fig. 4.9B and C). The *I2*^{X} T0 plants tested all developed greater lesions than the control plants and were depicted as susceptible (Fig. 4.9B and C). Genotypic characterization of the tomato plants tested revealed that all of them contain the *I2* gene, with the exception of the *I2*^{X} plants that don't carry the full *I2* gene (Fig. A2.8-Appendix 2).

These results suggest that tomato plants carrying *I2*^{I141N} confer resistance against *P. infestans* lines carrying *Avr3a*^{KI} and partial resistance against to *P. infestans* lines carrying *Avr3a*^{EM}, which is in agreement with the transient assays (Fig. 4.7). However, additional infection assays on progeny of the lines generated are required to draw any final conclusions. In this experiment, *I2*^{I141N}-5, developed no lesion after infection with either of *P. infestans* strains used. As this was the only T0 plant showing exactly the same phenotype in response to both *P. infestans* strains used, the possibility of failure of infection is ruled out. It will be very interesting to test the progeny of this line for resistance against *P. infestans*. Even though these results are overall promising, they are preliminary and additional characterization revealing number of insertions in all the plants tested, along with infection assays on their progeny are required.

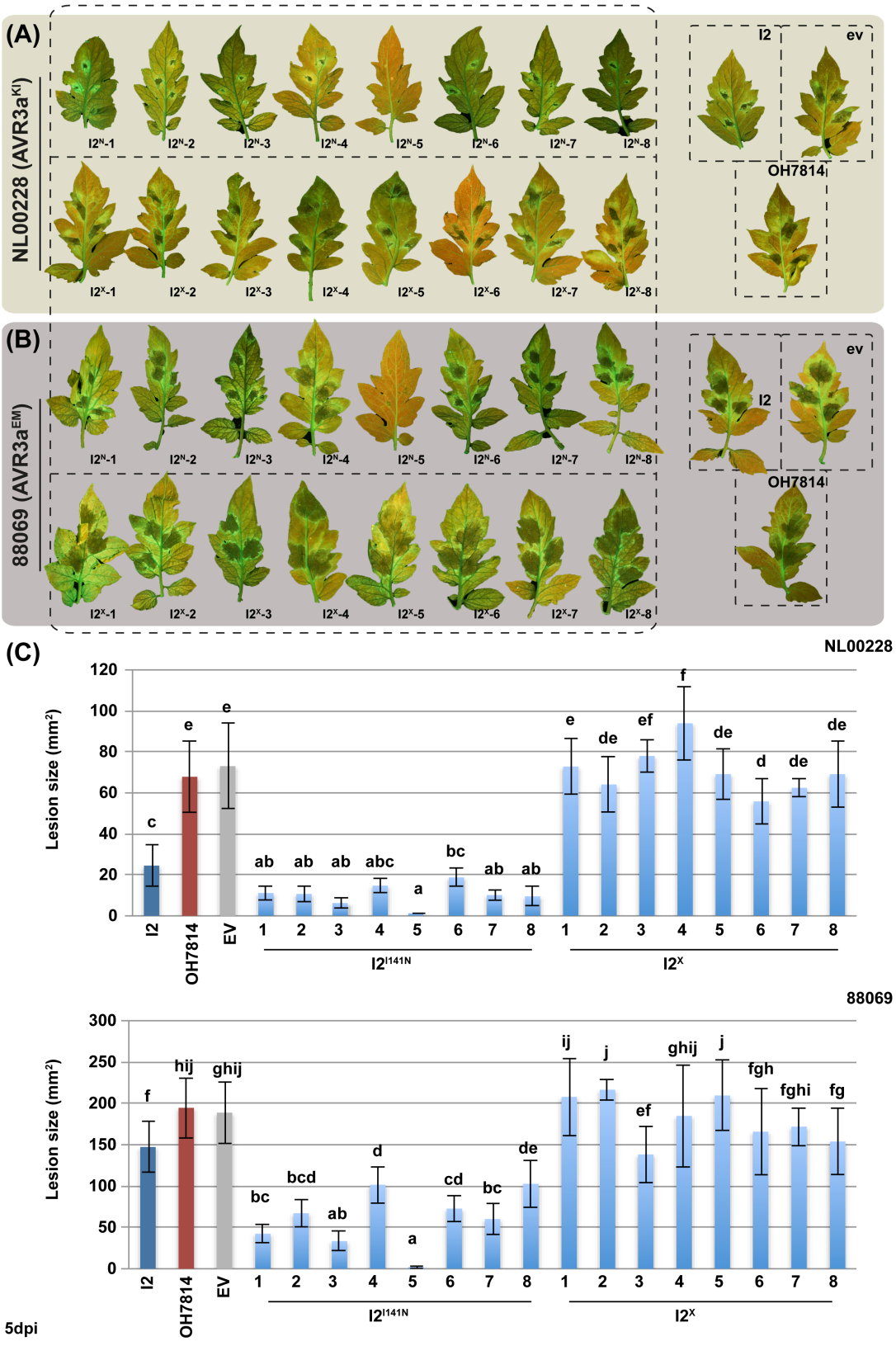

Figure 4.9: Plants carrying *I2*^{I141N} are resistant to *P. infestans*.

Leaves from three- to four-week-old tomato plants were subjected to *P. infestans* infection. Primary transformants (T0 generation) of *I2*^{I141N} (eight lines) and *I2*^{X} (eight lines), two *I2* and two EV plants (T2 generation) were used in this experiment. For simplicity, only one *I2* and one EV plants are shown in the figure. A, Tomato leaves

infected with *P. infestans* strain NL00228 (homozygous for *Avr3a*^{KI}). B, Tomato leaves infected with *P. infestans* strain 88069 (homozygous for *Avr3a*^{EM}). Pictures were taken 5 days post-inoculation (5 dpi). C, Lesion size following inoculation with *P. infestans* strain NL00228 (upper panel) or *P. infestans* strain 88069 (lower panel) was calculated using Image J software (paragraph 2.7.1). Bars represent the average of 6 lesions. Error bars represent standard deviation. Different letters indicate statistically significant difference according to an ANOVA analysis followed by Fisher's LSD test with a 95% confidence interval.

4.3. Discussion

I2 from tomato and R3a from potato are the two orthologous NLR immune receptors that have been previously described as mediating resistance to fungi and oomycetes, respectively. In this study, I discovered that I2 weakly responds to the AVR3a^{KI} effector from *P. infestans* and also confers resistance to a strain of this pathogen that expresses this effector (Fig. 4.1, Fig. 4.7). Targeted mutagenesis of the *I2* gene resulted in the identification of an I2 mutant protein, I2^{I141N}, with enhanced response specificities to both AVR3a^{KI} and the stealthy AVR3a^{EM} isoform that is produced by R3a-virulent races of *P. infestans* (Fig 4.5). Remarkably, I2^{I141N} conferred partial resistance to an R3a-breaking strain of *P. infestans* that expresses *Avr3a*^{EM} (Fig. 4.7). I further showed that I2^{I141N} responds to two out of three *F. oxysporum f. sp. lycopersici* AVR2 stealthy variants that evade response by the wild-type I2 (Fig. 4.8). Preliminary data also suggest that transgenic tomato plants carrying the gain-of-response *I2*^{I141N} mutant are resistant to *P. infestans* (Fig. 4.9). These findings open up exciting perspectives for the budding field of synthetic disease resistance NLR receptors (Farnham and Baulcombe 2006, Harris, Slootweg et al. 2013, Segretin, Pais et al. 2014). I have showed that knowledge generated on one NLR receptor can be exploited to improve homologous NLRs from other plant species. Furthermore, I suggest that synthetic NLR immune receptors can be engineered to confer resistance to phylogenetically divergent pathogens. Overall, these approaches can be applied to develop synthetic immune receptors that are beneficial to agriculture.

The study focused on two previously identified mutations at the N-terminal part of R3a (R3a^{I148F} and R3a^{N336Y}) which were transferred to I2 based on the high level of homology the two proteins exert at this region. The I2 mutants that were generated resulted in a loss-of-response (I2^{I141F}) and autoactive phenotype (I2^{N330Y}) respectively. Little is known about the underlying mechanisms in the I2 and R3a

systems. Based on the previous study by Segretin *et al.*, (Segretin, Pais et al. 2014) I propose that the amino acid positions identified are important for the activity of these NLR receptors. It is worth mentioning that the amino acids surrounding these two positions in the CC and NB-ARC domain of I2 (141 and 330) are different in R3a. Therefore, it is possible that when these residues are combined with the introduced substitutions, they affect the protein activity by preventing interaction with downstream signalling components ($I2^{I141F}$) or by changing the overall conformation of the protein leading to a constitutive activated state ($I2^{N330Y}$). Based on the structural modelling, the position 141 of I2 is located after the structurally defined CC domain, at an inter-domain region between the CC and NB-ARC regions (Fig. 4.2B). Therefore, it is possible that a change in this residue perturbs domain-domain interactions, affecting the function of this region and interfering with the overall performance of the protein. Previous studies have highlighted the involvement of the CC domain in pathogen perception and downstream signaling (Rairdan and Moffett 2006, Maekawa, Cheng et al. 2011, Chen, Liu et al. 2012, Hao, Collier et al. 2013). Rairdan *et al.*, have previously proposed that motifs in the CC domain of the potato CNL Rx protein, including the highly conserved EDVID, mediate interactions important for the function of the protein (Rairdan, Collier et al. 2008). However, position 141 in the I2 CC domain doesn't appear to be close to the EDVID motif (Fig. 4.2), therefore we cannot be sure about the mechanism underlying the mutation in that position. In the same study, Rairdan *et al*., further suggest a model where the signaling activity of the NB domain is defined by the joint function of both the CC and LRR domains and that this regulation is recognition dependent (Rairdan, Collier et al. 2008). Therefore, it is also possible that the specific amino acid change in the CC domain perturbs intramolecular interactions with the LRR domain thus enhancing the signaling activity of I2.

The position 330 is located near the predicted nucleotide-binding pocket of I2 (Fig. 4.2B), a region proposed to play a switch role between the active and inactive state of NLR proteins (Tameling, Vossen et al. 2006). A previous study has shown that single-amino acid mutations near the nucleotide-binding pocket of the potato NLR protein Rx, enhanced the expanded response conferred by a single mutation in the LRR domain, resulting in resistance to PopMV (Harris, Slootweg et al. 2013). However, saturation mutagenesis in position 330 in I2 did not result in expanded response phenotypes. It is possible that mutations in this position affect the affinity or catalysis of the ATP/ADP nucleotide. Further analysis is required before any firm conclusions can be drawn.

Stirnweis *et al.*, identified two positions in the NB-ARC domain of the wheat powdery mildew resistance gene *Pm3*, that when mutated enhance the ability of the protein to trigger cell death in *N. benthamiana* and also result in expanded resistance of the *Pm3f* allele in wheat. They further showed that the same mutations affected the activity of another CNL immune receptor in rice, Bph14, highlighting the importance of these two amino acids in a distantly related protein (Stirnweis, Milani et al. 2014). In addition, Ashikawa *et al.*, working on two members of the Pik locus in rice, the broad-spectrum *Pikm1-TS* and narrow spectrum *Pik1-KA* gene, generated chimeras to identify which domains define the recognition specificity. They found that a combination of the CC-NB of Pikm1-TS and the LRR of Pik1-KA was sufficient for resistance to a blast fungus isolate virulent only to Pik1-KA. Their results suggested that one or more of the polymorphic amino acids in the CC and/or NBS domain are responsible for the recognition specificity (Ashikawa 2012). Overall, these studies support the view that the N-terminal part of NLR proteins is implicated in the perception of the pathogen. In conclusion, although our $I2^{I141N}$ mutant appears to be sensitized it may also have altered specificity. Future work aiming at identifying the mechanisms mediating the observed expanded response of the $I2^{I141N}$ mutant protein and also addressing whether this response translates to resistance are required.

My results showed that transfer of the precise mutations previously identified in R3a (Segretin, Pais et al. 2014) to I2 did not yield the desirable phenotype, however it helped me focus my screens for improved I2 mutants. The $I2^{I141N}$ mutant identified in this study has expanded response to both AVR3a isoforms from *P. infestans* (Fig. 4.5) and also to two AVR2 variants from *F. oxysporum f. sp. lycopersici* race 3 (Fig. 4.8). This mutant however, shows a weak HR in the absence of effectors, suggesting that it has increased activation sensitivity. Most likely, this sensitized “trigger-happy” mutant has a lower threshold for activation compared to wild-type I2 and is more easily activated by weak elicitors. The western blot assays revealed altered accumulation levels in the $I2^{I141N}$ mutant protein (Fig. 4.6) which could be an indication that this mutation affects the overall conformation of the protein in a way that could make it easier for the protein to get activated (Schornack 2006). Alternatively, that mutated protein could have an altered ATP binding ability. In the wild-type I2 protein, both forms (ATP-bound, “on”; ADP-bound, “off”) are kept in a dynamic equilibrium and in the absence of an elicitor I2 would predominantly be inactive. In a previous study, an autoactive version of I2 was shown to be impaired in nucleotide hydrolysis (Tameling, Vossen et al. 2006). Similarly, an autoactive version

of the flax M NLR protein shows increased preference for binding ATP (Williams, Sornaraj et al. 2011). To examine the possibility that this mutation in the N-terminal part of I2 modifies the threshold for activation by altering the ability of the protein to bind ATP, further biochemical tests on $I2^{I141N}$ are required.

The pathogenicity assays showed that I2 confers resistance to a *P. infestans* isolate homozygous for the $Avr3a^{KI}$ allele (Fig. 5.7) and the preliminary data of the transgenic tomato lines presented (Fig. 5.9) also suggest that tomato lines carrying this gene may confer strain-specific resistance to *P. infestans*. However, the level of HR observed between I2 and $AVR3a^{KI}$ was relatively weak therefore we cannot rule out that other effectors present in this *P. infestans* determine the observed I2-mediated resistance. The vast majority of late blight lineages can infect both potato and tomato plants (Goodwin, Smart et al. 1998), although some lineages primarily infect tomato and are not likely to cause disease on potato plants in the field (Hu, Perez et al. 2012). An intensive screen of 45 *P. infestans* isolates from Canada, Mexico, US, Argentina, Ecuador, Denmark, Netherlands and Scotland revealed that 40 of them were homozygous for the $Avr3a^{EM}$ allele, 14 carried both $Avr3a^{KI}$ and $Avr3a^{EM}$ while only 1 was homozygous for $Avr3a^{KI}$ (Armstrong, Whisson et al. 2005). In a more recent study Yoshida *et al*., compared the genomes of 11 ancient *P. infestans* strains with 15 modern isolates, and revealed that the $Avr3a^{KI}$ allele was dominant in ancient populations whereas both *Avr3a* alleles are found in modern isolates, with lineages homozygous for $Avr3a^{EM}$ being more common (Yoshida, Schuenemann et al. 2013). Even though in many *P. infestans* populations the $Avr3a^{EM}$ allele dominates, epidemics are often caused by clonal lineages. *I2*-expressing tomatoes may provide some level of resistance to epidemics caused by strains homozygous for $Avr3a^{KI}$ however these races are rare in modern *P. infestans* populations. It is therefore clear that improved mutants with a broader spectrum of resistance to the dominant $Avr3a^{EM}$ carrying *P. infestans* races are needed. Unfortunately, the previously identified R3a+ mutants failed providing resistance against *P. infestans* (Chapman, Stevens et al. 2014, Segretin, Pais et al. 2014). The $I2^{I141N}$ mutant identified in this study gives partial resistance to *P. infestans* strains carrying either of the *Avr3a* alleles in the transient assays used (Fig. 4.7). Remarkably, preliminary data from pathogenicity assays on stable transgenic tomato lines carrying $I2^{I141N}$ show resistance against *P. infestans* (Fig. 4.9). Also, the $I2^{I141N}$ tomato lines tested showed no phenotypic abnormality, proposing that the weak autoactivation phenotype observed in the transient HR assays does not result in obvious morphological changes in the transgenic lines. These results overall suggest

that tomato lines carrying the *I2*^{I141N} mutant could confer resistance against *P. infestans* in the field.

NLR genes constitute a useful tool for generating sustainable disease resistant crops. Tomato is a characteristic example where traditional breeding approaches based on these genes have been used extensively (Andolfo, Jupe et al. 2014). Efficient transfer of *R* genes between plant species has become possible by recent transgenic approaches (Wulff, Horvath et al. 2011, Horvath, Stall et al. 2012, Narusaka, Kubo et al. 2013). However, the low occurrence of *R* genes with the useful response specificities has hampered the deployment of *NLR* genes through both conventional breeding and transgenic approaches. In this study, I showed that a synthetically generated NLR mutant protein has expanded response specificities towards two different pathogens. This approach could prove helpful in designing and engineering NLRs with novel activities, where mutants identified in one gene could be transferred to homologs. Similar to *I2* and *R3a* which share a high sequence homology, other *R* genes with high sequence similarity could benefit from this approach. Such examples are *RPP8*, *RCY1* and *HRT* from *Arabidopsis thaliana*, *Rx* and *Gpa2* from potato, *Mi-1.2* and *Rpi-blb2* from tomato and *Solanum bulbocastanum*, respectively. Random mutagenesis screens like the one leading to the identification of the R3a+ mutants (Chapman, Stevens et al. 2014, Segretin, Pais et al. 2014) have been extremely useful to determine critical positions affecting the response profile of *R* proteins. Recently, the advent of genome editing in plants (Feng, Zhang et al. 2013, Jiang, Zhou et al. 2013, Li, Norville et al. 2013, Mao, Zhang et al. 2013, Miao, Guo et al. 2013, Nekrasov, Staskawicz et al. 2013, Shan, Wang et al. 2013, Xie and Yang 2013) has opened a completely new era in the field of plant biotechnology. The application of genome editing to generate synthetic *R* genes with expanded response specificities could significantly broaden the perspectives for breeding crop plants with a far-ranging resistance.

CHAPTER 5: Mutants of the I2 tomato immune receptor confer resistance to race 3 of *Fusarium oxysporum f. sp. lycopersici*

5.1. Introduction

The wilt causing fungus *Fusarium oxysporum f. sp. lycopersici* is among the most destructive plants pathogens of tomato. This fungus is a perennial threat of tomato plants, since once the pathogen is established in a region there is no effective way of eliminating it (Agrios 2005). The only sustainable control practice is the use of resistant tomato varieties. A race-cultivar specific trend characterizes the interaction between *Fusarium oxysporum f. sp. lycopersici* and tomato as discussed earlier in chapter 1 and to date, three host-specific races of the pathogen have been described (Bohn and Tucker 1939, Alexander 1945, Grattidge and Obrien 1982, Volin and Jones 1982). Resistant tomato varieties for all three races of *F. oxysporum f. sp. lycopersici* are available following the introgression of resistance traits identified in wild tomato species into the cultivated *Lycopersicum esculentum.* As previously described, race-specific disease resistance in plants involves cell surface and intracellular immune receptors encoded by *R* genes, that recognise pathogen-secreted molecules called effectors, and subsequently activate immune responses (Dangl and Jones 2001, Dodds and Rathjen 2010, Win, Chaparro-Garcia et al. 2012). So far, tomato receptors responding to *F. oxysporum f. sp. lycopersici* effectors have been identified for all three races (Takken and Rep 2010). Incorporation of *R*-gene-mediated disease resistance as a crop improvement approach has been widely used, however the real challenge is to engineer crop plants with a broad-spectrum resistance, carrying resistance genes with expanded specificities, to counteract fast evolving pathogenic races.

As described previously, the vast majority of intracellular immune receptors belong to the nucleotide binding and leucine rich repeat (NLR) family of proteins, which constitutes an important defence element to the plant and also animal system (Maekawa, Cheng et al. 2011, Jacob, Vernaldi et al. 2013). In tomato, *R3a* and *I2* are two important resistance genes that belong to CNL clade 8. *R3a* in potato mediates strain-specific resistance to the late blight oomycete pathogen, *Phytophthora infestans* and *R3a*-carrying plants are resistant to strains of the

pathogen carrying the *Avr3a*^{KI} effector gene (Armstrong, Whisson et al. 2005, Bos, Kanneganti et al. 2006).

I2, the *R3a* ortholog in tomato, confers resistance to race 2 of the wilt fungus *F. oxysporum f. sp. lycopersici* (Simons, Groenendijk et al. 1998, Takken and Rep 2010). As mentioned earlier in chapter 1, the I2 immune receptor responds to the AVR2 effector present in race 2 of *F. oxysporum f. sp. lycopersici* (Takken and Rep 2010). In race 3 of *F. oxysporum f. sp. lycopersici* single point mutations in AVR2 (V41M, R45H, and R45P) abolish I2 recognition, without however altering the virulence of the fungus (Houterman, Ma et al. 2009). Ever since the first introgression of *I* genes in tomato back in 1939 (Bohn and Tucker 1939), there has been an arms race between tomato and *F. oxysporum f. sp. lycopersici* with a new race emerging approximately 20 years following introgression of each *R* gene (Alexander 1945, Booth 1971, Grattidge and Obrien 1982). To date, *R* genes that confer resistance to stealthy AVR2 variants in race 3 have not been reported.

In a previous study Segretin *et al*., identified eight single site R3a mutant proteins, termed R3a+ mutants, with expanded response to the AVR3a^{EM} variant that cannot be recognised by the wild-type R3a protein (Segretin, Pais et al. 2014). However, plants stably transformed with these mutants failed to provide resistance against *P. infestans* strains carrying the *Avr3a*^{EM} allele (Segretin, Pais et al. 2014).

In this study, I examined the extent to which the previously identified mutants in R3a with expanded response specificities can expand the response spectrum of its tomato ortholog, I2. As discussed previously in chapter 4, the initial hypothesis was that the N-terminal R3a+ positions are hotspots for sensitized phenotypes. This hypothesis was based on the fact that R3a+ mutants residing at the N-terminal part of R3a are conserved in I2, and that the two proteins share the highest similarity in this amino terminal part. Indeed, in chapter 4 I showed that these positions are important for the I2 response specificity; however, different amino acid substitutions expand the response spectrum of R3a and I2 (chapter 4, paragraph 4.3).

Here, I investigated the possibility that transfer of additional mutants identified in R3a to I2 would expand the response spectrum to its cognate effector AVR2 and/or the AVR2 variants that evade recognition by the wild-type I2 protein. The specific objectives were 1) to investigate whether transfer of the R3a+ mutations to the equivalent positions in I2, can expand the response spectrum to the stealthy AVR2

variants in *F. oxysporum f. sp. lycopersici*, 2) to test if tomato lines carrying the *I2* mutant genes with expanded response spectrum provide resistance towards races 2 and/or 3 of *F. oxysporum f. sp. lycopersici*, and 3) to gain insight into the underlying mechanisms mediating these I2/AVR2 interaction.

I showed that transfer of the eight R3a+ mutations in I2 resulted in a gain-of-response phenotype in only one case: the I2 mutant, $I2^{C967R}$, carrying a substitution at a conserved position between R3a and I2 at the LRR domain. Saturation mutagenesis at amino acid positions 141 (CC domain) and 330 (NB-ARC) in I2 revealed five more gain-of-response mutants (three at position 141 and two at position 330 respectively). For the generation of stable transgenic tomato lines, I selected five I2 gain-of-response mutants, responding to one or more of the AVR2 variants in race 3 of *F. oxysporum f. sp. lycopersici* while retaining the AVR2 recognition from race 2. Remarkably, infection assays with transgenic tomato lines carrying these *I2* mutant genes showed resistance to race 2 and 3 of the wilt pathogen *F. oxysporum f. sp. lycopersici* consistent with the gain-of-response noted in the HR assays.

5.2. Results

5.2.1. I2 responds to AVR2 from *F. oxysporum f. sp. lycopersici* race 2

To establish the experimental system, I first tested I2 wild-type with each of the AVR2 variants in races 2 and 3 of *F. oxysporum f. sp. lycopersici*. I co-expressed I2 with each of the AVR2 variants using *Agrobacterium tumefaciens*-mediated transient transformation (agroinfiltration) in the model plant *Nicotiana benthamiana* and scored for hypersensitive cell death phenotypes. I found that I2 responds to AVR2 (HR index ~2.5 on a scale of 0 to 3 at 6 days post-infiltration (dpi)) from race 2 of *F. oxysporum f. sp. lycopersici* (Fig. 5.1). Occasionally, I2 showed a weak response to the $AVR2^{V>M}$ variant (HR index ~0.6) but no cell death was observed when I2 was co-expressed with $AVR2^{R>P}$ and/or $AVR2^{R>H}$ (Fig. 5.1). All AVR2 variants were co-expressed in *N. benthamiana* with the binary vector pK7WG2 (Karimi, Inze et al. 2002) to exclude any possibility of weak autoactivity of these constructs (Fig. A3.1-Appendix 3). No cell death reaction was seen upon transient co-expression of either AVR2 variants with pK7WG2 (Fig. A3.1-Appendix 3), suggesting that the I2/AVR2 cell death is specific. These results confirmed previous studies supporting that I2 recognises only

AVR2 from race 2 but not any of the AVR2 variants found in race 3 of *F. oxysporum f. sp. lycopersici* (Houterman, Ma et al. 2009).

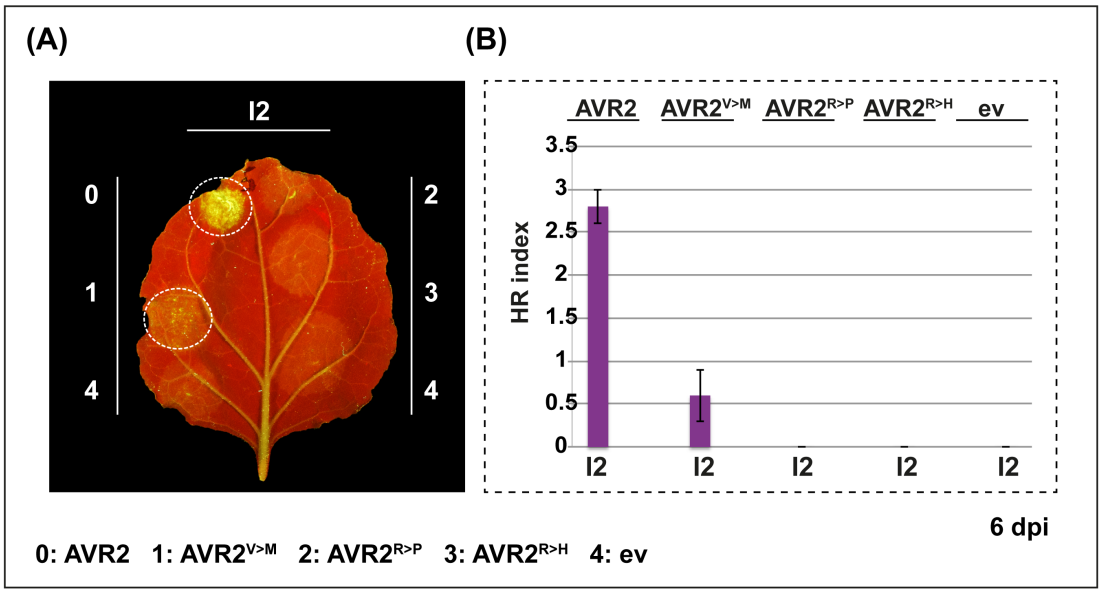

Figure 5.1: The tomato resistance protein I2 responds to AVR2 from *F. oxysporum f. sp. lycopersici*.
A, Hypersensitive response (HR) phenotypes of wild-type I2 after co-expression with the *F. oxysporum f. sp. lycopersici* AVR2 variants in *N. benthamiana* leaves. Wild-type *I2* and *Avr2* isoforms were under transcriptional control of the *Cauliflower mosaic virus* 35S promoter. I2 wild-type and I2 mutants were expressed form the Gateway binary vector pK7WG2 (Karimi, Inze et al. 2002) and AVR2 variants were expressed from a CTAPi vector (Rohila, Chen et al. 2004). The picture was taken at 6 days post-infiltration (dpi). B, HR indices corresponding to the experiment described in A. Values scored at 6 dpi are plotted. Bars represent the average of 20 replicas for each combination of constructs; error bars represent standard deviation. Scoring of the HR was obtained according to an arbitrary scale (Fig. A2.2), as previously described (Bos, Kanneganti et al. 2006, Segretin, Pais et al. 2014). Circulated areas represent examples of different levels of HR.

5.2.2. I2 and R3a are divergent in the LRR domain

Even though R3a and I2 share a high level of similarity at their N-terminal domains (82% an 87% amino acid similarity at the CC and NB-ARC domains respectively), they are more divergent in the C-terminal LRR domain (73% amino acid similarity) (Huang, van der Vossen et al. 2005). To investigate whether the R3a+ positions identified by Segretin *et al.*, (Segretin, Pais et al. 2014) are conserved in I2, I aligned the LRR domains of the two proteins (Fig. 5.2A). Sequence alignment of the two proteins revealed that three (E958, C967 and E1000) out of the six R3a+ positions in the LRR are conserved in I2 (highlighted in orange yellow and pink for I2,

respectively) (Fig. 5.2A). Interestingly, two of these three conserved positions (E958 and E1000) along with another one (Q939 for I2, highlighted in white) are predicted to be in residues exposed on the R3a protein surface (Segretin, Pais et al. 2014). Homology structure model for the LRR domain of I2 was generated based on protein fold recognition algorithms implemented by IntFold (Fig. 5.2B) (Roche, Buenavista et al. 2011). The LRR domain was modelled using 2 templates; Toll-like receptor 3 (PDB code 2a0z) (Bell, Botos et al. 2005) and Toll-like receptor 8 (PDB code 3w3g) (Tanji, Ohto et al. 2013) which were the top score in IntFold. The structure model showed that the E958, E1000 and Q939 positions in I2 are also exposed on the surface of the protein, however the rest of the R3a+ LRR positions occur in I2 folds that could possibly affect the overall conformation of the protein when mutated (Fig. 5.2B). I therefore proceeded with the generation of the following six I2 mutants, in the LRR domain; R660P, Q939E, E958K, C967R, E1000K, and N1234R. These I2 positions correspond to the equivalent R3a+ positions, as revealed by the alignment (Fig. 5.2A).

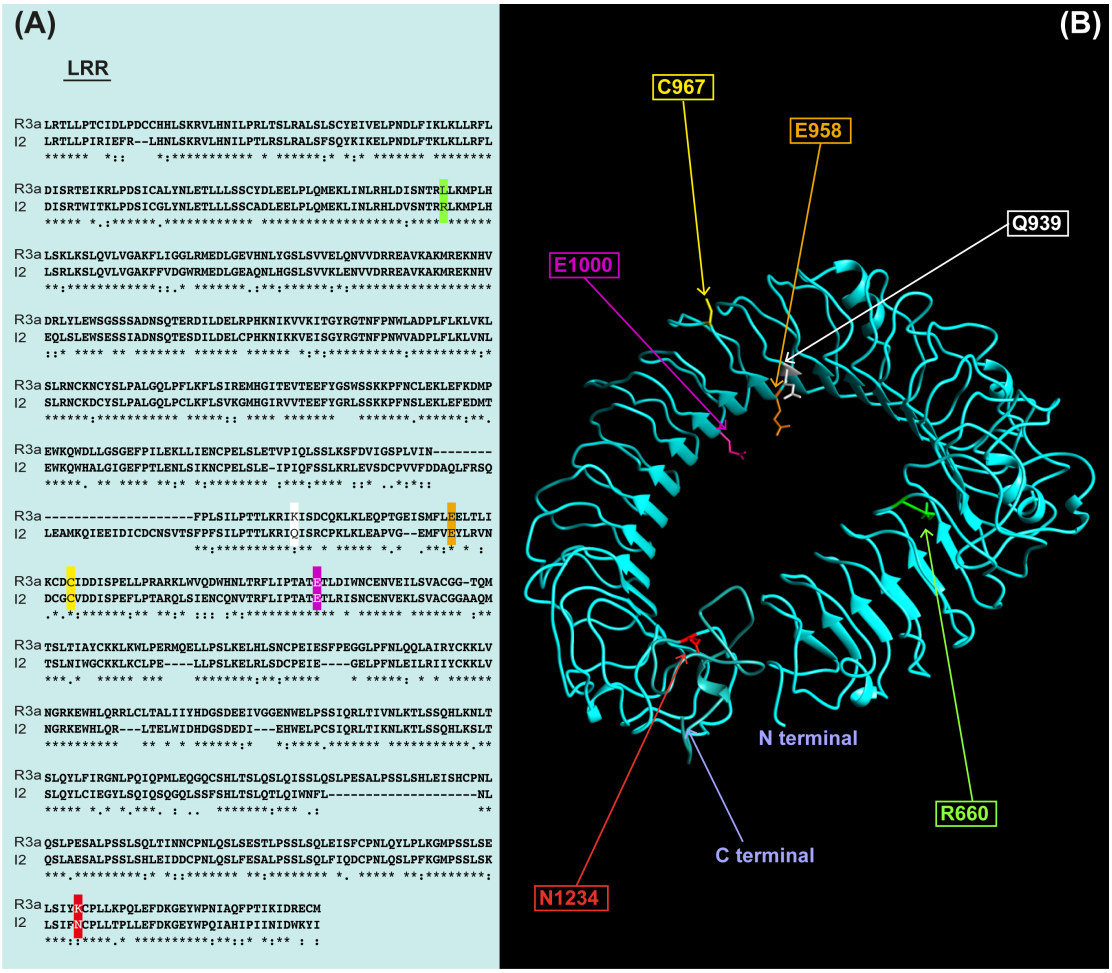

Figure 5.2: I2 and R3a are highly divergent in the C-terminal region.

A, Protein sequence alignment of the LRR domains of I2 and R3a. The amino acid positions that were subjected to mutation are highlighted in different colours (I2 amino acid positions: R660 green, Q939 white, E958 orange, C967 yellow, E1000 purple, N1234 red). B, Structural model of the LRR domain of I2. Model was generated by remote homology modeling using the INTFold2 server (Roche, Buenavista et al. 2011). Amino acids corresponding to the single-residue I2 mutations are indicated with arrows and are shown in coloured stick representation according to the colour of the respective highlighted position in A.

5.2.3. $I2^{C967R}$ has an expanded response to $AVR2^{V>M}$ and $AVR2^{R>P}$

I generated I2 mutants carrying the equivalent to R3a+ mutations ($R3a^{L668P}$, $R3a^{K920E}$, $R3a^{E941K}$, $R3a^{C950R}$, $R3a^{E983K}$ and $R3a^{K1250R}$) in the LRR domain. The I2 mutants were then tested with the *F. oxysporum* effectors AVR2, $AVR2^{V>M}$, $AVR2^{R>P}$ and $AVR2^{R>H}$ using agroinfiltration in *N. benthamiana*. Of the I2 mutants generated ($I2^{R660P}$, $I2^{Q939E}$, $I2^{E958K}$, $I2^{C967R}$, $I2^{E1000K}$ and $I2^{N1234R}$), only $I2^{C967R}$ showed an expanded response phenotype (Fig. 5.3). $I2^{C967R}$ responded to AVR2 (HR index ~2.5) and weakly to $AVR2^{V>M}$ (HR index between 0.8 and 1.3) and $AVR2^{R>P}$ (HR index between 0.6 and 1) (Fig. 5.3). $I2^{R660P}$ displayed a loss-of-response as it did not trigger any cell death when co-expressed with either one of the AVR2 variants (Fig. A2.4). $I2^{Q939E}$ and $I2^{E1000K}$ were autoactive as they triggered cell death (HR index ~2.5) even in the absence of effector proteins (Bendahmane, Farnham et al. 2002, Howles, Lawrence et al. 2005, van Bentem, Vossen et al. 2005, Tameling, Vossen et al. 2006, Van Ooijen, Mayr et al. 2008) (Fig. A2.4). Finally $I2^{E958K}$ and $I2^{N1234R}$ had a similar phenotype to the wild-type I2 protein as they triggered cell death only in the presence of AVR2 (HR index ~2.5) (Fig. A2.4). These results indicate that the specific R3a+ amino acid substitutions typically do not confer expanded response phenotypes to I2. However, given that I2 activity was altered in 4 out of the 6 mutants, I conclude that these positions are important for I2 activity.

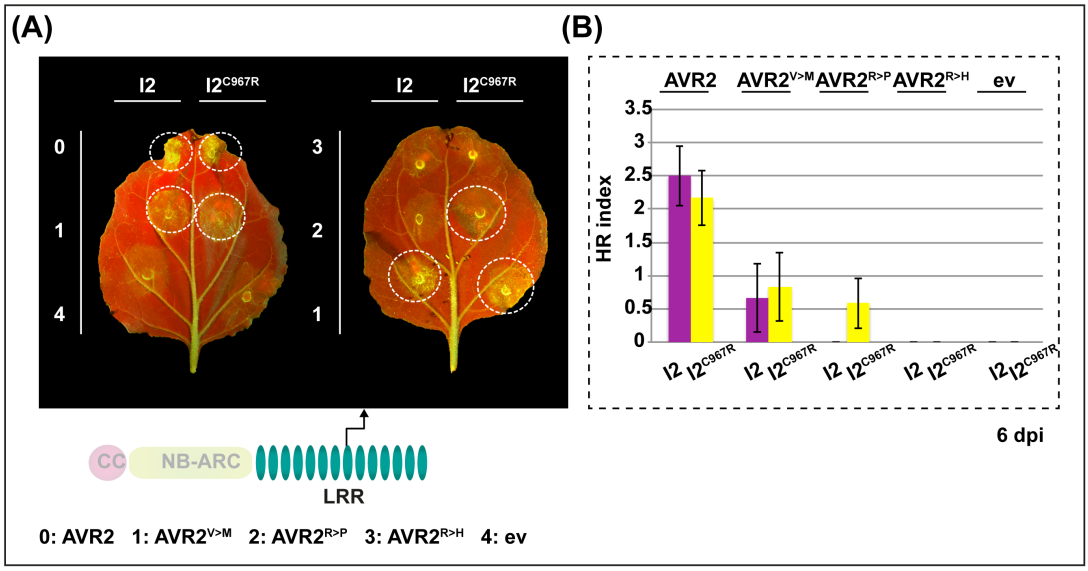

Figure 5.3: I2^{C967R} mutant responds to AVR2 and AVR2$^{V>M}$, AVR2$^{R>P}$ variants.
A, Hypersensitive response (HR) phenotypes of wild-type I2, and I2^{C967R} after co-expression with the *F. oxysporum f. sp. lycopersici* AVR2 variants in *N. benthamiana* leaves. Wild-type *I2*, *I2* mutants and *Avr2* isoforms were under transcriptional control of the *Cauliflower mosaic virus* 35S promoter. The pictures were taken at 6 days post-infiltration (dpi). B, HR indices corresponding to the experiment described in A. Values scored at 6 dpi are plotted. The cartoon indicates the approximate positions of the mutations. Bars represent the average of 20 replicas for each combination of constructs; error bars represent standard deviation. Empty vector (ev) corresponds to the binary vector CTAPi (Rohila, Chen et al. 2004) and was used as a negative control in this experiment. Scoring of the HR was obtained according to an arbitrary scale (Fig. A2.2), as previously described (Bos, Kanneganti et al. 2006, Segretin, Pais et al. 2014). Circulated areas represent examples of different levels of HR.

5.2.4. I2 mutants at the N-terminal part of the protein show expanded response to *F. oxysporum f. sp. lycopersici* race 3 AVR2 variants

To test whether the I2 mutants that were generated at the N-terminal part of the protein at positions 141 and 330 (described in chapter 4, paragraph 4.2.4) have an altered response towards the AVR2 variants of *F. oxysporum f. sp. lycopersici,* I screened the I2I141X and I2N330X mutants (Fig. 5.4A) using the established cell death assays in the model plant *N. benthamiana*. The cell death phenotypes I acquired grouped the I2 mutant clones in four categories: autoactive (HR index ~3 in the absence of effectors), loss-of-response (no HR phenotype), similar profile to wild-type I2, and gain-of-response (expanded response to AVR2 variants). Substitutions of the Asn in position 330 with Cys, His, Leu, Tyr, Arg, Thr, Ser, Val, Trp, Phe, Met and Ile resulted in autoactive mutants; Glu gave a loss-of-response phenotype; Gln, Pro, Gly and Ala had a similar response profile to the wild-type I2

whereas Lys and Asp gave a gain-of-response phenotype (Fig. 5.4). Substitution of the Ile in position 141 with Tyr resulted in an autoactive mutant; Arg, Pro, Phe, Ala, Lys, Thr and Asp showed a loss-of-response phenotype; Gly had a similar response profile to the wild-type I2 and Val, Leu and Asn gave a gain-of-response phenotype (Fig. 5.4). These results suggested that these specific positions at the N-terminal part of the I2 protein can modulate the ability of the protein to respond to the AVR2 effectors of *F. oxysporum f. sp. lycopersici*.

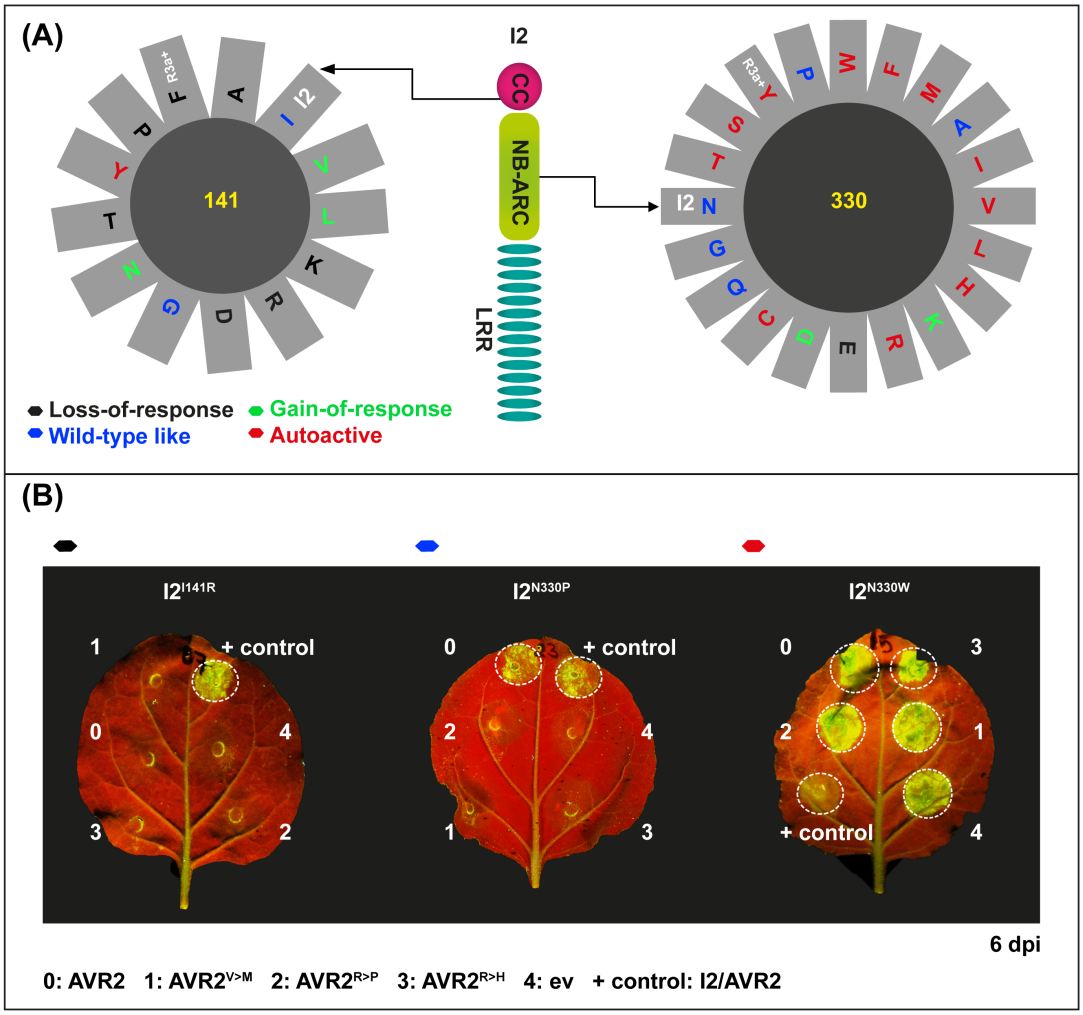

Figure 5.4: I2 mutants carrying randomized amino acids at positions 141 and 330 show variable responses to AVR2 variants.

The I2 mutant library described in chapter 4 was screened for gain-of-response phenotypes by co-agroinfiltration in *N. benthamiana* of the I2 mutant clones with *F. oxysporum f. sp. lycopersici* AVR2 variants. A, Amino acid substitutions are coloured according to the response phenotypes obtained: black (loss-of-response), blue (wild-type like), green (gain-of-response), red (autoactive). Wild-type amino acids at these positions and amino acids corresponding to the R3a+ mutants are indicated by the I2 and R3a+ labels respectively. B, Hypersensitive response (HR) phenotypes of selected I2 mutants generated in this library ($I2^{I141R}$, $I2^{N330P}$, $I2^{N330W}$) after co-expression with the *F. oxysporum f. sp. lycopersici* AVR2 variants in *N. benthamiana* leaves, representing a loss-of-response, a wild-type like and an autoactive phenotypic example respectively. Positive control (+), represents I2 wild-type co-

expressed with AVR2 in each leaf. Empty vector (ev) corresponds to the binary vector CTAPi (Rohila, Chen et al. 2004) and was used as a negative control in this experiment. Circulated areas represent examples of different levels of HR.

5.2.5. $I2^{I141V}$ and $I2^{I141L}$ respond to *F. oxysporum f. sp. lycopersici* AVR2 effectors form races 2 and 3

The gain-of-response $I2^{I141V}$, $I2^{I141L}$ and $I2^{I141N}$ identified in my screen were selected for further characterization. The $I2^{I141N}$ was characterised already in chapter 4 (paragraph 4.2.9), so in this chapter I focused on the two other gain-of-response I2 mutants, $I2^{I141V}$ and $I2^{I141L}$, residing at the CC domain of the protein. $I2^{I141V}$ and $I2^{I141L}$ were co-expressed with all the AVR2 variants using *N. benthamiana* agroinfiltration. $I2^{I141V}$ responded to AVR2 (HR index ~3) and also to $AVR2^{V>M}$ (HR index between 1.2 and 1.8) (Fig. 5.5). $I2^{I141L}$ responded to AVR2 (HR index ~3), $AVR2^{V>M}$ (HR index ~2.5) and $AVR2^{R>H}$ (HR index between 1.5 and 1.8) (Fig. 5.5). $I2^{I141L}$ also exhibited a weak response in the absence of effectors (HR index ~0.5), which was lower than the response to all the AVR2 variants. These results indicate that a single-amino acid change in the CC domain of I2 (I141V or I141L) is sufficient to expand the response profile of the wild-type I2 receptor to race 3 AVR2 variants and further suggests that distinct amino acid substitutions differentially affect the ability of the protein to respond to AVR2 effectors secreted by *F. oxysporum f. sp. lycopersici*.

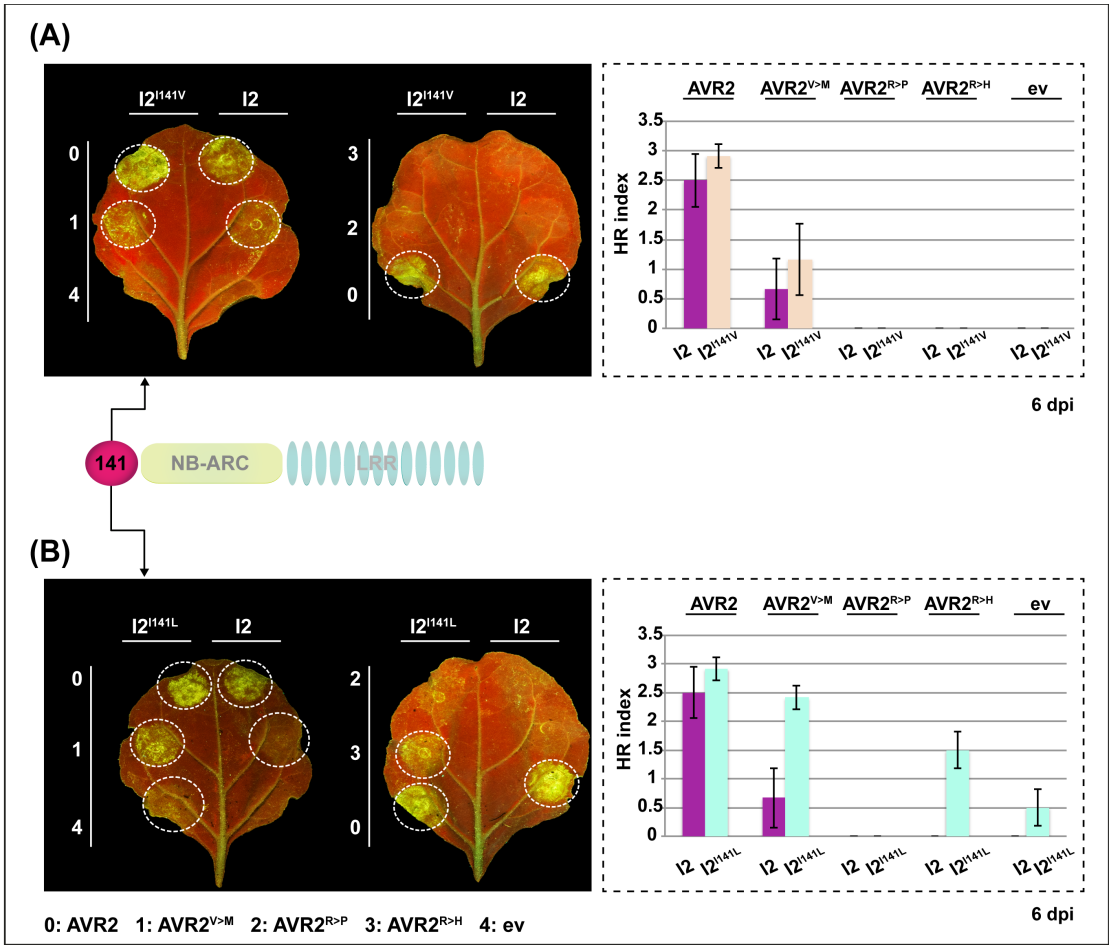

Figure 5.5: CC-domain I2 mutants, I2^{I141V} and I2^{I141L} show expanded response to AVR2 variants from race 3 of *F. oxysporum f. sp. lycopersici*.

A, Hypersensitive response (HR) phenotypes of wild-type I2 and I2^{I141V} after co-expression with the *F. oxysporum f. sp. lycopersici* AVR2 variants in *N. benthamiana* leaves. HR indices correspond to the experiment described. The wild-type, mutant *I2* and *Avr2* isoforms were under transcriptional control of the *Cauliflower mosaic virus* 35S promoter. The pictures were taken at 6 days post-infiltration (dpi). B, Hypersensitive response (HR) phenotypes of wild-type I2 and I2^{I141L} after co-expression with the *F. oxysporum f. sp. lycopersici* AVR2 variants in *N. benthamiana* leaves. HR indices correspond to the experiment described. The wild-type, mutant *I2* and *Avr2* isoforms were under transcriptional control of the *Cauliflower mosaic virus* 35S promoter. The pictures were taken at 6 days post-infiltration (dpi). For the HR indices shown values scored at 6 dpi are plotted. Empty vector (ev) corresponds to the binary vector CTAPi (Rohila, Chen et al. 2004) and was used as a negative control in this experiment. The cartoon indicates the approximate positions of the mutations. Bars represent the average of 20 replicas for each combination of constructs; error bars represent standard deviation. Scoring of the HR was obtained according to an arbitrary scale (Fig. A2.2), as previously described (Bos, Kanneganti et al. 2006, Segretin, Pais et al. 2014). Circulated areas represent examples of different levels of HR.

5.2.6. $I2^{N330K}$ and $I2^{N330D}$ have expanded response to *F. oxysporum f. sp. lycopersici* AVR2 variants found in race 3

The screen of mutant libraries focused on the N-terminal part of the I2 protein (previously described in chapter 4) also revealed two gain-of-response mutants at the NB-ARC position 330, $I2^{N330K}$ and $I2^{N330D}$. Co-expression of both I2 mutants with all AVR2 variants showed that they have expanded response to AVR2 variants from race 3 while retaining the response to the race 2 AVR2. $I2^{N330K}$ responded to AVR2 (HR index ~3), $AVR2^{V>M}$ (HR index between 1.6 and 2), $AVR2^{R>P}$ (HR index between 0.5 and 0.8) and $AVR2^{R>H}$ (HR index ~1.5) (Fig. 5.6). $I2^{N330K}$ also exhibited a weak response in the absence of effectors (HR index ~0.2), which was lower than the response to all the AVR2 variants. $I2^{N330D}$ responded to AVR2 (HR index ~2.5), weakly to $AVR2^{R>H}$ (HR index ~0.5) and some times a weak response was observed to $AVR2^{V>M}$ (HR index ~0.2) (Fig. 5.6). These results highlight once more the importance for I2 activity of position 330, close to the predicted nucleotide-binding pocket in the NB-ARC domain. Additionally, as previously stated, these results indicate that the response specificity of I2 is dependent on different amino acid changes (N330K or N330D) in position 330 of the NB-ARC domain of I2.

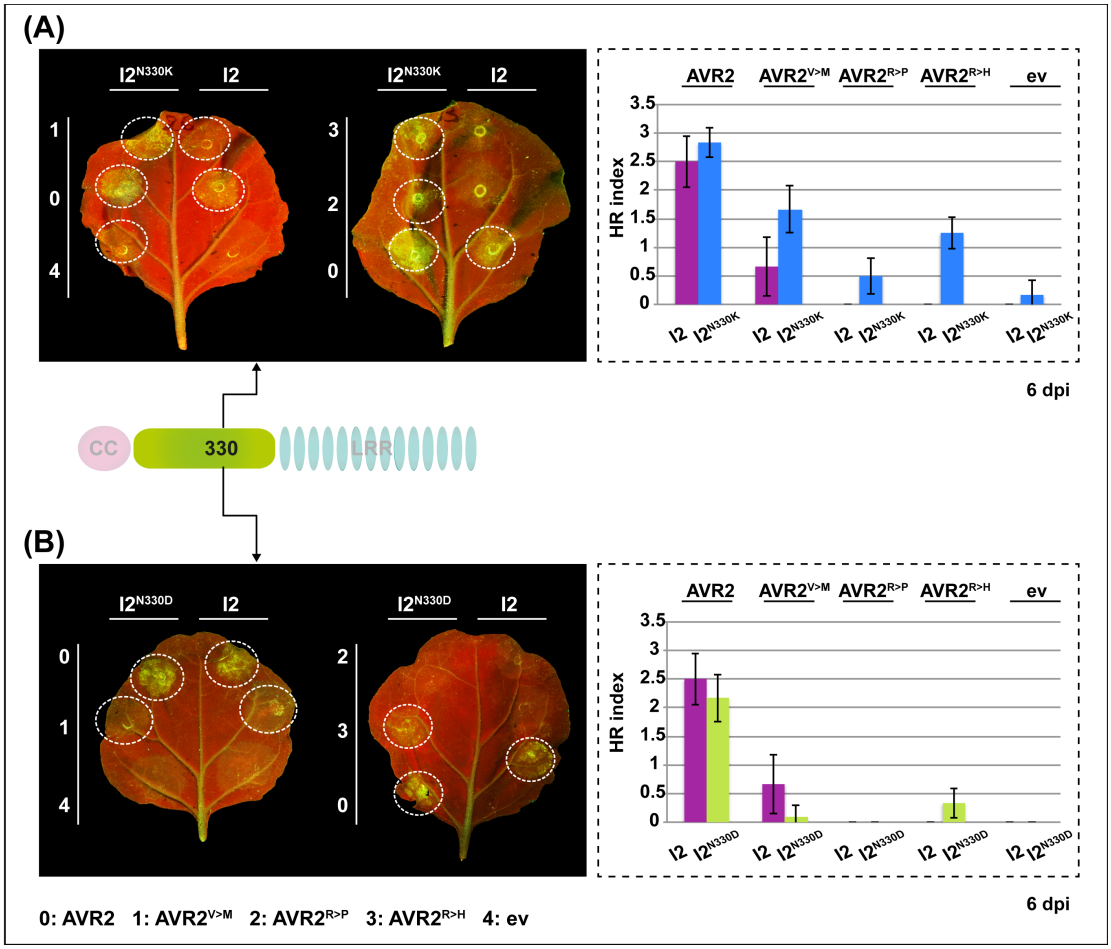

Figure 5.6: NB-domain I2 mutants, I2^{N330K} and I2^{N330D} show expanded response to AVR2 variants from race 3 of *F. oxysporum f. sp. lycopersici*.

A, Hypersensitive response (HR) phenotypes of wild-type I2 and I2^{N330K} after co-expression with the *F. oxysporum f. sp. lycopersici* AVR2 variants in *N. benthamiana* leaves. HR indices correspond to the experiment described. The wild-type, mutant *I2* and *Avr2* isoforms were under transcriptional control of the *Cauliflower mosaic virus* 35S promoter. The pictures were taken at 6 days post-infiltration (dpi). B, Hypersensitive response (HR) phenotypes of wild-type I2 and I2^{N330D} after co-expression with the *F. oxysporum f. sp. lycopersici* AVR2 variants in *N. benthamiana* leaves. HR indices correspond to the experiment described. The wild-type, mutant *I2* and *Avr2* isoforms were under transcriptional control of the *Cauliflower mosaic virus* 35S promoter. The pictures were taken at 6 days post-infiltration (dpi). For the HR indices shown values scored at 6 dpi are plotted. Empty vector (ev) corresponds to the binary vector CTAPi (Rohila, Chen et al. 2004) and was used as a negative control in this experiment. The cartoon indicates the approximate positions of the mutations. Bars represent the average of 20 replicas for each combination of constructs; error bars represent standard deviation. Scoring of the HR was obtained according to an arbitrary scale (Fig. A2.2), as previously described (Bos, Kanneganti et al. 2006, Segretin, Pais et al. 2014). Circulated areas represent examples of different levels of HR.

5.2.7. I2 gain-of-response mutant proteins have altered accumulation levels compared to the wild-type I2

The effect of the five I2 gain-of-response mutations (I141V, I141L, N330K, N330D, and C967R) on the stability of the I2 protein was investigated using western blot assays with a polyclonal antibody raised against the CC domain of R3a (previously described in chapter 4). *Nicotiana benthamiana* leaves were infiltrated using *A. tumefaciens* carrying the different constructs. Samples were collected at 2 and 3 dpi as I reasoned that this range of time points would allow us to detect potential differences in the protein levels between I2 and I2 mutant proteins. Interestingly, at 2 dpi, wild-type I2 gave a less intense signal than all $I2^{I141L}$, $I2^{N330K}$, $I2^{N330D}$, $I2^{C967R}$ mutants, while $I2^{I141V}$ had a similar signal to the wild-type I2 protein (Fig. 4.7). At 3 dpi, all of the mutants showed a less intense signal that the wild-type I2 protein with $I2^{I141L}$ and $I2^{C967R}$ being barely detectable (Fig. 4.7). These findings indicate that the expanded response of I2 mutants correlates with altered accumulation levels of the proteins, in agreement with our previous results (paragraph 4.2.6).

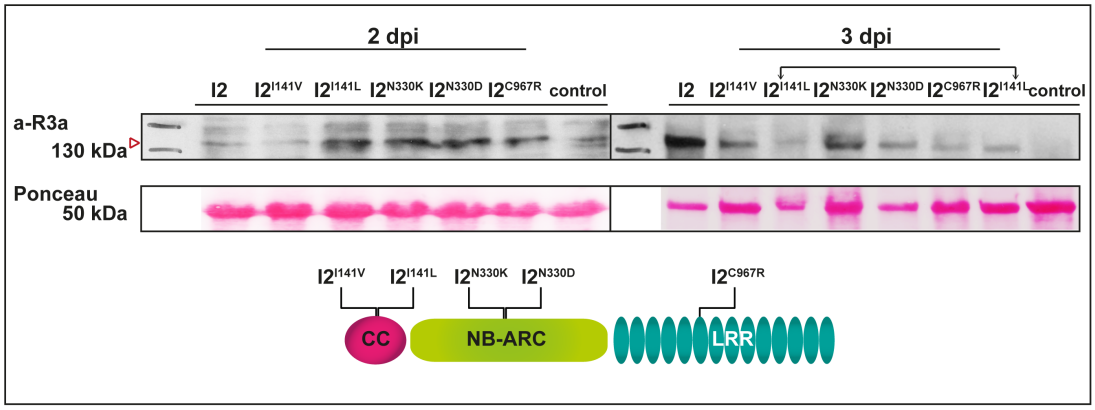

Figure 5.7: The I2 gain-of-response mutants accumulate to different levels compared to wild-type I2 *in planta*.
Nicotiana benthamiana leaves were agroinfiltrated with constructs to express wild-type and mutant I2 proteins. Total protein extracts from leaves sampled at 2 and 3 days post-infiltration (dpi) were subjected to SDS-PAGE followed by immunoblotting with a polyclonal antibody raised against the CC domain of R3a (a-R3a, upper panel). A band of approximately 145 kDa, indicated with a red arrow, corresponding to I2 was present in total extracts of the leaves infiltrated with the *I2* and $I2^{I141N}$ constructs. Ponceau S staining of Rubisco (lower panel) is shown as control of the amount of protein loaded and transferred in each lane. Sizes (in kDa) are indicated on the left. Control corresponds to the binary vector pK7WG2 (Karimi, Inze et al. 2002) and was used as a negative control in this experiment. Different boxes indicate different blots.

5.2.8. Generation of transgenic *I2* tomato lines

The *I2* mutant genes that led to gain-of-response I2 immune receptors were used for the generation of transgenic tomato lines. Tomato plants (*S. lycopersicum* accession OH7814 - SGN758) were transformed via *A. tumefaciens* with *I2* wild-type and mutant genes which were under transcriptional control of the *Cauliflower mosaic virus* 35S promoter. Transgenic T1 generation tomato plants were genotyped and the following *I2* containing lines were kept for further analysis: B8 and B14 lines carrying wild-type *I2*; B25 and B26 lines carrying $I2^{C967R}$; A36 and B2, lines carrying $I2^{I141L}$; A16 and A49 lines carrying $I2^{I141V}$; B1, B15 and B16 carrying $I2^{N330K}$, and EV1 and EV2 lines transformed empty vector pK7WG2 (Table 2.9.2) (Fig. A3.3-Appendix 3). Tomato lines carrying $I2^{N330D}$ or $I2^{I141N}$ were not included in this experiment, as the transformation process was not completed for those genotypes. For clarity, I will be referring to the original T1 selected lines as lines and to the T2 plants that derived from those lines as individuals.

5.2.9. Pathogen assays of I2 transgenic plants

To establish an infection assay, I first infected T1 tomato *I2* wild-type lines with *F. oxysporum f. sp. lycopersici* races 2 (Fol007) and 3 (Fol029, Fol035, Fol067) (Table 2.8.1). The presence of the pathogen and the identity of the strain was verified in tomato roots using AVR2 primers specific for each race of *F. oxysporum f. sp. lycopersici* (Fig. A3.4-Appendix 3).

To test the ability of the different 35S::*I2* individuals to confer resistance against races 2 and 3 of *F. oxysporum f. sp. lycopersici*, T2 individuals of the lines mentioned above (B8, B14, A36, B2, A16, A49, B1, B15, B16, B25, B26, EV1, EV2) were infected with each race. Briefly, approximately two to five T2 individuals of each line were inoculated with each race (Table 5.2.1). Infection was performed in 10-day-old tomato seedlings; roots were deep inoculated into a spore suspension (10^7 conidia ml^{-1}) and then were potted separately (for detailed description of infection see 2.8.1). Three and a half weeks post-inoculation the plant weight above cotyledons was scored and a phenotypic analysis of the symptoms developed was performed.

Table 5.2.1: Number of T2 individuals used for each infection assay with *F. oxysporum f. sp. lycopersici* strains

Line	Number of T2 individuals tested with each *F. oxysporum f. sp. lycopersici* strain			
	Strain Fol007 (AVR2)	Strain Fol069 ($AVR2^{V>M}$)	Strain Fol035 ($AVR2^{R>P}$)	Strain Fol029 ($AVR2^{R>H}$)
B8	4	-	-	-
B14	4	5	4	3
B2	2	3	2	3
A36	-	-	-	3
A16	4	5	-	-
A49	-	5	-	-
B1	2	2	2	1
B15	4	5	4	4
B16	4	4	2	4
B25	4	4	4	3
B26	5	5	4	5
EV1	3	1	1	3
EV2	3	2	2	1

5.2.10. Tomato plants carrying *I2* wild-type and mutant genes are resistant to *F. oxysporum f. sp. lycopersici* race 2 carrying *Avr2*

Inoculation of tomato individuals with *F. oxysporum f. sp. lycopersici* race 2 (strain Fol007, table 2.8.1) revealed that *I2* wild-type and mutant tomato individuals are resistant to this strain (Fig. 5.8). Representative examples of infected tomato plants are shown (Fig. 5.8A) and disease index of all the tomato individuals used was monitored (Fig. 5.8B). In detail, wilting symptoms including thin stem, leaves and branches dropping and even whole plants falling was apparent in all the individuals that did not contain the *I2* gene (No-*I2* and EV individuals) with an average plant weight of (~15 g), while all the mock individuals (water-inoculated) showed no symptoms and had relatively higher plant weight levels (~35 g). These results confirmed the success of the infection. All eight *I2* individuals tested (B8 and B14 lines) were resistant as no symptoms developed in the plants (Fig. 5.8 A) and the plant weight varied between 25 and 30 g (Fig. 5.8B). The two $I2^{I141L}$ individuals

tested (line B2) were also resistant as depicted by the lack of symptoms and plant weight of ~27 g (Fig. 5.8B). The four *I2*^{I141V} individuals tested (line A16) were resistant with plant weight reaching ~40 g (Fig. 5.8B). Tomato plants carrying *I2*^{N330K} had variable phenotypes as all four individuals from the B15 line were resistant (plant weight between 25 and 35 g), however 4 out of 6 individuals of lines B1 and B16 were susceptible with members showing wilting symptoms and plant weight ~17 g (Fig. 5.8B). Finally, only five out of nine tomato individuals carrying *I2*^{C967R} (lines B25 and B26) were resistant (Fig. 5.8B). Genotyping of the individuals used in this experiment confirmed the presence of *I2* in these lines (Appendix 3-Fig. A3.5 and A3.6). These results indicate that *I2* wild-type and *I2*^{I141L}, *I2*^{I141V}, *I2*^{I141K}, and *I2*^{C967R} tomato plants are resistance to *F. oxysporum f. sp. lycopersici* race 2, as at least three T2 individuals from more than one independent lines (with the exception of *I2*^{I141L} individuals that came from one line) carrying either of the *I2* constructs developed no symptoms and had an average plant weigh above ~25 g.

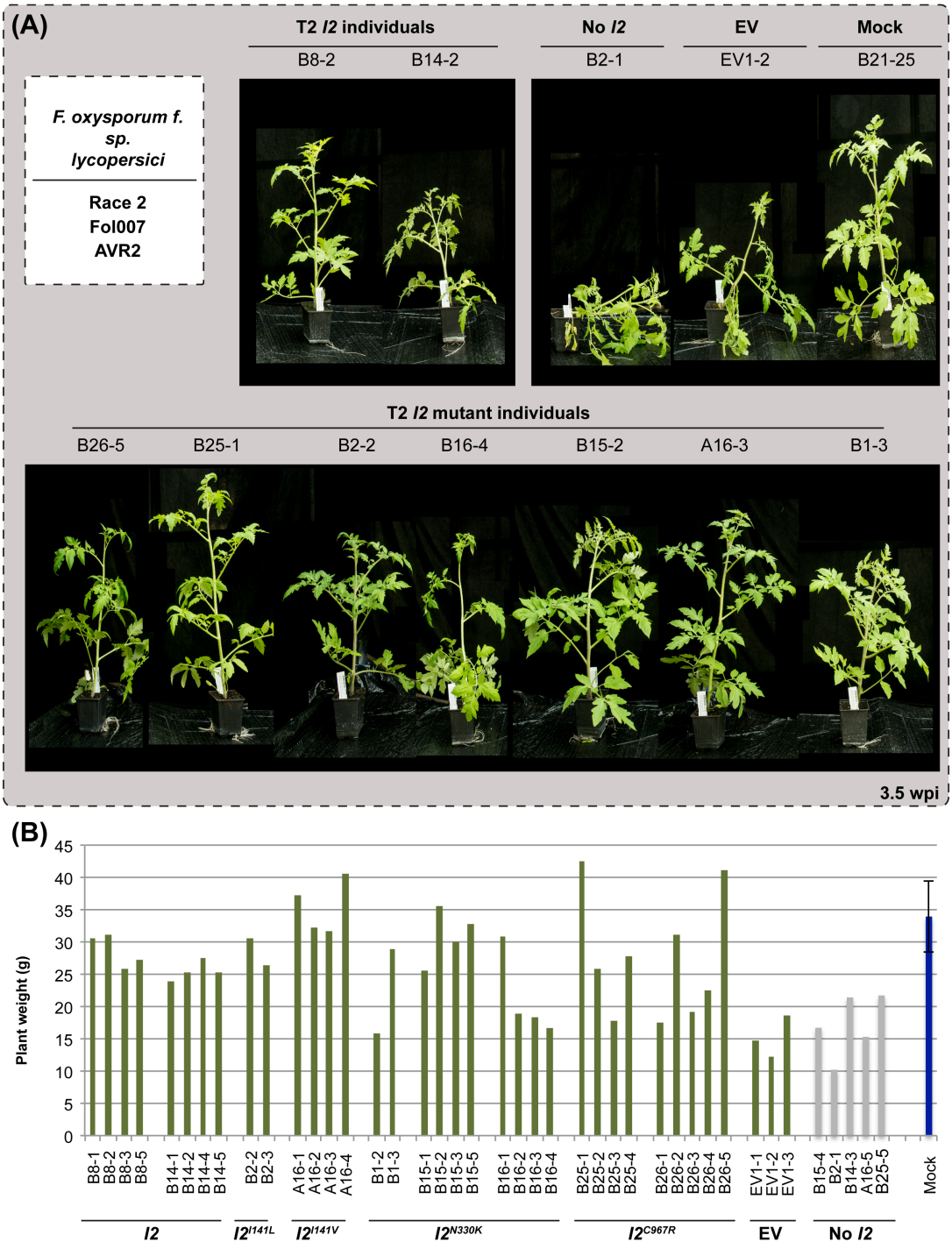

Figure 5.8: Disease assay on transgenic *I2* tomato plants with *F. oxysporum f. sp. lycopersici* race 2 Fol007.

A, Phenotypic analysis of tomato T2 individuals carrying *I2* wild-type or *I2* mutant genes. Inoculations were performed on 10-day-old seedlings. *I2* wild-type individuals, No-*I2* individuals (lacking the *I2* gene), EV individuals (transformed with pK7WG2) were used as controls in this experiment. Pictures were taken 3.5 weeks post inoculation (3.5 wpi). B, Disease index was monitored by determining the plant weight above cotyledons of each T2 individual. Mock bar represents the average of 60 different T2 individuals (including *I2* wild-type, *I2* mutant and EV tomato individuals) inoculated with water; error bar represents standard deviation. Individuals of the following lines were used: B8 and B14 (*I2*), A36 and B2 ($I2^{I141L}$),

A16 and A49 ($I2^{I141V}$), B1, B15 and B16 ($I2^{N330K}$), B25 and B26 ($I2^{C967R}$), and EV1 and EV2.

5.2.11. $I2^{I141V}$, $I2^{N330K}$ and $I2^{C967R}$ tomato plants are resistant to *F. oxysporum f. sp. lycopersici* race 3 carrying the $Avr2^{V>M}$ isoform

To examine the degree to which tomato individuals carrying *I2* mutant genes are resistant to *F. oxysporum f. sp. lycopersici* race 3 (strain Fol067, table 2.8.1) I performed a similar experiment as in the case of race 2 (Fig. 5.9). Representative examples of infected tomato plants are shown (Fig. 5.9A) and disease index of all the tomato individuals used was monitored (Fig. 5.9B). *I2* wild-type individuals developed wilting symptoms as expected Fig. 5.9), as race 3 is known to be virulent on *I2*-carrying plants. In addition all the individuals that did not contain the *I2* gene (No-*I2* and EV individuals) were infected with an average plant weight of ~15 g, while all the mock individuals (water-inoculated) showed no symptoms and had relatively higher plant weight levels (~35 g). These observations suggested that the infection was successful. The five $I2^{I141L}$ individuals tested (line B2) were all resistant as depicted by the lack of symptoms and plant weight of ~30 g (Fig. 5.9B). Five out of ten tomato individuals tested carrying $I2^{I141V}$ (lines A16 and A49) were resistant with an average plant weight of ~32 g (Fig. 5.9B). Ten out of eleven tomato individuals carrying $I2^{N330K}$ (lines B1, B15 and B16) were resistant (plant weight between 25 and 35 g) (Fig. 5.9B). Finally, seven out of nine individuals carrying $I2^{C967R}$ (lines B25 and B26) were resistant with an average plant weight of ~30 g (Fig. 5.9B). Genotyping of the individuals used in this experiment confirmed the presence of *I2* in these plants (Appendix 3-Fig. A3.5 and A3.6). These results indicate that the $I2^{I141L}$, $I2^{I141V}$, $I2^{I141K}$, and $I2^{C967R}$ mutant tomato plants are resistance to the specific strain of *F. oxysporum f. sp. lycopersici* race 3 Fol067, as at least three T2 individuals from more than one independent lines (with the exception of I2 and $I2^{I141L}$ individuals that came from one line each) carrying either of the *I2* constructs developed no symptoms and had an average plant weigh above ~25 g. Interestingly, $I2^{I141L}$ and $I2^{N330K}$ mutant tomato individuals (from lines B2 and B1, B15, B16 respectively) showed the highest level of resistance to *F. oxysporum f. sp. lycopersici* race 3 carrying $Avr2^{V>M}$ effector gene. These results confirm my HR transient assays where $I2^{I141L}$ and $I2^{N330K}$ showed the highest response to $AVR2^{V>M}$ (Fig. 5.5B and 5.6A).

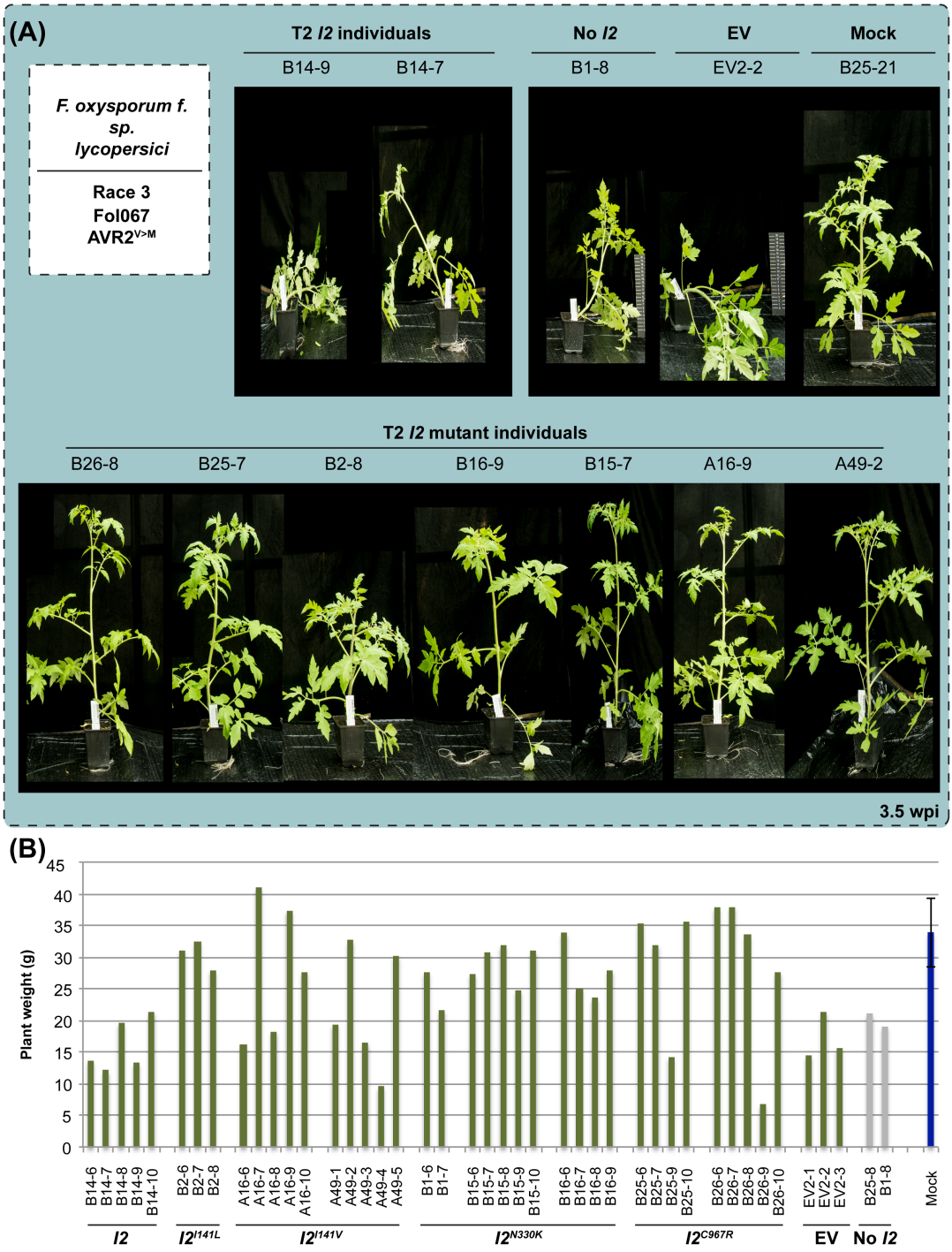

Figure 5.9: Disease assay on transgenic *I2* tomato plants with *F. oxysporum f. sp. lycopersici* race 3 Fol067.

A, Phenotypic analysis of T2 tomato individuals carrying *I2* wild-type or *I2* mutant genes. Inoculations were performed on 10-day-old seedlings. *I2* wild-type individuals, No-*I2* individuals (lacking the *I2* gene), EV individuals (transformed with pK7WG2) were used as controls in this experiment. Pictures were taken 3.5 weeks post inoculation (3wpi). B, Disease index was monitored by calculating the plant weight above cotyledons of each T2 individual. Mock bar represents the average of 60 different T2 individuals (including *I2* wild-type, *I2* mutant and EV tomato individuals) inoculated with water; error bar represents standard deviation.

Individuals of the following lines were used: B14 (*I2)*, B2 ($I2^{I141L}$), A16 and A49 ($I2^{I141V}$), B1, B15 and B16 ($I2^{N330K}$), B25 and B26 ($I2^{C967R}$), and EV1 and EV2.

5.2.12. $I2^{C967R}$ tomato plants are resistant to *F. oxysporum f. sp. lycopersici* race 3 carrying the $Avr2^{R>P}$ isoform

I2 wild-type and mutant tomato individuals were infected with *F. oxysporum f. sp. lycopersici* race 3 (strain Fol035, table 2.8.1) and screened for resistance. Representative examples of infected tomato plants are shown (Fig. 5.10A) and disease index of all the tomato individuals used was monitored (Fig. 5.10B). *I2* wild-type individuals and all the individuals that did not contain the *I2* gene (No-*I2* and EV individuals) presented wilting symptoms, however the average plant weight was ~20 g, while all the mock individuals (water-inoculated) showed no symptoms and had relatively higher plant weight levels (~35 g). This gave me confidence that the infection was successful. The two $I2^{I141L}$ individuals tested (line B2) were resistant as depicted by the lack of symptoms and plant weight of ~30 g (Fig. 5.10B). Three out of eight $I2^{N330K}$ tomato individuals (lines B1, B15 and B16) were resistant (plant weight ~30 g) (Fig. 5.10B), however most individuals showed wilting symptoms and had an average plant weight of ~15 g (Fig. 5.10A). Finally, six out of eight individuals carrying $I2^{C967R}$ (lines B25 and B26) were resistant as they showed no symptoms and had an average plant weight of ~30 g (Fig. 5.10B). Genotyping of the individuals used in this experiment confirmed the presence of *I2* in these plants (Appendix 3-Fig. A3.5 and A3.6). These results indicate that $I2^{C967R}$ mutant tomato plants are resistance to *F. oxysporum f. sp. lycopersici* race 3 strain Fol035, as most of the individuals tested, from two independent lines (B25, B26) showed no wilting symptoms. These phenotypes are in agreement with the results from the HR assays where $I2^{C967R}$ shows the highest response to $AVR2^{R>P}$ (Fig. 5.3) among the I2 mutants. Surprisingly the two $I2^{I141L}$ mutant tomato individuals that were tested (line B2), were resistant to *F. oxysporum f. sp. lycopersici* race 3 carrying $Avr2^{R>P}$ effector gene in contrast to the HR results from the transient assays where $I2^{I141L}$ shows no response to $AVR2^{R>P}$ (Fig. 5.5B).

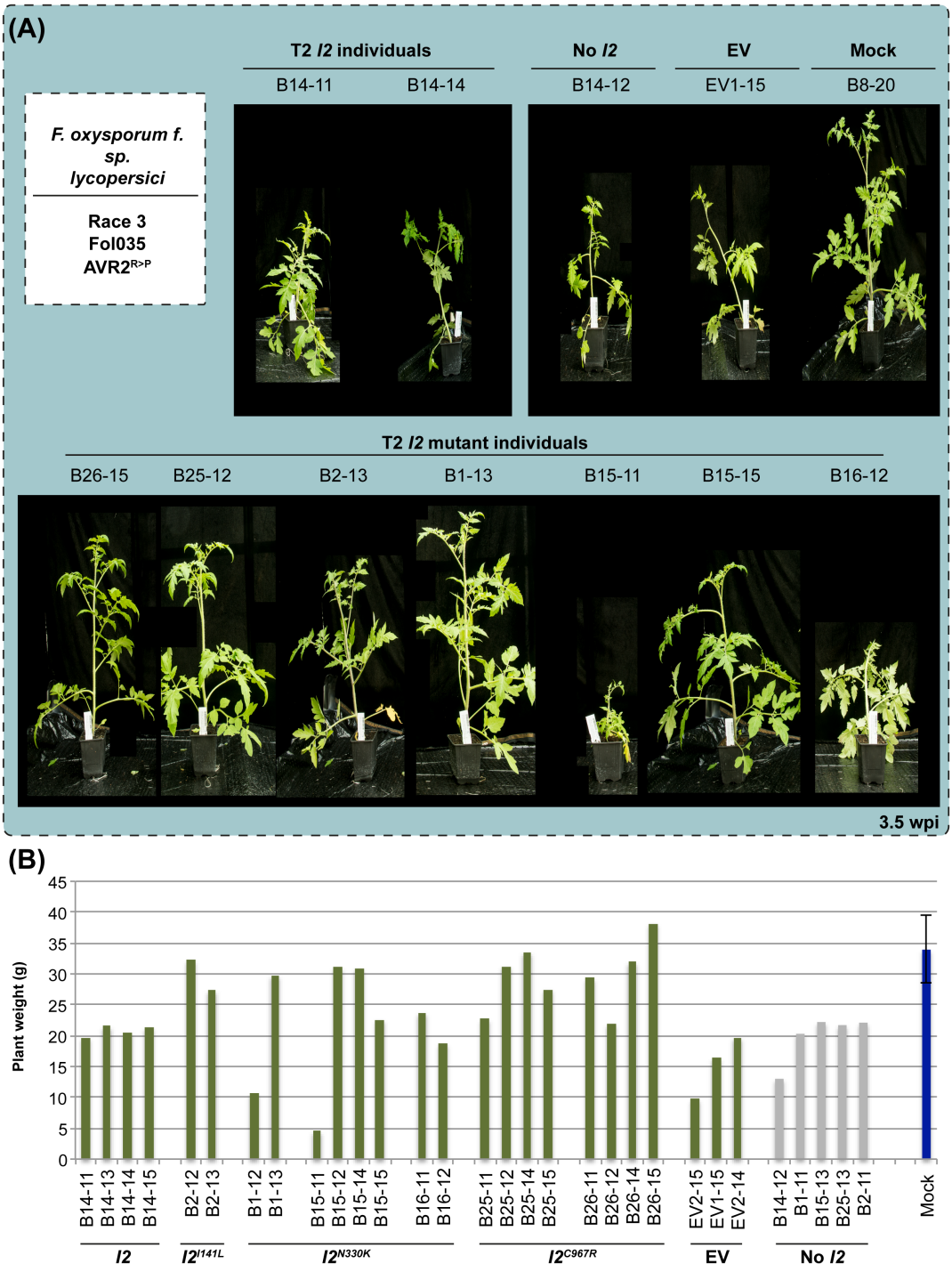

Figure 5.10: Disease assay on transgenic *I2* tomato plants with *F. oxysporum f. sp. lycopersici* race 3 Fol035.

A, Phenotypic analysis of T2 tomato individuals carrying *I2* wild-type or *I2* mutant genes. Inoculations were performed on 10-day-old seedlings. *I2* wild-type individuals, No-*I2* individuals (lacking the *I2* gene), EV individuals (transformed with pK7WG2) were used as controls in this experiment. Pictures were taken 3.5 weeks post inoculation (3wpi). B, Disease index was monitored by calculating the plant weight above cotyledons of each T2 individual. Mock bar represents the average of 60 different T2 individuals (including *I2* wild-type, *I2* mutant and EV tomato individuals) inoculated with water; error bar represents standard deviation.

Individuals of the following lines were used: B14 (*I2)*, B2 ($I2^{I141L}$), B1, B15 and B16 ($I2^{N330K}$), B25 and B26 ($I2^{C967R}$), and EV1 and EV2.

5.2.13. $I2^{I141L}$ tomato plants are resistant to *F. oxysporum f. sp. lycopersici* race 3 carrying the $Avr2^{R>H}$ isoform

I2 wild-type and mutant tomato individuals were infected with *F. oxysporum f. sp. lycopersici* race 3 (strain Fol029, table 2.8.1) and screened for resistance. Representative examples of infected tomato plants are shown (Fig. 5.11A) and disease index of all the tomato individuals used was monitored (Fig. 5.11B). *I2* wild-type individuals and all the individuals that did not contain the *I2* gene (No-*I2* and EV individuals) presented wilting symptoms, and the plant weight was between ~15 and ~20 g, while all the mock individuals (water-inoculated) showed no symptoms and had relatively higher plant weight levels (~35 g). This indicated that the infection was successful. Five out of six $I2^{I141L}$ individuals tested (lines B2 and A36) were resistant as depicted by the lack of symptoms and plant weight of ~30 g (Fig. 5.11B). Five out of nine $I2^{N330K}$ individuals (lines B1, B15 and B16) were resistant with an average plant weigh of ~30 g (Fig. 5.11). For tomato plants carrying $I2^{C967R}$, five out of eight individuals tested (lines B25 and B26) were susceptible with obvious wilting symptoms and plant weight ~15 g (Fig. 5.11B), however a few individuals were symptomless with a plant weight around ~30 g (Fig. 5.11B). Genotyping of the individuals used in this experiment confirmed the presence of *I2* in these plants (Appendix 3-Fig. A3.5 and A3.6). These results indicate that $I2^{I141L}$ mutant tomato plants are resistant to *F. oxysporum f. sp. lycopersici* race 3 strain Fol029, as five out of six T2 individuals from two independent lines (B2 and A36) developed no symptoms and had an average plant weigh above ~25 g. This result is in agreement with my transient HR assays where $I2^{I141L}$ shows the highest response to $AVR2^{R>H}$ (Fig. 5.5B).

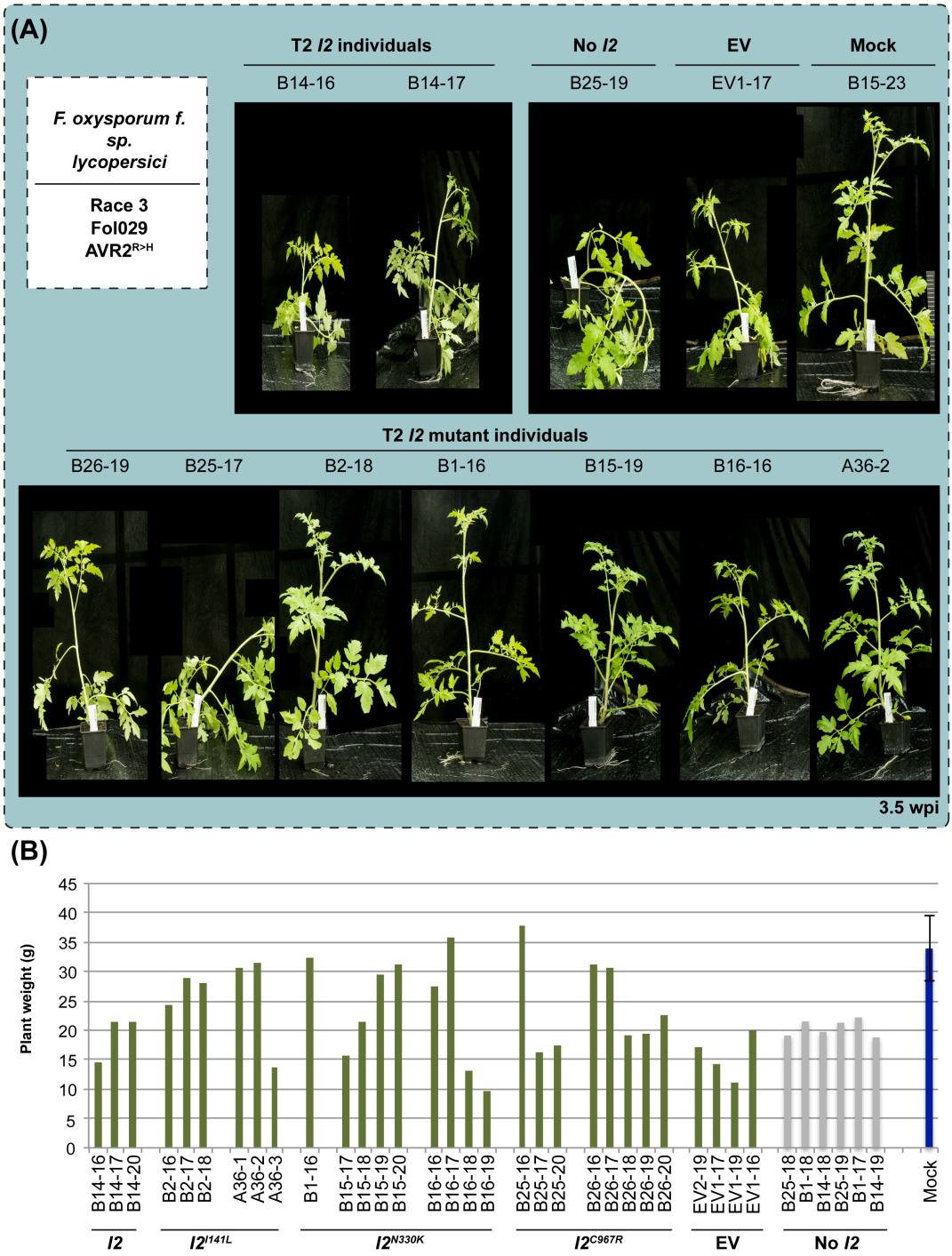

Figure 5.11: Disease assay on transgenic *I2* tomato plants with *F. oxysporum f. sp. lycopersici* race 3 Fol029.

A, Phenotypic analysis of T2 tomato individuals carrying *I2* wild-type or *I2* mutant genes. Inoculations were performed on 10-day-old seedlings. *I2* wild-type individuals, No *I2* individuals (lacking the *I2* gene), EV individuals (transformed with pK7WG2) were used as controls in this experiment. Pictures were taken 3.5 weeks post inoculation (3wpi). B, Disease index was monitored by calculating the plant weight above cotyledons of each T2 individual. Mock bar represents the average of 60 different T2 individuals (including *I2* wild-type, *I2* mutant and EV tomato individuals) inoculated with water; error bar represents standard deviation.

Individuals of the following lines were used: B14 (*I2)*, A36 and B2 ($I2^{I141L}$), B1, B15 and B16 ($I2^{N330K}$), B25 and B26 ($I2^{C967R}$), and EV1 and EV2 (pK7WG2).

5.3. Discussion

The tomato immune receptor I2 mediates resistance towards race 2 of the wilt-causing fungus *F. oxysporum f. sp. lycopersici* (Ori, Eshed et al. 1997, Simons, Groenendijk et al. 1998, Takken and Rep 2010). Co-expression of AVR2 effector from race 2 of *F. oxysporum f. sp. lycopersici* and I2 in *N. benthamiana* results in a hypersensitive response (Fig. 5.1). However AVR2 variants present in race 3 of the pathogen evade recognition by I2 (Fig. 5.2) (Houterman, Ma et al. 2009).

In this study, I tested whether previously identified mutations in the I2 ortholog, R3a, can expand the response spectrum of I2 to the AVR2 variants found in races 3 of *F. oxysporum f. sp. lycopersici*. I generated six I2 mutant proteins each carrying a single amino acid substitution at the LRR domain ($I2^{R660P}$, $I2^{Q939E}$, $I2^{E958K}$, $I2^{C967R}$, $I2^{E1000K}$ and $I2^{N1234R}$). Of these only $I2^{C967R}$ displayed an expanded response to $AVR2^{V>M}$ and $AVR2^{R>P}$ (Fig. 5.3). Saturation mutagenesis of positions 141 and 330 at the CC and NB-ARC domains of I2 respectively, revealed five additional I2 mutant proteins with expanded response to AVR2 race-3 variants; $I2^{I141N}$, $I2^{I141V}$, $I2^{I141L}$, $I2^{N330K}$ and $I2^{N330D}$ (Fig. 5.4-5.6). All the I2 gain-of-response mutants retained the ability to respond to the AVR2 variant in race 2. Also, I found that the I2 gain-of-response mutant proteins accumulate to a different level than the I2 wild-type proteins at both time points tested (Fig. 5.7). To examine the degree to which the expanded response observed in the transient assays associates with an expanded resistance phenotype I generated *35S::I2* transgenic tomato lines and performed pathogenicity tests with races 2 and 3 of *F. oxysporum f. sp. lycopersici* (Fig. 5.8-5.11). First, I found that all *I2* tomato individuals (carrying either *I2* wild-type or *I2* mutant genes) tested are resistant to race 2 of *F. oxysporum f. sp. lycopersici* (Fig. 5.8). Additionally, I showed that *I2* mutant tomato individuals are resistant against different races 3 of *F. oxysporum f. sp. lycopersici*, confirming the expanded response phenotypes observed in the transient assays (Fig. 5.8-5.11). These results confirm the initial hypothesis and previous studies on the use of synthetic NLR proteins as a source for broad-spectrum disease resistance (Farnham and Baulcombe 2006, Harris, Slootweg et al. 2013, Chapman, Stevens et al. 2014, Segretin, Pais et al. 2014). Overall the results presented suggest that synthetic NLR

immune receptors can be engineered to provide disease resistance against different *F. oxysporum f. sp. lycopersici* races in the field.

The I2 mutants generated carrying single-site substitutions at the LRR domain had variable response phenotypes to the AVR2 effectors from *F. oxysporum f. sp. lycopersici*. Of the I2 mutants generated, $I2^{C967R}$ was the only one that gained response to AVR2 race 3 variants (Fig. 5.3) whereas $I2^{R660P}$ was the only one that lost its ability to respond to AVR2 from race 2 (Fig. A3.2). $I2^{Q939E}$ and $I2^{E1000K}$ were autoactive and the remaining $I2^{E958K}$ and $I2^{N1234R}$ mutants showed a similar response spectrum to the wild-type I2 protein (Fig. A3.2-Appendix 3). Interestingly, both $I2^{Q939E}$ and $I2^{E1000K}$ autoactive mutants carry substitutions at exposed residues in I2 (Fig. 5.2). Therefore, substitutions in exposed residues that are either conservative (Q>E, polar to acidic) or radical (E>K, acidic to positive) depending on the amino acid properties changing, may be sufficient to trigger a conformational change so the protein is constitutively in an "on" state. However, although the E958K mutation is also located in an exposed residue in I2 the protein still behaves similar to the I2 wild-type with respect to its response to the AVR2 effectors. This suggests that positions Q939 and E1000 in I2 might be more important for I2 activity that position E958. Q939E, E958K, C967R and E1000K mutations are all located in LRRs 15 to 18, a region of I2 previously shown to be the binding site of a small heat-shock protein, RSI2 (van Ooijen, Lukasik et al. 2010). Van Ooijen *et al.*, showed that RSI2 is required for I2 stability and I2-mediated HR (van Ooijen, Lukasik et al. 2010). $I2^{C967R}$ was the only LRR mutant showing an expanded response to race 3 AVR2 variants without being autoactive (Fig. 5.3). Those mutations in this RSI2 dependent region could affect the ability of the protein to bind to RSI2 resulting in an altered protein state. The gain-of-response $I2^{C967R}$ mutant indeed showed an altered accumulation than the wild-type I2 protein when transiently expressed in *N. benthamiana* (Fig. 5.7).

$I2^{R660P}$ loss-of-response mutant in the N-terminal half of the LRR domain suggests that this position is critical for I2 activity. It is worth mentioning that the equivalent R3a+ mutant ($R3a^{L668P}$) gave a gain-of-response phenotype for the $AVR3a^{EM}$ variant of *P. infestans* (Segretin, Pais et al. 2014). This suggests that although the position is not conserved between the two proteins, it is critical for the activity of both I2 and R3a. The current model of NLR protein activation postulates that the N-terminal part of the LRR is folded inside the NB-ARC domain stabilizing the protein and keeping it in an "off" state (Takken and Goverse 2012). Therefore, the R660P mutation could

be affecting the way that the N-terminal part of the LRR domain interacts with the NB-ARC. It would be interesting to determine whether additional mutations in that position of I2 could affect the ability of the I2 protein to respond to AVR2 effectors from races 2 and 3. Overall these results suggest that there is no clear correlation between mutations in exposed residues in the I2 surface and subsequent activation of the protein, as not all cases of the I2 mutant immune receptors in exposed positions led to an altered I2 response. It rather seems that certain positions in the I2 protein define its ability to get activated, interact directly with the effector or mediate the interaction with intermediate components that are involved in the perception and/or activation of the receptor.

The saturation mutagenesis in positions 141 and 330 at the CC and NB-ARC domains of I2 respectively helped us identify key amino acids in those positions (paragraph 4.3). I141N, I141V and I141L at the CC domain and N330K and N330D in the NB-ARC domain of I2 all led to an expanded response phenotype of the I2 protein to AVR2 variants from race 3 of *F. oxysporum f. sp. lycopersici*, while retaining the response to the AVR2 effector from race 2. Our knowledge of the mechanisms mediating the I2/AVR2 interaction is limited. However, as previously proposed by Segretin *et al*., and others there are two main mechanisms that can explain the phenotypes of the mutants presented (Lukasik and Takken 2009, Takken and Goverse 2012, Harris, Slootweg et al. 2013, Segretin, Pais et al. 2014). The first one involves sensitized "trigger-happy" receptors with a lower threshold for activation, as proposed for the $I2^{I141N}$ mutant extensively discussed in chapter 4 (paragraph 4.3). The second model suggests that the gain-of-response mutants have altered recognition specificity, being able to sense an extended range of effectors, directly or indirectly. The present view on structure-function associations in NLR proteins suggests that mutations in the C-terminal part of the LRR domain affect the recognition specificity whereas mutations in the N-terminal part of the LRR as well as in the CC and NB-ARC domains affect activation and signalling threshold (Takken and Goverse 2012). From our mutation analysis, it seems that most of the gain-of-response mutants ($I2^{I141V}$, $I2^{N330D}$ and $I2^{C967R}$) have an altered response specificity. $I2^{C967R}$ is located in a region of the protein that could be influencing specificity whereas $I2^{I141V}$, $I2^{N330D}$ occur in regions of the protein potentially involved in signal transduction. The remaining $I2^{I141L}$ and $I2^{N330K}$ gain-of-response mutants seem to be sensitized "trigger-happy" since both of them exert a weak response in the absence of an effector, suggesting that these proteins can be activated easier than the wild-type I2 protein. However, additional biochemical tests are required to

assess the mechanisms by which these N-terminal mutations of I2 modify the activation threshold.

Pathogenicity assays showed that tomato lines carrying the *I2* mutant genes are resistant to *I2*-breaking races 3 of *F. oxysporum f. sp. lycopersici* (Fig. 5.8-5.11). It is interesting to note that the $I2^{I141L}$ and $I2^{N330K}$ tomato plants displayed no phenotypic abnormality suggesting that the slight autoactivity that the proteins showed in the HR transient assays (Fig. 5.5B and 5.6A) does not result in obvious morphological changes in the transgenic plants. For the generation of the transgenic tomato lines, the *S. lycopersicum* accession OH7814 - SGN758 was used as the background tomato variety. The OH7814 already contains the *I1* gene for resistance to *F. oxysporum f. sp. lycopersici* race 1 (Berry and Gould 1983) and is more tolerant to race 2 and 3 of the pathogen. This explains the intensity of the symptoms observed in the susceptible transgenic plants following inoculation with *F. oxysporum f. sp. lycopersici* races 3 of the pathogen. As previously discussed in chapter 1 (paragraph 1.3.2), a combination of *I1* and *I3* genes in tomato cultivars is the optimal solution so far for durable resistance against *F. oxysporum f. sp. lycopersici* given the current pathogen race makeup. However, as F. Takken and Rep highlighted, a tomato cultivar carrying *I1* and *I3* would not be sufficient to resist a potential race 4 outburst, possibly caused by single point mutations in the *Avr3* effector gene (Takken and Rep 2010). The *I2* mutant lines could provide resistance even in that extreme scenario, since the presence of *I1* combined with the *I2* mutants responding to the *Avr2* variants present in races 3 of the pathogen would still be sufficient for resistance. These results suggest that the *I2* lines presented here constitute an important source of resistance against *F. oxysporum f. sp. lycopersici*. However further phenotypic analysis is required to define the degree to which these lines have a potential market profile. In more detail, even though those lines displayed no obvious morphological abnormalities, other morphological, physiological characters (firmness, flavor, colour, shape, texture) and quality traits (shelf life) of the fruits produced need to be examined. Even so, and taking into account that these lines exert some good level of resistance in the field, whether they would constitute a desirable product for the consumers is an open possibility. Overall these findings give rise to exciting prospects on the use of synthetic NLR receptors for breeding crop plants with a broad-spectrum disease resistance. As previously discussed in chapter 4, this strategy could efficiently contribute to the control of economically important plant pathogens. The introduction of crops in the field with such powerful NLR receptors

could minimize the use of chemicals, leading at the same time to a reduction of overall costs in the cultivation process.

CHAPTER 6: Is the *I2* locus involved in the resistance of tomato cultivar PVO 43143 against *P. infestans*?

6.1. Introduction

I2 was the first of the *I* genes to be cloned from tomato, and it confers race specific resistance against the wilt pathogen *Fusarium oxysporum f. sp. lycopersici* (Ori, Eshed et al. 1997, Simons, Groenendijk et al. 1998, Takken and Rep 2010). In the 1960's, Stall and Walter introgressed *I2* from the wild species *Solanum pimpinellifolium* to the cultivated tomato for resistance against race 2 of *Fusarium oxysporum f. sp. lycopersici* (Stall and Walter 1965). Since then, a lot of commercial cultivars have been bred to contain the *I2* gene. In chapter 4, I discovered that I2 responds to effector AVR3a^{KI} secreted by the oomycete *P. infestans* during infection and is able to restrict the growth of the pathogen in transient assays (chapter 4, Fig. 4.1 and 4.7).

In this study, I initiated genetic analyses that aim at determining the extent to which the *I2* locus is a contributing factor to the resistance observed in tomato PVO 43143 cultivar against *P. infestans* strain NL00228 carrying *Avr3a^{KI}*. The specific objectives were to 1) examine whether the resistance observed in tomato cultivar PVO 43143 against *P. infestans* is due to the presence of the *I2* locus in that cultivar, 2) examine whether the presence of the *I2* gene into a tomato cultivar which has no background response to AVR3a^{KI}, correlates with resistance against *P. infestans*, 3) understand why the tomato cultivar MoneyMaker, which lacks *I2* (*i2i2*), shows a similar level of resistance against *P. infestans* as PVO 431413 (*I2I2*). The initial observation came from transient assays indicating that I2 responds to *P. infestans* AVR3a^{KI} and further arrests growth of *P. infestans* strain NL00228 homozygous for *Avr3a^{KI}* (chapter 4). Inoculation of two tomato cultivars, MoneyMaker (*i2i2*) and PVO 43143(*I2I2*) with *P. infestans* strains carrying either of the *Avr3a* variants revealed that both cultivars are resistant to *P. infestans* strain carrying *Avr3a^{KI}*, and susceptible to *P. infestans* strain carrying *Avr3a^{EM}*.

To help address these questions, I crossed tomato cultivars OH7814 (*i2i2,* susceptible to NL00228 *P. infestans* strain) and PVO 43143 (*I2I2,* resistant to NL00228 *P. infestans* strain) and screened the F1 generation for resistance against *P. infestans* strains carrying *Avr3a^{KI}*. All of the F1 lines tested were heterozygous for

I2 (*I2i2*), however showed variable resistance phenotypes towards the *P. infestans* AVR3a^{KI} strain tested. Screening for resistance in the F2 population revealed that resistant lines had either a homozygous or a heterozygous configuration for *I2*. Interestingly, a few F2 tomato plants which all contained the *I2* gene showed intermediate resistance against *P. infestans* strain 88069 carrying *Avr3a^{EM}*. Overall these results suggest that distinct loci, other than *I2* are involved or even define the PVO 43143 tomato resistance observed against *P. infestans* strain NL00228 carrying *Avr3a^{KI}*.

For clarity, I will refer to the F1 plants as lines and to the F2 plants that derived from those lines as individuals.

6.2. Results

6.2.1. Tomato cultivars MoneyMaker and PVO 43143 are resistant to *P. infestans* NL00228 strain (AVR3a^{KI}) but not to *P. infestans* strain 88069 (AVR3a^{EM})

The initial hypothesis was based on the previous discovery that I2 responds to AVR3a^{KI} from *P. infestans* after co-expression of both in the model plant *N. benthamiana* (chapter 4, Fig. 4.1) and additional evidence that I2 arrests *P. infestans* growth of strain NL00228 (AVR3a^{KI}) (chapter 4-Fig. 4.7). To test whether tomato cultivars carrying the *I2* gene are also resistant to *P. infestans* homozygous for AVR3a^{KI}, I inoculated leaves from tomato plants varieties PVO 43143 (I2I2) and MoneyMaker (i2i2) with *P. infestans* zoospores as previously described. Surprisingly, both varieties showed resistance to *P. infestans* strain NL00228 (AVR3a^{KI}) (Fig. 6.1A) but were susceptible to *P. infestans* strain 88069 (AVR3a^{EM}) (Fig. 6.1B). This result indicates that independent loci present at the MoneyMaker tomato background are involved to the resistance observed to *P. infestans* strain NL00228 carrying *Avr3a^{KI}*.

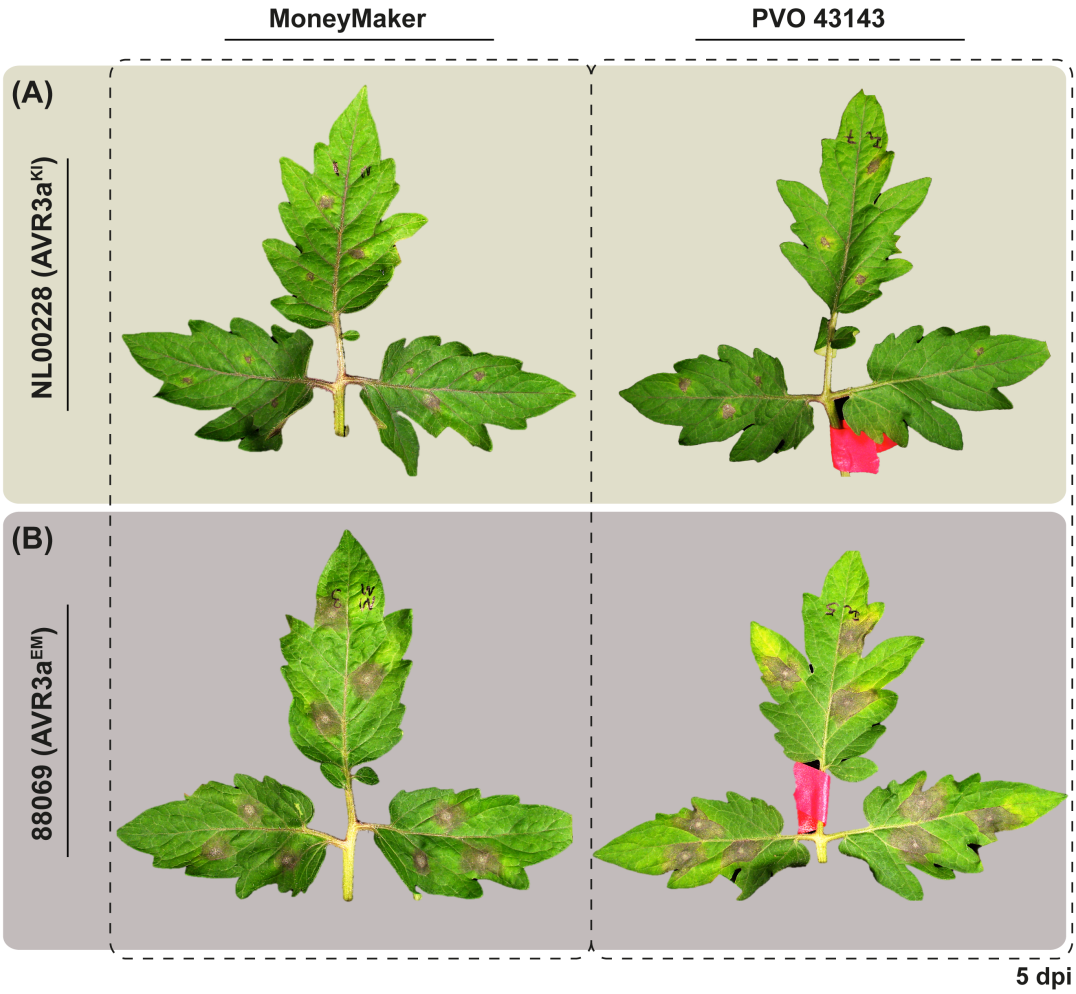

Figure 6.1: Tomato cultivars MoneyMaker and PVO 43143 are resistant to *P. infestans* carrying *Avr3a^{KI}*.
Three- to four-week-old tomato plants from cultivars MoneyMaker and PVO 43143 were subjected to *P. infestans* infection. A, Tomato leaves infected with *P. infestans* strain NL00228, homozygous for *Avr3a^{KI}*. B, Tomato leaves infected with *P. infestans* strain 88069 homozygous for *Avr3a^{EM}*. Pictures were taken 5 days post inoculation (5 dpi).

6.2.2. The Ohio 7814 (OH7814) tomato variety does not respond to AVR3a^{KI}

To investigate whether the resistance phenotype observed in MoneyMaker and PVO 43143 tomato cultivars correlates with a response to the AVR3a^{KI} variant of *P. infestans*, I performed an agroinfection experiment with *Potato Virus X* (Vleeshouwers, Driesprong et al. 2006). Briefly, cotyledon-stage plants from different tomato cultivars (table 2.9.1) were inoculated with *Agrobacterium tumefaciens* carrying a PVX-based vector expressing AVR3a^{KI}, AVR3a^{EM}, or a truncated version of green fluorescent protein (ΔGFP) (Fig. 6.2). This method is based on the ability of PVX to replicate inside the plant cells. Consequently, recombinant PVX transcripts

are produced and infect tissue that surrounds the inoculation site. The recombinant transcripts will express the insert and hypersensitive responce will appear in the case the encoded protein is recognised by a host factor (Takken, Luderer et al. 2000). Hypersensitive response to AVR3a^{KI} was observed for 4 out of 5 varieties tested, including PVO 43143, which is homozygous for the *I2* gene (Fig. 6.2), (table 6.2.1). OH7814 tomato plants (*i2i2*) were the only ones that did not show symptoms as a result of the inoculation. These results suggest that response to AVR3a^{KI} can be conferred independently of the *I2* locus.

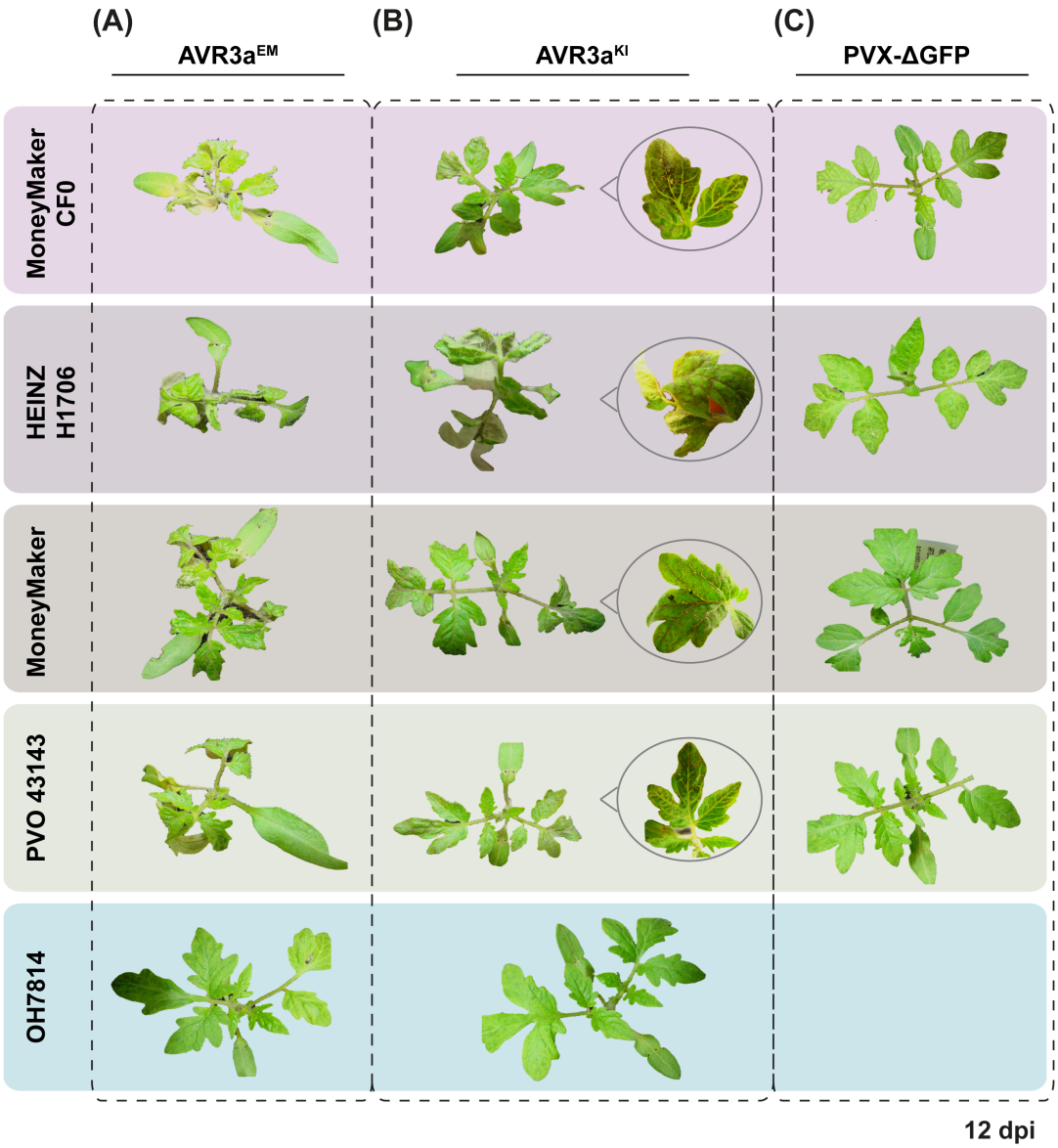

Figure 6.2: Tomato cultivar OH7814 does not respond to AVR3a^{KI}.
Tomato plants of different cultivars were assessed for their ability to respond to AVR3a variants. Plants at the cotyledon stage were inoculated with *Agrobacterium tumefaciens* carrying a binary *Potato virus X* (PVX)-based vector expressing *P. infestans* AVR3a^{KI} (A), AVR3a^{EM} (B), or a truncated version of green fluorescent protein (ΔGFP) (control) (C) according to know protocols (Vleeshouwers, Driesprong

et al. 2006, Du, Rietman et al. 2014). Hypersensitive response symptoms appear as a result of systemic spreading of the virus and expression of the effector gene. The following tomato varieties were used in this experiment: MoneyMaker CF0, HEINZ H1706, MoneyMaker, PVO 43143 and OH7814 (table 2.9.1).

Table 6.2.1: Response of different tomato cultivars to AVR3a from *P. infestans*

Tomato Cultivars	AVR3a^{KI}	AVR3a^{EM}	control	*I2* genotype
MoneyMaker CF0	**+**	**+/-**	**-**	*i2i2*
HEINZ H1706	**+**	**+/-**	**-**	*i2i2*
MoneyMaker	**+**	**+/-**	**-**	*i2i2*
PVO 43143	**+**	**+/-**	**-**	*I2I2*
OH7814	**-**	**-**	**-**	*i2i2*

(+) and/or (-) symbols reflect the presence and/or absence of hypersensitive response following Agroinfection of the indicated tomato cultivars with the PVX constructs indicated in Figure 6.2. Details on the cultivars used in this experiment can be found in Chapter 2 (table 2.9.1).

6.2.3. Crosses between OH7814 tomato cultivar (*i2i2*) and PVO 43143 (*I2I2*) tomato cultivar

The finding that OH7814 does not respond to AVR3a^{KI} or AVR3a^{EM} from *P. infestans* prompted me to cross this variety to PVO 43143. The underlying hypothesis was to initiate genetic analyses to determine whether the *I2* locus is sufficient to provide resistance against *P. infestans* NL00228 strain carrying *Avr3a^{KI}*. The OH7814 variety was used as the male donor, and PVO 43143 *I2*-containing variety as the female donor (carrying the resistance trait) (Fig. 6.3).

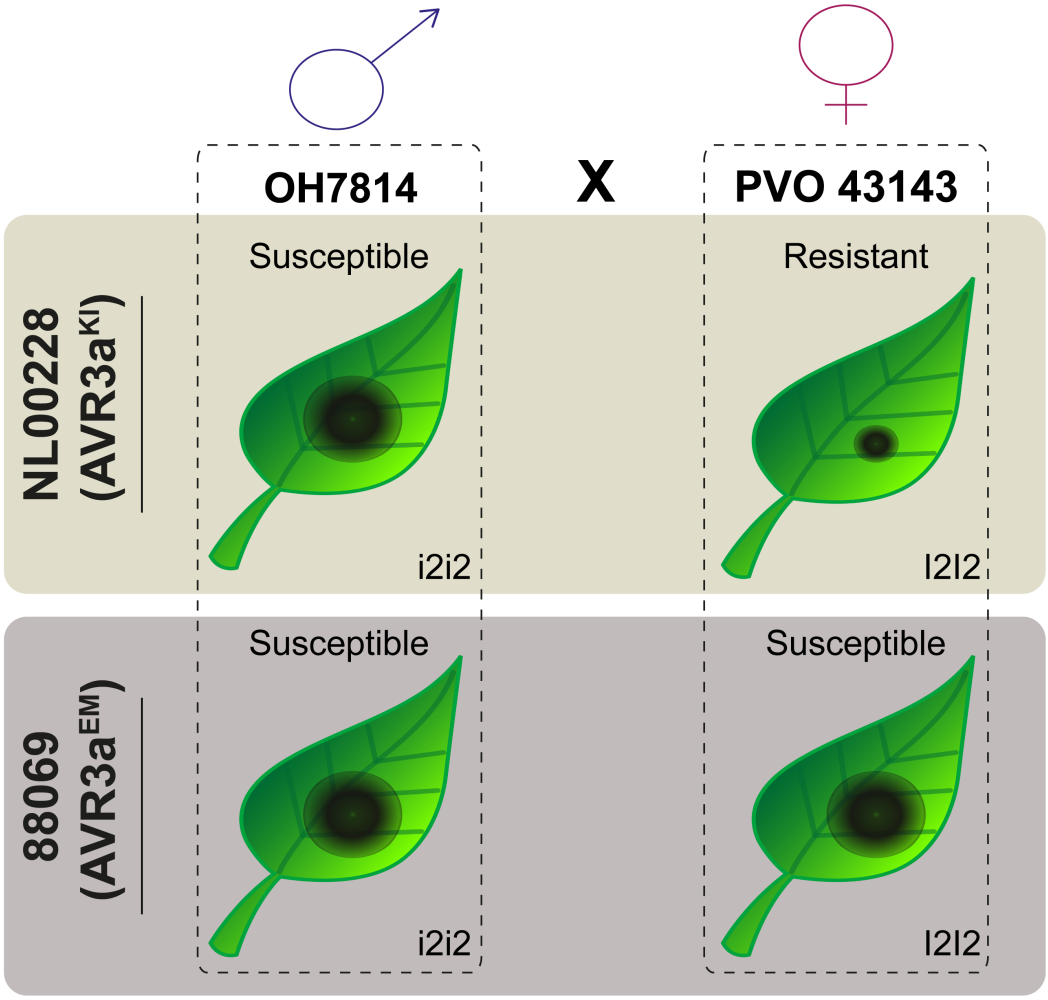

Figure 6.3: Schematic representation of the cross performed between OH7814 and PVO 43143 tomato cultivars.
The OH7814 (i2i2) tomato variety was used as the male donor for this cross and it is susceptible to both *P. infestans* strains (NL00228 and 88069). Tomato variety PVO 43143 (I2I2) was used as the female donor for this cross and it is resistant to *P. infestans* NL00228 (homozygous for *Avr3a*^{KI}), but susceptible *P. infestans* 88069 (homozygous for *Avr3a*^{EM}).

6.2.4. F1 tomato lines heterozygous for *I2* are partially resistant to *P. infestans* NL00228 strain

Ten individual F1 lines from the OH7814 X PVO 43143 cross were tested for resistance against *P. infestans* strains carrying either of the AVR3a variants. The lesions developed were quantified using the Image J analysis software (paragraph 2.7.1). Analysis of variance (ANOVA) followed by a Fisher's Least Significant Difference (LSD) test was carried out to reveal statistically significant differences in the lesion sizes among the different tomato lines tested. Of the 10 tomato lines

inoculated with *P. infestans* NL00228 strain (homozygous for *Avr3a*^{KI}), lines F1-[2,3,4,5,6,8,9] developed lesions statistically significant smaller in size than the susceptible OH7814 parent (and similar to the resistant parent PVO 43143) (Fig. 6.4A and C), (table 6.2.2). F1-7 line presented an intermediate resistance phenotype as it developed lesions significantly different in size than both parents but smaller than the susceptible OH7814 parent (Fig. 6.4A and C). Only two lines (F1-1 and F1-10) were depicted as susceptible, as they showed lesions similar to the susceptible parent OH7814 (Fig. 6.4A and C), (table 6.2.2). In the case of *P. infestans* 88069 strain (homozygous for *Avr3a*^{EM}), all the F1 lines tested developed lesions similar in size to both susceptible parents, OH7814 and PVO 43143 (Fig. 6.4B and C), (table 6.2.1). Genotypic characterization of the F1 lines tested revealed that all of them are heterozygous for *I2* (*I2i2*) (Fig. A4.1-Appendix 4). These results indicate that the *I2* gene, in the heterozygous configuration, does not confer resistance to *P. infestans* in these tomato lines. However, I pursued the hypothesis that a homozygous configuration for the *I2* gene being involved in the PVO 43143 tomato resistance observed.

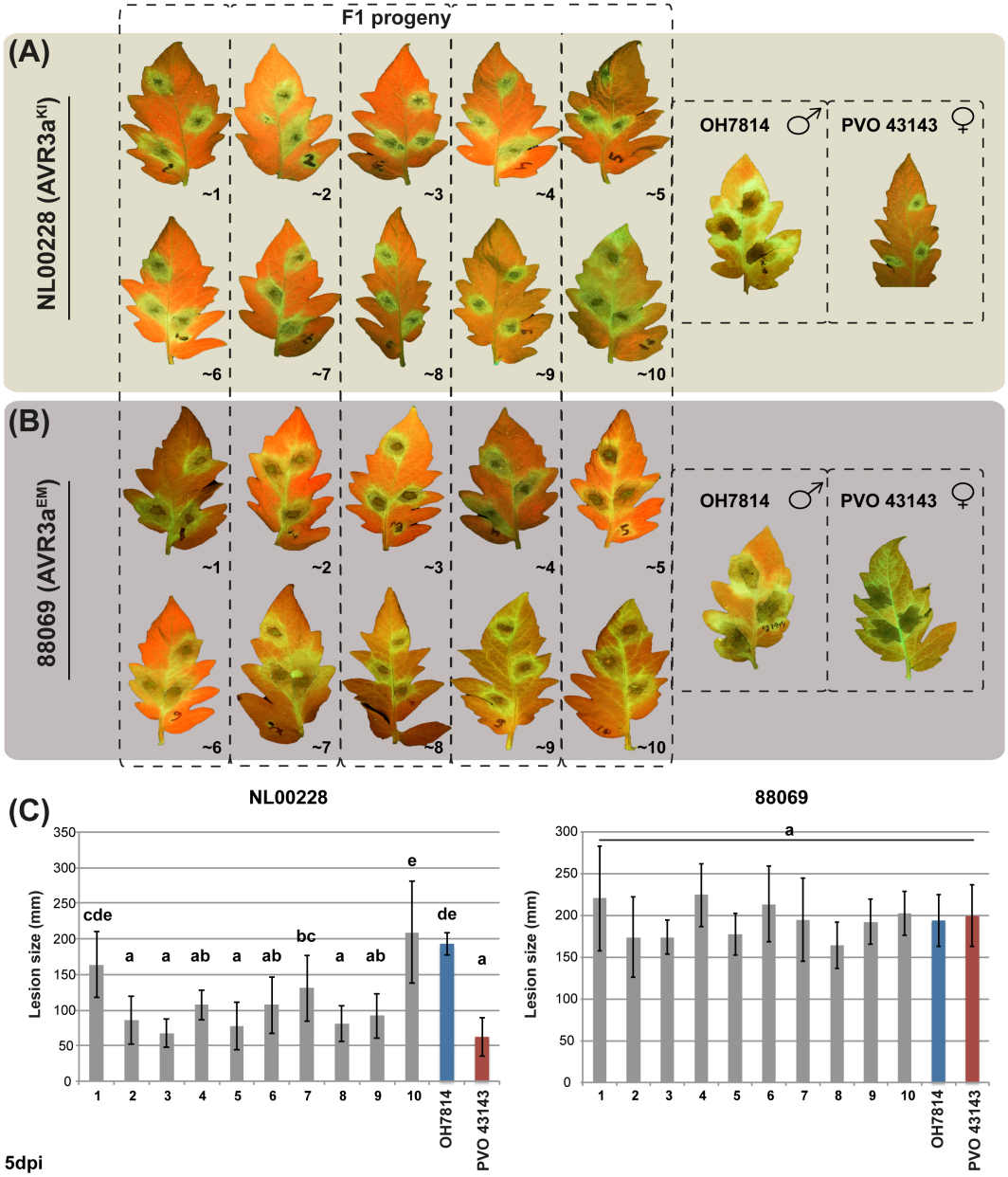

Figure 6.4: F1 lines show variable responses to *P. infestans* NL00228.

Leaves from three- to four-week-old F1 tomato plants were infected with *P. infestans*. A, Tomato leaves infected with *P. infestans* strain NL00228, (homozygous for *Avr3a*^{KI}). B, Tomato leaves infected with *P. infestans* strain 88069 (homozygous for *Avr3a*^{EM}). Pictures were taken 5 days post inoculation (5 dpi). C, Lesion size following inoculation with *P. infestans* strain NL00228 (left panel) or *P. infestans* strain 88069 (right panel) was calculated using Image J analysis software (paragraph 2.7.1). Bars represent the average value of 6 lesions. Error bars represent standard deviation. Different letters indicate statistically significant difference with a 95% confidence interval according to an ANOVA analysis followed by a Fisher's LSD test.

Table 6.2.2: Resistance phenotypes of the F1 lines against *P. infestans*

F1 tomato lines	*P. infestans* NL00228 ($AVR3a^{KI}$)	*P. infestans* 88069 ($AVR3a^{EM}$)	*I2* genotype
1	S	S	*I2i2*
2	R	S	*I2i2*
3	R	S	*I2i2*
4	R	S	*I2i2*
5	R	S	*I2i2*
6	R	S	*I2i2*
7	R/S	S	*I2i2*
8	R	S	*I2i2*
9	R	S	*I2i2*
10	S	S	*I2i2*
Parents			
OH7814	S	S	*i2i2*
PVO 43143	R	S	*I2I2*

R: Resistant, S: Susceptible, R/S: Intermediate resistance; Resistance and susceptibility phenotypes reflect quantitative data from the results shown in Figure 6.4 compared to the parental lines. The genotypic characterization reflects the results shown in Figure A4.1 (Appendix 4).

6.2.5. Resistance against *P. infestans* NL00228 in the F2 population

To further characterize the resistance against *P. infestans*, I selected five F2 individuals of each F1 line previously tested (F1-10) and performed infections assays with both *P. infestans* strains (NL00228 and 88069) (Fig. 6.5), (table 6.2.3). Inoculation of F2 individuals with *P. infestans* NL00228 strain revealed both resistant and susceptible plants (Fig. 6.5A). Using the image J analysis software I was able to quantify the infection lesions in each leaf (Fig. 6.5C). ANOVA followed by a Fisher's LSD test was carried out (Fig. A4.3A-Appendix 4), and revealed the following three categories; 1) F2 individuals that showed resistance to *P. infestans* NL00228 similar to the resistant parent PVO 43143 are designated with a red circle, displaying statistically significant difference from the susceptible parent OH7814, 2) F2 individuals that were susceptible to *P. infestans* NL00228 showing infection lesions similar to the susceptible parent OH7814 are designated with a blue circle and 3) F2 individuals that showed an intermediate resistance phenotype and developed lesions statistically significant in size from both parents (are not designated) (Fig. 6.5C). Homogeneous groups that arose from the full statistical analysis with Fisher's LSD test are also shown (Fig. A4.3A-Appendix 4). Genotypic characterization of these plants revealed that the resistant F2 individuals were either homozygous or heterozygous for *I2* (Fig. A4.2-Appendix 4), (table 6.2.3). Out of the five F2 individuals which were depicted as susceptible (F2-1.2, F2-3.3, F2-5.3, F2-6.4, F2-

8.1, F2-8.3) only F2-3.3, F2-6.4 and F2-8.1 were heterozygous for *I2* while the rest did not contain the *I2* gene (Fig. A4.2-Appendix 4), (table 6.2.3). These results are in agreement with the results of the F1 lines where two plants that were heterozygous for *I2* were susceptible to *P. infestans* NL00228 strain (Fig. 6.4), (table 6.2.2). Overall it is not clear from these results whether *I2* is involved in the tomato resistance observed to *P. infestans* NL00228. A full segregation analysis for each of the F1 lines generated is required to address this question and also reveal the degree to which other loci are involved.

6.2.6. Does the *I2* locus contribute to resistance against *P. infestans* strain 88069?

The F2 population was also screened with *P. infestans* strain 88069 (homozygous for *Avr3a*^{EM}) (Fig. 6.5B and D), (table 6.2.3). Both parents were susceptible to that strain as revealed by the extended lesions developed (Fig. 6.5B). ANOVA followed by a Fisher's LSD test was carried out (Fig. A4.3B-Appendix 4) after quantification of the infection, and revealed the following three categories; 1) F2 individuals that were susceptible and developed lesions similar in size to both parental lines (OH7814 and PVO 43143), non designated; 2) F2 individuals that were more susceptible than the parental lines, developing lesions greater in size, designated with a black circle; and 3) F2 individuals that showed an intermediate resistance phenotype and developed infection lesions statistically significant in size than both parental lines, designated with an open circle (Fig. 6.5D and A4.3B-Appendix 4). Interestingly, the four F2 individuals (F2-3.5, F2-7.4, F2-9.5, F2-10.3) showing intermediate resistance to *P. infestans* 88069 carrying *Avr3a*^{EM} were either homozygous or heterozygous for *I2* (Fig. A4.2-Appendix 4). Out of these four individuals, an *I2* heterozygous individual restricted *P. infestans* growth to the highest level, and developed the smallest infection lesions, F2-10.3, (Fig. 6.5B and A4.2-Appendix 4). Taking into account that none of the heterozygous F1 lines tested showed such a resistance phenotype to 88069 (Fig. 6.4) this result implicates a recessive gene being involved in this resistance. As previously mentioned, a full segregation analysis for each of the F1 lines generated is necessary to further characterize which loci are involved in the resistance phenotypes observed. The preliminary results presented in this study do not clearly support the involvement of the *I2* locus in either of the resistance phenotypes noted.

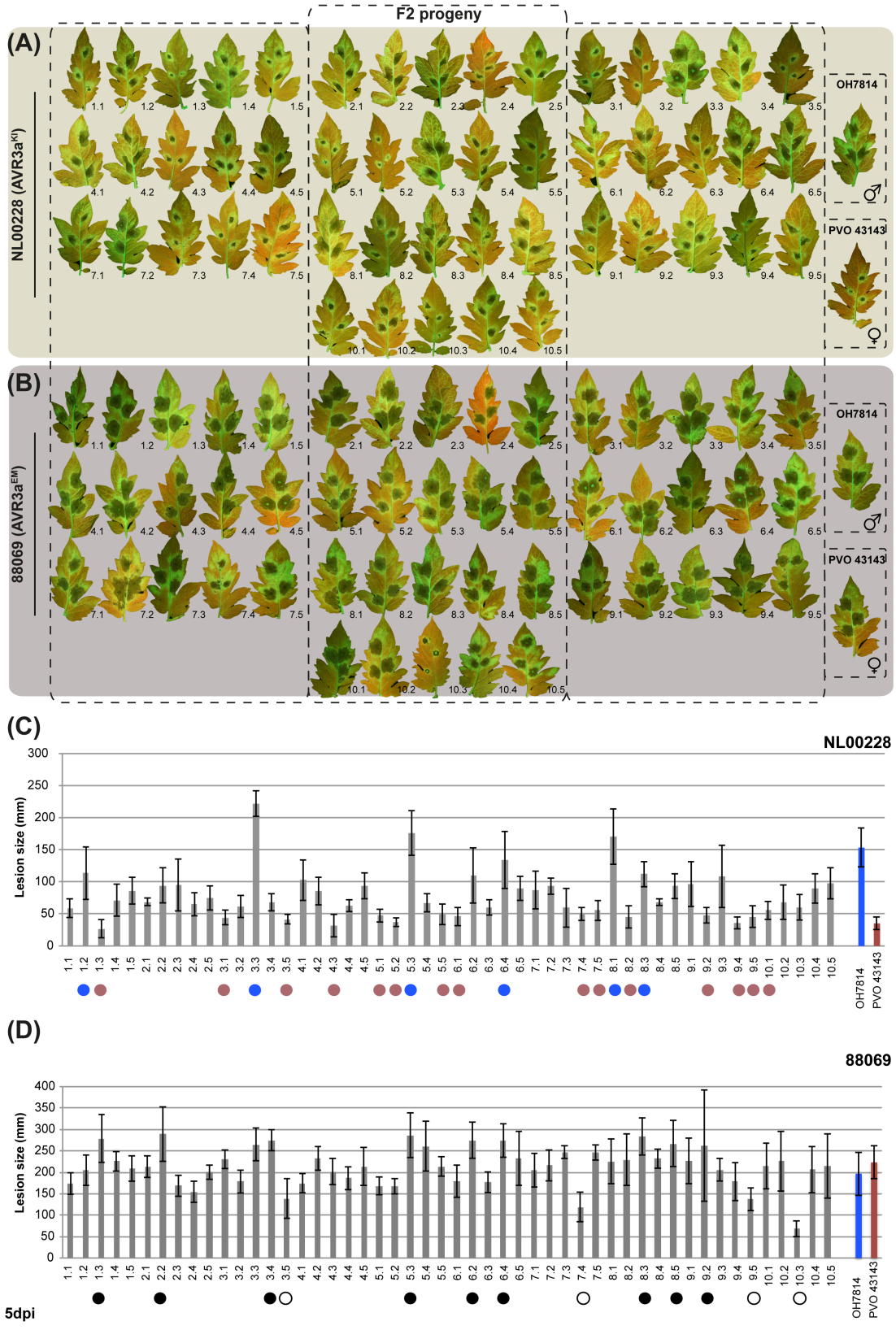

Figure 6.5: F2 individuals show resistance to *P. infestans*.

Leaves from five F2 individual from each F1 line (F1-1 to F1-10) were subjected to *P. infestans* infection. A, Tomato leaves infected with *P. infestans* strain NL00228, (homozygous for *Avr3a*^{KI}). B, Tomato leaves infected with *P. infestans* strain 88069 (homozygous for *Avr3a*^{EM}). Pictures were taken 5 days post inoculation (5 dpi). C, D, Lesion size following inoculation with *P. infestans* strain NL00228 or *P. infestans*

strain 88069 was calculated using Image J analysis software (paragraph 2.7.1). Bars represent the average value of 6 lesions. Error bars represent standard deviation. Red circles indicate plants that were infected similar to the PVO 43143 line (statistically significant difference from the OH7814); blue circles indicate plants that were infected similar to the OH7814 line (statistically significant difference from the PVO 43143); open circles indicate plants that showed an intermediate resistance phenotype (statistically significant difference from both OH7814 and PVO 43143 parents) and black circles indicate plants that were more susceptible than the parents (statistically significant difference from both OH7814 and PVO 43143 parents). Statistical analysis was carried out using ANOVA and Fisher's LSD test with a 95% confidence interval.

Table 6.2.3: Resistance phenotypes of the F2 individuals against *P. infestans*

F2 individuals	*P. infestans* NL00228 (AVR3a^{KI})	*P. infestans* 88069 (AVR3a^{EM})	*I2* genotype
1.1	R/S	S	*I2i2*
1.2	S ●	S	*i2i2*
1.3	R ●	SS ●	*I2I2*
1.4	R/S	S	*i2i2*
1.5	R/S	S	*I2I2*
2.1	R/S	S	*I2i2*
2.2	R/S	SS ●	*I2i2*
2.3	R/S	S	*I2I2*
2.4	R/S	S	*I2I2*
2.5	R/S	S	*I2i2*
3.1	R ●	S	*I2i2*
3.2	R/S	S	*I2i2*
3.3	S ●	S	*I2i2*
3.4	R/S	SS ●	*I2I2*
3.5	R ●	R/S ○	*I2I2*
4.1	R/S	S	*I2I2*
4.2	R/S	S	*I2i2*
4.3	R ●	S	*I2i2*
4.4	R/S	S	*I2i2*
4.5	R/S	S	*I2i2*
5.1	R ●	S	*I2I2*
5.2	R ●	S	*I2I2*
5.3	S ●	SS ●	*i2i2*
5.4	R/S	S	*I2i2*
5.5	R ●	S	*I2i2*
6.1	R ●	S	*I2i2*
6.2	R/S	SS ●	*I2i2*
6.3	R/S	S	*I2i2*
6.4	S ●	SS ●	*I2i2*
6.5	R/S	S	*i2i2*
7.1	R/S	S	*I2i2*
7.2	R/S	S	*i2i2*
7.3	R/S	S	*I2i2*
7.4	R ●	R/S ○	*I2I2*
7.5	R ●	S	*I2i2*
8.1	S ●	S	*I2i2*
8.2	R ●	S	*I2i2*

8.3	S ●	SS ●	*i2i2*
8.4	R/S	S	*I2I2*
8.5	R/S	SS ●	*I2i2*
9.1	R/S	S	*I2i2*
9.2	R ●	SS ●	*I2i2*
9.3	R/S	S	*I2i2*
9.4	R ●	S	*I2i2*
9.5	R ●	R/S ○	*I2i2*
10.1	R ●	S	*I2I2*
10.2	R/S	S	*I2i2*
10.3	R/S	R/S ○	*I2i2*
10.4	R/S	S	*i2i2*
10.5	R/S	S	*I2I2*
Parents			
OH7814	S ●	S	*i2i2*
PVO 43143	R ●	S	*I2I2*

P. infestans NL00228: [R ●: Resistant, S ●: Susceptible, R/S: Intermediate resistance]; Resistance and susceptibility phenotypes reflect quantitative data from the results shown in Figure 6.5. The genotypic characterization reflects the results shown in Figure A4.2 (Appendix 4).
P. infestans 88069: [S: Susceptible, R/S ○: Intermediate resistance, SS ●: More Susceptible than both parents]; Resistance and susceptibility phenotypes reflect quantitative data from the results shown in Figure 6.5. The genotypic characterization reflects the results shown in Figure A4.3 (Appendix 4).

6.3. Discussion

I2 is a tomato immune receptor from S. *pimpinellifolium*, which has been introgressed into cultivated tomato to mediate resistance towards race 2 of the wilt-causing fungus, *F. oxysporum f. sp. lycopersici* (Stall and Walter 1965, Ori, Eshed et al. 1997, Simons, Groenendijk et al. 1998, Takken and Rep 2010). In this study I investigated the extent to which the *I2* locus contributes to the resistance that I detected in tomato cultivar PVO 43143 against *P. infestans* NL00228 (AVR3a^{KI}). The initial observation that a non *I2*-cultivar, MoneyMaker (*i2i2*) was resistant to *P. infestans* NL00228 to the same extent with PVO 43143 (I2I2) was indicative of one or more resistance loci distinct from *I2*. OH7814 tomato cultivar (*i2i2*) was crossed with the PVO 43143 (*I2I2*), based on the observation that it does not respond to AVR3a from *P. infestans* (Fig. 6.2), (Table 6.2.1). Infection assays on the F1 progeny revealed that *I2* does not confer resistance to *P. infestans* NL00228 in a heterozygous configuration (Fig. 6.4 and A4.1-Appendix 4), (Table 6.2.2). Infection assays on the F2 population revealed that individuals that were resistant to *P. infestans* strain NL00228 contained the *I2* gene either in a homozygous or a

heterozygous configuration (Fig. 6.5 and A4.2-Appendix 4), (table 6.2.3). Also, a few lines showed resistance to *P. infestans* 88069, which indicates that a recessive gene may be involved in that phenotype (Fig. 6.5 and A4.2-Appendix 4), (table 6.2.3). It is important to state here that resistant and susceptible phenotypes were based on quantitative data (lesion size). Overall these results support the idea that a locus or multiple loci other than *I2* primarily control the resistance of tomato PVO 43143 towards *P. infestans* strain NL00228. Also, I cannot rule out the possibility that this resistance in PVO 43143 does not depend on AVR3a response.

The following points also rose from the results analysis: 1) tomato cultivars MoneyMaker (*i2i2*) and OH7814 (*i2i2*), although both lacking the *I2* gene, show resistance and susceptibility to *P. infestans* NL00228, respectively. It is possible that the locus responsible for the resistance in MoneyMaker is not present in OH7814; 2) PVO 43143 (*I2I2*) is resistant to *P. infestans* NL00228. However, my results do not clearly support the involvement of *I2* in that resistance.

As previously discussed, future work is required to address these points. First, it is important to perform a full segregation analysis on the F1 lines generated, where at least sixteen F2 individuals of each line are tested with *P. infestans*. The emerging phenotypes will help identify the putative pattern of inheritance of the resistance trait, for example mendelian, dominant autosomal or epistatic. Additionally, it would be useful to perform infection assays on progeny of the F2 individuals that were identified as resistant to examine whether the resistance trait is retained. The resistant plants identified in this study from both F1 and F2 populations can be used for backcrossing to the resistant parent (PVO 43143), subsequent rounds of which process will help isolating the resistance trait. Another approach would be marker-assisted linkage analysis, where the development of genetic markers would help the fine mapping of the gene/s that are involved in the strain specific resistance of tomato towards *P. infestans*. In order to identify the loci controlling the resistance of MoneyMaker to *P. infestans* NL00228, it would be useful to cross MoneyMaker with the susceptible OH7814 variety and assess the progeny for resistance to *P. infestans*.

One interesting observation that arose form the results presented in this study was that a few F2 individuals which all contained the *I2* gene (in a homozygous or heterozygous configuration) showed intermediate resistance to *P. infestans* 88069 strain ($AVR3a^{EM}$). Considering that no such phenotype was observed in the F1

progeny, it is possible that a recessive gene is controlling that phenotype. *Ty-2*, is a dominant resistance gene in tomato conferring resistance to the *Tomato Yellow Leaf Curl Virus* (TYLC) pathogen and is in close proximity of the *I2* gene in chromosome 11 (Ji, Scott et al. 2009). It is possible that this region in chromosome 11 is a hotspot for resistance traits in tomato. Future experiments are however required so as to identify the key players in the resistance phenotypes presented.

CHAPTER 7: General discussion and Outlook

Throughout evolution, plants acquired a multilayered defence arsenal to defend against pathogens. In return, pathogens have developed ways to successfully colonize plants, by overcoming their defence mechanisms. In the work presented in this thesis, I studied two approaches to engineer disease resistance against filamentous plant pathogens. An important aspect of the plant innate immunity is the inducible production of secondary metabolites as a result of pathogenic invasion (Kuc 1995, Mithoefer and Boland 2012). Plant secondary antimicrobial metabolites, termed phytoalexins, have been widely studied for their role in plant defence against pathogenic attack (Stoessl, Unwin et al. 1973, Jones, Unwin et al. 1975, Ward 1976, Hargreaves, Mansfield et al. 1977, Kurosaki and Nishi 1983, Hoffman and Heale 1987, Milat, Ducruet et al. 1991, Milat, Ricci et al. 1991, Delserone, Matthews et al. 1992, Mercier, Arul et al. 1993, Echeverri, Torres et al. 1997, Keller, Czernic et al. 1998, Ma 2008, Favaron, Lucchetta et al. 2009, Grosskinsky, Naseem et al. 2011, Timperio, D'Alessandro et al. 2012, Lachhab, Sanzani et al. 2014). Another important component of the plant defence system is mediated by specialized immune receptors encoded by *R* genes. During infection, pathogens facilitate their colonization and circumvent plant defence barriers by secreting effector molecules to the apoplastic space or to different compartments of the plant cell cytoplasm (Hogenhout, Van der Hoorn et al. 2009, Dodds and Rathjen 2010, Bozkurt, Schornack et al. 2012, Win, Chaparro-Garcia et al. 2012). In an incompatible interaction these effector proteins are perceived by immune receptors, which will then trigger further immune responses leading to disease resistance (Jones and Dangl 2006, Ooijen, Burg et al. 2007, Dodds and Rathjen 2010, Win, Chaparro-Garcia et al. 2012). The largest family of intracellular immune receptors is the nucleotide binding-leucine-rich repeat (NB-LRR or NLR) protein family, and constitutes an important element of defence in both plants and animals (Maekawa, Kufer et al. 2011, Jacob, Vernaldi et al. 2013).

As previously highlighted, the main objectives of this thesis were 1) to examine whether plant-derived antimicrobial compounds can determine host specificity in plant-microbe interactions and 2) to provide insights on how synthetically engineered immune receptors could open up new possibilities for breeding crop plants with a broad spectrum of disease resistance.

In chapter 3, I examined the effect of a pepper phytoalexin, capsidiol, against two *Phytophthora* species, the Irish potato famine pathogen *P. infestans* and the rot-causing vegetable pathogen *P. capsici*. This work confirmed earlier studies (Jones, Unwin et al. 1975, Ward 1976) that capsidiol differentially affects these two species by inhibiting their growth. Furthermore, I reported an additional intraspecific variation of several *P. infestans* isolates to capsidiol (chapter 3). The mechanism by which *P. capsici* tolerates capsidiol is still unclear, as well as the reason for the differential sensitivity of *P. infestans* to capsidiol.

In chapters 4 and 5, I examined the use of synthetic NLR immune receptors with expanded response specificities as an approach to engineer crop plants with a broad-spectrum disease resistance. I focused on two CNL proteins, the tomato I2 and the potato R3a proteins, which mediate resistance to *Fusarium oxysporum f. sp. lycopersici* and *Phytophthora infestans* respectively (Simons, Groenendijk et al. 1998, Takken and Rep 2010).

In chapter 4, I discovered that I2 responds weakly to AVR3a^{KI}, an effector from *P. infestans*. I also show that in transient assays I2 confers resistance to NL00228 strain of the pathogen that carries this effector. In a previous study, Segretin *et al.*, identified eight single-site R3a+ mutants with expanded response to the AVR3a^{EM} variant, which evades recognition by R3a (Segretin, Pais et al. 2014). Taking advantage of the high similarity that I2 and R3a share in their N-termini (Huang, van der Vossen et al. 2005), I transferred the two R3a+ mutations located at the CC and NB-ARC domains of R3a (R3a^{I148F} and R3a^{N336Y}), to the equivalent positions in I2 and assessed whether they expand the response of the later to the stealthy AVR3a^{EM} variant. The I2 mutants generated did not result in an expanded response phenotype. Saturation mutagenesis at these positions led to the identification of a CC-domain mutant, I2^{I141N}, which responds to both AVR3a variants from *P. infestans*. Interestingly, I2^{I141N} confers resistance to *P. infestans* strains carrying either of the AVR3a variants. I2^{I141N} also responds to AVR2 variants of *F. oxysporum f. sp. lycopersici* that evade recognition by the wild-type I2 protein. What could be the mode of action of the I2^{I141N} mutant? As discussed in chapter 4, I2^{I141N} seems to be a trigger-happy mutant, which means that its threshold for activation is lower than that of the wild-type I2 protein, so it is more easily activated by weak elicitors. Tameling *et al.* showed that an autoactive version of I2 was impaired in nucleotide hydrolysis (Tameling, Vossen et al. 2006). Also, an autoactive version of the flax M NLR protein

was shown to have increased preference for binding ATP (Williams, Sornaraj et al. 2011). We don't know whether or not $I2^{I141N}$ is affected in its ability to bind ATP, which in turn could modify its threshold for activation. Preliminary results from infection assays suggested that tomato lines carrying *I2*^{I141N} confer resistance against *P. infestans* growth. Additionally, these stable tomato lines did not present any obvious phenotypic abnormality, suggesting that the slight autoactivation observed in the transient assays did not result in deleterious effects in transgenic tomatoes.

In chapter 5, I investigated the extent to which the R3a+ mutations, when transferred to I2, expand its ability to respond to the stealthy AVR2 variants from races 3 of *F. oxysporum f. sp. lycopersici*. In total, I discovered five additional I2 mutant proteins, ($I2^{I141L}$, $I2^{I141V}$, $I2^{N330K}$, $I2^{N330D}$ and $I2^{C967R}$) with expanded response to the AVR2 variants found in different races 3 of the pathogen. Remarkably, stable transgenic tomato plants carrying those *I2* mutant genes displayed resistance against both races 2 and 3 of *F. oxysporum f. sp. lycopersici* correlating with the HR results of the transient assays. Additionally, all the tomato plants tested showed no obvious phenotypic abnormality, suggesting again that the weak autoactivation observed for two of the I2 mutant proteins ($I2^{I141L}$ and $I2^{N330K}$) does not result in a morphological penalty and that these I2+ mutants have promising potential for generating resistant varieties.

An interesting observation that emerged through my mutational analysis is that some of the I2 mutants generated behaved differently in response to AVR3a and AVR2 effectors from *P. infestans* and *F. oxysporum f. sp. lycopersici* respectively. The CC-domain mutants, $I2^{I141L}$ and $I2^{I141V}$ mutants showed a loss-of-response phenotype when transiently expressed with the AVR3a effectors, but a gain-of-response when tested with the AVR2 effectors. Similarly, $I2^{N330D}$ and $I2^{N330P}$ at the NB-ARC domain behaved as loss-of-response mutants with respect to the AVR3a variants. However, $I2^{N330D}$ showed expanded response to AVR2 variants of *F. oxysporum f. sp. lycopersici*, whereas $I2^{N330P}$ showed a response similar to the I2 wild-type when tested with the AVR2 effectors. Finally, $I2^{N330K}$, which showed a similar to the wild-type I2 response to the AVR3a variants, had an expanded response to race 3 AVR2 variants *F. oxysporum f. sp. lycopersici*. These differences point to the existence of the distinct mechanisms and/or threshold levels mediating the interaction of I2 and the effectors in each system. As previously discussed in chapter 1, our knowledge on the mechanisms underlying the I2/AVR2 interaction is yet very limited. Both direct

and indirect interaction scenarios are possible (Takken and Rep 2010). Regarding I2 and AVR3a interaction, I have shown that despite the weak I2 response to AVR3a^{KI}, it is possible to restrict growth of the pathogen strain NL00228 that carries AVR3a^{KI}. Therefore, I cannot rule out the possibility of I2 responding to other effectors present in this *P. infestans* strain.

Overall in chapters 4 and 5, I showed that the expanded response phenotypes observed in transient assays translated to resistance against *P. infestans* and *F. oxysporum f. sp. lycopersici* in stable transgenic plants. Preliminary results suggest that tomato lines carrying *I2^{I141N}* are resistant against *P. infestans* NL00228 strain carrying *Avr3a^{KI}* and are less susceptible to *P. infestans* 88069 strain carrying *Avr3a^{EM}* compared to plants carrying *I2* wild-type and/or non-*I2* tomato lines. Infection assays on tomato plants carrying the following *I2* gain-of-response mutants identified in this work (I2^{I141L}, I2^{I141V}, I2^{N330K} and I2^{C967R}) showed resistance to races 2 and 3 of *F. oxysporum f. sp. lycopersici* which in most cases correlated with the expanded response phenotypes detected in the transient assays. Whether or not the resistance phenotypes observed are strictly dependent on the expanded response of the mutant proteins is unclear. F. Gawehns *et al.*, suggested that the resistance against *F. oxysporum f. sp. lycopersici* mediated by the I2 immune receptor is independent from the cell death observed in this system (Gawehns, Houterman et al. 2014). Their hypothesis was based on the observation that Six6, an effector from *F. oxysporum f. sp. lycopersici*, suppresses the hypersensitive response developed in *N. benthamiana* after co-expression of I2 and AVR2 but does not compromise resistance in tomato (Gawehns, Houterman et al. 2014). However, as Thomma *et al.* previously highlighted, the presence of HR after transient expression of both I2 and AVR2 in the model plant *N. benthamiana* can be an overexpression effect. Therefore, they suggested that this cell death response could be more easily suppressed than the one induced by immune receptors that rely on the HR for their function (Thomma, Nuernberger et al. 2011). F. Gawehns *et al.* thus hypothesized that Six6 is a weak suppressor and the I2-mediated cell death is an easy target for suppression (Gawehns, Houterman et al. 2014). These authors' idea was also supported by the fact that the I2-mediated resistance against the tomato wilt pathogen does not generally involve the HR (Beckman 2000). Additional evidence on the uncoupling of these two phenomena, HR and resistance, has emerged through different studies (Coll, Vercammen et al. 2010, Heidrich, Wirthmueller et al. 2011, Bai, Liu et al. 2012, Hao, Collier et al. 2013). Coll *et al.*, showed that cell death in *Arabidopsis* is antagonistically controlled by two type-I metacaspases, AtMC1 and

AtMC2. Knock-out atmc1, atmc1/atmc2 or atmc2 mutant *Arabidopsis* lines showed suppression or enhancement of RPM1-mediated HR respectively, following infection with *Pseudomonas syringae pv. tomato* (DC3000). However, the suppression of the HR did not affect pathogen proliferation (Coll, Vercammen et al. 2010).

K. Heidrich *et al.*, also observed that different subcellular compartments control different defence branches in the RPS4-EDS1/AvrRps4 system in *Arabidopsis*. A nuclear localization of AvrRps4 was necessary to restrict *Pseudomonas syringae* growth confirming the need for a nuclear RPS4/EDS1 accumulation (Wirthmueller, Zhang et al. 2007, Garcia, Blanvillain-Baufume et al. 2010, Heidrich, Wirthmueller et al. 2011). However a nucleo-cytoplasmic coordination was required for cell death elicitation in the host and transcriptional resistance reinforcement (Heidrich, Wirthmueller et al. 2011). Another study on the barley CNL receptor MLA10, showed that localization of the receptor to the nucleus is sufficient for disease resistance, however the MLA10-mediated HR required a cytoplasmic localization (Bai, Liu et al. 2012). This study further supports the hypothesis that different cell compartments control disease resistance and HR. In a more recent study, Wei Hao *et al.*, identified a mutant in the CC domain of the potato immune receptor Rx which compromised the *in vitro* interaction of the protein with its cofactor RanGAP2. This mutation did not affect the ability of Rx to induce HR after co-expression with the coat protein of PVX, but rather diminished its ability to control virus accumulation (Hao, Collier et al. 2013). All the above studies suggest that it is possible that in some systems the phenomenon of host cell death is independent of processes involved in pathogen restriction (Heidrich, Wirthmueller et al. 2011).

In chapter 6, I explored the hypothesis of *I2* being a determinant of the PVO 43143 tomato resistance observed against *P. infestans* NL00228 strain carrying the AVR3a^{KI} effector. The initial observation that tomato cultivars MoneyMaker (which does not contain *I2*, *i2i2*) and PVO 43143 (homozygous for *I2*, *I2I2*) are both resistant to *P. infestans* NL00228 isolate (AVR3a^{KI}) was already indicative of other loci controlling that resistance. I identified a tomato cultivar that bears no background response to AVR3a and does not contain the *I2* gene, OH7814 and crossed it with the *I2*-containing PVO 43143 tomato cultivar. The F1 lines generated were all heterozygous for the *I2* gene (*I2i2*) and showed both resistance and susceptibility phenotypes to *P. infestans* NL00228 strain (AVR3a^{KI}) whereas they were all susceptible to *P. infestans* 88069 strain (AVR3a^{EM}). Screening for resistance in the F2 population, resistant plants towards *P. infestans* NL00228 all contained the *I2*

gene, however a few plants heterozygous for *I2* were found to be susceptible. Overall these preliminary results cannot support the hypothesis that *I2* is involved in the PVO 43413 tomato resistance observed against *P. infestans* NL00228 strain. Surprisingly in the F2 population, a few *I2*-containing plants showed resistance against *P. infestans* 88069 isolate (AVR3a^{EM}). Such a result was not observed in the F1 population, suggesting that a recessive gene is responsible for that resistance phenotype.

Overall in this work, I have studied two of the many mechanisms plants deploy to defend themselves against invading pathogens. Looking at the role of phytoalexins, as members of the plant's antimicrobial repertoire, I confirmed studies that date back to the 1970s supporting that capsidiol inhibits *P. infestans* growth (Jones, Unwin et al. 1975, Ward 1976). However, whether capsidiol contributes to the inability of *P. infestans* to infect peppers, is still unclear. I have also highlighted the importance of *NLR* genes as a useful tool for generating sustainable disease resistant crops. I have showed that a synthetically generated NLR mutant protein has expanded response specificities towards two different pathogens. My results further support the hypothesis that tomato lines carrying these gain-of-response mutants confer resistance against *F. oxysporum f. sp. lycopersici* and possibly *P. infestans* (preliminary data). Therefore, this approach could prove helpful in designing and engineering NLRs with novel activities.

There are still many open questions regarding the mechanisms driving capsidiol antimicrobial function and also the I2 activation and downstream signaling that leads to immunity. Manipulation of phytoalexin biosynthesis in plants to engineer disease resistance has already proven successful for many cases (Jeandet, Clement et al. 2013). Future experiments should aim at identifying some critical aspects in the *Phytophthora*/capsidiol interaction. The characterization of the molecular targets of capsidiol in the different *Phytophthora* species is of extreme importance for understanding the mechanistic basis of that interaction. Another question that arose from the results presented in this study and needs to be addressed is whether there is any correlation between aggressiveness and tolerance to capsidiol among various *P. infestans* isolates. The ultimate challenge is to test whether transfer of the capsidiol biosynthetic pathway from pepper or tobacco to potato and tomato is sufficient to provide resistance against *P. infestans*. And even so, whether these lines will provide sufficient amounts of yield and/or carry desirable traits has to be investigated.

Several recent studies have highlighted the use of synthetic NLR receptors with an expanded response spectrum as an approach for resistance in the field (Chapman, Stevens et al. 2014, Segretin, Pais et al. 2014, Stirnweis, Milani et al. 2014). The I2 gain-of-response mutants generated in both I2/AVR2 and I2/AVR3a systems gave promising results when introduced to tomato. However, the underlying mechanisms mediating the expanded response observed have to be identified. In addition, even thought the tomato lines generated presented no obvious morphological changes, additional tests on fitness traits have to be conducted, as well as their ability to produce high amounts of yield. The level of disease resistance the tomato lines produced against both *P. infestans* and *F. oxysporum f. sp. lycopersici* is overall promising, however the extend to which this level will be sufficient to restrict the pathogens in the field conditions has to be determined. Furthermore, additional genetic analysis has to be curried out to determine the different locus or loci, which mediate resistance of the different tomato cultivars to P. infestans, and to examine whether the *I2* locus contributes to this phenotype.

It has been previously highlighted that this study opens up exciting possibilities for application in agriculture. So far, *NLR* genes have been efficiently used in breeding through transgenic approaches (Wulff, Horvath et al. 2011, Horvath, Stall et al. 2012, Narusaka, Kubo et al. 2013). However, these approaches, even though successful, are hampered by the low occurrence of *R* genes with the useful response specificities. The results presented here support that gain-of-response mutants identified in one gene can be transferred to homologs and have similar beneficial effects. Such an approach could prove helpful in designing and engineering NLRs with novel activities against divergent pathogens. This study also supports that these powerful immune receptors once introduced to crops lead to disease resistance in the conditions tested. To further address the translational nature of such an approach, an extensive fitness analysis of the lines produced along with additional pathogenicity tests, field trials and yield-estimation assays are required.

APPENDICES

Appendix 1

Supplementary figures for chapter 3: Variation in sensitivity to the phytoalexin capsidiol between the oomycete plant pathogens *Phytophthora infestans* and *Phytophthora capsici* is consistent with their host range

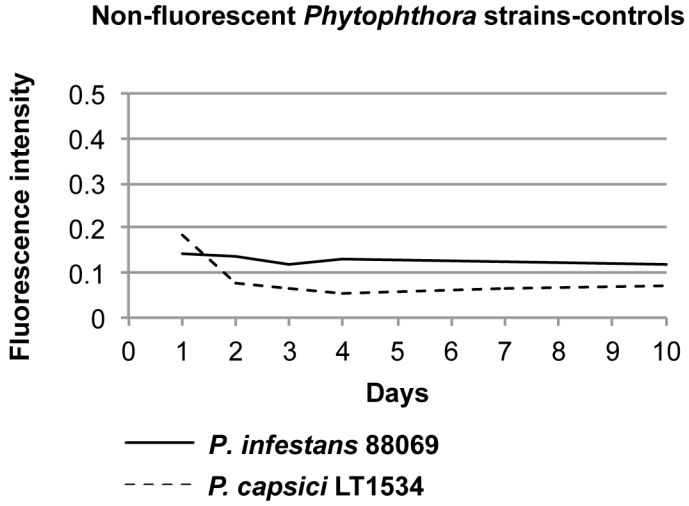

Figure A1.1: Fluorescence intensity of the non-fluorescent stains *P. infestans* 88069 and *P. capsici* LT1534.

Zoospores from two- to three-week-old *Phytophthora* plates were harvested and diluted to a final concentration of 50,000 spores/ml. Droplets of 10 µl were added to each well of a 96-well plate, previously filled with 250 µl of Plich medium, covered with a plastic lid and sealed with Parafilm. Plates were kept at 20°C in the dark for *P. infestans* and 25°C and illumination for *P. capsici*. At regular intervals, mycelial growth was monitored using a Varioscan Flash Multimode Reader (Thermo Scientific) by measuring emission of red fluorescence (excitation at 360 nm, emission at 465 nm). Fluorescence intensity of the non-fluorescent *P. infestans* 88069 and *P. capsici* LT1534 over time for a maximum of 10 days B, Each point in the plot represents the average value of three repeats. These strains were used as controls to verify that the signal in the fluorescent strains corresponds to fluorescence.

***P. infestans* 88069td** ***P. capsici* LT1534 tdtom**

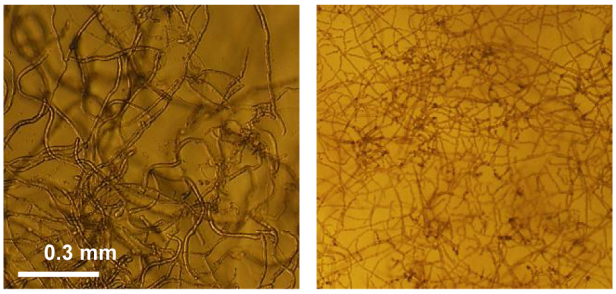

DMSO 1.5 % DMSO 2.36 %

Figure A1.2: Growth behaviour of *P. infestans* 88069td and *P. capsici* LT1534 tdtom after exposure to DMSO.

Zoospores from two- to three-week-old *Phytophthora* plates were harvested and diluted to a final concentration of 50,000 spores/ml. Droplets of 10 µl were added to each well of a 96-well plate, previously filled with 250 µl of Plich medium, covered with a plastic lid and sealed with Parafilm. Plates were kept at 20°C in the dark for *P. infestans* and 25°C and illumination for *P. capsici*. Both *Phytophthora* strains were exposed to 1.5% and 2.36% (v/v) DMSO/Plich for 10 days. DMSO levels correspond to the maximum capsidiol solution that was used in each experiment. The experiment was performed 3 times. Mycelial growth was imaged using a Zeiss Axiovert 25 microscope in transmission light mode with 10x magnification at 10 days post inoculation (10 dpi). The experiment was performed 3 times with similar results.

Appendix 2

Supplementary figures for chapter 4: I2 immune receptor mutant confers partial resistance to the Irish potato famine pathogen *Phytophthora infestans*

Figure A2.1: Sequence alignment of the *I2* sequence (GenBank AF118127.1) and Motelle (PVO 43143) *I2* sequence that was used in this study.

In this study I used the *I2* construct received from Dr. Frank Takken. Sequencing of the clone revealed the following two sequence polymorphisms in the LRR domain with respect to the published sequence: C to A in position 1743 (bp) leading to a silent change from GCC (Alanine) to GCA (Alanine), and C to G in position 2035 (bp) leading to an amino acid change from CCC (Proline) to GCC (Alanine). The sequence of the clone was verified by comparison with the *I2* sequence in the Motelle (PVO 43143) tomato cultivar (*I2I2*) and submitted to GenBank. The following GenBank number was given to the new *I2* sequence: KR108299. Sequence polymorphisms are indicated with boxes in the figure.

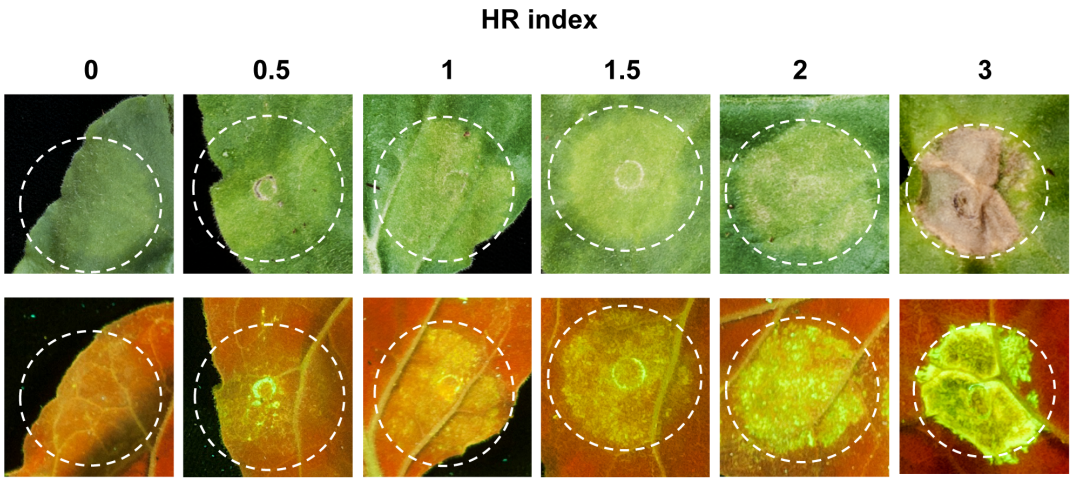

Figure A2.2: **The hypersensitive response (HR) index.**
The index was scored according to an arbitrary scale from 0 (no HR phenotype) to 3 (confluent necrosis on the infiltrated area). Representative pictures for different values of HR index are shown. The arbitrary scale was based on a previously established HR scale (Segretin, Pais et al. 2014), to measure intensity of the HR phenotypes induced (Bos, Kanneganti et al. 2006).

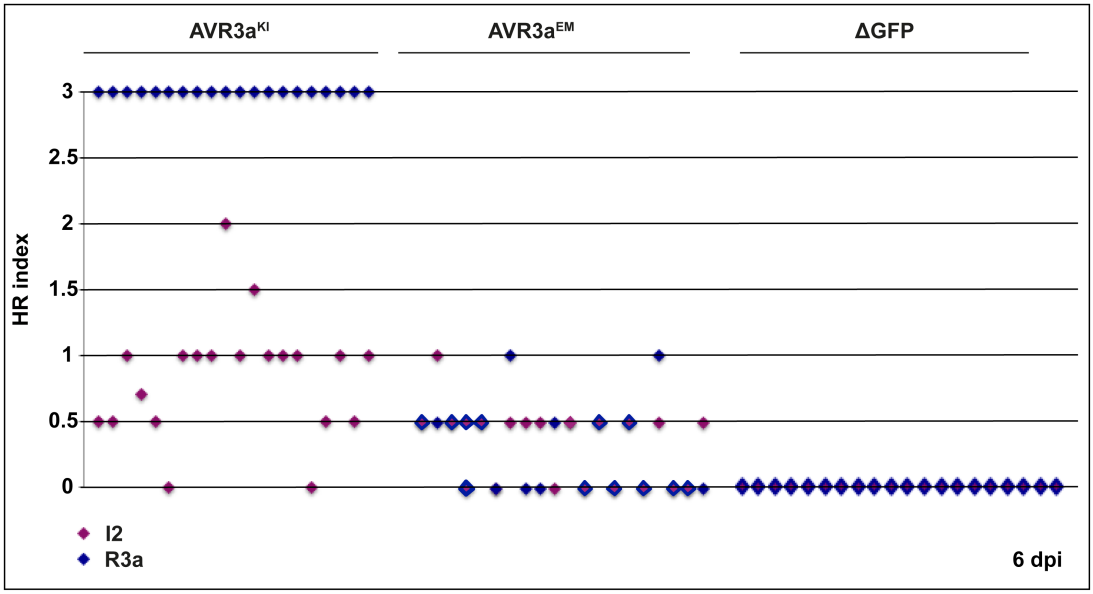

Figure A2.3: Example of Scatter plot analysis for the evaluation of the Hypersensitive response phenotypes.

Hypersensitive response (HR) indices of wild-type I2 after co-expression with the *P. infestans* AVR3a variants in *N. benthamiana* leaves, corresponding to the experiment described in **Fig. 4.1.** Wild-type *I2* was under transcriptional control of the *Cauliflower mosaic virus* 35S promoter and AVR3a^{KI}, AVR3a^{EM} or a truncated version of green fluorescent protein (ΔGFP) were expressed from a *Potato Virus X* (PVX)-based vector. Values of 20 replicas for each combination of constructs scored at 6 days post-infiltration (dpi) are plotted. The values were obtained by scoring the *N. benthamiana* leaves for presence of HR according to the arbitrary scale described previously in Fig. A2.2. Dark violet dots represent the HR indices of I2 and dark blue dots represent the HR indices of R3a, with each of the AVR3a variants or the control (ΔGFP). Double-coloured dots represent overlayed values for I2 and R3a.

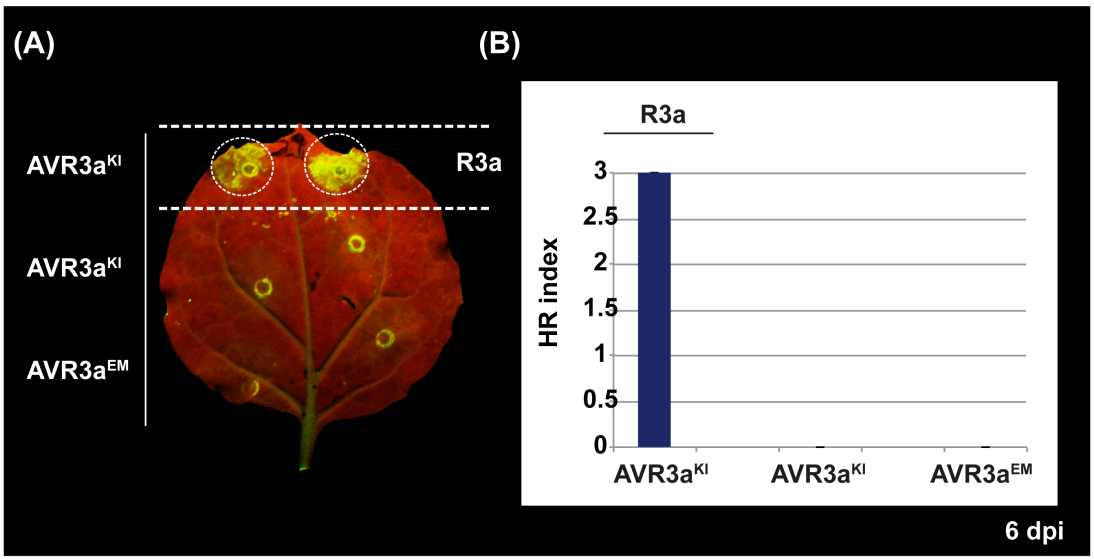

Figure A2.4: **AVR3a variants do not cause cell death after transient expression in *Nicotiana benthamiana*.**

A, Hypersensitive response (HR) phenotypes of the *Phythophthora infestans* AVR3a variants after transient expression in *N. benthamiana* leaves. Co-expression of wild-type R3a with the AVR3a^{KI} variant in *N. benthamiana* leaves was used as a positive control in this experiment. Wild-type *R3a* was under transcriptional control of the *Rpi-vnt1.1* promoter and AVR3a^{KI}, AVR3a^{EM} were expressed from a *Potato Virus X* (PVX)-based vector. The picture was taken at 6 days post-infiltration (dpi). B, HR indices corresponding to the experiment described in A. Values scored at 6 dpi are plotted. Bars represent the average of 16 replicas for each combination of constructs; error bars represent standard deviation.

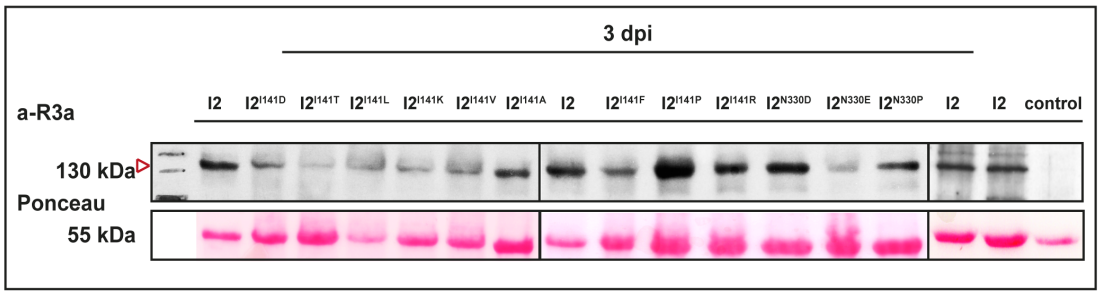

Figure A2.5: The I2 loss-of-response mutants have altered accumulation levels compared to the wild-type I2 protein *in planta.*

Nicotiana benthamiana leaves were agroinfiltrated with constructs to express wild-type and mutant I2 protein or a truncated version of green fluorescent protein, ΔGFP (control). Total protein extracts from leaves sampled at 3 days post-infiltration (dpi) were subjected to SDS-PAGE followed by immunoblotting with a polyclonal antibody raised against the CC domain of R3a (a-R3a, upper panel). A band of approximately 145 kDa, indicated with a red arrow, corresponding to I2 was present in total extracts of the leaves infiltrated with the *I2* and *I2* mutant constructs. Ponceau S staining of Rubisco (lower panel) is shown as control of the amount of protein loaded and transferred in each lane. Sizes (in kDa) are indicated on the left. Different boxes indicate different blots.

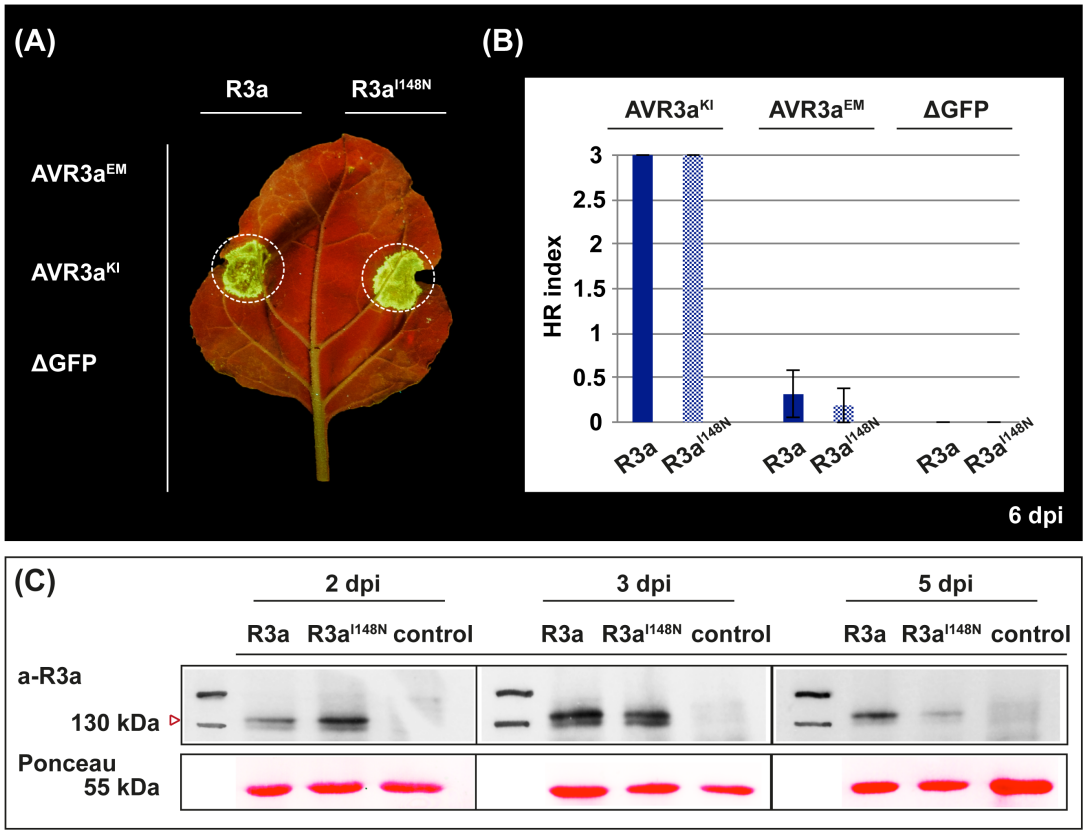

Figure A2.6: R3a^{I148N} response to the AVR3a variants is similar to that of wild-type R3a.

A, Hypersensitive response (HR) phenotypes of wild-type R3a and R3a^{I148N} after co-expression with the *Phythophthora infestans* AVR3a variants in *N. benthamiana* leaves. Wild-type and mutant *R3a* were under transcriptional control of the *Rpi-vnt1.1* promoter and AVR3a^{KI}, AVR3a^{EM} or a truncated version of green fluorescent protein (ΔGFP) were expressed from a *Potato Virus X* (PVX)-based vector. The picture was taken at 6 days post-infiltration (dpi). B, HR indices corresponding to the experiment described in A. Values scored at 6 dpi are plotted. Bars represent the average of 18 replicas for each combination of constructs; error bars represent standard deviation. C, Western blot assays were performed on total protein extracts from *N. benthamiana* leaves infiltrated with the *R3a* constructs described in A. The binary vector pCBNptII-vnt1.1P/T (Segretin, Pais et al. 2014) was included as negative control. Total protein extracts were obtained at 2, 3 and 5 dpi and subjected to SDS-PAGE followed by immunoblotting with a polyclonal antibody raised against the CC domain of R3a (a-R3a). A band of approximately 146 kDa, indicated with a red arrow, corresponding to R3a was present in the total extracts from the leaves infiltrated with the *R3a* constructs. Ponceau S staining of Rubisco (lower panel) is shown as control of the amount of protein loaded and transferred in each lane. Sizes (in kDa) are indicated on the left. Different boxes indicate different blots.

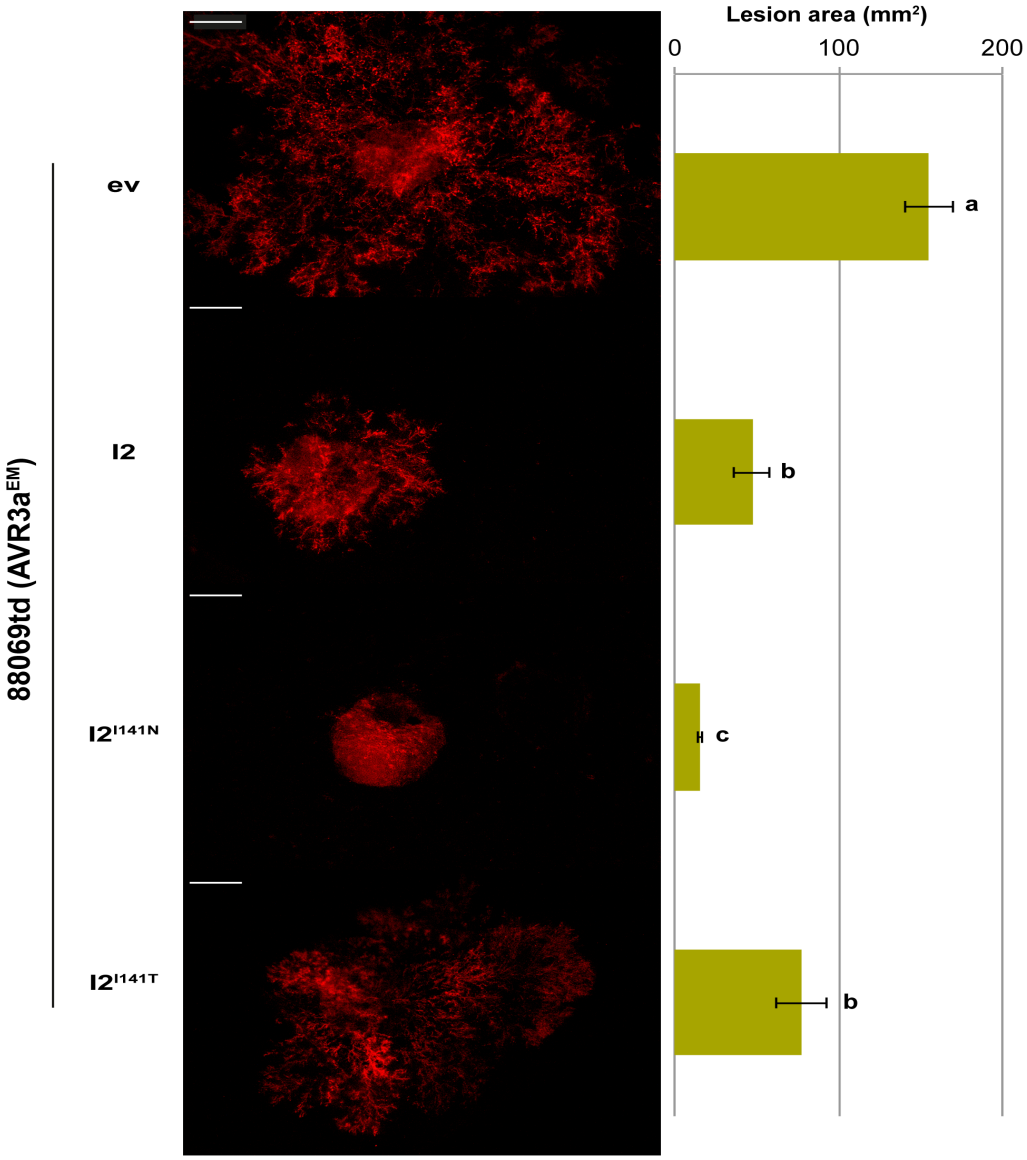

Figure A2.7: I2^{I141N} prevents *Phytophthora infestans* 88069td growth.
Wild-type and mutant *I2* were expressed in *N. benthamiana* leaves under transcriptional control of the *Cauliflower mosaic virus* 35S promoter. After approximately 15 hours, the infiltrated leaves were drop-inoculated with a *P. infestans*-zoospore suspension corresponding to the 88069td strain (AVR3a^{EM}). 88069td is a transgenic strain expressing the red fluorescent marker tandem-dimer RFP, known as tdTomato. The pictures were taken at 6 days post-inoculation. The area of *P. infestans* lesions was determined by analyzing the fluorescent signal with a bioimage analysis software by Dr. Ji Zhou (paragraph 2.7.2). Values corresponding to 6 days post-inoculation are plotted. Bars represent the average of 24 replicas for each treatment; error bars represent standard deviation. The experiment was performed 3 times and a representative repeat is shown. The Gateway binary vector pK7WG2 was included as negative control (empty vector, ev). I2^{I141T} is a loss-of-response I2 mutant and was used as an additional negative control in this experiment. Significant differences between the groups are indicated by letters and were determined in an analysis of variance (ANOVA), followed by a Fisher's Least Significance Difference (LSD), with a 95% confidence interval.

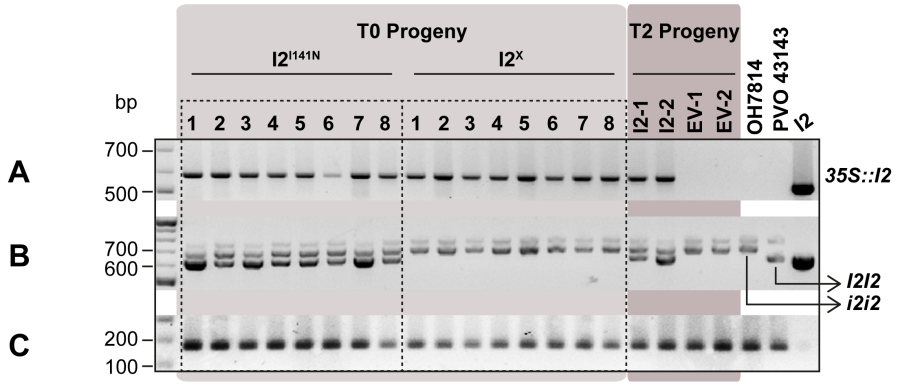

Figure A2.8: Genotyping of transgenic tomato plants containing *I2* wild-type and mutant genes.

All three blots in the panel show the genotypic characterization of different T0 and T2 transgenic tomato plants. A, PCR with primers 35S_F and I2_CC_R (table 2.12.1) was performed using genomic DNA from the tomato plants as template. The band indicates presence of the transgene in the tomato plant. B, PCR with primers I2hh_F and I2hh_R (table 2.12.1) was performed using genomic DNA from the tomato lines as template. OH7814 (*i2i2*) band (693 bp) is present in all the samples. PVO 43143 (*I2I2*) band (633 bp) is present only in the samples that contain *I2*. The extra band (above 700 bp) is non-specific. C, PCR with primers Actin-F and Actin-R (table 2.12.1) was performed using genomic DNA from the tomato plants as template. Actin was used as a control for constitutively expressed genes in tomato. Tomato lines OH7814 (*i2i2*), PVO 43143 (*I2I2*) and the pK7WG2::I2 construct were used as controls for the genotyping.

Appendix 3

Supplementary figures for chapter 5: Mutants of the I2 tomato immune receptor confer resistance to race 3 of *Fusarium oxysporum f. sp. lycopersici*

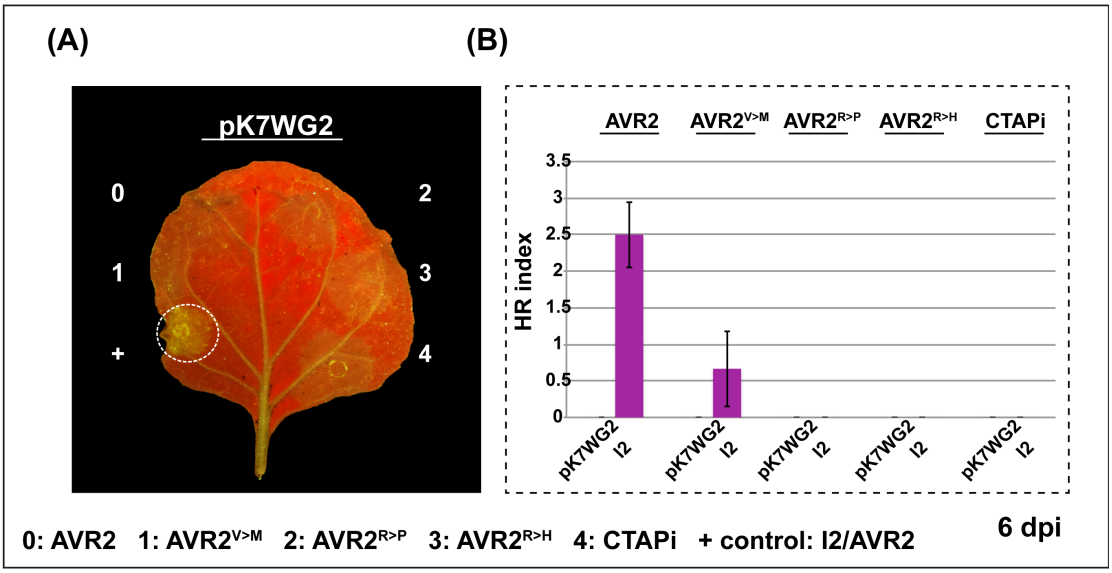

Figure A3.1: **AVR2 variants do not cause cell death after transient expression in *Nicotiana benthamiana*.**

A, Hypersensitive response (HR) phenotypes of the binary vector pK7WG2 (Karimi, Inze et al. 2002) after co-expression with the *F. oxysporum f. sp. lycopersici* AVR2 variants in *N. benthamiana* leaves. Co-expression of wild-type I2 with AVR2 in *N. benthamiana* leaves was used as a positive control (+) in this experiment. Wild-type *I2* and *Avr2* isoforms were under transcriptional control of the *Cauliflower mosaic virus* 35S promoter. I2 was expressed form the Gateway binary vector pK7WG2 (Karimi, Inze et al. 2002) and AVR2 variants were expressed from a CTAPi vector (Rohila, Chen et al. 2004). The picture was taken at 6 days post-infiltration (dpi). B, HR indices corresponding to the experiment described in A. Values scored at 6 dpi are plotted. Bars represent the average of 20 replicas for each combination of constructs; error bars represent standard deviation.

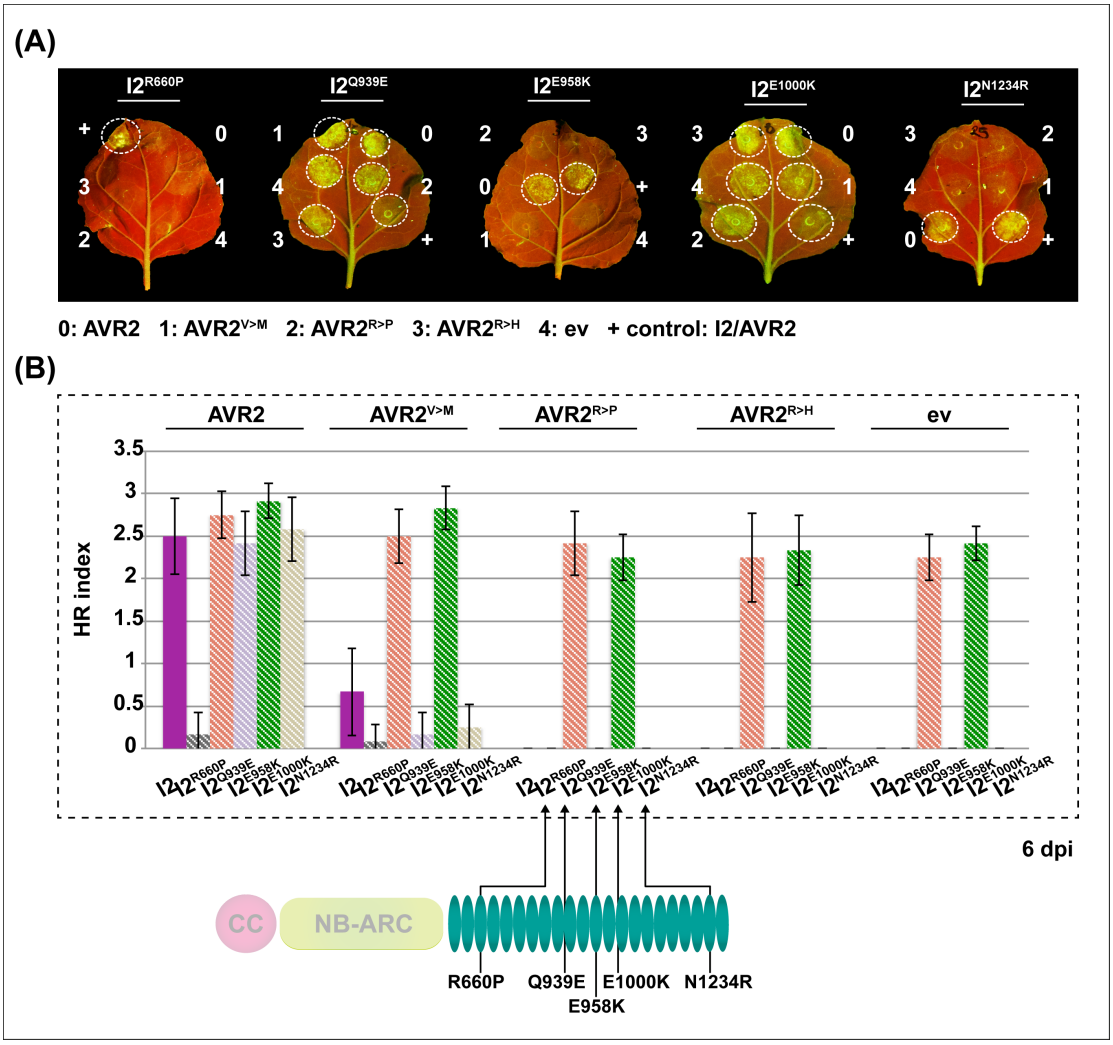

Figure A3.2: I2 mutants at the LRR domain do not show an expanded response phenotype.

A, Hypersensitive response (HR) phenotypes of $I2^{R660P}$, $I2^{Q939E}$ $I2^{E958K}$ $I2^{E1000K}$ $I2^{N1234R}$ after co-expression with the *F. oxysporum f. sp. lycopersici* AVR2 variants in *N. benthamiana* leaves. Wild-type *I2*, *I2* mutants and *Avr2* isoforms were under transcriptional control of the *Cauliflower mosaic virus* 35S. The pictures were taken at 6 days post-infiltration (dpi). B, HR indices corresponding to the experiment described in A. Values scored at 6 dpi are plotted. The cartoon indicates the approximate positions of the mutations. Bars represent the average of 20 replicas for each combination of constructs; error bars represent standard deviation. Positive control (+), represents I2 wild-type co-expressed with AVR2 in each leaf. Empty vector (ev) corresponds to the binary vector CTAPi (Rohila, Chen et al. 2004) and was used as a negative control in this experiment.

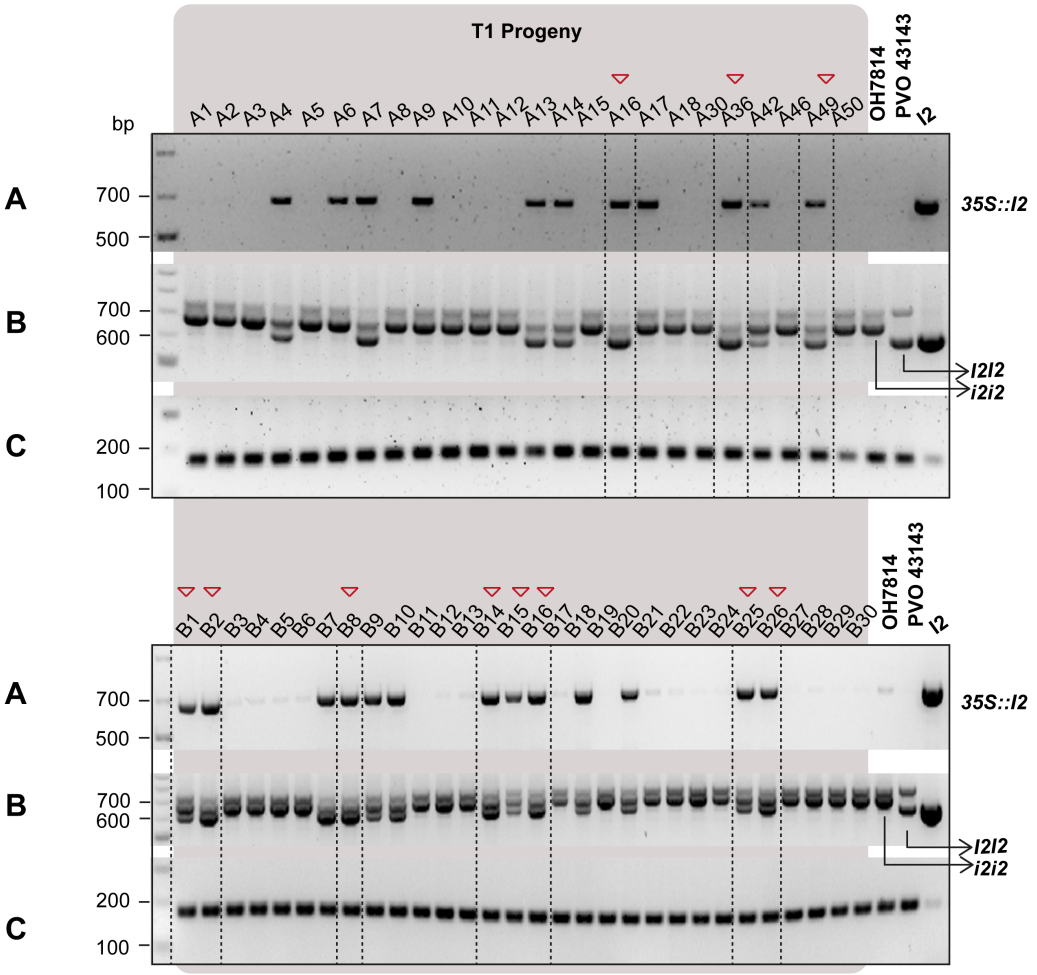

Figure A3.3: Genotyping of T1 transgenic tomato lines containing *I2* wild-type and mutant genes.

All three panels (upper, middle and low) show the genotypic characterization of different T1 transgenic tomato lines, namely: B8 and B14 (*I2)*, B25 and B26 ($I2^{C967R}$), A36 and B2 ($I2^{I141L}$), A16 and A49 ($I2^{I141V}$), B1, B15 and B16 ($I2^{N330K}$), and EV1 and EV2 (transformed with pK7WG2). A, PCR with primers 35S_F and I2_CC_R (table 2.12.1) was performed using genomic DNA from the tomato lines as template. The band indicates presence of the transgene in the tomato line. B, PCR with primers I2hh_F and I2hh_R (table 2.12.1) was performed using genomic DNA from the tomato lines as template. OH7814 (*i2i2*) band is present in all the samples. PVO 43143 (*I2I2*) band is present only in the samples that contain *I2*. The extra band (above 700 bp) is non-specific. C, PCR with primers Actin-F and Actin-R (table 2.12.1) was performed using genomic DNA from the tomato lines as template. Actin was used as a control for constitutively expressed genes in tomato. Tomato lines OH7814 (*i2i2*), PVO 43143 (*I2I2*) and the pK7WG2::I2 construct were used as controls for the genotyping. Red arrows indicate positive transgenic tomato lines that were selected for further characterization. Dashed lines indicate the genotyping of the selected tomato lines.

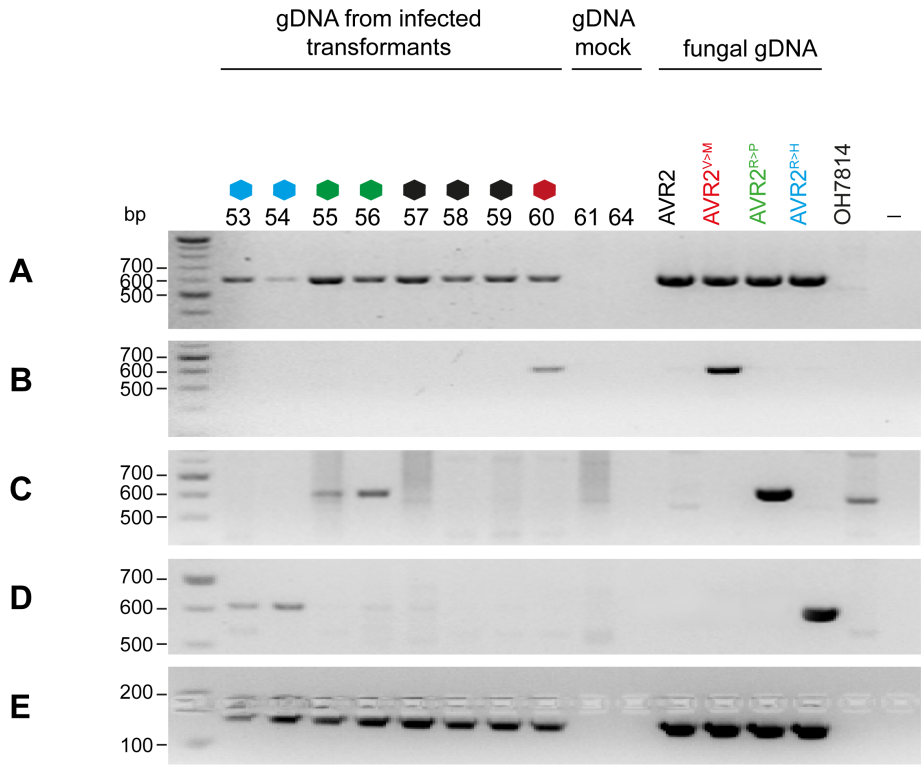

Figure A3.4: Genotyping of *F. oxysporum f. sp. lycopersici* strains isolated from infected tomato roots.

Genomic DNA was extracted from tomato roots infected with all 3 races of *F. oxysporum f. sp. lycopersici*. Tomato lines 53 and 54 were infected with *F. oxysporum f. sp. lycopersici* race 3 (AVR2$^{R>H}$); lines 55 and 56 were infected with *F. oxysporum f. sp. lycopersici* race 3 (AVR2$^{R>P}$); lines 57, 58 and 59 were infected with *F. oxysporum f. sp. lycopersici* race 2 (AVR2); line 60 was infected with *F. oxysporum f. sp. lycopersici* race 3 (AVR2$^{V>M}$); and lines 61 and 64 were mock inoculated with water. Fungal DNA was also extracted from *F. oxysporum f. sp. lycopersici* race 2 and 3 cultures. A, PCR performed with primers SIX3-F1 and SIX3-R2 (table 2.12.1). The band indicates presence of the *AVR2* effector gene in the tomato root samples. B, PCR with primers AVR2V>M_F and SIX3-R2 (table 2.12.1). The band indicates presence of the *Avr2$^{V>M}$* effector gene in the tomato root samples. C, PCR with primers AVR2R>P_F and SIX3-R2 (table 2.12.1). The band indicates presence of the *Avr2$^{R>P}$* effector gene in the tomato root samples. D, PCR with primers AVR2R>H_F and SIX3-R2 (table 2.12.1). The band indicates presence of the *Avr2$^{R>H}$* effector gene in the tomato root samples. E, PCR with primers FP157_F and FP157_R (table 2.12.1). The band indicates presence of the *FEM1* gene in the tomato root samples, which was used as a control for constitutively expressed genes in *F. oxysporum f. sp. lycopersici*.

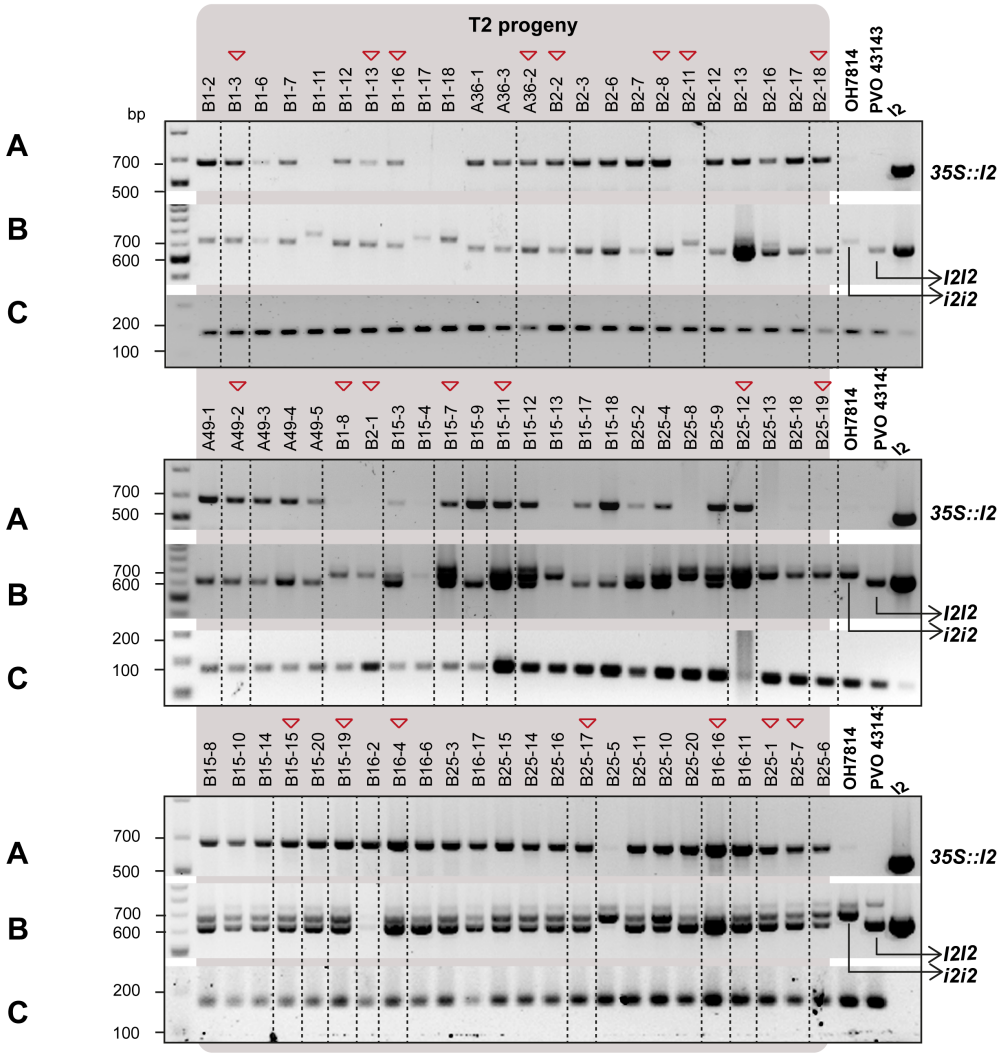

Figure A3.5: Genotyping of T2 transgenic tomato individuals containing *I2* wild-type and mutant genes.

All three panels (upper, middle and low) represent genotypic characterization of different T2 transgenic tomato individuals, namely: B8 and B14 (*I2)*, A36 and B2 ($I2^{I141L}$), A16 and A49 ($I2^{I141V}$), B1, B15 and B16 ($I2^{N330K}$), B25 and B26 ($I2^{C967R}$), and EV1 and EV2 (transformed with pK7WG2). A, PCR with primers 35S_F and I2_CC_R (table 2.12.1) was performed using genomic DNA from the tomato plants as template. The band indicates presence of the transgene in the tomato plant. B, PCR with primers I2hh_F and I2hh_R (table 2.12.1) was performed using genomic DNA from the tomato plants as template. OH7814 (*i2i2*) band is present in all the samples. PVO 43143 (*I2I2*) band is present only in the samples that contain *I2*. The extra band (above 700 bp) is non-specific. C, PCR with primers Actin-F and Actin-R (table 2.12.1) was performed using genomic DNA from the tomato plants as template. Actin was used as a control for constitutively expressed genes in tomato. Tomato lines OH7814 (*i2i2*), PVO 43143 (*I2I2*) and the pK7WG2::I2 construct were used as controls for the genotyping. Red arrows indicate representative examples of transgenic tomato plants used in figures 5.8-5.11. Dashed lines indicate the genotyping of the selected tomato plants used in figures 5.8-5.11.

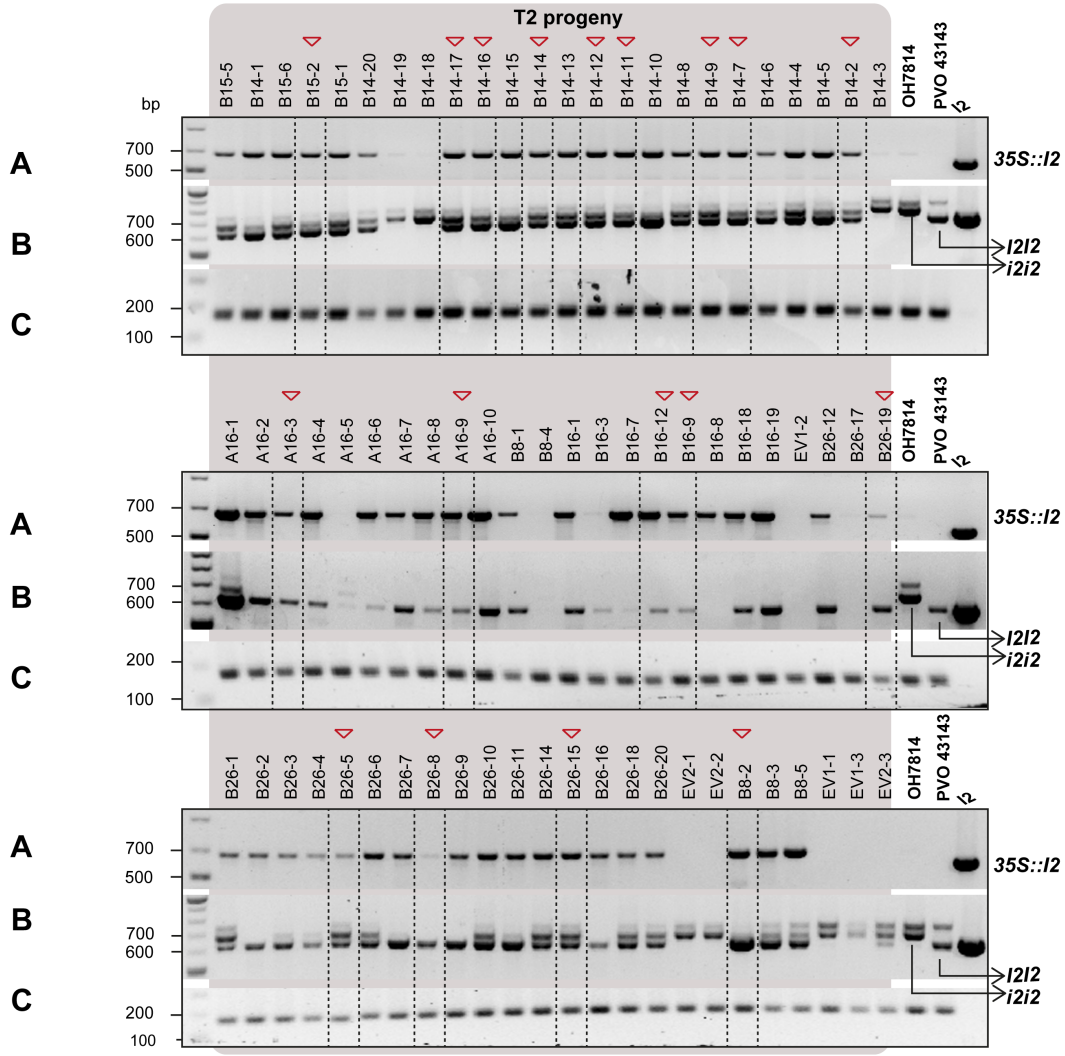

Figure A3.6: Genotyping of T2 transgenic tomato individuals containing *I2* wild-type and mutant genes.

All three panels (upper, middle and low) represent genotypic characterization of different T1 transgenic tomato lines, namely: B8 and B14 (*I2)*, A36 and B2 ($I2^{I141L}$), A16 and A49 ($I2^{I141V}$), B1, B15 and B16 ($I2^{N330K}$), B25 and B26 ($I2^{C967R}$), and EV1 and EV2 (transformed with pK7WG2). A, PCR with primers 35S_F and I2_CC_R (table 2.12.1) was performed using genomic DNA from the tomato plants as template. The band indicates presence of the transgene in the tomato plant. B, PCR with primers I2hh_F and I2hh_R (table 2.12.1) was performed using genomic DNA from the tomato plants as template. OH7814 (*i2i2*) band is present in all the samples. PVO 43143 (*I2I2*) band is present only in the samples that contain *I2*. The extra band (above 700 bp) is non-specific. C, PCR with primers Actin-F and Actin-R (table 2.12.1) was performed using genomic DNA from the tomato plants as template. Actin was used as a control for constitutively expressed genes in tomato. Tomato lines OH7814 (*i2i2*), PVO 43143 (*I2I2*) and the pK7WG2::I2 construct were used as controls for the genotyping. Red arrows indicate representative examples of transgenic tomato plants used in figures 5.8-5.11. Dashed lines indicate the genotyping of the selected tomato plants used in figures 5.8-5.11.

Appendix 4

Supplementary figures for chapter 6: Is the *I2* locus involved in the resistance of tomato cultivar PVO 43143 against *P. infestans?*

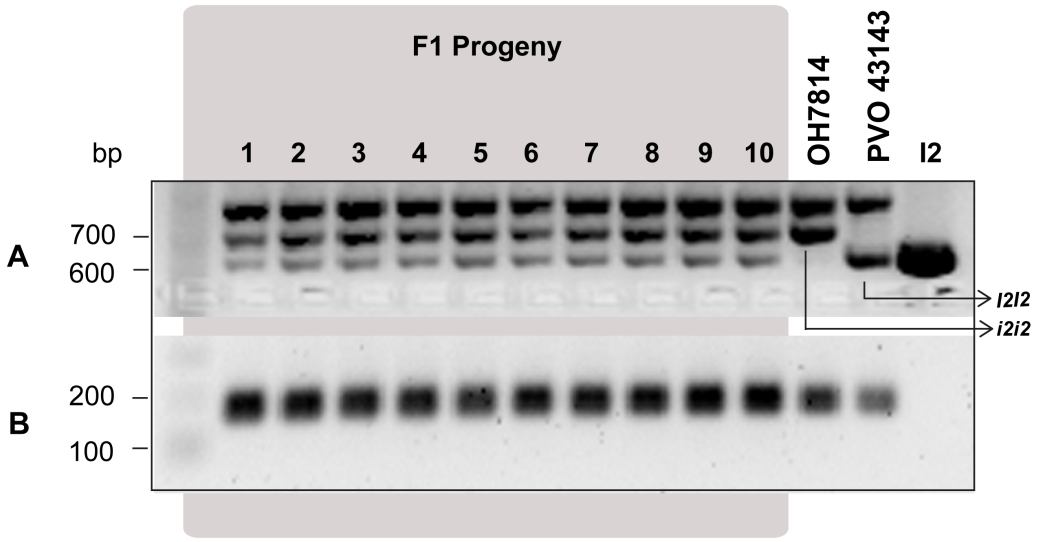

Figure A4.1: F1 tomato lines are heterozygous for *I2.*
The panel shows the genotypic characterization of different F1 tomato lines resulting from the following cross: OH7814 X PVO 43143. A, PCR with primers I2hh_F and I2hh_R (table 2.12.1) was performed using genomic DNA from the tomato lines as template. OH7814 (*i2i2*) band (693 bp) indicates presence of the *i2* gene (693 bp). PVO 43143 (*I2I2*) band (633 bp) is present only in the samples that carry *I2*. Presence of both bands indicates a heterozygous plant (*I2i2*), while presence of each of the individual bands only indicates a homozygous plant (*I2I2* or *i2i2*). The extra band (above 700 bp) is non-specific. B, PCR with primers Actin-F and Actin-R (table 2.12.1) was performed using genomic DNA from the tomato lines as template. Actin was as a control for constitutively expressed genes in tomato. Tomato lines OH7814 (*i2i2*), PVO 43143 (*I2I2*) and pK7WG2::I2 constructs were used as controls for the genotyping.

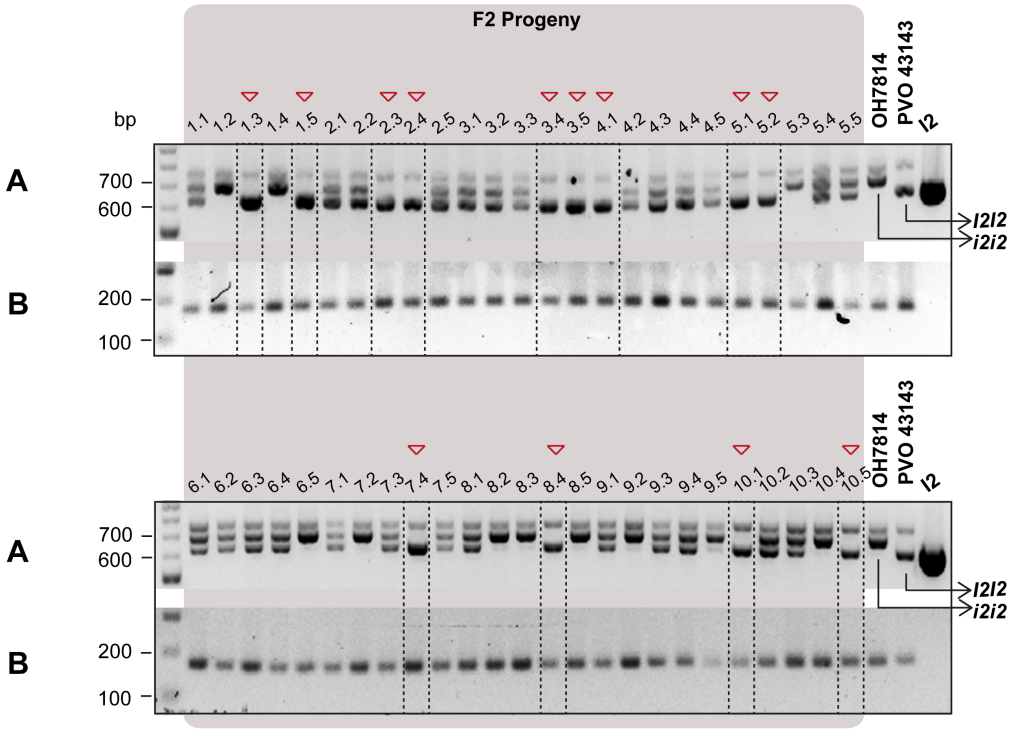

Figure A4.2: Genotyping of F2 tomato individuals.

Both panel (upper and lower) show the genotypic characterization of different F2 tomato individuals following self-crossing of the 10 F1 lines presented in A4.1. A, PCR with primers I2hh_F and I2hh_R (table 2.12.1) was performed using genomic DNA from the tomato plants as template. OH7814 (*i2i2*) band (693 bp) indicates presence of the *i2* gene (693 bp). PVO 43143 (*I2I2*) band (633 bp) is present only in the samples that carry *I2*. Presence of both bands indicates a heterozygous plant (*I2i2*), while presence of each of the individual bands only indicates a homozygous plant (*I2I2* or *i2i2*). The extra band (above 700 bp) is non-specific. B, PCR with primers Actin-F and Actin-R (table 2.12.1) was performed using genomic DNA from the tomato plants as template. Actin was as a control for constitutively expressed genes in tomato. Tomato lines OH7814 (*i2i2*), PVO 43143 (*I2I2*) and pK7WG2::I2 constructs were used as controls for the genotyping. Dashed lines indicate the F2 individuals that are homozygous for the *I2* gene (*I2I2*).

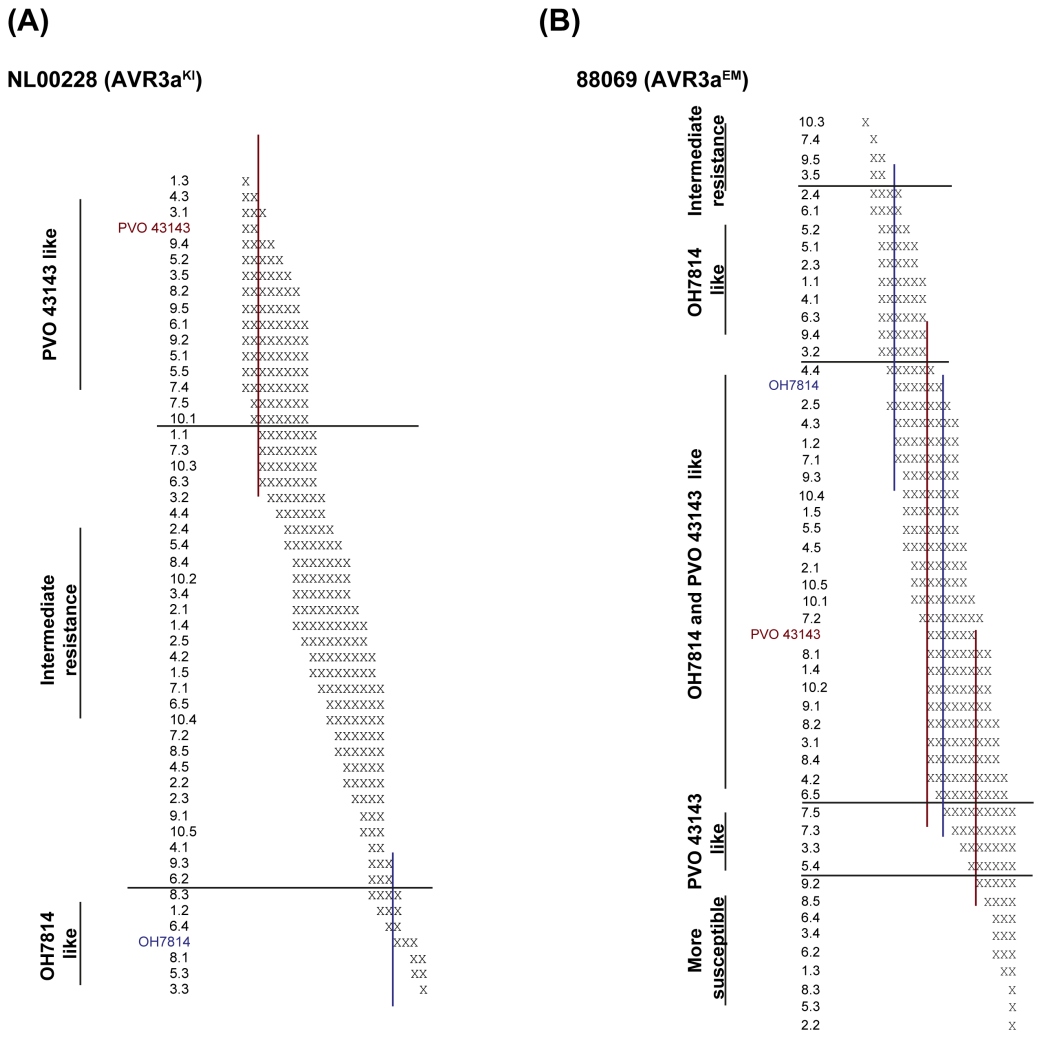

Figure: A4.3: Homogenous groups of F2 population following infection with *P. infestans.*

Homogenous groups are identified using columns of X's. Within each column, the levels containing X's from a group of means within which there are no statistically significant differences. The method that is used to discriminate among the means is Fisher's LSD test, with a 95% confidence level. A, Homogenous groups formed following quantification of the infection with *P. infestans* NL00228 strain, B, Homogenous groups formed following quantification of the infection with *P. infestans* 88069 strain. Red and blue lines have been used to further categorize the F2 population in response to how different their infection was to the PVO 43143 and OH7814 parent lines respectively.

LIST OF TABLES

LIST OF FIGURES

REFERENCES

Agarwal, K. C. (1996). Therapeutic actions of garlic constituents. Medicinal Research Reviews 16(1): 111-124.

Agrios, G. N. (2005). Plant pathology, Elsevier Academic Press.

Ahmed Sid, A., C. Perez Sanchez and M. Emilia Candela (2000). Evaluation of induction of systemic resistance in pepper plants (Capsicum annuum) to Phytophthora capsici using Trichoderma harzianum and its relation with capsidiol accumulation. European Journal of Plant Pathology 106(9): 817-824.

Ahuja, I., R. Kissen and A. M. Bones (2012). Phytoalexins in defense against pathogens. Trends in plant science 17(2): 73-90.

Aime, S., C. Cordier, C. Alabouvette and C. Olivain (2008). Comparative analysis of PR gene expression in tomato inoculated with virulent Fusarium oxysporum f. sp lycopersici and the biocontrol strain F. oxysporum Fo47. Physiological and Molecular Plant Pathology 73(1-3): 9-15.

Alexander, L. J. a. T., C.M. (1945). Physiologic specialization in the tomato wilt fungus Fusarium oxysporum f.sp. lycopersici. Journal of Agricultural Research 70: 303-313.

Alfano, J. R. and A. Collmer (2004). Type III secretion system effector proteins: Double agents in bacterial disease and plant defense. Annual Review of Phytopathology 42: 385-414.

Alonso-Villaverde, V., F. Voinesco, O. Viret, J.-L. Spring and K. Gindro (2011). The effectiveness of stilbenes in resistant Vitaceae: Ultrastructural and biochemical events during Plasmopara viticola infection process. Plant Physiology and Biochemistry 49(3): 265-274.

Ament, K., V. Krasikov, S. Allmann, M. Rep, F. L. W. Takken and R. C. Schuurink (2010). Methyl salicylate production in tomato affects biotic interactions. Plant Journal 62(1): 124-134.

Amini, J. and D. F. Sidovich (2010). The effects of fungicides on Fusarium oxysporum f. sp. lycopersici associated with fusarium wilt of tomato. Journal of Plant Protection Research 50(2): 172-178.

Anderson, J. P., E. Badruzsaufari, P. M. Schenk, J. M. Manners, O. J. Desmond, C. Ehlert, D. J. Maclean, P. R. Ebert and K. Kazan (2004). Antagonistic interaction between abscisic acid and jasmonate-ethylene signaling pathways modulates defense gene expression and disease resistance in Arabidopsis. Plant Cell 16(12): 3460-3479.

Andolfo, G., F. Ferriello, L. Tardella, A. Ferrarini, L. Sigillo, L. Frusciante and M. R. Ercolano (2014). Tomato Genome-Wide Transcriptional Responses to Fusarium Wilt and Tomato Mosaic Virus. Plos One 9(5).

Andolfo, G., F. Jupe, K. Witek, G. J. Etherington, M. R. Ercolano and J. D. G. Jones (2014). Defining the full tomato NB-LRR resistance gene repertoire using genomic and cDNA RenSeq. Bmc Plant Biology 14.

Andolfo, G., W. Sanseverino, S. Rombauts, Y. Van de Peer, J. M. Bradeen, D. Carputo, L. Frusciante and M. R. Ercolano (2013). Overview of tomato (Solanum lycopersicum) candidate pathogen recognition genes reveals important Solanum R locus dynamics. New Phytologist 197(1): 223-237.

Aoki, K., R. Ishida and M. Kasai (1997). Isolation and characterization of a cDNA encoding a Translin-like protein, TRAX. Febs Letters 401(2-3): 109-112.

Armstrong, G. M. a. A., J.K. (1981). Formae speciales and races of Fusarium oxysporum causing wilt diseases. Fusarium: Diseases, Biology and Taxonomy. P. E. Nelson, Toussoun, and R. J. T.A.. and Cook. University Park, PA, USA., The Pennsylvania State University Press,: 391-399.

Armstrong, M. R., S. C. Whisson, L. Pritchard, J. I. B. Bos, E. Venter, A. O. Avrova, A. P. Rehmany, U. Bohme, K. Brooks, I. Cherevach, N. Hamlin, B. White, A. Frasers, A. Lord, M. A. Quail, C. Churcher, N. Hall, M. Berriman, S. Huang, S. Kamoun, J. L. Beynon and P. R. J. Birch (2005). An ancestral oomycete locus contains late blight avirulence gene Avr3a, encoding a protein that is recognized in the host cytoplasm. Proceedings of the National Academy of Sciences of the United States of America 102(21): 7766-7771.

Ashikawa, I. (2012). Regions outside the leucine-rich repeat domain determine the distinct resistance specificities of the rice blast resistance genes Pik and Pik-m. Molecular Breeding 30(3): 1531-1535.

Atamian, H. S., T. Eulgem and I. Kaloshian (2012). SlWRKY70 is required for Mi-1-mediated resistance to aphids and nematodes in tomato. Planta 235(2): 299-309.

Axtell, M. J. and B. J. Staskawicz (2003). Initiation of RPS2-specified disease resistance in Arabidopsis is coupled to the AvrRpt2-directed elimination of RIN4. Cell 112(3): 369-377.

Azevedo, C., S. Betsuyaku, J. Peart, A. Takahashi, L. Noel, A. Sadanandom, C. Casais, J. Parker and K. Shirasu (2006). Role of SGT1 in resistance protein accumulation in plant immunity. Embo Journal 25(9): 2007-2016.

Bai, S., J. Liu, C. Chang, L. Zhang, T. Maekawa, Q. Wang, W. Xiao, Y. Liu, J. Chai, F. L. W. Takken, P. Schulze-Lefert and Q.-H. Shen (2012). Structure-Function Analysis of Barley NLR Immune Receptor MLA10 Reveals Its Cell Compartment Specific Activity in Cell Death and Disease Resistance. Plos Pathogens 8(6).

Beattie, B. C. F. a. G. A. (2008). An Overview of Plant Defenses against Pathogens and Herbivores. The Plant Health Instructor.

Beckman, C. H. (2000). Phenolic-storing cells: keys to programmed cell death and periderm formation in wilt disease resistance and in general defence responses in plants? Physiological and Molecular Plant Pathology 57(3): 101-110.

Bednarek, P., M. Pislewska-Bednarek, E. V. L. van Themaat, R. K. Maddula, A. Svatos and P. Schulze-Lefert (2011). Conservation and clade-specific diversification of pathogen-inducible tryptophan and indole glucosinolate metabolism in Arabidopsis thaliana relatives. New Phytologist 192(3): 713-726.

Bell, J. K., I. Botos, P. R. Hall, J. Askins, J. Shiloach, D. M. Segal and D. R. Davies (2005). The molecular structure of the Toll-like receptor 3 ligand-binding domain. Proceedings of the National Academy of Sciences of the United States of America 102(31): 10976-10980.

Bendahmane, A., G. Farnham, P. Moffett and D. C. Baulcombe (2002). Constitutive gain-of-function mutants in a nucleotide binding site-leucine rich repeat protein encoded at the Rx locus of potato. Plant Journal 32(2): 195-204.

Berg, A. (1926). Tomato late blight and its relation to late blight of potato. Bull. West Virginia Agrl Expt. Sta. 25: 1-31.

Bernoux, M., T. Ve, S. Williams, C. Warren, D. Hatters, E. Valkov, X. Zhang, J. G. Ellis, B. Kobe and P. N. Dodds (2011). Structural and Functional Analysis of a Plant Resistance Protein TIR Domain Reveals Interfaces for Self-Association, Signaling, and Autoregulation. Cell Host & Microbe 9(3): 200-211.

Berry, S. Z. and W. A. Gould (1983). OHIO-7814 TOMATO. Hortscience 18(4): 494-496.

Bhattacharjee, S., N. L. Hiller, K. Liolios, J. Win, T.-D. Kanneganti, C. Young, S. Kamoun and K. Haldar (2006). The malarial host-targeting signal is conserved in the Irish potato famine pathogen. PLoS pathogens 2(5): e50-e50.

Birch, P. R. J., P. C. Boevink, E. M. Gilroy, I. Hein, L. Pritchard and S. C. Whisson (2008). Oomycete RXLR effectors: delivery, functional redundancy and durable disease resistance. Current Opinion in Plant Biology 11(4): 373-379.

Birker, D., K. Heidrich, H. Takahara, M. Narusaka, L. Deslandes, Y. Narusaka, M. Reymond, J. E. Parker and R. O'Connell (2009). A locus conferring resistance to Colletotrichum higginsianum is shared by four geographically distinct Arabidopsis accessions. Plant Journal 60(4): 602-613.

Birnbaum, G. I. S., A.; Grover, S.H.; Stothers, J.B. (1974). The complete stereostructure of capsidiol, X-ray analysis and 13C nuclear magnetic resonance of eremophilane derivatives having trans-vicinal methyl groups. Can. J. Chem 52: 993-1005.

Block, A., G. Li, Z. Q. Fu and J. R. Alfano (2008). Phytopathogen type III effector weaponry and their plant targets. Current Opinion in Plant Biology 11(4): 396-403.

Blum, M., M. Boehler, E. Randall, V. Young, M. Csukai, S. Kraus, F. Moulin, G. Scalliet, A. O. Avrova, S. C. Whisson and R. Fonne-Pfister (2010). Mandipropamid targets the cellulose synthase-like PiCesA3 to inhibit cell wall biosynthesis in the oomycete plant pathogen, Phytophthora infestans. Molecular Plant Pathology 11(2): 227-243.

Blum, M., M. Waldner and U. Gisi (2010). A single point mutation in the novel PvCesA3 gene confers resistance to the carboxylic acid amide fungicide mandipropamid in Plasmopara viticola. Fungal Genetics and Biology 47(6): 499-510.

Bohman, S., J. Staal, B. Thomma, M. L. Wang and C. Dixelius (2004). Characterisation of an Arabidopsis-Leptosphaeria maculans pathosystem: resistance partially requires camalexin biosynthesis and is independent of salicylic acid, ethylene and jasmonic acid signalling. Plant Journal 37(1): 9-20.

Bohn, G. W. and C. M. Tucker (1939). IMMUNITY TO FUSARIUM WILT IN THE TOMATO. Science (New York, N.Y.) 89(2322): 603-604.

Bonardi, V. and J. L. Dangl (2012). How complex are intracellular immune receptor signaling complexes? Frontiers in Plant Science 3.

Booth, C. (1971). The Genus Fusarium. Kew, Surrey, England, Commonwealth Mycological Institute.

Bos, J. I. B. (2007). Function, structure and evolution of the RXLR effector AVR3a of Phytophthora infestans. Doctor of Philosophy, Ohio State University.

Bos, J. I. B., A. Chaparro-Garcia, L. M. Quesada-Ocampo, B. B. M. Gardener and S. Kamoun (2009). Distinct Amino Acids of the Phytophthora infestans Effector AVR3a Condition Activation of R3a Hypersensitivity and Suppression of Cell Death. Molecular Plant-Microbe Interactions 22(3): 269-281.

Bos, J. I. B., T.-D. Kanneganti, C. Young, C. Cakir, E. Huitema, J. Win, M. R. Armstrong, P. R. J. Birch and S. Kamoun (2006). The C-terminal half of Phytophthora infestans RXLR effector AVR3a is sufficient to trigger R3a-mediated hypersensitivity and suppress INF1-induced cell death in Nicotiana benthamiana. Plant Journal 48(2): 165-176.

Boter, M., B. Amigues, J. Peart, C. Breuer, Y. Kadota, C. Casais, G. Moore, C. Kleanthous, F. Ochsenbein, K. Shirasu and R. Guerois (2007). Structural and functional analysis of SGT1 reveals that its interaction with HSP90 is required for the accumulation of Rx, an R protein involved in plant immunity. Plant Cell 19(11): 3791-3804.

Bozkurt, T. O., S. Schornack, M. J. Banfield and S. Kamoun (2012). Oomycetes, effectors, and all that jazz. Current Opinion in Plant Biology 15(4): 483-492.

Bozkurt, T. O., S. Schornack, J. Win, T. Shindo, M. Ilyas, R. Oliva, L. M. Cano, A. M. E. Jones, E. Huitema, R. A. L. van der Hoorn and S. Kamoun (2011). Phytophthora infestans effector AVRblb2 prevents secretion of a plant immune protease at the haustorial interface. Proceedings of the National Academy of Sciences 108(51): 20832-20837.

Brasier, C. (2009). Phytophthora biodiversity: how many Phytophthora species are there? General Technical Report - Pacific Southwest Research Station, USDA Forest Service(PSW-GTR-221): 101-115.

Cane, D. E. (1990). ENZYMATIC FORMATION OF SESQUITERPENES. Chemical Reviews 90(7): 1089-1103.

Catanzariti, A.-M., P. N. Dodds, T. Ve, B. Kobe, J. G. Ellis and B. J. Staskawicz (2010). The AvrM Effector from Flax Rust Has a Structured C-Terminal Domain and Interacts Directly with the M Resistance Protein. Molecular Plant-Microbe Interactions 23(1): 49-57.

Catanzariti, A.-M., G. T. T. Lim and D. A. Jones (2015). The tomato I-3 gene: a novel gene for resistance to Fusarium wilt disease. New Phytologist: n/a-n/a.

Catanzariti, A. M., P. N. Dodds, G. J. Lawrence, M. A. Ayliffe and J. G. Ellis (2006). Haustorially expressed secreted proteins from flax rust are highly enriched for avirulence elicitors. Plant Cell 18(1): 243-256.

Cesari, S., M. Bernoux, P. Moncuquet, T. Kroj and P. N. Dodds (2014). A novel conserved mechanism for plant NLR protein pairs: the 'integrated decoy' hypothesis. Frontiers in Plant Science 5.

Cesari, S., G. Thilliez, C. Ribot, V. Chalvon, C. Michel, A. Jauneau, S. Rivas, L. Alaux, H. Kanzaki, Y. Okuyama, J.-B. Morel, E. Fournier, D. Tharreau, R. Terauchi and T. Kroj (2013). The Rice Resistance Protein Pair RGA4/RGA5 Recognizes the Magnaporthe oryzae

Effectors AVR-Pia and AVR1-CO39 by Direct Binding. Plant Cell 25(4): 1463-1481.

Chakrabarti, A., M. Rep, B. Wang, A. Ashton, P. Dodds and J. Ellis (2011). Variation in potential effector genes distinguishing Australian and non-Australian isolates of the cotton wilt pathogen Fusarium oxysporum f.sp vasinfectum. Plant Pathology 60(2): 232-243.

Chaparro-Garcia, A., R. C. Wilkinson, S. Gimenez-Ibanez, K. Findlay, M. D. Coffey, C. Zipfel, J. P. Rathjen, S. Kamoun and S. Schornack (2011). The Receptor-Like Kinase SERK3/BAK1 Is Required for Basal Resistance against the Late Blight Pathogen Phytophthora infestans in Nicotiana benthamiana. Plos One 6(1).

Chapman, S., L. J. Stevens, P. C. Boevink, S. Engelhardt, C. J. Alexander, B. Harrower, N. Champouret, K. McGeachy, P. S. M. Van Weymers, X. Chen, P. R. J. Birch and I. Hein (2014). Detection of the Virulent Form of AVR3a from Phytophthora infestans following Artificial Evolution of Potato Resistance Gene R3a. Plos One 9(10).

Chen, Y., Z. Liu and D. A. Halterman (2012). Molecular Determinants of Resistance Activation and Suppression by Phytophthora infestans Effector IPI-O. Plos Pathogens 8(3).

Cho, Y. S., V. M. Chennathukuzhi, M. A. Handel, J. Eppig and N. B. Hecht (2004). The relative levels of translin-associated factor X (TRAX) and testis brain RNA-binding protein determine their nucleocytoplasmic distribution in male germ cells. Journal of Biological Chemistry 279(30): 31514-31523.

Chowdappa, P., N. B. J. Kumar, S. Madhura, M. S. P. Kumar, K. L. Myers, W. E. Fry, J. N. Squires and D. E. L. Cooke (2013). Emergence of 13_A2 Blue Lineage of Phytophthora infestans was Responsible for Severe Outbreaks of Late Blight on Tomato in South-West India. Journal of Phytopathology 161(1): 49-58.

Coleman, J. J., G. J. White, M. Rodriguez-Carres and H. D. VanEtten (2011). An ABC Transporter and a Cytochrome P450 of Nectria haematococca MPVI Are Virulence Factors on Pea and Are the Major Tolerance Mechanisms to the Phytoalexin Pisatin. Molecular Plant-Microbe Interactions 24(3): 368-376.

Coll, N. S., D. Vercammen, A. Smidler, C. Clover, F. Van Breusegem, J. L. Dangl and P. Epple (2010). Arabidopsis Type I Metacaspases Control Cell Death. Science 330(6009): 1393-1397.

Consonni, C., P. Bednarek, M. Humphry, F. Francocci, S. Ferrari, A. Harzen, E. V. L. van Themaat and R. Panstruga (2010). Tryptophan-Derived Metabolites Are Required for Antifungal Defense in the Arabidopsis mlo2 Mutant. Plant Physiology 152(3): 1544-1561.

Cook, R. J. (2000). Advances in plant health management in the twentieth century. Annual Review of Phytopathology 38: 95-116.

Cooke, D. E. L., L. M. Cano, S. Raffaele, R. A. Bain, L. R. Cooke, G. J. Etherington, K. L. Deahl, R. A. Farrer, E. M. Gilroy, E. M. Goss, N. J. Gruenwald, I. Hein, D. MacLean, J. W. McNicol, E. Randall, R. F. Oliva, M. A. Pel, D. S. Shaw, J. N. Squires, M. C. Taylor, V. G. A. A. Vleeshouwers, P. R. J. Birch, A. K. Lees and S. Kamoun (2012). Genome Analyses of an Aggressive and Invasive Lineage of the Irish Potato Famine Pathogen. Plos Pathogens 8(10).

Coutos-Thevenot, P., B. Poinssot, A. Bonomelli, H. Yean, C. Breda, D. Buffard, R. Esnault, R. Hain and M. Boulay (2001). In vitro tolerance to Botrytis cinerea of grapevine 41B rootstock in transgenic plants expressing the stilbene synthase Vst1 gene under the control of a pathogen-inducible PR 10 promoter. Journal of Experimental Botany 52(358): 901-910.

Dangl, J. L., D. M. Horvath and B. J. Staskawicz (2013). Pivoting the Plant Immune System from Dissection to Deployment. Science 341(6147): 746-751.

Dangl, J. L. and J. D. G. Jones (2001). Plant pathogens and integrated defence responses to infection. Nature 411(6839): 826-833.

Davis, R. M., K. A. Kimble and J. J. Farrar (1988). A 3RD RACE OF FUSARIUM-OXYSPORUM F-SP LYCOPERSICI IDENTIFIED IN CALIFORNIA. Plant Disease 72(5): 453-453.

De Marino, S., N. Borbone, F. Gala, F. Zollo, G. Fico, R. Pagiotti and M. Iorizzi (2006). New constituents of sweet Capsicum annuum L. fruits and evaluation of their biological activity. Journal of Agricultural and Food Chemistry 54(20): 7508-7516.

Delserone, L. M., D. E. Matthews and H. D. Vanetten (1992). DIFFERENTIAL TOXICITY OF ENANTIOMERS OF MAACKIAIN AND PISATIN TO PHYTOPATHOGENIC FUNGI. Phytochemistry 31(11): 3813-3819.

Dempsey, D. M. A. and D. F. Klessig (2012). SOS - too many signals for systemic acquired resistance? Trends in Plant Science 17(9): 538-545.

Deslandes, L., J. Olivier, N. Peeters, D. X. Feng, M. Khounlotham, C. Boucher, I. Somssich, S. Genin and Y. Marco (2003). Physical interaction between RRS1-R, a protein conferring resistance to bacterial wilt, and PopP2, a type III effector targeted to the plant nucleus. Proceedings of the National Academy of Sciences of the United States of America 100(13): 8024-8029.

Deverall, B. J. (1982). Introduction. In Phytoalexins;. Phytoalexins. M. J. W. Bailey J.A. Glasgow and London, UK: 1-20.

Divon, H. H. and R. Fluhr (2007). Nutrition acquisition strategies during fungal infection of plants. Fems Microbiology Letters 266(1): 65-74.

Dixon, R. A. (2001). Natural products and plant disease resistance. Nature 411(6839): 843-847.

Dodds, P. N., G. J. Lawrence, A. M. Catanzariti, T. Teh, C. I. A. Wang, M. A. Ayliffe, B. Kobe and J. G. Ellis (2006). Direct protein interaction underlies gene-for-gene specificity and coevolution of the flax resistance genes and flax rust avirulence genes. Proceedings of the National Academy of Sciences of the United States of America 103(23): 8888-8893.

Dodds, P. N. and J. P. Rathjen (2010). Plant immunity: towards an integrated view of plant-pathogen interactions. Nature Reviews Genetics 11(8): 539-548.

Domingo, C., F. Andres, D. Tharreau, D. J. Iglesias and M. Talon (2009). Constitutive Expression of OsGH3.1 Reduces Auxin Content and Enhances Defense Response and Resistance to a Fungal Pathogen in Rice. Molecular Plant-Microbe Interactions 22(2): 201-210.

Dorant, E., P. A. Vandenbrandt, R. A. Goldbohm, R. J. J. Hermus and F. Sturmans (1993). GARLIC AND ITS SIGNIFICANCE FOR THE PREVENTION OF CANCER IN HUMANS - A CRITICAL-VIEW. British Journal of Cancer 67(3): 424-429.

Du, J., H. Rietman and V. G. A. A. Vleeshouwers (2014). Agroinfiltration and PVX Agroinfection in Potato and Nicotiana benthamiana. Jove-Journal of Visualized Experiments(83).

Echeverri, F., F. Torres, W. Quinones, G. Cardona, R. Archbold, J. Roldan, I. Brito, J. G. Luis and E. H. Lahlou (1997). Danielone, a phytoalexin from papaya fruit. Phytochemistry 44(2): 255-256.

Egea, C., M. D. Alcazar and M. E. Candela (1996). Capsidiol: Its role in the resistance of Capsicum annuum to Phytophthora capsici. Physiologia Plantarum 98(4): 737-742.

Engelhardt, S., P. C. Boevink, M. R. Armstrong, M. B. Ramos, I. Hein and P. R. J. Birch (2012). Relocalization of Late Blight Resistance Protein R3a to Endosomal Compartments Is Associated with Effector Recognition and Required for the Immune Response. Plant Cell 24(12): 5142-5158.

Erb, M., S. Meldau and G. A. Howe (2012). Role of phytohormones in insect-specific plant reactions. Trends in Plant Science 17(5): 250-259.

Ewing, B., L. Hillier, M. C. Wendl and P. Green (1998). Base-calling of automated sequencer traces using phred. I. Accuracy assessment. Genome Research 8(3): 175-185.

F.L., W. (1939). A technique for studying host resistance and pathogenicity in tomato Fusarium wilt. Phytopathology(29): 945-956.

Faix, J. and R. Grosse (2006). Staying in shape with formins. Developmental Cell 10(6): 693-706.

Farnham, G. and D. C. Baulcombe (2006). Artificial evolution extends the spectrum of viruses that are targeted by a disease-resistance gene from potato. Proceedings of the National Academy of Sciences of the United States of America 103(49): 18828-18833.

Favaron, F., M. Lucchetta, S. Odorizzi, A. T. P. da Cunha and L. Sella (2009). THE ROLE OF GRAPE POLYPHENOLS ON TRANS-RESVERATROL ACTIVITY AGAINST BOTRYTIS CINEREA AND OF FUNGAL LACCASE ON THE SOLUBILITY OF PUTATIVE GRAPE PR PROTEINS. Journal of Plant Pathology 91(3): 579-588.

Fay, J. C. and W. E. Fry (1997). Effects of hot and cold temperatures on the survival of oospores produced by United States strains of Phytophthora infestans. American Potato Journal 74(5): 315-323.

Feng, Z., B. Zhang, W. Ding, X. Liu, D.-L. Yang, P. Wei, F. Cao, S. Zhu, F. Zhang, Y. Mao and J.-K. Zhu (2013). Efficient genome editing in plants using a CRISPR/Cas system. Cell Research 23(10): 1229-1232.

Fillatti, J. J., J. Kiser, R. Rose and L. Comai (1987). EFFICIENT TRANSFER OF A GLYPHOSATE TOLERANCE GENE INTO TOMATO USING A BINARY AGROBACTERIUM-TUMEFACIENS VECTOR. Bio-Technology 5(7): 726-730.

Fisher, M. C., D. A. Henk, C. J. Briggs, J. S. Brownstein, L. C. Madoff, S. L. McCraw and S. J. Gurr (2012). Emerging fungal threats to animal, plant and ecosystem health. Nature 484(7393): 186-194.

Flor, H. H. (1955). HOST-PARASITE INTERACTION IN FLAX RUST - ITS GENETICS AND OTHER IMPLICATIONS. Phytopathology 45(12): 680-685.

Fry, W. (2008). Phytophthora infestans: the plant (and R gene) destroyer. Molecular Plant Pathology 9(3): 385-402.

Galindo, J. and M. E. Gallegly (1960). THE NATURE OF SEXUALITY IN PHYTOPHTHORA INFESTANS. Phytopathology 50(2): 123-128.

Gallegly, M. E. and J. Galindo (1958). MATING TYPES AND OOSPORES OF PHYTOPHTHORA INFESTANS IN NATURE IN MEXICO. Phytopathology 48(5): 274-277.

Gan, P., K. Ikeda, H. Irieda, M. Narusaka, R. J. O'Connell, Y. Narusaka, Y. Takano, Y. Kubo and K. Shirasu (2013). Comparative genomic and transcriptomic analyses reveal the hemibiotrophic stage shift of Colletotrichum fungi. New Phytologist 197(4): 1236-1249.

Garcia, A. V., S. Blanvillain-Baufume, R. P. Huibers, M. Wiermer, G. Li, E. Gobbato, S. Rietz and J. E. Parker (2010). Balanced Nuclear and Cytoplasmic Activities of EDS1 Are Required for a Complete Plant Innate Immune Response. Plos Pathogens 6(7).

Garnica, D. P., A. Nemri, N. M. Upadhyaya, J. P. Rathjen and P. N. Dodds (2014). The Ins and Outs of Rust Haustoria. Plos Pathogens 10(9).

Gassmann, W., M. E. Hinsch and B. J. Staskawicz (1999). The Arabidopsis RPS4 bacterial-resistance gene is a member of the TIR-NBS-LRR family of disease-resistance genes. Plant Journal 20(3): 265-277.

Gawehns, F., P. M. Houterman, F. A. Ichou, C. B. Michielse, M. Hijdra, B. J. C. Cornelissen, M. Rep and F. L. W. Takken (2014). The Fusarium oxysporum Effector Six6 Contributes to Virulence and Suppresses I-2-Mediated Cell Death. Molecular Plant-Microbe Interactions 27(4): 336-348.

Gebhardt, C. and J. P. T. Valkonen (2001). Organization of genes controlling disease resistance in the potato genome. Annual Review of Phytopathology 39: 79-102.

Gershenzon, J. and N. Dudareva (2007). The function of terpene natural products in the natural world. Nature Chemical Biology 3(7): 408-414.

Gimenez-Ibanez, S. and R. Solano (2013). Nuclear jasmonate and salicylate signaling and crosstalk in defense against pathogens. Frontiers in Plant Science 4.

Giorcelli, A., F. Sparvoli, F. Mattivi, A. Tava, A. Balestrazzi, U. Vrhovsek, P. Calligari, R. Bollini and M. Confalonieri (2004). Expression of the stilbene synthase (StSy) gene from grapevine in transgenic white poplar results in high accumulation of the antioxidant resveratrol glucosides. Transgenic Research 13(3): 203-214.

Goodwin, S. B., C. D. Smart, R. W. Sandrock, K. L. Deahl, Z. K. Punja and W. E. Fry (1998). Genetic change within populations of Phytophthora infestans in the United States and Canada during 1994 to 1996: Role of migration and recombination. Phytopathology 88(9): 939-949.

Grattidge, R. and R. G. Obrien (1982). OCCURRENCE OF A 3RD RACE OF FUSARIUM-WILT OF TOMATOES IN QUEENSLAND. Plant Disease 66(2): 165-166.

Grosskinsky, D. K., M. Naseem, U. R. Abdelmohsen, N. Plickert, T. Engelke, T. Griebel, J. Zeier, O. Novak, M. Strnad, H. Pfeifhofer, E. van der Graaff, U. Simon and T. Roitsch (2011). Cytokinins Mediate Resistance against Pseudomonas syringae in Tobacco through Increased Antimicrobial Phytoalexin Synthesis Independent of Salicylic Acid Signaling. Plant Physiology 157(2): 815-830.

Haas, B. J., S. Kamoun, M. C. Zody, R. H. Y. Jiang, R. E. Handsaker, L. M. Cano, M. Grabherr, C. D. Kodira, S. Raffaele, T. Torto-Alalibo, T. O. Bozkurt, A. M. V. Ah-Fong, L. Alvarado, V. L. Anderson, M. R. Armstrong, A. Avrova, L. Baxter, J. Beynon, P. C. Boevink, S. R. Bollmann, J. I. B. Bos, V. Bulone, G. Cai, C. Cakir, J. C. Carrington, M. Chawner, L. Conti, S. Costanzo, R. Ewan, N. Fahlgren, M. A. Fischbach, J. Fugelstad, E. M. Gilroy, S. Gnerre, P. J. Green, L. J. Grenville-Briggs, J. Griffith, N. J. Gruenwald, K. Horn, N. R. Horner, C.-H. Hu, E. Huitema, D.-H. Jeong, A. M. E. Jones, J. D. G. Jones, R. W. Jones, E. K. Karlsson, S. G. Kunjeti, K. Lamour, Z. Liu, L. Ma, D. MacLean, M. C. Chibucos, H. McDonald, J. McWalters, H. J. G. Meijer, W. Morgan, P. F. Morris, C. A. Munro, K. O'Neill, M. Ospina-Giraldo, A. Pinzon, L. Pritchard, B. Ramsahoye, Q. Ren, S. Restrepo, S. Roy, A. Sadanandom, A. Savidor, S. Schornack, D. C. Schwartz, U. D. Schumann, B. Schwessinger, L. Seyer, T. Sharpe, C. Silvar, J. Song, D. J. Studholme, S. Sykes, M. Thines, P. J. I. van de Vondervoort, V. Phuntumart, S. Wawra, R. Weide, J. Win, C. Young, S. Zhou, W. Fry, B. C. Meyers, P. van West, J. Ristaino, F. Govers, P. R. J. Birch, S. C. Whisson, H. S. Judelson and C. Nusbaum (2009). Genome sequence and analysis of the Irish potato famine pathogen Phytophthora infestans. Nature 461(7262): 393-398.

Hain, R., H. J. Reif, E. Krause, R. Langebartels, H. Kindl, B. Vornam, W. Wiese, E. Schmelzer, P. H. Schreier, R. H. Stocker and K. Stenzel (1993). DISEASE RESISTANCE RESULTS FROM FOREIGN PHYTOALEXIN EXPRESSION IN A NOVEL PLANT. Nature 361(6408): 153-156.

Hammerschmidt, R. (1999). Phytoalexins: What have we learned after 60 years? Annual Review of Phytopathology 37: 285-306.

Hao, W., S. M. Collier, P. Moffett and J. Chai (2013). Structural Basis for the Interaction between the Potato Virus X Resistance Protein (Rx) and Its Cofactor Ran GTPase-activating Protein 2 (RanGAP2). Journal of Biological Chemistry 288(50): 35868-35876.

Harborne, J. B. (1999). The comparative biochemistry of phytoalexin induction in plants. Biochemical Systematics and Ecology 27(4): 335-367.

Hargreaves, J. A., J. W. Mansfield and S. Rossall (1977). CHANGES IN PHYTOALEXIN CONCENTRATIONS IN TISSUES OF BROAD BEAN PLANT (VICIA-FABA L) FOLLOWING INOCULATION WITH SPECIES OF BOTRYTIS. Physiological Plant Pathology 11(3): 227-&.

Harris, C. J., E. J. Slootweg, A. Goverse and D. C. Baulcombe (2013). Stepwise artificial evolution of a plant disease resistance gene. Proceedings of the National Academy of Sciences of the United States of America 110(52): 21189-21194.

Hawkes, J. G. (1990). The potato: evolution, biodiversity and genetic resources.

Heidrich, K., L. Wirthmueller, C. Tasset, C. Pouzet, L. Deslandes and J. E. Parker (2011). Arabidopsis EDS1 Connects Pathogen Effector Recognition to Cell Compartment-Specific Immune Responses. Science 334(6061): 1401-1404.

Hellens, R., P. Mullineaux and H. Klee (2000). A guide to Agrobacterium binary Ti vectors. Trends in Plant Science 5(10): 446-451.

Hipskind, J. D. and N. L. Paiva (2000). Constitutive accumulation of a resveratrol-glucoside in transgenic alfalfa increases resistance to Phoma medicaginis. Molecular Plant-Microbe Interactions 13(5): 551-562.

Hoffman, R. and J. B. Heale (1987). CELL-DEATH, 6-METHOXYMELLEIN ACCUMULATION, AND INDUCED RESISTANCE TO BOTRYTIS-CINEREA IN CARROT ROOT SLICES. Physiological and Molecular Plant Pathology 30(1): 67-75.

Hogenhout, S. A., R. A. L. Van der Hoorn, R. Terauchi and S. Kamoun (2009). Emerging Concepts in Effector Biology of Plant-Associated Organisms. Molecular Plant-Microbe Interactions 22(2): 115-122.

Horvath, D. M., R. E. Stall, J. B. Jones, M. H. Pauly, G. E. Vallad, D. Dahlbeck, B. J. Staskawicz and J. W. Scott (2012). Transgenic Resistance Confers Effective Field Level Control of Bacterial Spot Disease in Tomato. Plos One 7(8).

Houterman, P. M., B. J. C. Cornelissen and M. Rep (2008). Suppression of plant resistance gene-based immunity by a fungal effector. Plos Pathogens 4(5).

Houterman, P. M., L. Ma, G. van Ooijen, M. J. de Vroomen, B. J. C. Cornelissen, F. L. W. Takken and M. Rep (2009). The effector protein Avr2 of the xylem-colonizing fungus Fusarium oxysporum activates the tomato resistance protein I-2 intracellularly. Plant Journal 58(6): 970-978.

Houterman, P. M., D. Speijer, H. L. Dekker, C. G. de Koster, B. J. C. Cornelissen and M. Rep (2007). The mixed xylem sap proteome of Fusarium oxysporum-infected tomato plants. Molecular Plant Pathology 8(2): 215-221.

Howles, P., G. Lawrence, J. Finnegan, H. McFadden, M. Ayliffe, P. Dodds and J. Ellis (2005). Autoactive alleles of the flax L6 rust resistance gene induce non-race-specific rust resistance associated with the hypersensitive response. Molecular Plant-Microbe Interactions 18(6): 570-582.

Hu, C.-H., F. G. Perez, R. Donahoo, A. McLeod, K. Myers, K. Ivors, G. Secor, P. D. Roberts, K. L. Deahl, W. E. Fry and J. B. Ristaino (2012). Recent Genotypes of Phytophthora infestans in the Eastern United States Reveal Clonal Populations and Reappearance of Mefenoxam Sensitivity. Plant Disease 96(9): 1323-1330.

Huang, S. W., E. A. G. van der Vossen, H. H. Kuang, V. Vleeshouwers, N. W. Zhang, T. J. A. Borm, H. J. van Eck, B. Baker, E. Jacobsen and R. G. F. Visser (2005). Comparative genomics enabled the isolation of the R3a late blight resistance gene in potato. Plant Journal 42(2): 251-261.

Hubert, D. A., P. Tornero, Y. Belkhadir, P. Krishna, A. Takahashi, K. Shirasu and J. L. Dangl (2003). Cytosolic HSP90 associates with and modulates the Arabidopsis RPM1 disease resistance protein. Embo Journal 22(21): 5679-5689.

Inami, K., C. Yoshioka-Akiyama, Y. Morita, M. Yamasaki, T. Teraoka and T. Arie (2012). A Genetic Mechanism for Emergence of Races in Fusarium oxysporum f. sp lycopersici: Inactivation of Avirulence Gene AVR1 by Transposon Insertion. Plos One 7(8).

Ingham, J. L. (1982). Phytoalexins from the Leguminosae. Phytoalexins. J. A. Bailey, Mansfield, J.W. Glasgow and London, UK: 21-80.

Ishizaka, N., K. Tomiyama, N. Katsui, A. Murai and T. Masamune (1969). BIOLOGICAL ACTIVITIES OF RISHITIN,AN ANTIFUNGAL COMPOUND ISOLATED FROM DISEASED POTATO TUBERS,AND ITS DERIVATIVES. Plant and Cell Physiology 10(1): 183-&.

Jacob, F., S. Vernaldi and T. Maekawa (2013). Evolution and Conservation of Plant NLR Functions. Frontiers in immunology 4: 297-297.

Jeandet, P., C. Clement, E. Courot and S. Cordelier (2013). Modulation of Phytoalexin Biosynthesis in Engineered Plants for Disease Resistance. International Journal of Molecular Sciences 14(7): 14136-14170.

Ji, Y., J. W. Scott and D. J. Schuster (2009). Toward Fine Mapping of the Tomato Yellow Leaf Curl Virus Resistance Gene Ty-2 on Chromosome 11 of Tomato. Hortscience 44(3): 614-618.

Jia, Y., S. A. McAdams, G. T. Bryan, H. P. Hershey and B. Valent (2000). Direct interaction of resistance gene and avirulence gene products confers rice blast resistance. Embo Journal 19(15): 4004-4014.

Jiang, W., H. Zhou, H. Bi, M. Fromm, B. Yang and D. P. Weeks (2013). Demonstration of CRISPR/Cas9/sgRNA-mediated targeted gene modification in Arabidopsis, tobacco, sorghum and rice. Nucleic Acids Research 41(20).

Jones, D. A. (1988). GENETIC PROPERTIES OF INHIBITOR GENES IN FLAX RUST THAT ALTER AVIRULENCE TO VIRULENCE ON FLAX. Phytopathology 78(3): 342-344.

Jones, D. R., C. H. Unwin and E. W. B. Ward (1975). POSTINFECTIONAL INHIBITORS FROM PLANTS .21. CAPSIDIOL INDUCTION IN PEPPER FRUIT DURING INTERACTIONS WITH PHYTOPHTHORA-CAPSICI AND MONILINIA-FRUCTICOLA. Phytopathology 65(12): 1417-1419.

Jones, D. R., C. H. Unwin and E. W. B. Ward (1975). SIGNIFICANCE OF CAPSIDIOL INDUCTION IN PEPPER FRUIT DURING AN INCOMPATIBLE INTERACTION WITH PHYTOPHTHORA-INFESTANS. Phytopathology 65(11): 1286-1288.

Jones, J. D. G. and J. L. Dangl (2006). The plant immune system. Nature 444(7117): 323-329.

Jones, J. D. G., K. Witek, W. Verweij, F. Jupe, D. Cooke, S. Dorling, L. Tomlinson, M. Smoker, S. Perkins and S. Foster (2014). Elevating crop disease resistance with cloned genes. Philosophical Transactions of the Royal Society B-Biological Sciences 369(1639).

Jones, L. R., Giddings, N.J. and Lutman, B.F. (1912). Investigations of the potato fungus, Phytophthora infestans. Vermont Agricultural Experiment Station Bulletin, 168.

Judelson, H. S. (1997). Expression and inheritance of sexual preference and selfing potential in Phytophthora infestans. Fungal Genetics and Biology 21(2): 188-197.

Judelson, H. S. (1997). The genetics and biology of Phytophthora infestans: Modern approaches to a historical challenge. Fungal Genetics and Biology 22(2): 65-76.

Judelson, H. S. and G. Senthil (2006). Investigating the role of ABC transporters in multifungicide insensitivity in Phytophthora infestans. Molecular Plant Pathology 7(1): 17-29.

Jupe, J., R. Stam, A. J. M. Howden, J. A. Morris, R. Zhang, P. E. Hedley and E. Huitema (2013). Phytophthora capsici-tomato interaction features dramatic shifts in gene expression associated with a hemi-biotrophic lifestyle. Genome Biology 14(6).

Kale, S. D., B. Gu, D. G. S. Capelluto, D. Dou, E. Feldman, A. Rumore, F. D. Arredondo, R. Hanlon, I. Fudal, T. Rouxel, C. B. Lawrence, W. Shan and B. M. Tyler (2010). External Lipid PI3P Mediates Entry of Eukaryotic Pathogen Effectors into Plant and Animal Host Cells. Cell 142(2): 284-295.

Kamoun, K. L. a. S. (2009). Oomycete Genetics and Genomics: Diversity, INteractions and Research tools, WILLEY-BLACKWELL.

Kamoun, S. (2006). A catalogue of the effector secretome of plant pathogenic oomycetes. Annual Review of Phytopathology. 44: 41-60.

Kamoun, S. (2007). Groovy times: filamentous pathogen effectors revealed. Current Opinion in Plant Biology 10(4): 358-365.

Kamoun, S. and S. B. Goodwin (2007). Fungal and oomycete genes galore. New Phytologist 174(4): 713-717.

Kamoun, S., E. Huitema and V. Vleeshouwers (1999). Resistance to oomycetes: a general role for the hypersensitive response? Trends in Plant Science 4(5): 196-200.

Kamoun, S. and C. D. Smart (2005). Late blight of potato and tomato in the genomics era. Plant Disease 89(7): 692-699.

Kamoun, S., T. van der Lee, G. van den Berg-Velthuis, K. E. de Groot and F. Govers (1998). Loss of production of the elicitor protein INF1 in the clonal lineage US-1 of Phytophthora infestans. Phytopathology 88(12): 1315-1323.

Kamoun, S., P. vanWest, A. J. deJong, K. E. deGroot, V. Vleeshouwers and F. Govers (1997). A gene encoding a protein elicitor of Phytophthora infestans is down-regulated during infection of potato. Molecular Plant-Microbe Interactions 10(1): 13-20.

Kanzaki, H., K. Yoshida, H. Saitoh, K. Fujisaki, A. Hirabuchi, L. Alaux, E. Fournier, D. Tharreau and R. Terauchi (2012). Arms race co-evolution of Magnaporthe oryzae AVR-Pik and rice Pik genes driven by their physical interactions. Plant Journal 72(6): 894-907.

Karimi, M., D. Inze and A. Depicker (2002). GATEWAY((TM)) vectors for Agrobacterium-mediated plant transformation. Trends in Plant Science 7(5): 193-195.

Katan, T. (1999). Current status of vegetative compatibility groups in Fusarium oxysporum. Phytoparasitica 27(1): 51-64.

Katan, T. and P. Di Primo (1999). Current status of vegetative compatibility groups in Fusarium oxysporum: Supplement (1999). Phytoparasitica 27(4): 273-277.

Katsui, N. M., A.; Masamune, T (1974). The structure of lubimin, oxylubimin, antifungal metabolites from diseased potato tubers. Tetrahedron Lett 15: 4483-4486.

Katsui, N. M., A.; Takasugi, M.; Imaizumi, K.; Masamune, T. (1968). The structure of rishitin, a new anfifungal compound from diseased potato tubers. J. Chem. Soc. Chem. Comm: 43-44.

Keller, H., P. Czernic, M. Ponchet, P. H. Ducrot, K. Back, J. Chappell, P. Ricci and Y. Marco (1998). Sesquiterpene cyclase is not a

determining factor for elicitor- and pathogen-induced capsidiol accumulation in tobacco. Planta 205(3): 467-476.

Kleemann, J., L. J. Rincon-Rivera, H. Takahara, U. Neumann, E. V. L. van Themaat, H. C. van der Does, S. Hacquard, K. Stueber, I. Will, W. Schmalenbach, E. Schmelzer and R. J. O'Connell (2012). Sequential Delivery of Host-Induced Virulence Effectors by Appressoria and Intracellular Hyphae of the Phytopathogen Colletotrichum higginsianum. Plos Pathogens 8(4).

Klement, Z., K. Rudolph and D. C. Sands (1990). Methods in phytobacteriology.

Kliebenstein, D. J., H. C. Rowe and K. J. Denby (2005). Secondary metabolites influence Arabidopsis/Botrytis interactions: variation in host production and pathogen sensitivity. Plant Journal 44(1): 25-36.

Kobayashi, S., C. K. Ding, Y. Nakamura, I. Nakajima and R. Matsumoto (2000). Kiwifruits (Actinidia deliciosa) transformed with a Vitis stilbene synthase gene produce piceid (resveratrol-glucoside). Plant Cell Reports 19(9): 904-910.

Kodera, Y., H. Matsuura, S. Yoshida, T. Sumida, Y. Itakura, T. Fuwa and H. Nishino (1989). ALLIXIN, A STRESS COMPOUND FROM GARLIC. Chemical & Pharmaceutical Bulletin 37(6): 1656-1658.

Koornneef, A., A. Verhage, A. Leon-Reyes, R. Snetselaar, L. Van Loon and C. M. Pieterse (2008). Towards a reporter system to identify regulators of cross-talk between salicylate and jasmonate signaling pathways in Arabidopsis. Plant signaling & behavior 3(8): 543-546.

Kuc (1982). Phytoalexins from the Solanaceae. Phytoalexins. J. A. Bailey, Mansfield, J.W. Glasgow and London, UK: 81-105.

Kuc, J. (1957). A BIOCHEMICAL STUDY OF THE RESISTANCE OF POTATO TUBER TISSUE TO ATTACK BY VARIOUS FUNGI. Phytopathology 47(11): 676-680.

Kuc, J. (1995). PHYTOALEXINS, STRESS METABOLISM, AND DISEASE RESISTANCE IN PLANTS. Annual Review of Phytopathology 33: 275-297.

Kurosaki, F. and A. Nishi (1983). ISOLATION AND ANTI-MICROBIAL ACTIVITY OF THE PHYTOALEXIN 6-METHOXYMELLEIN FROM CULTURED CARROT CELLS. Phytochemistry 22(3): 669-672.

Lachhab, N., S. M. Sanzani, M. Adrian, A. Chiltz, S. Balacey, M. Boselli, A. Ippolito and B. Poinssot (2014). SOYBEAN AND CASEIN HYDROLYSATES INDUCE GRAPEVINE IMMUNE RESPONSES AND RESISTANCE AGAINST PLASMOPARA VITICOLA. Frontiers in Plant Science 5.

Lamour, K. H., J. Mudge, D. Gobena, O. P. Hurtado-Gonzales, J. Schmutz, A. Kuo, N. A. Miller, B. J. Rice, S. Raffaele, L. M. Cano, A. K. Bharti, R. S. Donahoo, S. Finley, E. Huitema, J. Hulvey, D. Platt, A. Salamov, A. Savidor, R. Sharma, R. Stam, D. Storey, M. Thines, J. Win, B. J. Haas, D. L. Dinwiddie, J. Jenkins, J. R. Knight, J. P. Affourtit, C. S. Han, O. Chertkov, E. A. Lindquist, C. Detter, I. V. Grigoriev, S. Kamoun and S. F. Kingsmore (2012). Genome Sequencing and Mapping Reveal Loss of Heterozygosity as a Mechanism for Rapid Adaptation in the Vegetable Pathogen Phytophthora capsici. Molecular Plant-Microbe Interactions 25(10): 1350-1360.

Laterrot, H. (1976). Localisation chromosomique de I2 chez la tomate controlant la resistance au pathotype 2 de Fusarium oxysporum f.sp. lycopersici. ANNALES DE L AMELIORATION DES PLANTES(26): 485-491.

Lazo, G. R., P. A. Stein and R. A. Ludwig (1991). A DNA TRANSFORMATION-COMPETENT ARABIDOPSIS GENOMIC LIBRARY IN AGROBACTERIUM. Bio-Technology 9(10): 963-967.

Leckband, G. and H. Lorz (1998). Transformation and expression of a stilbene synthase gene of Vitis vinifera L. in barley and wheat for increased fungal resistance. Theoretical and Applied Genetics 96(8): 1004-1012.

Lee, G. J., A. M. Roseman, H. R. Saibil and E. Vierling (1997). A small heat shock protein stably binds heat-denatured model substrates and can maintain a substrate in a folding-competent state. Embo Journal 16(3): 659-671.

Lee, G. J. and E. Vierling (2000). A small heat shock protein cooperates with heat shock protein 70 systems to reactivate a heat-denatured protein. Plant Physiology 122(1): 189-197.

Leipe, D. D., E. V. Koonin and L. Aravind (2004). STAND, a class of P-loop NTPases including animal and plant regulators of programmed cell death: Multiple, complex domain architectures, unusual phyletic patterns, and evolution by horizontal gene transfer. Journal of Molecular Biology 343(1): 1-28.

Li, F. and S.-W. Ding (2006). Virus counterdefense: Diverse strategies for evading the RNA-silencing immunity. Annual Review of Microbiology. 60: 503-531.

Li, F., D. Pignatta, C. Bendix, J. O. Brunkard, M. M. Cohn, J. Tung, H. Sun, P. Kumar and B. Baker (2012). MicroRNA regulation of plant innate immune receptors. Proceedings of the National Academy of Sciences of the United States of America 109(5): 1790-1795.

Li, J.-F., J. E. Norville, J. Aach, M. McCormack, D. Zhang, J. Bush, G. M. Church and J. Sheen (2013). Multiplex and homologous recombination-mediated genome editing in Arabidopsis and Nicotiana benthamiana using guide RNA and Cas9. Nature Biotechnology 31(8): 688-691.

Li, R., C.-S. Tee, Y.-L. Jiang, X.-Y. Jiang, P. N. Venkatesh, R. Sarojam and J. Ye (2015). A terpenoid phytoalexin plays a role in basal defense of Nicotiana benthamiana against Potato virus X. Scientific Reports 5.

Li, Y., T. van der Lee, J. H. Zhu, G. H. Jin, C. Z. Lan, S. X. Zhu, R. F. Zhang, B. W. Liu, Z. J. Zhao, G. Kessel, S. W. Huang and E. Jacobsen (2013). Population structure of Phytophthora infestans in China - geographic clusters and presence of the EU genotype Blue_13. Plant Pathology 62(4): 932-942.

Li, Y., T. A. J. van der Lee, A. Evenhuis, G. B. M. van den Bosch, P. J. van Bekkum, M. G. Forch, M. P. E. van Gent-Pelzer, H. M. G. van Raaij, E. Jacobsen, S. W. Huang, F. Govers, V. G. A. A. Vleeshouwers and G. J. T. Kessel (2012). Population Dynamics of Phytophthora infestans in the Netherlands Reveals Expansion and Spread of Dominant Clonal Lineages and Virulence in Sexual Offspring. G3-Genes Genomes Genetics 2(12): 1529-1540.

Liang, H., J. Zheng, X. Y. Duan, B. Q. Sheng, S. G. Jia, D. W. Wang, J. W. Ouyang, J. Y. Li, L. C. Li, W. Z. Tian, R. Hain and X. Jia (2000). A transgenic wheat with a stilbene synthase gene resistant to powdery mildew obtained by biolistic method. Chinese Science Bulletin 45(7): 634-638.

Lievens, B., P. M. Houterman and M. Rep (2009). Effector gene screening allows unambiguous identification of Fusarium oxysporum f.sp lycopersici races and discriminationfrom other formae speciales. Fems Microbiology Letters 300(2): 201-215.

Lim, J. D., S. J. Yun, I. M. Chung and C. Y. Yu (2005). Resveratrol synthase transgene expression and accumulation of resveratrol glycoside in Rehmannia glutinosa. Molecular Breeding 16(3): 219-233.

Literakova, P., J. Lochman, Z. Zdrahal, Z. Prokop, V. Mikes and T. Kasparovsky (2010). Determination of Capsidiol in Tobacco Cells Culture by HPLC. Journal of Chromatographic Science 48(6): 436-440.

Liu, Y., H. Wang, H. C. Ye and G. F. Li (2005). Advances in the plant isoprenoid biosynthesis pathway and its metabolic engineering. Journal of Integrative Plant Biology 47(7): 769-782.

Liu, Y. L., T. Burch-Smith, M. Schiff, S. H. Feng and S. P. Dinesh-Kumar (2004). Molecular chaperone Hsp90 associates with resistance protein n and its signaling proteins SGT1 and Rar1 to modulate an innate

immune response in plants. Journal of Biological Chemistry 279(3): 2101-2108.

Liu, Z., C. Zhuang, S. Sheng, L. Shao, W. Zhao and S. Zhao (2011). Overexpression of a resveratrol synthase gene (PcRS) from Polygonum cuspidatum in transgenic Arabidopsis causes the accumulation of trans-piceid with antifungal activity. Plant Cell Reports 30(11): 2027-2036.

Llorente, F., P. Muskett, A. Sanchez-Vallet, G. Lopez, B. Ramos, C. Sanchez-Rodriguez, L. Jorda, J. Parker and A. Molina (2008). Repression of the auxin response pathway increases Arabidopsis susceptibility to necrotrophic fungi. Molecular Plant 1(3): 496-509.

Locci, R. K., J. (1967). Steroid glycoalkaloids as compounds produced by potato tuber slices under stress. Phytopathology 57: 1272-1273.

Lozano-Torres, J. L., R. H. P. Wilbers, P. Gawronski, J. C. Boshoven, A. Finkers-Tomczak, J. H. G. Cordewener, A. H. P. America, H. A. Overmars, J. W. Van 't Klooster, L. Baranowski, M. Sobczak, M. Ilyas, R. A. L. van der Hoorn, A. Schots, P. J. G. M. de Wit, J. Bakker, A. Goverse and G. Smant (2012). Dual disease resistance mediated by the immune receptor Cf-2 in tomato requires a common virulence target of a fungus and a nematode. Proceedings of the National Academy of Sciences of the United States of America 109(25): 10119-10124.

Lozovaya, V. V., A. V. Lygin, O. V. Zernova, S. X. Li, G. L. Hartman and J. M. Widholm (2004). Isoflavonoid accumulation in soybean hairy roots upon treatment with Fusarium solani. Plant Physiology and Biochemistry 42(7-8): 671-679.

Lu, R., I. Malcuit, P. Moffett, M. T. Ruiz, J. Peart, A. J. Wu, J. P. Rathjen, A. Bendahmane, L. Day and D. C. Baulcombe (2003). High throughput virus-induced gene silencing implicates heat shock protein 90 in plant disease resistance. Embo Journal 22(21): 5690-5699.

Lukasik, E. and F. L. W. Takken (2009). STANDing strong, resistance proteins instigators of plant defence. Current Opinion in Plant Biology 12(4): 427-436.

Lukasik-Shreepaathy, E., J. H. Vossen, W. I. L. Tameling, M. J. de Vroomen, B. J. C. Cornelissen and F. L. W. Takken (2012). Protein-protein interactions as a proxy to monitor conformational changes and activation states of the tomato resistance protein I-2. Journal of Experimental Botany 63(8): 3047-3060.

Ma, C. J. (2008). Cellulase elicitor induced accumulation of capsidiol in Capsicum annumm L. suspension cultures. Biotechnology Letters 30(5): 961-965.

Ma, L., B. J. C. Cornelissen and F. L. W. Takken (2013). A nuclear localization for Avr2 from Fusarium oxysporum is required to activate the tomato resistance protein I-2. Frontiers in Plant Science 4.

Mackey, D., B. F. Holt, A. Wiig and J. L. Dangl (2002). RIN4 interacts with Pseudomonas syringae type III effector molecules and is required for RPM1-mediated resistance in Arabidopsis. Cell 108(6): 743-754.

Maekawa, T., W. Cheng, L. N. Spiridon, A. Toeller, E. Lukasik, Y. Saijo, P. Liu, Q.-H. Shen, M. A. Micluta, I. E. Somssich, F. L. W. Takken, A.-J. Petrescu, J. Chai and P. Schulze-Lefert (2011). Coiled-Coil Domain-Dependent Homodimerization of Intracellular Barley Immune Receptors Defines a Minimal Functional Module for Triggering Cell Death. Cell Host & Microbe 9(3): 187-199.

Maekawa, T., T. A. Kufer and P. Schulze-Lefert (2011). NLR functions in plant and animal immune systems: so far and yet so close. Nature Immunology 12(9): 818-826.

Mahady, G. B., H. Matsuura and S. L. Pendland (2001). Allixin, a phytoalexin from garlic, inhibits the growth of Helicobacter pylori in vitro. American Journal of Gastroenterology 96(12): 3454-3455.

Maldonado-Bonilla, L. D., M. Betancourt-Jimenez and E. Lozoya-Gloria (2008). Local and systemic gene expression of sesquiterpene phytoalexin biosynthetic enzymes in plant leaves. European Journal of Plant Pathology 121(4): 439-449.

Mao, Y., H. Zhang, N. Xu, B. Zhang, F. Gou and J.-K. Zhu (2013). Application of the CRISPRCas System for Efficient Genome Engineering in Plants. Molecular Plant 6(6): 2008-2011.

Marquenet, E. and E. Richet (2007). How integration of positive and negative regulatory signals by a STAND signaling protein depends on ATP hydrolysis. Molecular Cell 28(2): 187-199.

Martin, G. B., A. J. Bogdanove and G. Sessa (2003). Understanding the functions of plant disease resistance proteins. Annual Review of Plant Biology 54: 23-61.

Matsukawa, M., Y. Shibata, M. Ohtsu, A. Mizutani, H. Mori, P. Wang, M. Ojika, K. Kawakita and D. Takemoto (2013). Nicotiana benthamiana Calreticulin 3a Is Required for the Ethylene-Mediated Production of Phytoalexins and Disease Resistance Against Oomycete Pathogen Phytophthora infestans. Molecular plant-microbe interactions : MPMI 26(8): 880-892.

McGrath, D. J., D. Gillespie and L. Vawdrey (1987). INHERITANCE OF RESISTANCE TO FUSARIUM-OXYSPORUM FSP LYCOPERSICI RACE-2 AND RACE-3 IN LYCOPERSICON-PENNELLII. Australian Journal of Agricultural Research 38(4): 729-733.

McGrath, D. J. and J. E. Maltby (1989). FUSARIUM WILT RACE 3 RESISTANCE IN TOMATO. Acta Horticulturae (Wageningen)(247): 107-110.

Melhus, I. E. (1915). Germination and infection with the fungus of the late blight of potato (Phytophthora infestans). Madison, WI: University of Wisconsin Agr. Exp. Sta.

M**endgen, K., C. Struck, R. T. Voegele and M. Hahn** (2000). Biotrophy and rust haustoria. Physiological and Molecular Plant Pathology 56(4): 141-145.

Mercier, J., J. Arul, R. Ponnampalam and M. Boulet (1993). INDUCTION OF 6-METHOXYMELLEIN AND RESISTANCE TO STORAGE PATHOGENS IN CARROT SLICES BY UV-C. Journal of Phytopathology-Phytopathologische Zeitschrift 137(1): 44-54.

Mes, J. J., A. A. van Doorn, J. Wijbrandi, G. Simons, B. J. C. Cornelissen and M. A. Haring (2000). Expression of the Fusarium resistance gene I-2 colocalizes with the site of fungal containment. Plant Journal 23(2): 183-193.

Miao, J., D. Guo, J. Zhang, Q. Huang, G. Qin, X. Zhang, J. Wan, H. Gu and L.-J. Qu (2013). Targeted mutagenesis in rice using CRISPR-Cas system. Cell Research 23(10): 1233-1236.

Michelmore, R. W., M. Christopoulou and K. S. Caldwell (2013). Impacts of Resistance Gene Genetics, Function, and Evolution on a Durable Future. Annual Review of Phytopathology, Vol 51 51: 291-319.

Michielse, C. B., R. van Wijk, L. Reijnen, E. M. M. Manders, S. Boas, C. Olivain, C. Alabouvette and M. Rep (2009). The Nuclear Protein Sge1 of Fusarium oxysporum Is Required for Parasitic Growth. Plos Pathogens 5(10).

Milat, M. L., J. M. Ducruet, P. Ricci, F. Marty and J. P. Blein (1991). PHYSIOLOGICAL AND STRUCTURAL-CHANGES IN TOBACCO-LEAVES TREATED WITH CRYPTOGEIN, A PROTEINACEOUS ELICITOR FROM PHYTOPHTHORA-CRYPTOGEA. Phytopathology 81(11): 1364-1368.

Milat, M. L., P. Ricci, P. Bonnet and J. P. Blein (1991). CAPSIDIOL AND ETHYLENE PRODUCTION BY TOBACCO CELLS IN RESPONSE TO CRYPTOGEIN, AN ELICITOR FROM PHYTOPHTHORA-CRYPTOGEA. Phytochemistry 30(7): 2171-2173.

Mithoefer, A. and W. Boland (2012). Plant Defense Against Herbivores: Chemical Aspects. Annual Review of Plant Biology, Vol 63 63: 431-450.

Mizubuti, E. S. G. and W. E. Fry (1998). Temperature effects on developmental stages of isolates from three clonal lineages of Phytophthora infestans. Phytopathology 88(8): 837-843.

Monaghan, J. and C. Zipfel (2012). Plant pattern recognition receptor complexes at the plasma membrane. Current Opinion in Plant Biology 15(4): 349-357.

Morgan, W. and S. Kamoun (2007). RXLR effectors of plant pathogenic oomycetes. Current Opinion in Microbiology 10(4): 332-338.

Moriguchi, T., H. Matsuura, Y. Itakura, H. Katsuki, H. Saito and N. Nishiyama (1997). Allixin, a phytoalexin produced by garlic, and its analogues as novel exogenous substances with neurotrophic activity. Life Sciences 61(14): 1413-1420.

Müller, K. O. B., H. (1940). Experimentelle untersuchungen über die Phytophthora resistenz der Kartoffel. Arbeit. Biol. Reichsant Land Forstwirtsch 23: 189–231.

Nafisi, M., S. Goregaoker, C. J. Botanga, E. Glawischnig, C. E. Olsen, B. A. Halkier and J. Glazebrook (2007). Arabidopsis cytochrome P450 monooxygenase 71A13 catalyzes the conversion of indole-3-acetaldoxime in camalexin synthesis. Plant Cell 19(6): 2039-2052.

Narusaka, M., Y. Kubo, K. Hatakeyama, J. Imamura, H. Ezura, Y. Nanasato, Y. Tabei, Y. Takano, K. Shirasu and Y. Narusaka (2013). Interfamily Transfer of Dual NB-LRR Genes Confers Resistance to Multiple Pathogens. Plos One 8(2).

Narusaka, M., K. Shirasu, Y. Noutoshi, Y. Kubo, T. Shiraishi, M. Iwabuchi and Y. Narusaka (2009). RRS1 and RPS4 provide a dual Resistance-gene system against fungal and bacterial pathogens. Plant Journal 60(2): 218-226.

Nekrasov, V., B. Staskawicz, D. Weigel, J. D. G. Jones and S. Kamoun (2013). Targeted mutagenesis in the model plant Nicotiana benthamiana using Cas9 RNA-guided endonuclease. Nature Biotechnology 31(8): 691-693.

Nishino, H. N., A.; Takayasu, J.; Iwashima, A.; Itakura, Y.; Kodera, Y.; Matsuura, H.; Fuwa, T. (1990). Antitumor-promoting activity of allixin, a stress compound produced by garlic. `Cncer Journal(3): 20-21.

Nombela, G., V. M. Williamson and M. Muniz (2003). The root-knot nematode resistance gene Mi-1.2 of tomato is responsible for resistance against the whitefly Bemisia tabaci. Molecular Plant-Microbe Interactions 16(7): 645-649.

O'Maille, P. E., A. Malone, N. Dellas, B. A. Hess, Jr., L. Smentek, I. Sheehan, B. T. Greenhagen, J. Chappell, G. Manning and J. P. Noel (2008). Quantitative exploration of the catalytic landscape

separating divergent plant sesquiterpene synthases. Nature Chemical Biology 4(10): 617-623.

Olson, S. A. (1994). MacVector: an integrated sequence analysis program for the Macintosh. Methods in molecular biology (Clifton, N.J.) 25: 195-201.

Ooijen, G. v., H. A. v. d. Burg, B. J. C. Cornelissen and F. L. W. Takken (2007). Structure and function of resistance proteins in solanaceous plants. Annual Review of Phytopathology 45: 43-72.

Ori, N., Y. Eshed, I. Paran, G. Presting, D. Aviv, S. Tanksley, D. Zamir and R. Fluhr (1997). The I2C family from the wilt disease resistance locus I2 belongs to the nucleotide binding, leucine-rich repeat superfamily of plant resistance genes. Plant Cell 9(4): 521-532.

P. Król, R. I., S. Pollmann, E. Kepczynska, (2015). Priming of seeds with methyl jasmonate induced resistance to hemi-biotroph Fusarium oxysporum f.sp. lycopersici in tomato via 12-oxo-phytodienoic acid, salicylic acid, and flavonol accumulation. Journal of Plant Physiology 179: 122-132.

Padmanabhan, M. S., S. P. Gorepoker, S. Golem, H. Shiferaw and J. N. Culver (2005). Interaction of the tobacco mosaic virus replicase protein with the Aux/IAA protein PAPI/IAA26 is associated with disease development. Journal of Virology 79(4): 2549-2558.

Padmanabhan, M. S., H. Shiferaw and J. N. Culver (2006). The Tobacco mosaic virus replicase protein disrupts the localization and function of interacting Aux/IAA proteins. Molecular Plant-Microbe Interactions 19(8): 864-873.

Pan, Q. L., J. Wendel and R. Fluhr (2000). Divergent evolution of plant NBS-LRR resistance gene homologues in dicot and cereal genomes. Journal of Molecular Evolution 50(3): 203-213.

Pandey, S. P., M. Roccaro, M. Schoen, E. Logemann and I. E. Somssich (2010). Transcriptional reprogramming regulated by WRKY18 and WRKY40 facilitates powdery mildew infection of Arabidopsis. Plant Journal 64(6): 912-923.

Paul, J.-Y., D. K. Becker, M. B. Dickman, R. M. Harding, H. K. Khanna and J. L. Dale (2011). Apoptosis-related genes confer resistance to Fusarium wilt in transgenic 'Lady Finger' bananas. Plant Biotechnology Journal 9(9): 1141-1148.

Pearl, L. H. and C. Prodromou (2006). Structure and mechanism of the Hsp90 molecular chaperone machinery. Annual Review of Biochemistry. 75: 271-294.

Pennisi, E. (2010). Armed and Dangerous. Science 327(5967): 804-805.

Pieterse, C. M. J., D. Van der Does, C. Zamioudis, A. Leon-Reyes and S. C. M. Van Wees (2012). Hormonal Modulation of Plant Immunity. Annual Review of Cell and Developmental Biology, Vol 28 28: 489-521.

Raffaele, S., R. A. Farrer, L. M. Cano, D. J. Studholme, D. MacLean, M. Thines, R. H. Y. Jiang, M. C. Zody, S. G. Kunjeti, N. M. Donofrio, B. C. Meyers, C. Nusbaum and S. Kamoun (2010). Genome Evolution Following Host Jumps in the Irish Potato Famine Pathogen Lineage. Science 330(6010): 1540-1543.

Rafiqi, M., P. H. P. Gan, M. Ravensdale, G. J. Lawrence, J. G. Ellis, D. A. Jones, A. R. Hardham and P. N. Dodds (2010). Internalization of Flax Rust Avirulence Proteins into Flax and Tobacco Cells Can Occur in the Absence of the Pathogen. Plant Cell 22(6): 2017-2032.

Rairdan, G. J., S. M. Collier, M. A. Sacco, T. T. Baldwin, T. Boettrich and P. Moffett (2008). The coiled-coil and nucleotide binding domains of the potato Rx disease resistance protein function in pathogen recognition and signaling. Plant Cell 20(3): 739-751.

Rairdan, G. J. and P. Moffett (2006). Distinct domains in the ARC region of the potato resistance protein Rx mediate LRR binding and inhibition of activation. Plant Cell 18(8): 2082-2093.

Ralston, L., S. T. Kwon, M. Schoenbeck, J. Ralston, D. J. Schenk, R. M. Coates and J. Chappell (2001). Cloning, heterologous expression, and functional characterization of 5-epi-aristolochene-1,3-dihydroxylase from tobacco (Nicotiana tabacum). Archives of Biochemistry and Biophysics 393(2): 222-235.

Randall, E., V. Young, H. Sierotzki, G. Scalliet, P. R. J. Birch, D. E. L. Cooke, M. Csukai and S. C. Whisson (2014). Sequence diversity in the large subunit of RNA polymerase I contributes to Mefenoxam insensitivity in Phytophthora infestans. Molecular Plant Pathology 15(7): 664-676.

Rep, M. (2005). Small proteins of plant-pathogenic fungi secreted during host colonization. Fems Microbiology Letters 253(1): 19-27.

Rep, M., H. C. van der Does, M. Meijer, R. van Wijk, P. M. Houterman, H. L. Dekker, C. G. de Koster and B. J. C. Cornelissen (2004). A small, cysteine-rich protein secreted by Fusarium oxysporum during colonization of xylem vessels is required for I-3-mediated resistance in tomato. Molecular Microbiology 53(5): 1373-1383.

Reuveni, M. and Y. Cohen (1978). GROWTH RETARDATION AND CHANGES IN PHENOLIC COMPOUNDS, WITH SPECIAL REFERENCE TO SCOPOLETIN, IN MILDEWED AND ETHYLENE-TREATED TOBACCO PLANTS. Physiological Plant Pathology 12(2): 179-189.

Riedl, S. J., W. Y. Li, Y. Chao, R. Schwarzenbacher and Y. G. Shi (2005). Structure of the apoptotic protease-activating factor 1 bound to ADP. Nature 434(7035): 926-933.

Roche, D. B., M. T. Buenavista, S. J. Tetchner and L. J. McGuffin (2011). The IntFOLD server: an integrated web resource for protein fold recognition, 3D model quality assessment, intrinsic disorder prediction, domain prediction and ligand binding site prediction. Nucleic Acids Research 39: W171-W176.

Rogers, E. E., J. Glazebrook and F. N. Ausubel (1996). Mode of action of the Arabidopsis thaliana phytoalexin camalexin and its role in Arabidopsis-pathogen interactions. Molecular Plant-Microbe Interactions 9(8): 748-757.

Rohila, J. S., M. Chen, R. Cerny and M. E. Fromm (2004). Improved tandem affinity purification tag and methods for isolation of protein heterocomplexes from plants. Plant Journal 38(1): 172-181.

Rooney, H. C. E., J. W. van 't Klooster, R. A. L. van der Hoorn, M. Joosten, J. D. G. Jones and P. de Wit (2005). Cladosporium Avr2 inhibits tomato Rcr3 protease required for Cf-2-dependent disease resistance. Science 308(5729): 1783-1786.

Sambrook, J. and D. W. Russell (2001). Molecular cloning: A laboratory manual.

Sanchez-Vallet, A., B. Ramos, P. Bednarek, G. Lopez, M. Pislewska-Bednarek, P. Schulze-Lefert and A. Molina (2010). Tryptophan-derived secondary metabolites in Arabidopsis thaliana confer non-host resistance to necrotrophic Plectosphaerella cucumerina fungi. Plant Journal 63(1): 115-127.

Saunders, D. G. O., S. Breen, J. Win, S. Schornack, I. Hein, T. O. Bozkurt, N. Champouret, V. G. A. A. Vleeshouwers, P. R. J. Birch, E. M. Gilroy and S. Kamoun (2012). Host Protein BSL1 Associates with Phytophthora infestans RXLR Effector AVR2 and the Solanum demissum Immune Receptor R2 to Mediate Disease Resistance. Plant Cell 24(8): 3420-3434.

Schmidt, S. M., P. M. Houterman, I. Schreiver, L. Ma, S. Amyotte, B. Chellappan, S. Boeren, F. L. W. Takken and M. Rep (2013). MITEs in the promoters of effector genes allow prediction of novel virulence genes in Fusarium oxysporum. Bmc Genomics 14.

Schnee, S., O. Viret and K. Gindro (2008). Role of stilbenes in the resistance of grapevine to powdery mildew. Physiological and Molecular Plant Pathology 72(4-6): 128-133.

Schneider, C. A., W. S. Rasband and K. W. Eliceiri (2012). NIH Image to ImageJ: 25 years of image analysis. Nature Methods 9(7): 671-675.

Schornack, S. (2006). Struktur, Erkennungsspezifität und Regulationsmechanismus des Resistenzproteins Bs4 aus Tomate. PhD, Martin-Luther-University Halle-Wittenberg.

Schornack, S., M. van Damme, T. O. Bozkurt, L. M. Cano, M. Smoker, M. Thines, E. Gaulin, S. Kamoun and E. Huitema (2010). Ancient class of translocated oomycete effectors targets the host nucleus. Proceedings of the National Academy of Sciences of the United States of America 107(40): 17421-17426.

Scott, J. W. and J. P. Jones (1989). MONOGENIC RESISTANCE IN TOMATO TO FUSARIUM-OXYSPORUM F-SP LYCOPERSICI RACE-3. Euphytica 40(1-2): 49-53.

Segretin, M.-E., M. Pais, M. Franceschetti, A. Chaparro-Garcia, J. I. B. Bos, M. J. Banfield and S. Kamoun (2014). Single Amino Acid Mutations in the Potato Immune Receptor R3a Expand Response to Phytophthora Effectors. Molecular Plant-Microbe Interactions 27(7): 624-637.

Seppanen, S. K., L. Syrjala, K. von Weissenberg, T. H. Teeri, L. Paajanen and A. Pappinen (2004). Antifungal activity of stilbenes in in vitro bioassays and in transgenic Populus expressing a gene encoding pinosylvin synthase. Plant Cell Reports 22(8): 584-593.

Serazetdinova, L., K. H. Oldach and H. Lorz (2005). Expression of transgenic stilbene synthases in wheat causes the accumulation of unknown stilbene derivatives with antifungat activity. Journal of Plant Physiology 162(9): 985-1002.

Shan, L. B., V. K. Thara, G. B. Martin, J. M. Zhou and X. Y. Tang (2000). The pseudomonas AvrPto protein is differentially recognized by tomato and tobacco and is localized to the plant plasma membrane. Plant Cell 12(12): 2323-2337.

Shan, Q., Y. Wang, J. Li, Y. Zhang, K. Chen, Z. Liang, K. Zhang, J. Liu, J. J. Xi, J.-L. Qiu and C. Gao (2013). Targeted genome modification of crop plants using a CRISPR-Cas system. Nature Biotechnology 31(8): 686-688.

Shattock, R. C., Tooley, P.W. and Fry, W.E. (1986). The genetics of Phytophthora infestans: identification of recombination, segregation and selfing by isozyme analysis. Phytopathology 76: 410-413.

Shibata, Y., K. Kawakita and D. Takemoto (2010). Age-Related Resistance of Nicotiana benthamiana Against Hemibiotrophic Pathogen Phytophthora infestans Requires Both Ethylene- and Salicylic Acid-Mediated Signaling Pathways. Molecular Plant-Microbe Interactions 23(9): 1130-1142.

Simons, G., J. Groenendijk, J. Wijbrandi, M. Reijans, J. Groenen, P. Diergaarde, T. Van der Lee, M. Bleeker, J. Onstenk, M. de Both, M. Haring, J. Mes, B. Cornelissen, M. Zabeau and P. Vos (1998). Dissection of the Fusarium I2 gene cluster in tomato reveals six homologs and one active gene copy. Plant Cell 10(6): 1055-1068.

Smith, D. A. (1982). Toxicity of Phytoalexins. Phytoalexins. J. A. Bailey, Mansfield, J.W. Glasgow and London, UK: 218–252.

Smoot, J. J., F. J. Gough, H. A. Lamey, J. J. Eichenmuller and M. E. Gallegly (1958). PRODUCTION AND GERMINATION OF OOSPORES OF PHYTOPHTHORA-INFESTANS. Phytopathology 48(3): 165-171.

Snyder, W. C. H., H.N. (1940). The species concept in Fusarium. American Journal of Botany 27.

Spoel, S. H. and X. Dong (2012). How do plants achieve immunity? Defence without specialized immune cells. Nature Reviews Immunology 12(2): 89-100.

Staal, J., M. Kaliff, S. Bohman and C. Dixelius (2006). Transgressive segregation reveals two Arabidopsis TIR-NB-LRR resistance genes effective against Leptosphaeria maculans, causal agent of blackleg disease. Plant Journal 46(2): 218-230.

Stall, R. E. and J. M. Walter (1965). SELECTION AND INHERITANCE OF RESISTANCE IN TOMATO TO ISOLATES OF RACES 1 AND 2 OF FUSARIUM WILT ORGANISM. Phytopathology 55(11): 1213-&.

StarkLorenzen, P., B. Nelke, G. Hanssler, H. P. Muhlbach and J. E. Thomzik (1997). Transfer of a grapevine stilbene synthase gene to rice (Oryza sativa L). Plant Cell Reports 16(10): 668-673.

Stirnweis, D., S. D. Milani, T. Jordan, B. Keller and S. Brunner (2014). Substitutions of Two Amino Acids in the Nucleotide-Binding Site Domain of a Resistance Protein Enhance the Hypersensitive Response and Enlarge the PM3F Resistance Spectrum in Wheat. Molecular Plant-Microbe Interactions 27(3): 265-276.

Stoessl, A., C. H. Unwin and E. W. B. Ward (1972). Postinfectional Inhibitors from Plants. Journal of Phytopathology 74(2): 141-152.

Stoessl, A., C. H. Unwin and E. W. B. Ward (1973). POSTINFECTIONAL FUNGUS INHIBITORS FROM PLANTS - FUNGAL OXIDATION OF CAPSIDIOL IN PEPPER FRUIT. Phytopathology 63(10): 1225-1231.

Szabo, L. J. and W. R. Bushnell (2001). Hidden robbers: The role of fungal haustoria in parasitism of plants. Proceedings of the National Academy of Sciences of the United States of America 98(14): 7654-7655.

Takahashi, A., C. Casais, K. Ichimura and K. Shirasu (2003). HSP90 interacts with RAR1 and SGT1 and is essential for RPS2-mediated disease resistance in Arabidopsis. Proceedings of the National Academy of Sciences of the United States of America 100(20): 11777-11782.

Takken, F. and M. Rep (2010). The arms race between tomato and Fusarium oxysporum. Molecular Plant Pathology 11(2): 309-314.

Takken, F. L. W., M. Albrecht and W. I. L. Tameling (2006). Resistance proteins: molecular switches of plant defence. Current Opinion in Plant Biology 9(4): 383-390.

Takken, F. L. W. and A. Goverse (2012). How to build a pathogen detector: structural basis of NB-LRR function. Current Opinion in Plant Biology 15(4): 375-384.

Takken, F. L. W., R. Luderer, S. Gabriels, N. Westerink, R. Lu, P. de Wit and M. Joosten (2000). A functional cloning strategy, based on a binary PVX-expression vector, to isolate HR-inducing cDNAs of plant pathogens. Plant Journal 24(2): 275-283.

Takken, F. L. W. and W. I. L. Tameling (2009). To Nibble at Plant Resistance Proteins. Science 324(5928): 744-746.

Tameling, W. I. L., S. D. J. Elzinga, P. S. Darmin, J. H. Vossen, F. L. W. Takken, M. A. Haring and B. J. C. Cornelissen (2002). The tomato R gene products I-2 and Mi-1 are functional ATP binding proteins with ATPase activity. Plant Cell 14(11): 2929-2939.

Tameling, W. I. L., J. H. Vossen, M. Albrecht, T. Lengauer, J. A. Berden, M. A. Haring, B. J. C. Cornelissen and F. L. W. Takken (2006). Mutations in the NB-ARC domain of I-2 that impair ATP hydrolysis cause autoactivation. Plant Physiology 140(4): 1233-1245.

Tanji, H., U. Ohto, T. Shibata, K. Miyake and T. Shimizu (2013). Structural Reorganization of the Toll-Like Receptor 8 Dimer Induced by Agonistic Ligands. Science 339(6126): 1426-1429.

Thaler, J. S., P. T. Humphrey and N. K. Whiteman (2012). Evolution of jasmonate and salicylate signal crosstalk. Trends in Plant Science 17(5): 260-270.

Thatcher, L. F., D. M. Gardiner, K. Kazan and J. M. Manners (2012). A Highly Conserved Effector in Fusarium oxysporum Is Required for Full Virulence on Arabidopsis. Molecular Plant-Microbe Interactions 25(2): 180-190.

Thomma, B. P. H. J., T. Nuernberger and M. H. A. J. Joosten (2011). Of PAMPs and Effectors: The Blurred PTI-ETI Dichotomy. Plant Cell 23(1): 4-15.

Thomzik, J. E., K. Stenzel, R. Stocker, P. H. Schreier, R. Hain and D. J. Stahl (1997). Synthesis of a grapevine phytoalexin in transgenic tomatoes (Lycopersicon esculentum Mill.) conditions resistance against Phytophthora infestans. Physiological and Molecular Plant Pathology 51(4): 265-278.

Tian, D., M. B. Traw, J. Q. Chen, M. Kreitman and J. Bergelson (2003). Fitness costs of R-gene-mediated resistance in Arabidopsis thaliana. Nature 423(6935): 74-77.

Tian, M. Y., E. Huitema, L. da Cunha, T. Torto-Alalibo and S. Kamoun (2004). A Kazal-like extracellular serine protease inhibitor from Phytophthora infestans targets the tomato pathogenesis-related protease P69B. Journal of Biological Chemistry 279(25): 26370-26377.

Timperio, A. M., A. D'Alessandro, M. Fagioni, P. Magro and L. Zolla (2012). Production of the phytoalexins trans-resveratrol and delta-viniferin in two economy-relevant grape cultivars upon infection with Botrytis cinerea in field conditions. Plant Physiology and Biochemistry 50: 65-71.

Tomiyama, K., T. Sakuma, N. Ishizaka, N. Sato, N. Katsui, M. Takasugi and T. Masamune (1968). A NEW ANTIFUNGAL SUBSTANCE ISOLATED FROM RESISTANT POTATO TUBER TISSUE INFECTED BY PATHOGENS. Phytopathology 58(1): 115-&.

Trinh-Don, N., G. MacNevin and D.-K. Ro (2012). De Novo Synthesis of High-Value Plant Sesquiterpenoids in Yeast. Natural Product Biosynthesis by Microorganisms and Plants, Pt C. D. A. Hopwood. 517: 261-278.

Ueda, H., Y. Yamaguchi and H. Sano (2006). Direct interaction between the tobacco mosaic virus helicase domain and the ATP-bound resistance protein, N factor during the hypersensitive response in tobacco plants. Plant Molecular Biology 61(1-2): 31-45.

van Baarlen, P., E. J. Woltering, M. Staats and J. A. L. van Kan (2007). Histochemical and genetic analysis of host and non-host interactions of Arabidopsis with three Botrytis species: an important role for cell death control. Molecular Plant Pathology 8(1): 41-54.

van Bentem, S. D. F., J. H. Vossen, K. J. de Vries, S. van Wees, W. I. L. Tameling, H. L. Dekker, C. G. de Koster, M. A. Haring, F. L. W. Takken and B. J. C. Cornelissen (2005). Heat shock protein 90 and its co-chaperone protein phosphatase 5 interact with distinct regions of the tomato I-2 disease resistance protein. Plant Journal 43(2): 284-298.

van Damme, M., T. O. Bozkurt, C. Cakir, S. Schornack, J. Sklenar, A. M. E. Jones and S. Kamoun (2012). The Irish Potato Famine Pathogen

Phytophthora infestans Translocates the CRN8 Kinase into Host Plant Cells. Plos Pathogens 8(8).

van der Does, H. C., B. Lievens, L. Claes, P. M. Houterman, B. J. C. Cornelissen and M. Rep (2008). The presence of a virulence locus discriminates Fusarium oxysporum isolates causing tomato wilt from other isolates. Environmental Microbiology 10(6): 1475-1485.

van der Hoorn, R. A. L. and S. Kamoun (2008). From Guard to Decoy: A new model for perception of plant pathogen effectors. Plant Cell 20(8): 2009-2017.

van Ooijen, G., E. Lukasik, H. A. van den Burg, J. H. Vossen, B. J. C. Cornelissen and F. L. W. Takken (2010). The small heat shock protein 20 RSI2 interacts with and is required for stability and function of tomato resistance protein I-2. Plant Journal 63(4): 563-572.

van Ooijen, G., G. Mayr, M. Albrecht, B. J. C. Cornelissen and F. L. W. Takken (2008). Transcomplementation, but not Physical Association of the CC-NB-ARC and LRR Domains of Tomato R Protein Mi-1.2 is Altered by Mutations in the ARC2 Subdomain. Molecular Plant 1(3): 401-410.

Van Ooijen, G., G. Mayr, M. M. A. Kasiem, M. Albrecht, B. J. C. Cornelissen and F. L. W. Takken (2008). Structure-function analysis of the NB-ARC domain of plant disease resistance proteins. Journal of Experimental Botany 59(6): 1383-1397.

van West, P., A. J. de Jong, H. S. Judelson, A. M. C. Emons and F. Govers (1998). The ipiO gene of Phytophthora infestans is highly expressed in invading hyphae during infection. Fungal Genetics and Biology 23(2): 126-138.

Vleeshouwers, V., W. van Dooijeweert, F. Govers, S. Kamoun and L. T. Colon (2000). The hypersensitive response is associated with host and nonhost resistance to Phytophthora infestans. Planta 210(6): 853-864.

Vleeshouwers, V. G. A. A., J.-D. Driesprong, L. G. Kamphuis, T. Torto-Alalibo, K. A. E. Van't Slot, F. Govers, R. G. F. Visser, E. Jacobsen and S. Kamoun (2006). Agroinfection-based high-throughput screening reveals specific recognition of INF elicitins in Solanum. Molecular Plant Pathology 7(6): 499-510.

Vlot, A. C., D. M. A. Dempsey and D. F. Klessig (2009). Salicylic Acid, a Multifaceted Hormone to Combat Disease. Annual Review of Phytopathology. 47: 177-206.

Voegele, R. T. and K. Mendgen (2003). Rust haustoria: nutrient uptake and beyond. New Phytologist 159(1): 93-100.

Voegele, R. T., C. Struck, M. Hahn and K. Mendgen (2001). The role of haustoria in sugar supply during infection of broad bean by the rust fungus Uromyces fabae. Proceedings of the National Academy of Sciences of the United States of America 98(14): 8133-8138.

Volin, R. B. and J. P. Jones (1982). A NEW RACE OF FUSARIUM-WILT OF TOMATO IN FLORIDA AND SOURCES OF RESISTANCE. Proceedings of the Florida State Horticultural Society 95: 268-270.

W. F. O. Marasas, P. E. N. (1987). Mycotoxicology: Introduction to the Mycology, Plant Pathology, Chemistry, Toxicology, and Pathology of Naturally Occurring Mycotoxicoses in Animals, Pennsylvania State Univ Pr.

Ward, E. W. B. (1976). CAPSIDIOL PRODUCTION IN PEPPER LEAVES IN INCOMPATIBLE INTERACTIONS WITH FUNGI. Phytopathology 66(2): 175-176.

Ward, E. W. B. and A. Stoessl (1972). POSTINFECTIONAL INHIBITORS FROM PLANTS .3. DETOXIFICATION OF CAPSIDIOL, AN ANTIFUNGAL COMPOUND FROM PEPPERS. Phytopathology 62(10): 1186-1187.

Webster J, W. R. (2007). Introduction to fungi, New York: Camridge UniversityPress.

Wei, C., H. Kuang, F. Li and J. Chen (2014). The I2 resistance gene homologues in Solanum have complex evolutionary patterns and are targeted by miRNAs. Bmc Genomics 15.

Weiberg, A., M. Wang, F.-M. Lin, H. Zhao, Z. Zhang, I. Kaloshian, H.-D. Huang and H. Jin (2013). Fungal Small RNAs Suppress Plant Immunity by Hijacking Host RNA Interference Pathways. Science 342(6154): 118-123.

Westwood, J. H., J. I. Yoder, M. P. Timko and C. W. dePamphilis (2010). The evolution of parasitism in plants. Trends in Plant Science 15(4): 227-235.

Whisson, S. C., P. C. Boevink, L. Moleleki, A. O. Avrova, J. G. Morales, E. M. Gilroy, M. R. Armstrong, S. Grouffaud, P. van West, S. Chapman, I. Hein, I. K. Toth, L. Pritchard and P. R. J. Birch (2007). A translocation signal for delivery of oomycete effector proteins into host plant cells. Nature 450(7166): 115-+.

Williams, S. J., K. H. Sohn, L. Wan, M. Bernoux, P. F. Sarris, C. Segonzac, T. Ve, Y. Ma, S. B. Saucet, D. J. Ericsson, L. W. Casey, T. Lonhienne, D. J. Winzor, X. Zhang, A. Coerdt, J. E. Parker, P. N. Dodds, B. Kobe and J. D. G. Jones (2014). Structural Basis for Assembly and Function of a Heterodimeric Plant Immune Receptor. Science 344(6181): 299-303.

Williams, S. J., P. Sornaraj, E. deCourcy-Ireland, R. I. Menz, B. Kobe, J. G. Ellis, P. N. Dodds and P. A. Anderson (2011). An Autoactive Mutant of the M Flax Rust Resistance Protein Has a Preference for Binding ATP, Whereas Wild-Type M Protein Binds ADP. Molecular Plant-Microbe Interactions 24(8): 897-906.

Win, J., A. Chaparro-Garcia, K. Belhaj, D. G. O. Saunders, K. Yoshida, S. Dong, S. Schornack, C. Zipfel, S. Robatzek, S. A. Hogenhout and S. Kamoun (2012). Effector biology of plant-associated organisms: concepts and perspectives. Cold Spring Harbor symposia on quantitative biology 77: 235-247.

Wirthmueller, L., Y. Zhang, J. D. G. Jones and J. E. Parker (2007). Nuclear accumulation of the Arabidopsis immune receptor RPS4 is necessary for triggering EDS1-dependent defense. Current Biology 17(23): 2023-2029.

Wu, C.-H., K. V. Krasileva, M. J. Banfield, R. Terauchi and S. Kamoun (2015). The "sensor domains" of plant NLR proteins: more than decoys? Frontiers in plant science 6: 134-134.

Wulff, B. B. H., D. M. Horvath and E. R. Ward (2011). Improving immunity in crops: new tactics in an old game. Current Opinion in Plant Biology 14(4): 468-476.

Xiang, T., N. Zong, Y. Zou, Y. Wu, J. Zhang, W. Xing, Y. Li, X. Tang, L. Zhu, J. Chai and J.-M. Zhou (2008). Pseudomonas syringae effector AvrPto blocks innate immunity by targeting receptor kinases. Current Biology 18(1): 74-80.

Xiao, F., P. He, R. B. Abramovitch, J. E. Dawson, L. K. Nicholson, J. Sheen and G. B. Martin (2007). The N-terminal region of Pseudomonas type III effector AvrPtoB elicits Pto-dependent immunity and has two distinct virulence determinants. Plant Journal 52(4): 595-614.

Xie, K. and Y. Yang (2013). RNA-Guided Genome Editing in Plants Using a CRISPRCas System. Molecular Plant 6(6): 1975-1983.

Yadeta, K. and B. P. H. J. Thomma (2013). The xylem as battleground for plant hosts and vascular wilt pathogens. Frontiers in Plant Science 4.

Yamasaki, T., R. W. Teel and B. H. S. Lau (1991). EFFECT OF ALLIXIN, A PHYTOALEXIN PRODUCED BY GARLIC, ON MUTAGENESIS, DNA-BINDING AND METABOLISM OF AFLATOXIN-B1. Cancer Letters 59(2): 89-94.

Yoshida, K., H. A. Burbano, J. Krause, M. Thines, D. Weigel and S. Kamoun (2014). Mining herbaria for plant pathogen genomes: back to the future. PLoS pathogens 10(4): e1004028-e1004028.

Yoshida, K., V. J. Schuenemann, L. M. Cano, M. Pais, B. Mishra, R. Sharma, C. Lanz, F. N. Martin, S. Kamoun, J. Krause, M. Thines, D. Weigel and H. A. Burbano (2013). The rise and fall of the Phytophthora infestans lineage that triggered the Irish potato famine. Elife 2.

Yu, S.-C. and Y.-M. Zou (2008). A co-dominant molecular marker of fusarium wilt resistance gene I-2 derived from gene sequence in tomato. Yichuan 30(7): 926-932.

Zhai, C., Y. Zhang, N. Yao, F. Lin, Z. Liu, Z. Dong, L. Wang and Q. Pan (2014). Function and Interaction of the Coupled Genes Responsible for Pik-h Encoded Rice Blast Resistance. Plos One 9(6).

Zhang, P. F., H. Foerster, C. P. Tissier, L. Mueller, S. Paley, P. D. Karp and S. Y. Rhee (2005). MetaCyc and AraCyc. Metabolic pathway databases for plant research. Plant Physiology 138(1): 27-37.

Zhang, Y., S. Dorey, M. Swiderski and J. D. G. Jones (2004). Expression of RPS4 in tobacco induces an AvrRps4-independent HR that requires EDS1, SGT1 and HSP90. Plant Journal 40(2): 213-224.

Zhu, S., Y. Li, J. H. Vossen, R. G. F. Visser and E. Jacobsen (2012). Functional stacking of three resistance genes against Phytophthora infestans in potato. Transgenic Research 21(1): 89-99.

Zhu, Y. J., R. Agbayani, M. C. Jackson, C. S. Tang and P. H. Moore (2004). Expression of the grapevine stilbene synthase gene VST1 in papaya provides increased resistance against diseases caused by Phytophthora palmivora. Planta 220(2): 241-250.